Dissertation

submitted to the
Combined Faculties for the Natural Sciences and for Mathematics
of the Ruperto-Carola University of Heidelberg, Germany
for the degree of

Doctor of Natural Sciences

Induction and Regulation of Plasma Membrane Blebbing by SH4-Domains and the Diaphanous Related Formin FHOD1

presented by
Diplom-Biologe Sebastian Hannemann
born in: Hildesheim, Germany
Oral-examination:

Referees: Prof. Dr. Hans-Georg Kräusslich

Prof. Dr. Oliver Till Fackler

Meiner Familie

"Grau, teurer Freund, ist alle Theorie,
Und grün des Lebens goldner Baum."

Johann Wolfgang von Goethe
Faust, der Tragödie erster Teil, Studierzimmer

INDEX

1 PUBLICATIONS

Peer-Reviewed Original Papers:

- Haller, C., Rauch, S., Michel, N., **Hannemann, S.**, Lehmann, M. J., Keppler O.T. and Fackler, O.T. 2006. The HIV-1 Pathogenicity Factor Nef interferes With Maturation of Stimulatory T-lymphocyte Contacts by Modulation of N-Wasp Activity. J Biol Chem **281**(28), 19618-30.
- Kitzing T.M., Sahadevan A.S., Brandt D.T., Knieling H., **Hannemann S.**, Fackler O.T., Großhans J., Grosse R. 2007. Positive feedback between Dia1, LARG, and RhoA regulates cell morphology and invasion. Genes Dev, **21**(12), 1478-83.
- Tournaviti*, S., **Hannemann*, S.**, Terjung, S., Kitzing, T.M., Stegmayer, C., Ritzerfeld, J., Walther, P., Grosse, R., Nickel, W. and Fackler, O.T. 2007. SH4 Domain-Induced Plasma Membrane Dynamization Promotes Bleb-Associated Cell Motility. J Cell Sci, **in press** (*co-first author).

Oral Presentations at Meetings:

- **Sebastian Hannemann** (2005), 'Role of the Interaction of the Diaphanous Related Formin FHOD1 and the Rho-Kinase ROCK 1 in Membrane Blebbing', SFB 638 - Dynamics of macromolecular complexes in biosynthetic transport, Spring Meeting, Lindenfels-Winkel, Germany.

Abstract Presentations at Meetings:

- Judith E. Gasteier, **Sebastian Hannemann**, Ricardo Madrid, Jérôme Bouchet, Sebastian Schröder, Matthias Geyer, Serge Benichou, Oliver T. Fackler (2004), 'Oligomerization of the Diaphanous Related Formin FHOD1 Requires a Coiled-Coil Motif Critical for its Cytoskeletal and Transcriptional Activities', 3rd workshop "Cell Biology of Viral Infections" of the Society for Virology, Zeilitzheim, Germany.
- **Sebastian Hannemann**, Judith E. Gasteier, Ricardo Madrid, Serge Benichou, Oliver T. Fackler (2005), 'Non-apoptotic Membrane Blebbing Induced by the Diaphanous Related Formin FHOD1 and ROCK 1', 20th FEBS/ESF Advanced Workshop on Integrated Approaches in Cytoskeleton Research, Luxembourg-City, Luxembourg.
- **Sebastian Hannemann**, Stella Tournaviti, Carolin Stegmayer, Oliver T. Fackler and Walter Nickel (2006), 'Hydrophilic Acylated Surface Protein B, an SH4-containing Factor Expressed at the Cell Surface of Leishmania Parasites Induces Plasma Membrane Blebs', Annual Meeting of the German Society for Cell Biology, Braunschweig, Germany.
- **Sebastian Hannemann**, Stella Tournaviti, Stefan Terjung, Thomas M. Kitzing, Carolin Stegmayer, Julia Ritzerfeld, Paul Walther, Robert Grosse Walter Nickel and Oliver T. Fackler (2007), 'SH4-Domain Induced Plasma Membrane Dynamization Promotes Bleb-Associated Cell Motility', Gordon Research Conference, Motile and Contractile Systems, New London, New Hampshire, USA.

2 ABBREVIATIONS

- ABP280 — actin binding protein 280
- ADP — adenosine-diphosphate
- approx. — Approximately
- Arp — actin related protein
- ATP — adenosine-triphosphate
- BFA — Brefeldin A
- β-gal — β-galactosidase
- BrdU — Bromodeoxyuridine
- BS — Blebbistatin
- BSA — bovine serum albumine
- c-/v-Src — cellular/viral steroid receptor co-factor
- CC — coiled coil
- Cdc42 — cell division cycle 42 homolog protein
- cDNA — complementary DNA
- CFP — cyan fluorescent protein
- cGMP — cyclic guanosine monophosphate
- Chk — Csk-homologous kinase
- Chx — Cycloheximide
- Ci — Curie
- CoA — coenzyme A
- co-IP — co-immunoprecipitation
- CRD — cysteine rich domain
- CS — Coverslip
- Csk — C-terminal Src kinase
- CytoD — Cytochalasin D
- DAAM — dishevelled-associated activator of morphogenesis
- Dia — Diaphanous
- DIP — diaphanous interacting protein
- DMSO — Dimethylsulfoxide
- DNA — desoxyribonucleic acid

- dox — Doxicycline
- Drf — diaphanous related formin
- e.g. — *exempli gratia* (for example)
- EBV — Epstein-Barr virus
- ECM — extracellular matrix
- eGFP — enhanced GFP
- EIPA — 5-(N-ethyl-N-isopropyl)-amiloride
- ELISA — enzyme linked immunosorbend assay
- EM — electron micrograph
- ER — endoplasmatic reticulum
- ERK — extracellular signal regulated kinase
- ERM — ezrin-radixin-moesin
- et al. — *et alii* (and others)
- Eto — Etoposide
- FAK — focal adhesion kinase
- FCS — fetal calve serum
- FH1, FH2, FH3 — formin homology 1/2/3
- FHOD1 — formin homology 2 domain containing 1
- FMN — Formin
- FRET — fluorescence resonance energy transfer
- FRL — formin-related gene in lymphocytes
- FT — flow through
- g — Gram
- g — Gravity
- GAP — GTPase activating proteins
- GDI — guanine nucleotide dissociation inhibitors
- GDP — guanosine-diphosphate
- GEF — guanine exchange factor
- GFP — green fluorescent protein
- GTP — guanosine-triphosphate
- HASPB — hydrophilic acylated surface protein B
- HIV — Human immunodeficiency virus

- INF — inverted formin
- IP — Immunoprecipitation
- LIMK — LIM kinase
- LPA — lysophosphatic acid
- MAL — megakaryocytic acute leukemia
- MAP — mitogen activated protein
- MARCKS — myristoylated alanine-rich C kinase substrate
- MBP — myelin basic protein
- mDia — mammalian diaphanous
- MEF — mouse embryonal fibroblast
- MFI — mean fluorescence intensity
- MLC — myosin light chain
- MLCK — MLC kinase
- MLCP — MLC phosphatase
- MMP — Metalloprotease
- MQ — MilliQ water
- mRFP — monomeric Red Fluorescent Protein
- MTOC — microtubule organizing center
- MWCO — molecular weight cut-off
- n, μ, m — nano, mycro, milli
- NMT — N-myristoyl transferase
- OD — optical density
- PAGE — polyacrylamide gel electrophoresis
- PAK — p21 activated kinase
- PGK1 — cyclic GMP dependent protein kinase 1
- PH — pleckstrin homology
- PIP_2 — phosphatidylinositol-4,5-bisphosphate
- PKA — protein kinase A
- PKC — protein kinase C
- PM — plasma membrane
- PMA — phorbol myristate acetate
- PS — phosphatidyl serine

- PVDF — Polyvinylidenfluoride
- Rac — Ras-related C3 botulinum toxin substrate
- RBD — Rho binding domain
- Rho — Ras homolog protein
- RNAi — RNA interference
- ROCK — Rho associated coiled-coil containing protein kinase
- s, min, h — second, minute, hour
- S.E.M. — standard error of the mean
- Scar — suppressor of cAMP receptor
- SD — standard deviation
- SDS — sodium dodecyl sulfate
- SEM — scanning electron micrograph
- SH1, SH2, SH3, SH4 — Src homology 1/2/3/4
- shRNA — short hairpin RNA
- siRNA — silencer RNA
- SRE — serum response element
- SRF — serum response factor
- TdT — deoxynucleotidyl transferase
- TMR — Tetramethylrhodamine
- TNF-α — Tumor necrosis factor
- TUNEL — transferase-dUTP nick end labeling
- UTP — uridine-triphosphate
- v/v — volume per volume
- VASP — vasodilator stimulated phosphoprotein
- VCA — verproline-central-acidic domain
- VSV — vesicular stomatitis virus
- WASp — Wiskott-Aldrich-syndrome protein
- WAVE — WASp-verprolin homologous protein
- WH2 — WASp homology 2
- WISH — WASp interacting SH3-domain protein 1
- wt — Wildtype

3 SUMMARY

The plasma membrane (PM) of animal cells represents a dynamic lipid bilayer which is constantly remodeled and adapted to cellular demands *e.g.* by formation of protrusions such as lamellipodia, filopodia or membrane ruffles. Spherical PM blebs are another type of protrusions and are generated after exposure to specific triggers in distinct circumstances including *e.g.* apoptosis, secretion and cell motility. They are thought to be controlled by a common blebbing machinery which orchestrates bleb expansion, retention and retraction by influencing cytoskeletal organization and integrity as well as its interaction with the PM. A key factor in PM blebbing is the Rho kinase ROCK which activity is required for PM blebbing.

First, SH4-domains were identified as novel trigger for non-apoptotic PM blebbing. These anchoring domains of peripheric PM proteins such as the proto-oncogenic Src kinases or the cell surface protein HASPB of *Leishmania* parasites are attached to the PM *via* acetylated and saturated hydrocarbon chains, in some cases in combination with basic clusters. PM association was required for induction of PM blebbing which showed kinetics similar to other described PM blebbing phenotypes. Consistently, this dynamic process was controlled by Rho but not Rac or Cdc42 GTPase signaling pathways, was regulated by the activities of ROCK kinase and myosin II ATPase and was dependent on the integrity of F-actin as well as microtubules. In addition, Src kinases were identified as novel determinants in regulation of PM blebbing. Endogenous Src kinase activity was essential for PM blebbing in SH4-domain expressing cells. Active c-Src as well as active ROCK were enriched in PM blebs.

As a functional consequence, SH4-domain mediated PM blebbing correlated with enhancement of fluid-phase uptake as well as cell invasion in 3D matrices which is connected to the amoeboid mode of cell migration in metastasizing tumor cells. In fact, CHO cells expressing SH4-domains also showed PM blebbing in 3D environments and their invasiveness closely matched that of MDA-MB-435 breast cancer cells indicating a novel function of these anchoring domains.

Second, the diaphanous related formin FHOD1 was identified in RNAi based knockdown experiments to be involved in SH4-domain induced PM blebbing. Consistently, co-expressed with ROCK1, FHOD1 participated in non-apoptotic PM blebbing dependent on its formin specific ability to nucleate F-actin and possibly related to its binding to ROCK1. Induction of PM blebbing as well as binding required Src kinase activity, suggesting a direct interplay between these factors. In a here postulated hypothetical model, c-Src and ROCK1 are responsible for PM association and regulation of the blebbing machinery. In this scenario

FHOD1 mediated F-actin polymerization is required for cytoskeletal rearrangements during PM blebbing possibly in combination with other formins.

Finally, by application of a novel FHOD1 specific antibody it was demonstrated that endogenous FHOD1 localized in a perinuclear and Golgi related region. In knockdown experiments, however, additional functions beyond its contribution to PM blebbing were not detected, neither in relation to its Golgi association nor to its supposed capability of F-actin reorganization.

Collectively, Src kinases as well as FHOD1 were identified as compounds of a cellular machinery that involves Rho-ROCK activity and regulates SH4-domain triggered PM blebbing. These results suggest a novel interplay between SH4-domains, Src activity, ROCK signaling and FHOD1 mediated cytoskeletal rearrangements. Since PM blebbing was correlated with enhanced fluid-phase uptake and 3D motility, SH4-domain mediated PM dynamization might be a mechanism that influences invasiveness of cells transformed by SH4-domain containing oncoproteins.

4 ZUSAMMENFASSUNG

Die Plasmamembran (PM) tierischer Zellen besteht aus einer dynamischen, lipidhaltigen Doppelschicht, die beispielsweise bei der Bildung von Zellausläufern wie Lamellipodien, Filopodien oder Membranfalten abhängig von zellulären Bedürfnissen konstant umgestaltet wird. Die ballonartigen PM "blebs" stellen ebenfalls einen solchen Typ Zellausläufer dar und können zum Beispiel während Apoptose, Sekretion und Zellbeweglichkeit auftreten. Dabei werden Ausdehnung, Stabilisierung und Rückbildung der "blebs" vermutlich durch eine gemeinsame zelluläre Maschinerie kontrolliert, die sowohl die Organisation und Integrität des Zytoskeletts als auch dessen Interaktion mit der PM beeinflusst. Eine wichtige Rolle spielt dabei die Rho Kinase ROCK, deren Aktivität notwendig für PM "blebbing" ist.

In dieser Studie wurden SH4-Domänen als neuartiger Auslöser für PM "blebbing" identifiziert. SH4-Domänen sind die Ankerdomänen bestimmter peripherer PM Proteine wie der protoonkogenen Src Kinasen und des Oberflächenproteins HASPB des *Leishmania* Parasiten. Sie werden durch acetylierte und gesättigte Kohlenwasserstoffketten, teils unterstützt durch basische Bereiche in der Aminosäuresequenz an die PM gebunden. Es stellte sich heraus, dass diese Assoziation an die PM notwendig für die Induktion von SH4-Domänen vermitteltem PM "blebbing" war, welches Kinetiken aufwies, die vergleichbar mit beschriebenen PM "blebbing" Phänotypen waren. Darüber hinaus stand dieser dynamische Prozess allein unter der Kontrolle eines auf Rho, jedoch nicht auf Rac oder Cdc42 basierenden GTPase Signalweges, wurde durch ROCK Aktivität und Myosin II ATPase reguliert und benötigte sowohl F-Aktin- als auch Mikrotubuli-Integrität. Als neuer regulierender Faktor wurden Src Kinasen bestimmt, da endogene Src Kinase Aktivität essentiell für SH4-Domänen induziertes PM "blebbing" war. Darüber hinaus waren SH4-Domänen induzierte PM "blebs" sowohl mit aktivem c-Src als auch mit aktivem ROCK angereichert.

Es bestand eine funktionelle Korrelation von SH4-Domänen induziertem PM "blebbing" sowohl mit einer erhöhten zellulären Aufnahme flüssiger Bestandteile als auch mit einer erhöhten Zellinvasion in 3D Matrizen, welche in direktem Zusammenhang mit der amöboiden Form der Zellwanderung metastasierender Tumorzellen steht. Tatsächlich zeigten SH4-Domänen exprimierende CHO Zellen auch in 3D Umgebungen eine ähnliche "bleb" Morphologie und ihre Invasivität war vergleichbar mit der von MDA-MB-435 Brustkrebszellen, was auf eine neue zelluläre Funktion dieser Ankerdomänen hinweist.

Auch das "diaphanous related formin" FHOD1 konnte, basierend auf RNAi vermittelter Herunterregulierung, als Faktor für SH4-Domänen induziertes PM "blebbing" identifiziert werden. In Koexpression mit ROCK1 war FHOD1 in Abhängigkeit von seiner Fähigkeit zur F-Aktin-Nukleierung und möglicherweise durch direkte Interaktion mit ROCK1 an der Induktion von nicht-apoptotischem PM "blebbing" beteiligt. Dabei war Src Kinase Aktivität sowohl für die Induktion von PM "blebs" als auch für Interaktion von FHOD1 mit ROCK1 notwendig, was auf ein direktes Zusammenspiel dieser Faktoren hinweist. In einem in dieser Studie aufgestellten hypothetischen Modell sind c-Src und ROCK1 verantwortlich für PM Assoziation und Regulation der "blebbing" Maschinerie. FHOD1 vermittelte F-Aktin Polymerisierung ist hingegen notwendig für die Organisation des Zytoskeletts während des "blebbing" Vorganges, möglicherweise mit Unterstützung anderer Formine.

Schließlich konnte unter Verwendung eines neuen FHOD1 spezifischen Antikörpers gezeigt werden, dass endogenes FHOD1 in tierischen Zellen in perinukleären, Golgi ähnlichen Bereichen lokalisierte. Zusätzlich zu seiner Rolle in SH4-Domänen vermitteltem PM "blebbing" war es jedoch durch RNAi vermittelte Herunterregulierung nicht möglich, weitere Funktionen für FHOD1 zu ermitteln, weder in Bezug auf seine Golgi Assoziation noch auf seine postulierten Funktion für F-Aktin-Organisation.

Zusammenfassend wurden sowohl Src Kinasen als auch FHOD1 als neue Bestandteile einer zellulären Maschinerie identifiziert, die von Rho-ROCK Aktivität abhängig war und von SH4-Domänen gesteuert wurde. Ferner weisen die hier beschriebenen Ergebnisse auf ein neuartiges Zusammenspiel von SH4-Domänen, Src Aktivität, ROCK Signalwirkung und FHOD1 vermittelte Zytoskelett Umgestaltung hin. Da PM "blebbing" mit erhöhter zellulärer Aufnahme flüssiger Bestandteile und erhöhter Zellwanderung in 3D Umgebungen korrelierte, könnte SH4-Domänen vermittelte PM Dynamik einen Mechanismus darstellen, der die Invasivität von Zellen beeinflusst, die durch SH4-Domänen-haltige Onkoproteine transformiert wurden.

5 INTRODUCTION

Dynamic processes are found at each level of organization and determine the life cycle of all organisms. In vertebrates, the blood circulates in vessels, a process driven by the muscular activity of the heart. During infections, the immune system specifically reacts to germs affecting the organism. Therefore, specialized immune cells actively migrate through tissues, an ability that is also ascribed to metastasizing tumor cells. For delivery of cellular determinants, vesicles are actively carried through the whole cell. Most of the secretory proteins, for instance, are transported and processed by the Golgi apparatus. Compositions of cellular structures like plasma membranes are constantly reconstructed and altered similarly to the shape of the whole cell. Cells form several kinds of protrusions like filopodia, lamellipodia, membrane ruffles or plasma membrane blebs on their surface that are needed for active locomotion and are specifically formed even in the process of dying. Required for all these actions is the dynamic cytoskeleton consisting of three different types of protein-polymers: The F-actin filaments that made of G-actin monomers representing the microfilament system, the intermediate filaments consisting of heterologous monomers, and the microtubules composed of tubulin monomers forming a tubular structure. Polymerization of the cytoskeletal components itself is very organized and depends on active signaling events of regulatory proteins like Rho-GTPases or Src kinases as well as on proteins that directly facilitate the assembly process. Nucleation of F-actin filament polymerization in particular is catalyzed by molecular machineries such as the Arp2/3 complex, the spire proteins as well as by diaphanous related formins (Drfs).

This work deals with the influence of Src kinases and of the Drf FHOD1 on several dynamic cellular processes. A particular focus is put on cellular motility and PM blebbing, two processes that have been shown to correlate in certain situations.

5.1 The Microfilament System

The cytoskeleton of eukaryotic cells is the basis for various dynamic cellular processes. It is also involved in cellular adhesion, migration, polarity, development and cytokinesis and mediates stability of the cell as well as intracellular transportation. The three main components of the cytoskeleton have in common that they consist of monomers with the capacity for non-covalent polymerization and formation of filaments. The biggest filamentous structures found within a cell are the microtubules. These polarized filaments of about 25 nm in diameter and consist of polymerized heterodimers of α-tubulin and β-tubulin. Usually, they originate from the

microtubule organizing center (MTOC) which is associated with the nucleus and is divided during cytokinesis, thus playing a pivotal role in chromatin separation. By binding of motor proteins, microtubules are important structures for delivery of cellular determinants. They are therefore directly involved in organization of intracellular traffic that is related *e.g.* to the Golgi apparatus (Brinkley, 1997, Pellegrini and Budman, 2005, Wade *et al.*, 1998). The next smaller polymers are the very stable intermediate filaments with a size of approximately 10-12 nm in diameter. Intermediate filaments are built up of homo- or heterodimers that are successively organized to proto-filaments and non polarized filaments. They have been suggested to play a tissue specific role in which their principal function is a structural one: By providing mechanical support they are thought to play a pivotal role in reinforcement of the cell and organization of cells into tissues (Kim and Coulombe, 2007). Keratins for example are typically expressed in epithelial cells and therefore give rise to hairs or nails. Vimentin on the other hand can be found in leukocytes, fibroblasts and other cells types where it supports cellular membranes and contributes to the localization of cellular organelles (Lodish *et al.*, 2000). The smallest polymerized compounds of the cytoskeleton are the microfilaments which consist of F-actin. These filaments with a diameter of 5-7 nm are homopolymers of single globular G-actin proteins. Their cellular role, structure, organization and dynamics are the topics of the following chapters.

5.1.1 The Actin Protein and Microfilaments

The actin cytoskeleton or microfilament system is the main component of most eukaryotic cells and contributes to many processes including polarization, protrusion, contraction, nuclear segregation, cytokinesis, gene transcription and vesicle trafficking (Evangelista *et al.*, 2003, Pederson and Aebi, 2005, Pollard and Borisy, 2003). Six isoforms of the globular actin monomer with a size of 42-45 kDa encoded by separate genes have been described in mammals and are divided into three classes: α-actins are mainly present in muscle cells (α-skeletal, α-aortic smooth, α-cardiac and γ2-enteric smooth), whereas β- and γ-actins are primarily found in non-muscle cells (β- and γ1-cytoplasmic) (Vandekerckhove and Weber, 1978). Despite small differences in sequence and properties between the isoforms, all actins polymerize non-covalently into microfilaments. Thereby, G-actin monomers that are bound to adenosine-triphosphate (ATP) assemble under physiological conditions to F-actin filaments (Laki *et al.*, 1950). Following irreversible hydrolysis of ATP to adenosine-diphosphate (ADP) in the middle section of a newly formed linear and unbranched microfilament, the resulting structure develops certain stability. Detected by electron microscopy, F-actin filaments show a clear polarity

following treatment with myosin heads that specifically decorate these filaments: They have a fast growing barbed or plus end and a slow growing pointed or minus end (fig. 1). This diversity in kinetics results from a higher affinity of ATP-bound G-actin to the barbed end leading *in vitro* to a less critical concentration for assembly at this site (K_d = 0.12 µM) compared to the pointed end (K_d = 0.6 µM, fig. 1) (Pollard and Borisy, 2003).

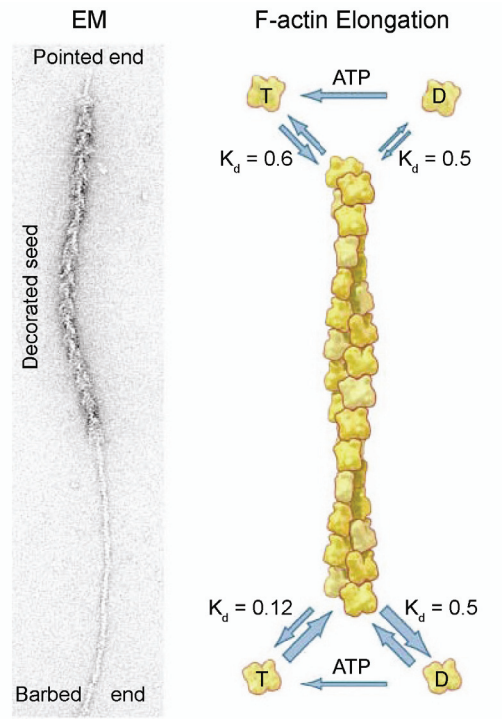

Figure 1: Elongation of F-actin filaments.

An electron micrograph (EM) of an F-actin seed that is decorated with myosin heads to indicate the barbed and the pointed end of the filament. The non decorated parts are newly added G-actin monomers indicating a slow assembly rate at the pointed end, but a fast polymerization at the barbed end. The dissociation equilibrium constants K_d [µM] for these elongation reactions are depicted in the schematic presentation of a microfilament on the right. Addition of ADP bound G-actin (= D) to any end as well as addition of ATP bound G-actin (= T) to the pointed end are energetically not favorable reactions. In contrast, its addition to the barbed end is energetically preferred (adapted from Pollard and Borisy, 2003).

In non-muscle cells the concentrations of ATP bound G-actin has been shown to exceed 100 µM (Pollard *et al.*, 2000). To prevent spontaneous polymerization, the concentration of free G-actin is highly adjusted by binding to regulatory proteins like thymosin-β4 or members of the profilin family. These G-actin binding proteins reduce the amount of free cytosolic ATP bound G-actin, thereby inhibiting uncontrolled self assembly to filaments (Pollard *et al.*, 2000). Furthermore, profilins are able to stimulate the nucleotide exchange of ADP to ATP which is available in excess, resulting in a regeneration of the ATP bound G-actin pool. The G-actin binding capacity of profilins is regulated by its binding to membrane bound phosphatidylinositol-4,5-bisphosphate (PIP_2) (Lassing and Lindberg, 1985). Additionally, profilins have a high affinity and directly bind to proline rich regions of several proteins that control F-actin nucleation such as the Wiskott-Aldrich-syndrome protein (WASp) (Lu and Pollard, 2001) or formins (see chapter 5.1.2.2) (Frazier and Field, 1997, Tojo *et al.*, 2003, Wasserman, 1998, Watanabe *et al.*, 1997). Besides G-actin binding proteins there are additional classes of regulated proteins that maintain, modify or organize existing microfilament structures (fig. 2): Capping proteins either bind to the barbed (capping protein, AIP1) or to the pointed end (tropomodulin) of F-actin

filaments, thereby blocking further filament growth or shrinkage of the polymer. Severing proteins like gelsolin, villin or ADF/cofilin induce destruction of existing F-actin filaments resulting in their depolymerization but also in formation of new F-actin filaments.

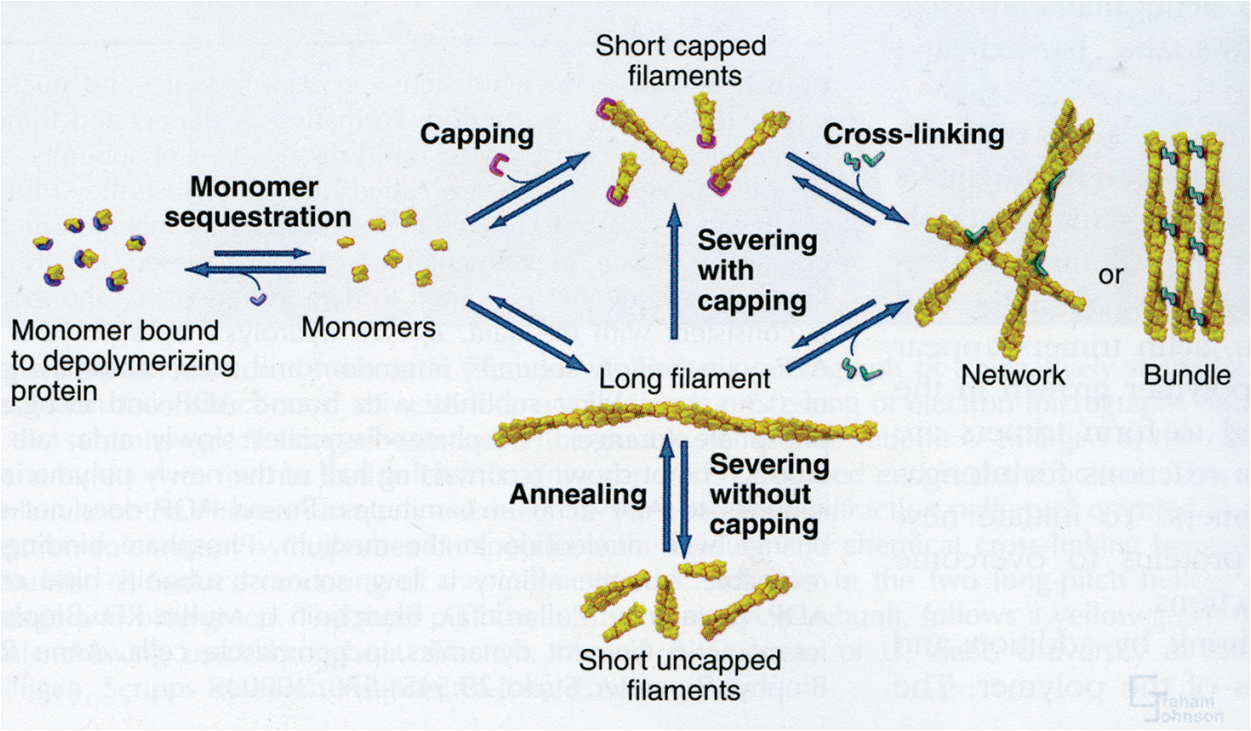

Figure 2: The cellular appearance of actin and the role of associated proteins.

In the cytosol, the appearance of actin is organized by highly regulated actin associated proteins: Spontaneous assembly to F-actin filaments is prevented by binding of the monomers to G-actin binding proteins. Nucleation and polymerization is controlled by nucleating compounds like formins, the Arp2/3 complex and spire, but is also initialized by severing proteins that are involved in destruction of existing microfilaments. F-actin filaments are protected for depolymerization by capping proteins and are linked to each other by crosslinking and bundling proteins (Pollard and Earnshaw, 2004).

Crosslinking proteins like α-actinin or filamins connect and organize single F-actin filaments. Similarly, motor proteins like myosins contribute to bundling of microfilaments to stress fibers as well as provide contractility (Ruegg *et al.*, 2002, Siripala and Welch, 2007, Siripala and Welch, 2007, Stossel *et al.*, 2001, Wang *et al.*, 2007, Weeds and Maciver, 1993). Finally, there are specific proteins and protein complexes that facilitate nucleation of F-actin polymerization. These proteins, their regulation and their specific mechanisms of polymerization will be described in the following chapters.

5.1.2 The Dynamics of the Microfilament System

The limiting step in actin polymerization is the nucleation of new filaments. Since spontaneous association of G-actin monomers is a very unlikely process, there are at least three types of nucleators that function with distinct mechanisms: The Arp2/3-complex, the spire protein and the

family of formins (fig. 3) (Mullins *et al.*, 1998, Pruyne *et al.*, 2002, Quinlan *et al.*, 2005, Welch and Mullins, 2002).

5.1.2.1 Nucleation of F-Actin Polymerization

The Arp2/3-complex is composed of seven strongly associated proteins: The two actin related proteins (Arp) Arp2 and Arp3 and the five unique proteins ARPC1, ARPC2, ARPC 3, ARPC4 and ARPC5 form a complex with a stoichiometry of 1:1 (Millard *et al.*, 2004). The Arp2/3-complex itself represents the nucleus that binds to the pointed end of a newly formed microfilament (fig. 3). Following this initial assembly step the filament growth proceeds at the barbed end independent of Arp2/3. However, to induce nucleation, Arp2/3 binds to an existing microfilament at an angle of 70° leading to a meshwork of short and branched filaments (Blanchoin *et al.*, 2000, Mullins *et al.*, 1998, Pollard *et al.*, 2000). The activity of the Arp2/3-compex is controlled by the family of WASp adaptor proteins with WASp, its brain isoform N-WASP, WAVE (WASp-verprolin homologous protein) and Scar (suppressor of cAMP receptor) (Machesky and Insall, 1998, Machesky *et al.*, 1999). The structural components that are needed for their activity are combined in the VCA-module that is located at the C-terminal end: The WH2 (WASp homology 2) or verprolin (V) domain is required for binding of G-actin monomers, the acidic (A) domain binds to the Arp2/3-complex and the central (C) domain induces conformational changes that are required for nucleation (Higgs and Pollard, 2001). The WASp/N-WASP proteins are activated by binding of GTP bound Cdc42 and PIP_2 that release an intramolecular autoinhibition (Millard *et al.*, 2004). In contrast, the WAVE/Scar proteins function in a complex that includes Sra1 and further proteins. By binding of the Rho-GTPase Rac1 to Sra1 the complex is activated and regulates the activity of the Arp2/3-complex (Kunda *et al.*, 2003). WAVE proteins are also activated by binding of IRSp53, another effector of Rac that plays a role in Arp2/3-complex activation (Miki *et al.*, 2000). Since the Arp2/3-complex is directly involved in F-actin polymerization at the leading edge of migrating cells, it plays a pivotal role in cell motility by formation of the branched microfilament network in lamellipodia (Higgs and Pollard, 2001, Pollard and Borisy, 2003).

The second class of F-actin nucleators is represented by the spire protein. Its functional unit consists of four G-actin binding WH2-domains, which are also present in the family of WASp related proteins as described above. Spire presumably nucleates unbranched F-actin filaments at the pointed end by recruitment and organization of G-actin monomers into a prenucleation complex that templates filament formation from the side (fig. 3) (Baum and Kunda, 2005, Kerkhoff, 2006).

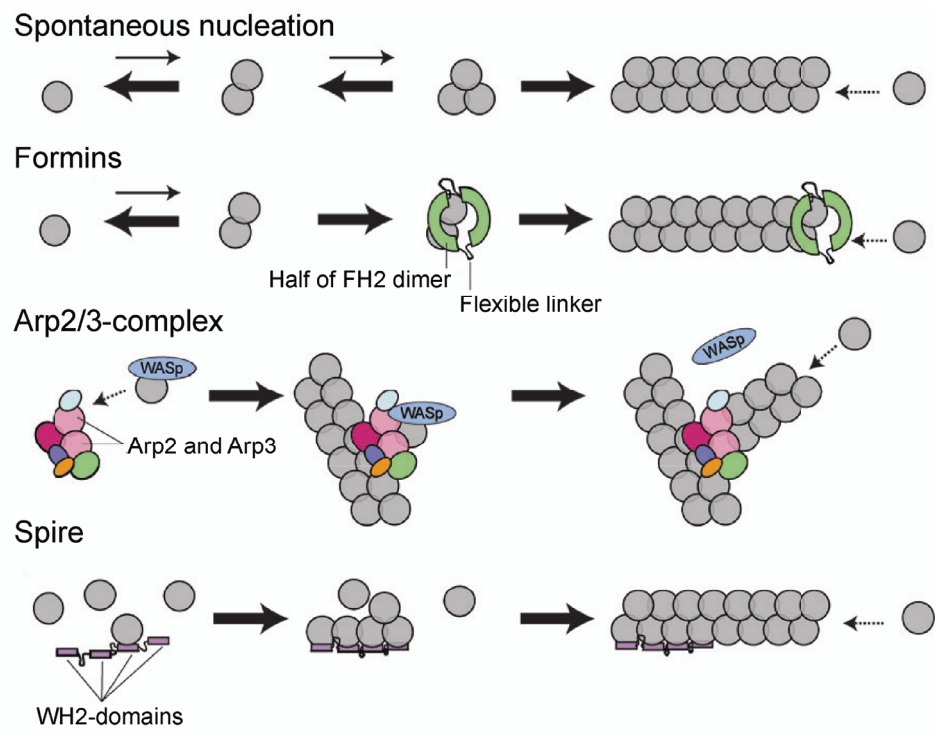

Figure 3: Nucleation of F-actin polymerization.

The limiting step in polymerization of F-actin filaments is the nucleation process. Therefore, at least three ATP bound G-actin monomers have to assemble in order to form the very unstable initiating seed or nucleus. *In vivo*, this **spontaneous nucleation** is extremely unlikely. In cellular systems, certain different mechanisms exist to mediate nucleation. **Formins** are "leaky cappers" that bind to the barbed end of growing F-actin filaments by their FH2-domains. They are thought to stabilize intermediates like short actin dimers. The **Arp2/3-complex** binds to an existing microfilament and also requires adaptor proteins like WASp that are also bound to G-actin monomers. Therefore, the Arp2/3-complex is associated to the pointed end of newly formed F-actin filaments that stick out of the mother filament at an angle of 70°. The elongation, however, proceeds at the barbed end without a contribution of the Arp2/3-complex, resulting in the formation of meshwork of short and branched microfilaments. Similarly, **spire** also binds to the pointed end of newly formed microfilaments by its array of WH2-domains, thus stabilizing the nucleus by a prenucleation complex (Goode and Eck, 2007).

The capacity of spire to nucleate F-actin polymerization has only been discovered recently (Quinlan *et al.*, 2005), even though the *spire*-gene has been identified in 1989 (Manseau and Schupbach, 1989). The cellular functions of spire are related to intracellular vesicle transport and Golgi organization as well as to organization of the cortical actin network (Kerkhoff, 2006, Kerkhoff *et al.*, 2001).

Similar to spire, formins form unbranched F-actin filaments. However, the mechanism is completely different and will be described in the following.

5.1.2.2 Formins

Formins are a large family of ubiquitous and highly conserved multidomain proteins generally consisting of over 1000 amino acid residues (Faix and Grosse, 2006, Higgs, 2005). The term "formin" originates from transgene insertion into the *limb deformity* gene resulting in limb

formation defects in mice (Mass *et al.*, 1990, Woychik *et al.*, 1990). However, it was shown recently that the adjacent *gremlin* gene rather than formins is required for limb bud patterning (Zuniga *et al.*, 2004). Formins are involved in a variety of actin-based processes in eukaryotic cells. Their common characteristic is the unique and highly conserved C-terminal formin homology 2 (FH2)-domain of about 400 amino acid residues that is preceded by an N-terminally proline-rich FH1-domain (fig. 8A) (Faix and Grosse, 2006). Typically, the FH2 core-domain and the intervening linker region between the FH1- and the FH2-domain are necessary and sufficient to nucleate F-actin polymerization from G-actin monomers *in vitro* (Kovar *et al.*, 2003, Pruyne *et al.*, 2002, Sagot *et al.*, 2002). During filament elongation, the formin remains at its barbed end resulting in long unbranched F-actin filaments. The central motif of the FH2-domain is a conserved stretch of amino acids with the consensus sequence G-N-X-M-N (where G is glutamine, N is asparagine, M is methionine and X is any amino acid) (Wasserman, 1998). The FH1-domain binds to SH3-domains (see chapter 5.3.1.2) and WW-domains (W for tryptophan) as well as in a low micromolar range to the G-actin binding protein profilin (see chapter 5.1.1), recruiting G-actin monomers in close proximity to the FH2-domain and to the barbed end of F-actin filaments (Bedford *et al.*, 1997, Chang *et al.*, 1997). Profilin has the capacity to increase the elongation rate of several FH1-FH2-domains *in vitro*, but it is not required for all formins (Kovar and Pollard, 2004, Romero *et al.*, 2004). The nucleation of new microfilaments is thought to be facilitated by stabilization of an F-actin dimer (fig. 3) (Pring *et al.*, 2003). During polymerization, formins remain at the barbed end of the newly generated F-actin filament and are directly involved in the elongation process (Higashida *et al.*, 2004, Kovar and Pollard, 2004, Pruyne *et al.*, 2002). In line with this, they can inhibit and replace capping proteins that stay at the barbed end. Therefore, formins are also termed as "leaky cappers" (Harris and Higgs, 2004, Kovar *et al.*, 2003, Zigmond *et al.*, 2003) and the mechanism they provide for nucleation and elongation is referred to as "processive capping" (Goode and Eck, 2007). According to this model, a dimer of the FH2-domain is required (Harris *et al.*, 2004, Harris *et al.*, 2006, Li and Higgs, 2005, Moseley *et al.*, 2004). Structural analysis of the FH2-domain of the yeast formin Bni1p also revealed a dimer that is flexibly linked by a lasso-domain and forms a doughnut-like structure (Otomo *et al.*, 2005, Xu *et al.*, 2004). Disruption of this lasso-domain inhibits dimerization and thus F-actin polymerization (Moseley *et al.*, 2004). During nucleation, this structure presumably forms a scaffold for assembly of the first actin subunits (fig. 3). During elongation, the two halves of an FH2-domain dimer localize at the barbed end and are proposed to alternately assume one of two states, which are referred to as the "bound" state and the "migrating" state (fig. 4).

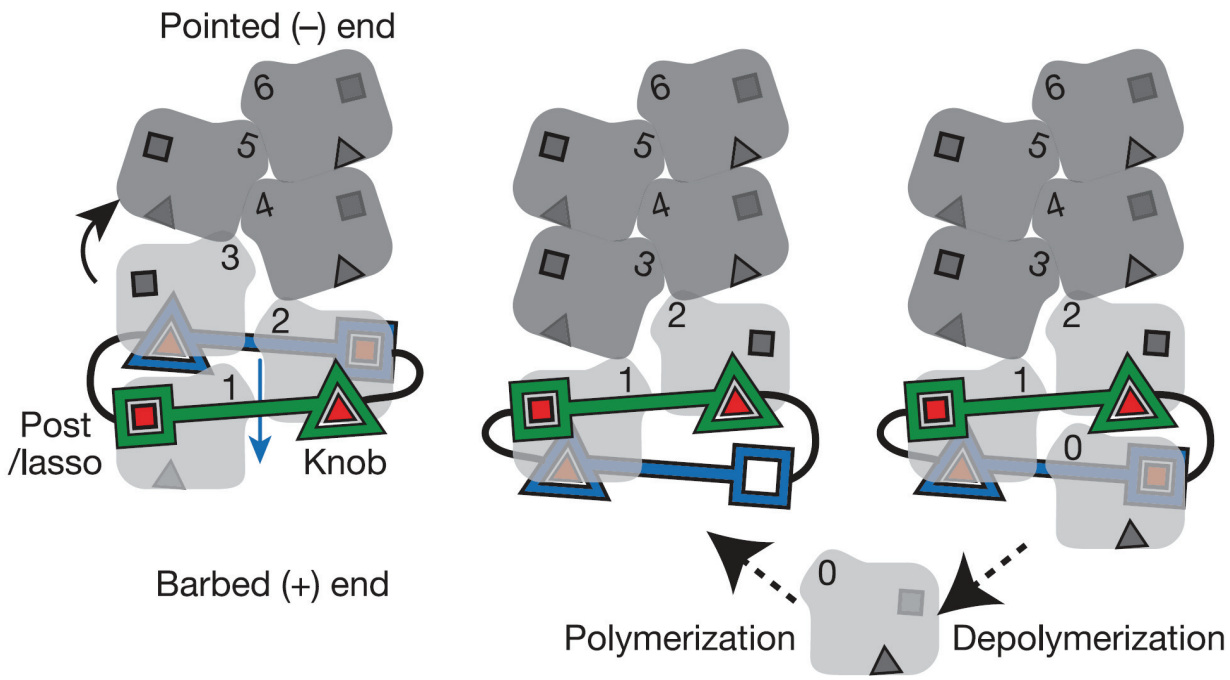

Figure 4: Model for elongation of microfilaments by processive capping of formins.

The FH2-domain (blue) which is tightly bound to the two terminal actin subunits (light grey 2 and 3) is linked by a lasso structure to the second FH2-domain (green) of the dimer **(left panel)**. Addition of a new actin subunit (1) to the barbed end leads to conformational changes in the FH2-domain dimer resulting in a release of actin binding of the first FH2-domain (blue) that becomes the "migrating" unit, and a strengthening of the second one (green). The migrating unit is now capable of binding new G-actin monomers (0) resulting in polymerization **(middle panel)**. In this state, the actin subunit can also be released leading to depolymerization **(right panel)**. This process is also known as stair-stepping mode of elongation (Otomo *et al.*, 2005).

The bound FH2-domain tightly interacts with the two terminal actin subunits at the barbed end, whereas the migrating unit interacts only weakly and therefore facilitates addition of new G-actin monomers. This migrating FH2-domain is also supposed to be in a dynamic equilibrium between an open or accessible and a closed or blocked conformation, in which actin subunits can also dissociate under certain conditions. Addition of a new subunit to the filament in the open conformation of the migrating FH2-domain causes a conformational switch in the FH2-domain dimer, consequently their roles reverse. This model allows that one subunit of the FH2-dimer is always bound to the microfilament and proposes a stair-stepping mode of elongation (Goode and Eck, 2007). However, this mechanism implies that the formin circles around the filament, which has been shown to be not the case (Kovar and Pollard, 2004). Until now, this rotation paradox is not understood.

According to a phylogenetic analysis of the FH2-domain, seven subgroups of formins in metazoans have been classified: Dia (diaphanous), DAAM (dishevelled-associated activator of morphogenesis), FRL (formin-related gene in lymphocytes), FHOD (formin homology 2 domain

containing protein), INF (inverted formin), FMN (formin) and delphilin (Higgs and Peterson, 2004).

5.1.2.3 Regulation of the Cytoskeleton by Rho-GTPases

Rho-GTPases are major regulators of cytoskeletal organization and comprise a family of eukaryotic highly conserved regulatory proteins that are members of the superfamily of Ras related Rho-GTPases. In mammals, 22 Rho-GTPases have been identified, whereupon the most prominent and investigated members are Rho (Ras homolog protein), Rac (Ras-related C3 *clostridium botulinum* toxin substrate) and Cdc42 (cell division cycle 42 homolog protein). Three isoforms of Rho have been described (RhoA, RhoB and RhoC) and four isoforms of Rac (Rac1, Rac2, Rac3 and RhoG) (Aspenstrom *et al.*, 2004, Jaffe and Hall, 2005). Most of the Rho-GTPases are modified by prenylation and carboxymethylation of a conserved cysteine at the C-terminal end. Rho, Rac and Cdc42 are prenylated by a geranylgeranylgroup that contributes to their localization at membrane structures (Adamson *et al.*, 1992, Marshall, 1993). Furthermore, Rho and Rac have been shown to be targeted to lipid-rafts in the plasma membrane through interaction with integrins (del Pozo *et al.*, 2004, Palazzo *et al.*, 2004).

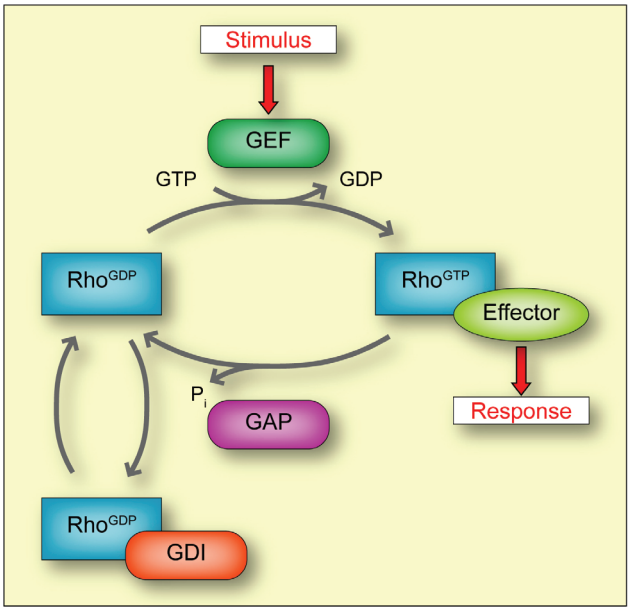

Figure 5: The GTPase cycle.

Rho-GTPases cycle between an inactive GDP-bound form and an active GTP-bound form. This activity is regulated by associated proteins that stimulate GDP to GTP exchange (GEF = guanine nucleotide exchange factor) and activate the Rho-GTPase, stimulate hydrolysis of bound GTP to GDP (GAP = GTPase activating protein) and inactivate the Rho-GTPase or block spontaneous activation (GDI = guanine nucleotide dissociation inhibitor). Active Rho-GTPases interact with effector proteins to mediate a response (adapted from Jaffe and Hall, 2005).

The activity of Rho-GTPases is determined by their binding to guanine-nucleotides. Thus they act as molecular switches cycling between an active form that is bound to guanosine-triphosphate (GTP) and an inactive state in which the protein is bound to guanosine-diphosphate (GDP). This activity is controlled by three types of associated proteins (fig. 5): GTPase activating proteins (GAPs) stimulate the intrinsic GTPase activity to facilitate the hydrolysis of GTP to GDP and lead to its deactivation. Guanine nucleotide dissociation inhibitors (GDIs)

block spontaneous activation of the GTPase, whereas guanine nucleotide exchange factors (GEFs) catalyze the exchange of GDP to GTP, thus leading to an activation of the GTPase (Jaffe and Hall, 2005). Mutation of certain amino acid residues alters the intrinsic GAP stimulated activation of Rho-GTPases and leads to their deregulation. As discovered first for Ras, Rho-GTPases often carry a proto-oncogenic capacity (Campbell and Der, 2004). According to Rac numbering, constitutively active forms of Rho-GTPases are usually mutated at amino acid residue 12, where glycine is substituted with valine (G12V), or at residue 61, where glutamine is substituted with leucine (Q61L), whereas dominant negative forms are mutated at residue 17, by substitution of threonine with asparagine (T17N) (Bishop and Hall, 2000). Rho-GTPases have been suggested to facilitate most of their interaction to effector proteins by their effector regions switch I and switch II which facilitate GDP and GTP binding (Bishop and Hall, 2000). Through activation of a large array of effector proteins, Rho-GTPases indirectly regulate the organization of the cytoskeleton and therefore play a role in various cellular processes. Addition of the pro-inflammatory peptide Bradykinin stimulates the activation of Cdc42 and therefore the formation of microspikes and filopodia (fig. 6) (Allen *et al.*, 1997, Hall, 1998). These cellular protrusions are thought to be involved in exploration of the environment and therefore play an important role during cell motility and neurite outgrowth (Kater and Rehder, 1995, Ridley, 2006). Cdc42 activates diaphanous related formins and the Arp2/3-complex through WASp/N-WASP (see chapter 5.1.2.1 and 5.1.3), and is mainly localized at the Golgi apparatus indicating a role in vesicle transport (Qualmann and Mellor, 2003).

Treatment of cells with the platelet derived growth factor (PDGF) activates Rac and leads to the formation of lamellipodia and membrane ruffles by WAVE/Scar mediated activation of the Arp2/3-complex (fig. 6; see chapter 5.1.2.1) (Allen *et al.*, 1997, Norbury, 2006, Ridley, 2006). Furthermore, through p21 activated kinase (PAK) signaling, Rac induces the activation of myosin II and of LIM-kinases (LIMK) that regulate the activity of the F-actin severing protein ADF/cofilin. Rac also interacts with diaphanous related formins like FHOD1 and FRL, indicating that formins could play a role in formation of lamellipodia and cell migration (Gasteier *et al.*, 2003, Westendorf, 2001, Yayoshi-Yamamoto *et al.*, 2000).

Addition of growth factors like lysophosphatic acid (LPA) to animal cell cultures results in an activation of Rho and therefore in the formation of stress fibers, which are contractile bundles of F-actin filaments that are linked by myosins and other proteins (fig. 6) (Allen *et al.*, 1997, Hall, 1998). This stress fiber formation depends on the activity of the Rho effector proteins mDia for F-actin nucleation (see chapter 5.1.3) and ROCK for induction of filament bundling.

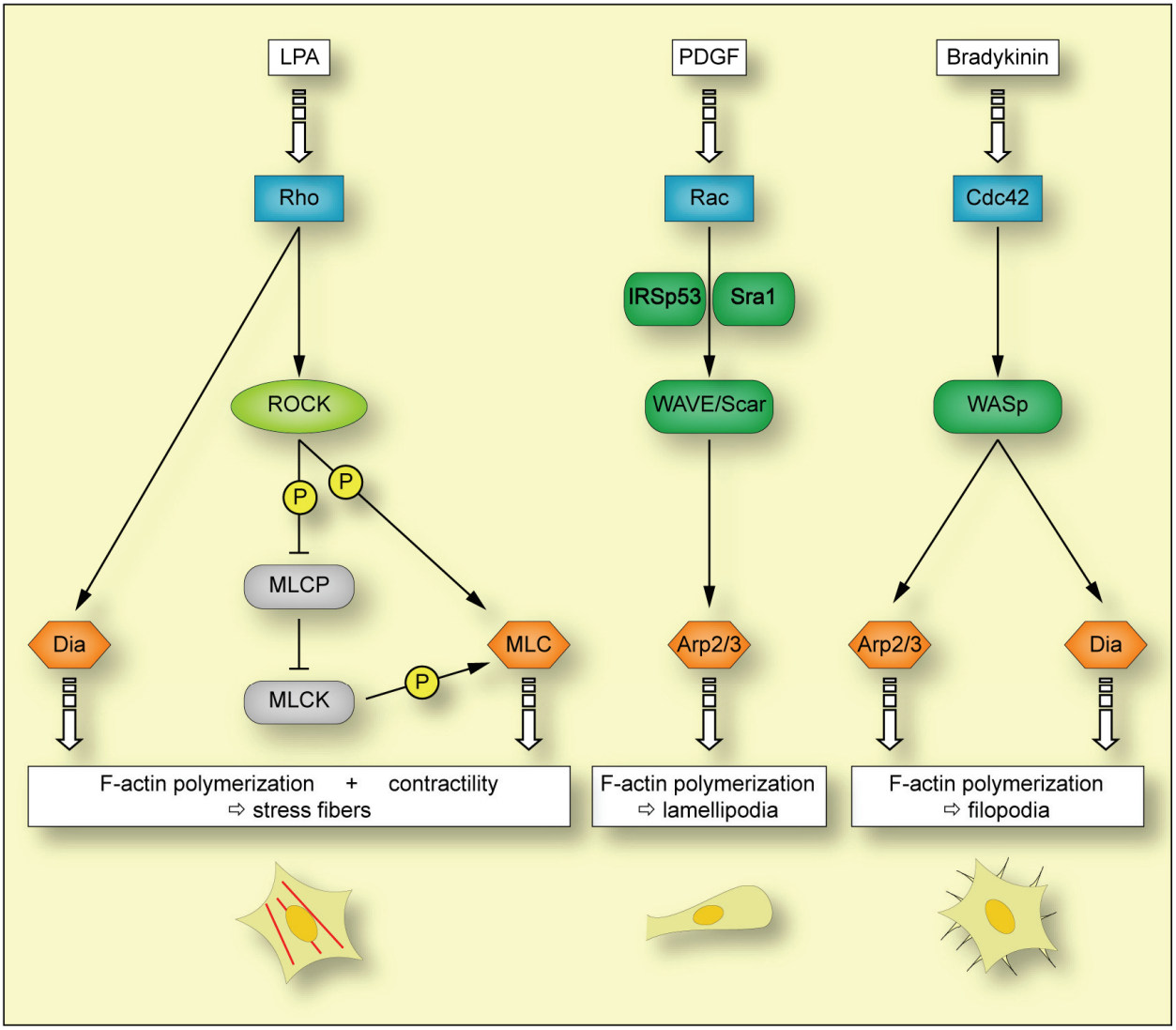

Figure 6: Signaling of Rho-GTPases.

Depicted are the Rho-GTPase signaling cascades that are involved in formation of cell protrusions: LPA = lysophosphatic acid, PDGF = platelet derived growth factor; blue rectangles = Rho-GTPases; light green ellipses = central serine/threosine kinases; dark green boxes = adaptor proteins; red diamonds = effector proteins; grey boxes = MLC phosphatase and MLC kinase; P = phosphorylation; black arrows = activation; black blocked lines = deactivation.

5.1.2.4 The family of ROCK proteins

The Rho associated coiled-coil containing protein kinases ROCK1 and ROCK2 form a family of serine/threonine kinases. They are Rho effector proteins required for induction of F-actin bundling and contractility at the rear of a motile cell (Bishop and Hall, 2000). The two isoforms show 65 % identity in their overall amino acid sequence and 92 % in their kinase domains at the N-terminal end (Riento and Ridley, 2003) (fig. 7). Inside their coiled-coil region between the kinase region and the C-terminal Pleckstrin Homology (PH) domain with its cysteine-rich region lays the Rho binding domain (RBD) that plays a role in ROCK activation. ROCK kinase activity is intramolecularly autoinhibited by independent binding of the RBD and the PH-domain to the

kinase domain (fig. 7) (Chen *et al.*, 2002). Therefore, ROCK proteins are thought to be activated by direct binding to active Rho-GTP and to lipids like arachidonic acid to the PH-domain (Dvorsky *et al.*, 2004, Riento and Ridley, 2003). In line with this, ROCK1 is constitutively activated by caspase-3 mediated and ROCK2 by granzyme B mediated cleavage of its carboxyl-terminus. This naturally occurs in apoptotic cells and causes extensive PM blebbing (Coleman *et al.*, 2001, Sebbagh *et al.*, 2005).

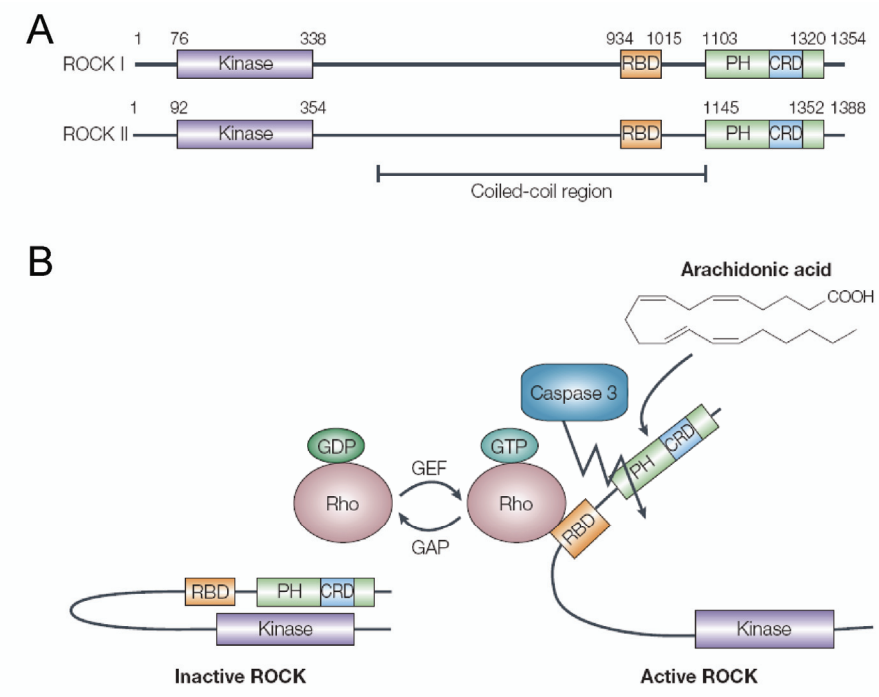

Figure 7: Organization and regulation of ROCK Rho kinases.

(A) Schematic presentation of ROCK proteins. The two isoforms ROCK1 and ROCK2 show 65 % overall amino acid sequence identity and 92 % in their kinase domains at the N-terminal end. The Rho binding domain (RBD) is situated within a predicted coiled-coil region that is followed by a Pleckstrin homology (PH) domain with a cysteine rich region (CRD) at the carboxyl terminus. **(B)** Regulation of ROCK kinases. The kinase domain of ROCK independently binds to its PH domain and RBD resulting in an intracellular autoinhibition. The kinase domain is released by binding of active Rho-GTP to the RBD, lipids like arachidonic acid to the PH domain or apoptotic cleavage by caspase-3 (ROCK1: residue 1113, DETD) or granzyme B (ROCK2: residue 1131, IGLD; not shown) (Riento and Ridley, 2003).

To understand how ROCK proteins mediate their activities to the microfilament system one has to have a closer look at their kinase activity and effector proteins. ROCK proteins are serine/threonine kinases with two consensus sequences for phosphorylation that are R/K-X-S/T and R/K-X-X-S/T (where R is arginine, K is lysine, S is serine, T is threonine and X is any amino acid). They can be auto-phosphorylated which is thought to contribute to their activation state as well, but their main target is the myosin II motor protein in non-muscle cells. The myosin II regulatory part myosin light chain (MLC) is phosphorylated directly by ROCK proteins at Ser19 and thereby activated (fig. 6). The phosphorylation state is furthermore

regulated by MLC kinase (MLCK) that stands in balance with MLC phosphatase (MLCP) leading to dephosphorylation and inactivation of MLC. ROCK proteins phosphorylate MLCP and thereby induce its release from MLC resulting in an indirect activation of MLC (Bishop and Hall, 2000, Matsumura, 2005). Active myosin II decorates F-actin fibers, aligns them to bundles and stress fibers and facilitates contraction in an ATP consuming process. Similar to the sacromeric structure of muscle cells, but not as organized, myosin II mediates the antagonistic gliding of F-actin filaments (Geeves and Holmes, 1999, Ruegg *et al.*, 2002).

5.1.3 Diaphanous Related Formins

A subfamily of formins, the diaphanous related formins (Drfs) interact with Rho-GTPases and are therefore thought to represent effectors of these regulatory proteins (see chapter 5.1.2.3). Drfs share a typical domain structure that mediates an intramolecular autoinhibition which initially had been identified in the *Drosophila* formin diaphanous (Wasserman, 1998). The autoinhibition is mediated by the C-terminal diaphanous autoregulatory domain (DAD) and the N-terminal regulatory domain (fig. 8A) (Wasserman, 1998, Watanabe *et al.*, 1997).

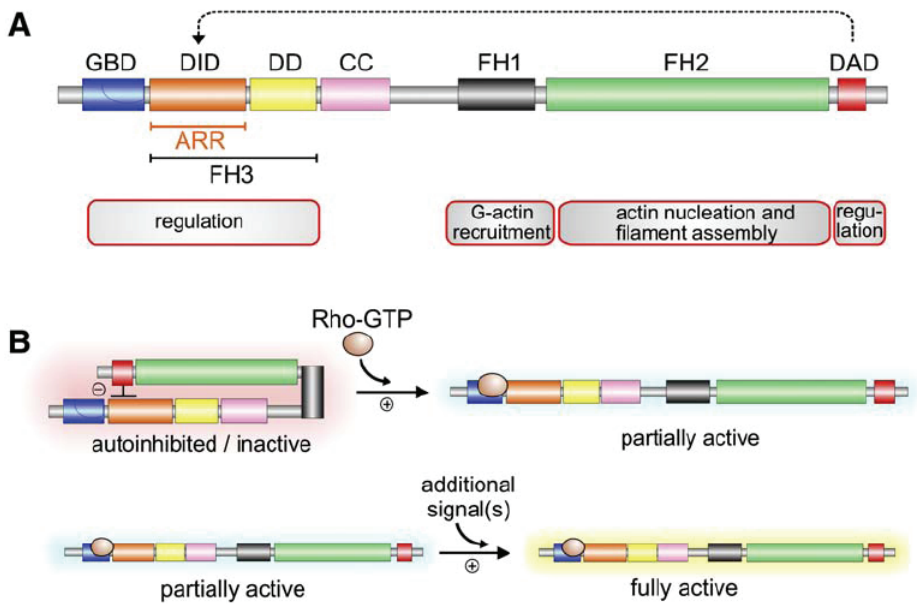

Figure 8: Diaphanous related formins and their activation.

(A) Formins consist of a proline rich FH1-domain that is capable to associate the G-actin binding protein profilin. The FH2-domain is located in an adjacent position facilitating the nucleation process. The FH3-domain is only poorly defined and in some formins it is involved in their cellular localization. Drfs are autoinhibited by an intramolecular binding of the C-terminal diaphanous autoregulatory domain (DAD) to the N-terminal regulatory domain consisting of a Rho-GTPase binding domain (GBD), a diaphanous inhibitory domain (DID) with an armadillo repeat region (ARR), a dimerization domain (DD) and a coiled-coil region (CC). **(B)** By binding of a GTP bound Rho-GTPase to the GBD the autoinhibition is partially released. Additional signals are required for full activation (Faix and Grosse, 2006).

The DAD represents a relatively small stretch of amino acids and is characterized by a highly conserved regulatory motif with the consensus sequence M-D-X-L-L (where D is aspartic acid, L is leucine, M is methionine and X is any amino acid) and a conserved regulatory region of basic amino acid residues (Alberts, 2001, Schonichen *et al.*, 2006). In contrast, the N-terminal regulatory domain is much bigger in size and includes a GTPase binding domain (GBD), a diaphanous inhibitory domain (DID) with an armadillo repeat region (ARR) and a dimerization domain (DD) (Alberts, 2001, Li and Higgs, 2005, Rose *et al.*, 2005). The DID and DD together loosely define the less characterized FH3-domain that contributes to the subcellular localization of some formins (Brandt *et al.*, 2007, Kato *et al.*, 2001, Kitayama and Uyeda, 2003). In its dormant state, the Drfs DAD is bound to the N-terminal regulatory domain and remains in a closed conformation (fig. 8B).

Upon binding of a Rho-GTPase to the GBD the autoinhibition is released (Alberts, 2001, Li and Higgs, 2003, Watanabe *et al.*, 1999). In mDia1, the Rho-GTPase interacts *via* its switch I and switch II effector regions with the GBD and the DID (Otomo *et al.*, 2005, Rose *et al.*, 2005). However, the DAD binding to the N-terminal region is not fully released, additional conformational changes of the DID are thought to be required (Lammers *et al.*, 2005). Therefore further factors are suggested to be required to fully activate Drfs (Li and Higgs, 2005).

5.1.3.1 Cellular Functions of Formins

Formins are involved in a variety of cellular processes that are related to the cytoskeleton. During cytokinesis, formins contribute to the formation of the contractile ring in mammalian and yeast cells (Castrillon and Wasserman, 1994, Evangelista *et al.*, 2002, Noguchi and Mabuchi, 2001). In line with this, formins like Bni1p play a pivotal role in polarization of yeast cells during cytokinesis and budding (Evangelista *et al.*, 1997). The Drf DAAM1 is involved in formation of the planar cell polarity in *Xenopus laevis*, a highly regulated process of morphogenesis and cell coordination during gastrulation (Habas *et al.*, 2001).

Additionally, endocytosis also depends on cytoskeletal interactions. A splice variant of hDia2 has been identified to regulate the motility of early endosomes along microfilaments in a Src dependent manner (see chapter 5.3.1.1) (Gasman *et al.*, 2003). Furthermore, other Drfs like mDia1 and mDia2 localize to endosomes as well (Tominaga *et al.*, 2000).

A possible role for Drfs in the formation of cellular protrusions like filopodia has also been proposed. Therefore, a combined activity of the vasodilator stimulated phosphoprotein (VASP) and the Drf mDia2 at the filopodia tip complex is suggested (Faix and Rottner, 2006). In line with this, dynamic rearrangement of the microfilament system is essential for cellular shape as

well as for cell-substrate and cell-cell adhesion. It has been shown for mDia1 that its expression is sufficient to induce focal adhesions in fibroblasts (Riveline *et al.*, 2001). This Drf as well as formin-1 also mediate the accumulation of integral adhesion proteins, suggesting a capacity for reshaping the PM (Kobielak *et al.*, 2004, Sahai and Marshall, 2002).

Furthermore, *de novo* synthesis of new microfilaments is required during cell motility as well. Various formins are thought to be involved in this process. The Drf mDia1 for instance is necessary for migration of fibroblasts in wound healing assays (Goulimari *et al.*, 2005), and the Drf FHOD1 has been shown to contribute to chemotaxis of fibroblasts (Koka *et al.*, 2003).

The ability of formins to reorganize the actin cytoskeleton also has transcriptional consequences on various cytoskeletal target genes. Many of them are upregulated by binding of the actin binding coactivator megakaryocytic acute leukemia (MAL) to the serum response factor (SRF) that recognizes a promoter region termed as serum response element (SRE) (Faix and Grosse, 2006). The SRF appears to be essential for cell adhesion, spreading and stress fiber formation. Drfs like mDia1, mDia2, FHOD1 and diaphanous have been shown to induce SRE activity (Boehm *et al.*, 2005, Gasteier *et al.*, 2003, Miralles *et al.*, 2003, Tominaga *et al.*, 2000, Westendorf, 2001).

Interestingly, not only the microfilament system is organized by formins. They assist in orientation and formation of stable microtubules presumably by binding to their tip (Gasteier *et al.*, 2005, Goulimari *et al.*, 2005, Palazzo *et al.*, 2001). Nevertheless, this function is actin-dependent as well (Wen *et al.*, 2004). Therefore, formins are thought to mediate the crosslink between microtubules and microfilaments (Gundersen *et al.*, 2004).

Many formins have been identified since the discovery of the *limp deformity* gene and most of their individual functions are supposed to be specific instead of redundant. It is thought that this individuality is directly linked to various factors such as cell-cycle steps, their expression pattern in tissues, their interaction partners and regulation mechanisms, their cellular localization as well as their specific mechanism for F-actin nucleation.

5.1.3.2 FHOD1

The mammalian FHOD1 (formin homology 2 domain containing 1) protein is a member of the Drf family. It has been identified in a Yeast-two-hybrid screen as an interaction partner of the transcription factor AML-1B (acute myelogenous leukemia protein-1B) and has initially been termed as FHOS (Formin Homologue Overexpressed in Spleen) (Koka *et al.*, 2003, Westendorf *et al.*, 1999, Westendorf *et al.*, 1998). The open reading frame with a size of 3945 basepairs is located on the human chromosome 16q22 resulting in a protein consisting of 1164 amino acid

residues (Westendorf *et al.*, 1999). The gene of its homolog FHOD2 is located on chromosome 18q12 and encodes 1422 amino acids (Kanaya *et al.*, 2005). FHOD1 is ubiquitously expressed, but is found in greatest abundance in spleen (Westendorf *et al.*, 1999). Its structural organization is similar to that of other formins, but also shows specific characteristics: The proline rich FH1-domain is located in the middle of the protein adjacent to the FH2-domain that follows in C-terminal direction and has the capability for oligomerization (fig. 9) (Madrid *et al.*, 2005).

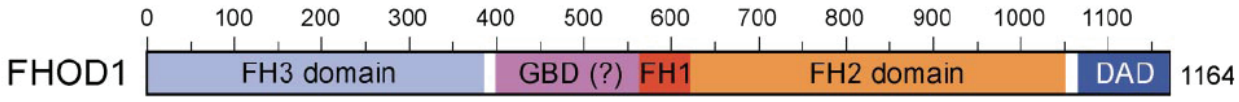

Figure 9: Schematic presentation of the Drf FHOD1.

Like other Drfs FHOD1 consists of a central FH1-domain adjacent to the FH2-domain. At the C-terminal end the diaphanous autoregulatory domain (DAD) that binds to the N-terminally located regulatory domain is located here depicted as FH3-domain. The poorly defined GTPase binding domain (GBD) binds the Rho-GTPase Rac1 (GDP and GTP bound) and is situated in between the FH1- and FH3-domain (Schonichen *et al.*, 2006).

The DAD is situated at the C-terminal end. In contrast to other Drfs, FHOD1 possesses two leucine rich consensus sequences (Schonichen *et al.*, 2006, Wallar and Alberts, 2003). At least the more C-terminally located one in combination with a basic stretch of amino acids contributes to the intramolecular autoinhibition by binding to the DID or FH3-domain that is located at the N-terminal end (Schonichen *et al.*, 2006). In contrast to other formins like mDia1 or Bni1, the poorly defined GBD was suggested to be located between the FH3- and the FH2-domain and shows no sequence homology to that of other Drfs (Westendorf, 2001). The Rho-GTPase Rac1 has been identified to bind to this GBD, however, in its GDP- as well as in its GTP-bound form (Gasteier *et al.*, 2003, Westendorf, 2001). Nevertheless, co-expression of constitutively active Rac1 with FHOD1 recruits the Drf to membrane ruffles, whereas over-expressed FHOD1 alone shows an unspecific cytoplasmic distribution (Gasteier *et al.*, 2003). Interestingly, expression of a C-terminally truncated FHOD1 mutant lacking its DAD results in formation of F-actin stress fibers (Gasteier *et al.*, 2003, Koka *et al.*, 2003, Takeya and Sumimoto, 2003). These fibers are bundled to thick cables and depend on the activity of the Rho-ROCK pathway. FHOD1 also decorates F-actin fibers generated by co-expression of constitutively active ROCK1 (Gasteier *et al.*, 2003). By induction of these stress fibers, FHOD1 organizes microtubules along these cables and thereby mediates cell elongation (Gasteier *et al.*, 2005). Motility is stimulated in cells stably expressing FHOD1 *via* acto-myosin contractility but is independent of integrin mediated cell adhesion (Koka *et al.*, 2003). Furthermore, the constitutively active FHOD1 mutant also induces SRE activity (Gasteier *et al.*, 2003, Westendorf, 2001). It has been shown that this activation depends on the activity of the ERK/MAP-kinase pathway (extracellular signal regulated

kinase/mitogen activated protein kinase) and that FHOD1 has the capacity to bind to ERK and Raf1, a further component of this pathway (Boehm *et al.*, 2005). Interestingly, the capacity of FHOD1 for SRE induction also requires the activity of Src kinases (see chapter 5.3), whereas depletion of Src activity has no influence on FHOD1 mediated stress fiber formation (Koka *et al.*, 2005). Additionally, Src kinases also interfere with FHOD1 gene expression (Koka *et al.*, 2005). FHOD1 interacts with F-actin and the FH1-domain of FHOD1 binds to profilin IIa, suggesting profilin to be the recruiting protein for G-actin (Takeya and Sumimoto, 2003, Tojo *et al.*, 2003). FHOD1 is phosphorylated at amino acid residue Ser1131 in vascular smooth muscle cells by cyclic GMP dependent protein kinase 1 (PGK1) which directly interacts with FHOD1 in the absence of cyclic guanosine monophosphate (cGMP) (Wang *et al.*, 2004). Furthermore, the C-terminus of FHOD1 co-localizes and binds to the cytoplasmic domain of the multifunctional receptor CD21 that interact with Epstein-Barr virus (EBV) particles (Gill *et al.*, 2004). Finally, FHOD2 had been suggested to represent a link between the microfilament system and the nestin intermediate filaments (Kanaya *et al.*, 2005).

5.1.4 The Regulation of the Microfilament System During Cell Motility

Directional motility is a fundamental cellular process essential for embryonic development, wound healing, immune response, development of tissues and metastization of tumors cells. The basic mechanism is directly connected to the cytoskeleton and requires a constant and dynamic reorganization of cytoskeletal components as well as stimulation by extracellular signals.

5.1.4.1 Cell Migration on Planar Surfaces

Crawling cell motility on planar surfaces involves a cycle of four steps: protrusion of the leading edge, adhesion to the substratum, retraction of the rear and de-adhesion (Pollard and Borisy, 2003). This process is highly regulated by Rho-GTPases and is mediated by the microfilament system. Therefore, Rac and Cdc42 are required at the front of a polarized cell: By regulation of formins and of Arp2/3-complex activity through WASp/N-WASP, Cdc42 induces the formation of filopodia which are thought to be involved in exploration of the cellular environment (see chapter 5.1.2.3) (Faix and Rottner, 2006). Activity of Rac mediates the protrusive force and controls the formation of lamellipodia which expand forward as the cell moves and forms the leading edge. This cortical actin structure reveals a characteristic dense meshwork of short, but branched microfilaments mainly formed by the activity of the Arp2/3-complex which is regulated by Rac through WAVE/Scar signaling (see chapter 5.1.2.1). Both Rac and Cdc42 are furthermore supposed to control formation and release of integrin-dependent matrix adhesion of

the cell to the surface (Raftopoulou and Hall, 2004). Activity of Rho at the rear of the cell is needed for retraction of the cell body. It induces formation of long F-actin filaments bundled to stress fibers, tethered to focal adhesions and reaching through the cytoplasm. The microfilaments are polymerized with the help of formins, whereas regulation of myosin activity through its effector kinase ROCK resulted in filament bundling and contractility (Pollard and Borisy, 2003, Raftopoulou and Hall, 2004).

5.1.4.2 Cell Migration in 3D-Environments – Cancer Cell Invasion

Compared to planar surfaces, three dimensional environments are characterized by completely different conditions: The extracellular matrix (ECM) for instance is a three dimensional network of polysaccharides, fibrous and adhesive proteins, secreted by animal cells and providing structural support in tissues. In order to cross this network, single tumor cells use at least two distinct strategies to invade this environment. The mesenchymal or elongated mode of motility is similar to migration on planar surfaces (fig. 10A):

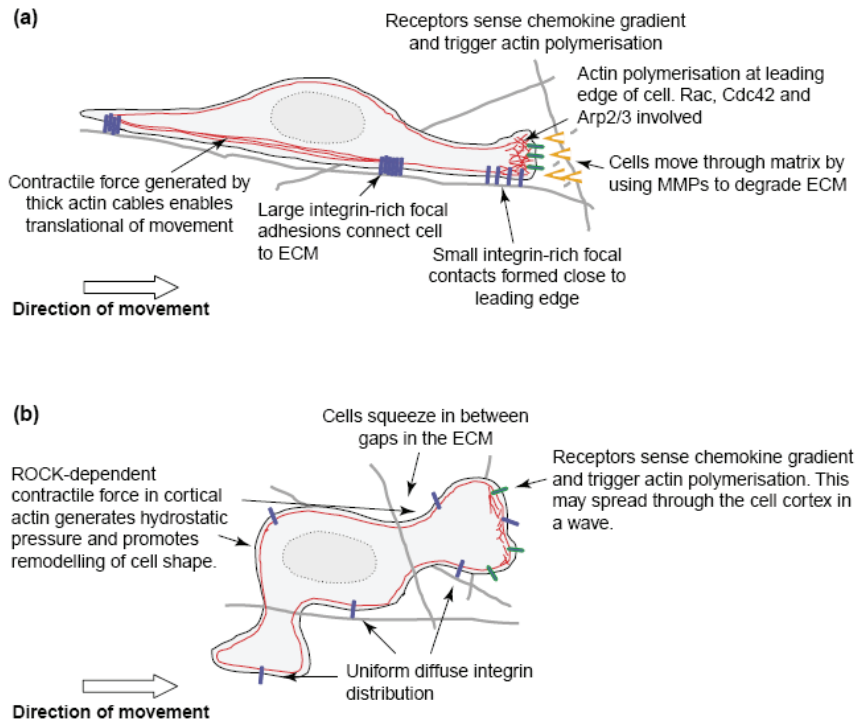

Figure 10: Different modes of cancer cell invasion.

Invasion of single metastasizing tumor cells in 3D-environments like tissues can be performed by two distinct mechanisms: **(A)** The mesenchymal or elongated mode of motility is characterized by an elongated morphology and is dependent on activities of metalloproteases (MMPs). **(B)** The amoeboid or rounded mode of motility is characterized by an amorphous cell shape or PM blebbing (Sahai, 2005).

Activated by external signals like chemokines and regulated by the already described signaling pathways, the cells form protrusions in the direction of the stimulus. These protrusions, referred to as invadopodia or pseudopodia, are related to lamellipodia and display an enrichment of cell substrate connections. Src kinases have been shown to play an important role in their formation (Linder and Aepfelbacher, 2003). For invasion, however, these cells locally destroy the ECM by secretion of proteases such as metalloproteases that are enriched in podosomes (Sahai, 2005, Yamazaki *et al.*, 2005). This mode of motility is highly regulated by Rac and Cdc42, whereas Rho and ROCK activity is dispensable (Sahai, 2005). This is in contrast to the second mode of motility termed amoeboid or rounded mode (fig. 10B). Here, the activity of Rho and ROCK is essential, whereas a degradation of the ECM does not occur (Wyckoff *et al.*, 2006). Instead, when imaged in the 3D environment, these cells show extensive PM blebbing at their surface which is directed to the stimulus (Sahai and Marshall, 2003). By this mechanism, cells are thought to be able to squeeze through small gaps of the ECM. In these cells, cell-substratum interactions are weak and dispersed over the whole PM. Under certain conditions, various tumor cell lines are able to switch between the elongated and blebbing mode of invasion (Sahai, 2005, Yamazaki *et al.*, 2005).

5.2 Plasma Membrane Blebbing

The generic term PM blebbing defines a dynamic process that alters the appearance of the PM surface of animal cells. It results in the formation of large spherical structures referred to as PM blebs. Depending on the reason for blebbing, PM blebs are either constantly formed and retracted (zeiotic blebs) or occasionally shed from the cellular surface (budding vesicles). Versatile physiological situations have been described in which PM blebbing occurs: The most noted one can be observed during programmed cell death or apoptosis. Initially it had been thought that PM blebbing contributes to cellular destruction and DNA fragmentation as well as to attraction of phagocytotic immune cells (Fadeel, 2004, Martinez *et al.*, 2005). However, opposing observations had been made that clearly uncouple PM blebbing and fragmentation events (Schulze-Osthoff *et al.*, 1994, Shiratsuchi *et al.*, 2002). Nevertheless, in late apoptotic stages these blebs bud from cells as apoptotic bodies finally leading to cellular disruption (Mills *et al.*, 1999, Zhang *et al.*, 1998). Second, secretion of certain proteins like galectins or IL-1β are directly linked to PM blebbing since vesicles containing these proteins bud from the cellular surface (MacKenzie *et al.*, 2001, Mehul and Hughes, 1997). However, contradictory observations have been made indicating two separate events that are not related (Verhoef *et al.*,

2003). Although viral budding has a similar appearance, it is not directly linked to PM blebbing since the vesicle scaffold is formed by viral proteins. However, *Vaccinia* viruses have been observed to induce PM blebbing during the entry process into host cells (A. Helenius and J. Mercer: 58. Mosbacher Kolloquium 2007), suggesting a connection to endocytosis. Other viruses cause PM blebbing simply by induction of apoptosis (Mosquera *et al.*, 2005). PM blebbing also occurs during mitosis of tissue cultured cells (Boss, 1955, Laster and Mackenzie, 1996) and following seeding in culture dishes before spreading (Bereiter-Hahn *et al.*, 1990, Erickson and Trinkaus, 1976). Finally, PM blebbing can be observed during cellular movement in embryonic development and at the leading edge of cellular sheets (Dipasquale, 1975, Trinkaus, 1973). PM blebs that are generated during migration in 3D environments and tissues, *e.g.* of certain amoebas or metastasizing tumor cells have been well investigated. This amoeboid or rounded mode of motility is distinct from the mesenchymal or elongated mode which in contrast is dependent on secretion of metalloproteases and formation of podosomes or invadopodia (see chapter 5.1.4.2) (Linder and Aepfelbacher, 2003, Sahai, 2005, Yamazaki *et al.*, 2005, Yoshida and Soldati, 2006).

PM blebbing has also been observed in several non-physiological situations as during 2D migration and can be specifically induced. M2 melanoma cells lacking the F-actin cross-linking protein filamin a (FLNa) bleb extensively and continuously because of defects in their cortical actin integrity (Byers *et al.*, 1991, Charras *et al.*, 2005, Cunningham, 1995, Cunningham *et al.*, 1992). Similarly, MEF (mouse embryonal fibroblast) knockout cells that are depleted in the cell cycle regulatory protein p53 have recently been shown to bleb constantly in a mode that is linked to cell invasion (Gadea *et al.*, 2007). Furthermore, over-expression of the Rho kinases ROCK1 or ROCK2 induce PM blebbing especially in a constitutively active form lacking the respective regulatory C-terminal end (Coleman *et al.*, 2001, Sebbagh *et al.*, 2005, Sebbagh *et al.*, 2001, Song *et al.*, 2002). PM blebbing has also been shown to be inducible by expression of a constitutively active mutant of the Rho-GTPase Rac1 (Rac1-L61A37) (Schwartz *et al.*, 1998). Disassembly of microtubules by colchicine leads to PM blebbing in Walker carcinosarcoma cells (Keller and Eggli, 1998). Stabilization of F-actin filaments by inhibition of the actin severing factor ADF/cofilin has been shown to induce PM blebbing as well (Amano *et al.*, 2001, Tomiyoshi *et al.*, 2004). Finally artificial detachment of the PM from the cortical actin layer by suction pressure also induces local PM blebbing (Rentsch and Keller, 2000, Sheetz *et al.*, 2006).

Although the specific function of any kind of PM blebbing is not clear and the circumstances in which PM occurs are different, the general machinery that is required for their dynamics is thought to be similar and will be discussed in the following.

5.2.1 Formation of PM Blebs and the Contribution of the Cortical Actin

The site of blebbing activity is the PM. This outer barrier of an animal cell is a lipid bilayer that separates the intracellular compartments from the external medium. Furthermore, the PM is the site where communication with the extracellular milieu takes place: For instance, intracellular proteins and signal peptides are secreted *via* the PM. The PM is enriched with membrane proteins that either traverse the PM by hydrophobic domains (integrated or transmembrane proteins) or are linked indirectly *via* lipid anchors. Some of them are part of receptor complexes that transmit external signals into the cell causing cellular responses. The PM also facilitates and regulates uptake of differently sized extracellular components by different mechanisms. However, the PM is also the place where blebbing occurs. At least for apoptotic cells, PM blebbing is thought to be a form of communication as well. Thereby the dying cell is opsonized to phagocytotic cells of the immune system (Fadeel, 2004).

The PM of animal cells is directly connected to the cortical actin meshwork that lies in parallel beneath lipid bilayer and plays a pivotal role in cell motility, adhesion, endo- and phagocytosis, cytokinesis and organization of integral proteins (Weed and Parsons, 2001). Lacking the cell wall that is usually found in plant cells, it antagonizes extra- and intracellular pressure by maintaining an isotropic tension. Thereby it provides both elastic and viscous properties forming a robust framework for the membrane (Bray and White, 1988). This web like organized and about 50–2000 nm thick layer is enriched in F-actin filaments and actin associated proteins like myosin II that are needed for contractility and other proteins that are required for its organization (Bray and White, 1988). How the cortical actin meshwork is tethered to the PM is not fully understood and depends on the cell type as well as on the specific setting of the cell. A major role is suggested for the ezrin–radixin–moesin (ERM) family of proteins. These proteins are attached to microfilaments by a highly conserved C-terminal actin binding site and associated to the PM by direct binding of their N-terminal FERM domain to integral PM proteins like CD44, ICAM-1-3 and CD43 or by indirect binding, respectively (Bretscher *et al.*, 2000, Bretscher *et al.*, 2002, Tsukita and Yonemura, 1999). In fact, in microinjection experiments, Charras and coworkers have shown a requirement for functional ezrin in tethering the PM to newly formed cortical actin (Charras *et al.*, 2006). In addition, a role for cortical F-actin attachment to the PM has been suggested for a variety of other proteins as well. Similarly by binding to integral PM proteins, proteins like cortactin, talin, vinculin, zyxin, filamins, catenins, α-actinins, spectrins, and others contribute to F-actin PM tethering (Daly, 2004, Siripala and Welch, 2007, Stossel *et al.*, 2006, Weed and Parsons, 2001). Peripheric PM proteins like the myristoylated

alanine-rich C kinase substrate (MARCKS) are also able to link F-actin filaments to the PM. Interestingly, a role for MARCKS in formation of podosomes that are different to PM blebs has been suggested recently (Sheetz *et al.*, 2006). However, a role for the cortical actin meshwork in PM blebbing is very likely, since it is constantly reorganized to form distinct types of dynamic protrusions that are coated by the PM. Activation of Cdc42 induces filopodia, whereas Rac activity is required for formation of lamellipodia and PM ruffles (see chapter 5.1.2.3), whose functions are not clear although they are thought to be involved in macropinocytosis (Norbury, 2006, Ridley, 2006). Nevertheless, the contribution of the cortical actin meshwork to PM blebbing is not fully understood. Some insights in its role have been obtained in the recent years and will be discussed here.

5.2.1.1 The Model of Poroelastic PM Bleb Formation

Zeiotic PM blebbing is defined by a cycle of processes that are described by certain characteristics: Following loss of tension of the cortical actin meshwork a PM bleb is formed which is subsequently stabilized by F-actin polymerization. Upon contractility of the microfilament system a bleb is retracted to PM levels. It is worth mentioning that a major contribution to our knowledge about PM blebbing originates from a cell line that has been isolated from a human cutaneous malignant melanoma (Byers *et al.*, 1991). These M2 cells lack the F-actin cross-linking protein FLNa and bleb extensively and constantly (Cunningham, 1995, Cunningham *et al.*, 1992). FLNa, also known as actin binding protein 280 (ABP280) is a 280 kDa protein that efficiently organizes F-actin filaments in an orthogonal meshwork (Bennett *et al.*, 1984, Brotschi *et al.*, 1978), thus stabilizing the microfilament system. FLNa is phosphorylated by several serine/threonine kinases including protein kinase A (PKA), protein kinase C (PKC), Ca^{2+}/calmodulin-dependent protein kinase II and p90 ribosomal S6 kinase (Stossel *et al.*, 2001). Although the physiological relevance of these modifications is unclear, phosphorylation by the Src kinase Lck is thought to regulate its F-actin cross linking activity as well as its membrane association (Goldmann, 2002, Pal Sharma and Goldmann, 2004). Furthermore, FLNa specifically binds to the PH domain of the serine/threonine kinase ROCK (Ueda *et al.*, 2003). Loss of FLNa in M2 cells is thought to cause defects in the integrity of the microfilament system pervading the whole cell and in particular in the cortical actin meshwork. In the model of poroelastic PM bleb formation (fig. 11) it is assumed that the cytoplasm is composed of a porous, actively contractile, elastic network (cytoskeletal filaments, organelles, ribosomes). Comparable to a sponge this network is infiltrated with an intestinal fluid (cytosol, water, ions, soluble proteins).

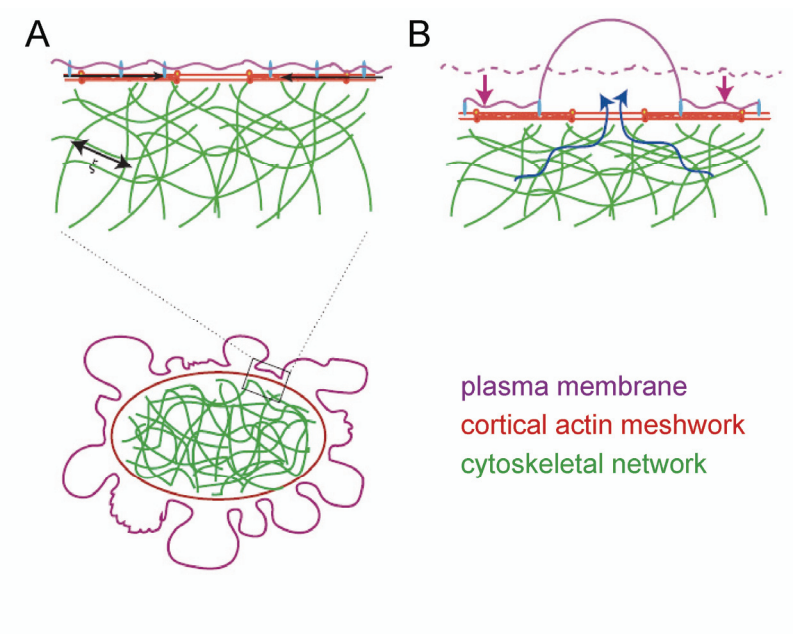

Figure 11: Poroelastic description of PM blebbing.

(A) Local contraction of the actin cortex meshwork by myosin II leads to a shortening of the cortical periphery and therefore to a compression of the cytoskeletal network that fills the cell creating a hydrostatic pressure. In FLNa depleted cells fluid cytosol infiltrating this porous network with an average pore size (ζ) squeezes through the cortical actin **(B)**, causing the protrusion of PM blebs (Charras *et al.*, 2005).

Contraction of the acto-myosin cortex would create a local hydrostatic pressure to the cytosol causing the intestinal fluid to flow out through the porous network which leads to PM detachment and bleb formation (Charras *et al.*, 2005). However, the initiating event is related to a weakening of the actin structure, since the blebs initially contain mainly monomeric actin (Cunningham, 1995). Subsequently, actin polymerization and actin cross-linking proteins limit bleb enlargement by production of a new cortical actin meshwork lining the inner leaflet of a bleb. This process is accompanied by incorporation of the PM tethering proteins of the ERM family. Finally, PM blebs are successively retracted in a myosin II dependent process, resulting in a stabilization and flattening of the PM (Charras *et al.*, 2006, Cunningham, 1995, Paluch *et al.*, 2005, Stossel *et al.*, 2001, Wyckoff *et al.*, 2006).

The loss of FLNa represents the trigger for bleb genesis in M2 cells leading to a weakening of the cortical actin meshwork. Although this FLNa deficiency creates an artificial situation, it provides a basic model for the cycle of PM blebbing which requires distinct signaling events. this has been shown by the involvement of regulatory proteins such as the Rho-GTPase Rho and its effector kinase ROCK.

5.2.1.2 The Roles of Rho, ROCK and Myosin II in PM Blebbing

During apoptosis, ROCK proteins are constitutively activated *via* cleavage of the carboxyl-terminus either by caspase-3 (ROCK1) or by granzyme B (ROCK2) which causes extensive PM blebbing (Coleman *et al.*, 2001, Sebbagh *et al.*, 2005). This process is independent of Rho activity but requires the kinase activity of the ROCK proteins. Active ROCK proteins mediate contractility and F-actin filament bundling by direct or indirect elevation of MLC

phosphorylation, which activate this regulatory compartment of myosin II (see chapter 5.1.2.4). In fact, the need for myosin activity in PM blebbing has been shown in several studies for different situations in which PM blebbing occurs. Treatment of blebbing cells with the myosin II specific drug Blebbistatin (BS) interfering with its ATPase activity (Allingham *et al.*, 2005, Ramamurthy *et al.*, 2004) abolishes PM blebbing in dividing cells, apoptotic cells and additionally in amoebae movement in a physiological milieu (Orlando *et al.*, 2006, Straight *et al.*, 2003, Yoshida and Soldati, 2006). During induction of PM blebbing, MLC is phosphorylated (Coleman *et al.*, 2001, Sebbagh *et al.*, 2005). This active form also localizes at PM blebs (Charras *et al.*, 2006, Keller *et al.*, 2002, Torgerson and McNiven, 1998). In line with the model of poroelastic PM bleb formation described for M2 cells lacking FLNa, ROCK activity is increased in local areas of the actin cortex mediated by ROCKs constitutive activation or over-expression. Subsequently, myosin II is activated resulting in limited but intensive contractility. This enhanced contractility might then lead to a loss of integrity of the cortical actin and would cause detachment of the PM resulting in bleb formation (Paluch *et al.*, 2005, Sahai and Marshall, 2003).

5.2.1.3 The Role of Nucleation of F-actin Polymerization in PM Blebbing

As introduced in the previous chapter, F-actin filaments are involved in PM blebbing. As the main component of the actin cortex, they are required to determine cell shape and form the scaffold for myosin II mediated contractility. F-actin has been shown to be newly polymerized in already formed PM blebs to stabilize the bleb structure and retract the PM bleb to its origin (Charras *et al.*, 2006, Cunningham, 1995). In general, nucleation of F-actin polymerization is mediated by the Arp2/3 complex and spire proteins as well as by Drfs in distinct mechanisms (see chapter 5.1.2.1). However, the contribution of any of these proteins during PM blebbing is unclear and requires further investigation.

5.3 Src Kinases and SH4-Domain Containing Proteins

Many formins functionally and physically interact with Src kinases. These non-receptor protein-tyrosine kinases bind to the formin FH1-domain and are suggested to contribute to their activation. This had been shown for DAAM1, FHOD1, mDia1 and mDia2 (Aspenstrom *et al.*, 2006, Koka *et al.*, 2005, Matusek *et al.*, 2006, Tominaga *et al.*, 2000, Uetz *et al.*, 1996, Yamana *et al.*, 2006), but Src kinase activity is also regulated by Drfs (Gasman *et al.*, 2003). Src kinases are a family of proto-oncogenic proteins playing a pivotal role in a variety of biological and

dynamic processes, such as cell morphology regulation, motility, proliferation and survival of animal cells. The first identified member of this group is the transforming protein v-Src (viral Src) of the oncogenic retrovirus Rous sarcoma virus, a chicken tumor virus discovered in 1911 by Peyton Rous (Martin, 2001). Its cellular homolog c-Src (cellular Src) is ubiquitously expressed in animal cells and localizes at endosomes, perinuclear membranes, secretory vesicles and the cytoplasmic part of the PM where it interacts with certain growth factors and integrin receptors. Additionally to c-Src ten further members of Src kinases in humans are thought to be partially redundant in some cellular functions. Similarly to c-Src, the Src kinases Fyn and Yes are ubiquitously expressed, whereas the other ones have been shown to be tissue specific: Srm is found in keratinocytes, Frk and Brk in a variety of cell types, and Blk, Fgr, Hck, Lck as well as Lyn are found in hematopoietic cells. The functionality of Src kinases is directly linked to their localization to cellular membranes *via* their N-terminal Src homology 4-domain (SH4-domain) (Frame, 2004, Resh, 1993, Resh, 1994, Roskoski, 2004, Thomas and Brugge, 1997).

5.3.1.1 Cellular Functions of Src Kinases

In line with their proto-oncogenic capacity, Src kinases are involved in versatile regulatory processes of animal cells that are related to gene transcription as well as to cell cycle control, cell-cell and cell-matrix contacts and cytoskeletal rearrangements (Martin, 2001). They functionally and physically interact with various cellular enzymes, adaptors, regulatory and cytoskeletal proteins. Activated by integrins for instance, Src kinases are directly involved in cell adhesion and spreading (Resh, 1999, Roskoski, 2004). The Src kinases c-Src, Fyn and Yes are thought to phosphorylate several proteins like focal adhesion kinase (FAK), talin, vinculin, tensin and others necessary for maintenance of focal adhesions. These contact sites are required for attachment of the cell to the extracellular matrix and for attachment of the intracellular microfilament system, since they are enriched with PM crossing integrin proteins. Therefore, Src kinases play an important role in cell migration where focal adhesion turnover is highly regulated (Resh, 1999, Roskoski, 2004). During migration on planar surfaces, cells develop lamellipodia at their leading edge. These highly dynamic F-actin meshworks are constantly formed at the front and destructed at the rear. In both processes Src kinases have the capacity to be involved: At least v-Src takes part in depolymerization of the microfilament system by causing dephosphorylation and thereby activation of the severing protein ADF/cofilin (Pawlak and Helfman, 2002). In addition to Drfs, the Arp2/3-complex is negatively regulated by tyrosine phosphorylation of cellular proteins like cortactin (Daly, 2004, Weed and Parsons, 2001). Interestingly, Src kinases also have the capacity to regulate the activity of Rho-GTPases, thus

controlling central regulators of cytoskeleton dynamics (DerMardirossian *et al.*, 2006, Meng *et al.*, 2004). In line with this, active Rho has been found in podosomes of Src transformed fibroblasts (Berdeaux *et al.*, 2004). Podosomes or invadopodia are developed during invasion of monocyte-derived cells and certain carcinoma cells during invasion (see chapter 5.1.4.2). Src kinases have been shown to play a crucial role in signaling events leading to formation of these protrusions (Linder and Aepfelbacher, 2003).

5.3.1.2 Structure and Regulation of Src kinases – The Src Homology Domains

The organization of the different Src kinases is very similar. These 52-62 kDa proteins are composed of six distinct functional regions (Martin, 2001, Roskoski, 2004, Thomas and Brugge, 1997). At the N-terminal end, the SH4-domain is located which is required for membrane association (fig. 12A). This domain is followed by a stretch of amino acids that is distinct for the different Src kinases (Unique-domain). The three subsequent domains represent modular structures in many classes of cellular proteins. The SH2- and SH3-domains are protein-binding domains as found in phosphatases, lipid kinases, cytoskeletal proteins, adaptor molecules, transcription factors and other proteins as well. The SH1-domain is connected to the SH2-domain by a linker region and embodies the kinase domain required for phosphorylation of several cellular targets. At the C-terminal end a short negative regulatory tail is located.

In its dormant state, in which the Src kinase shows basal activity only, the protein is phosphorylated at amino acid residue Y527 in the regulatory tail. This phosphorylation is mainly performed by C-terminal Src kinase (Csk) and Csk-homologous kinase (Chk) and results in an intramolecular binding of the tail region to the SH2-domain leading to a sterical hindrance of the SH2- as well as the SH3-domain, both required for protein-protein interactions. This autoinhibition is released *via* dephosphorylation of Y527 by a tyrosine phosphatase. Subsequently, amino acid residue Y416 can undergo autophosphorylation by another Src kinase molecule, stabilizing the enzyme in its active state with accessible SH2- and SH3-domains (fig. 12B).

Interestingly, the v-Src protein differs from c-Src mainly by a lack of the regulatory tail and its phosphorylation site. The site in Src kinases corresponding to position Y418 in c-Src is constantly phosphorylated in oncogenic enzymes. The SH3-domain is important for intra- as well as for intermolecular interactions regulating Src catalytic activity, Src localization and recruitment of substrates. With contribution of neighboring amino acid residues, SH3-domains bind to short proline rich amino acid sequences with a core consensus sequence of P-X-X-P (where P is proline and X is any amino acid). The SH2-domain is also required for protein-

protein interactions regulating the catalytic activity of the Src kinase as well as its localization or that of its binding partner. SH2-domains bind to short amino acid stretches containing phosphotyrosine and the subsequent 3-5 amino acid residues defining the specificity (Martin, 2001, Roskoski, 2004, Thomas and Brugge, 1997).

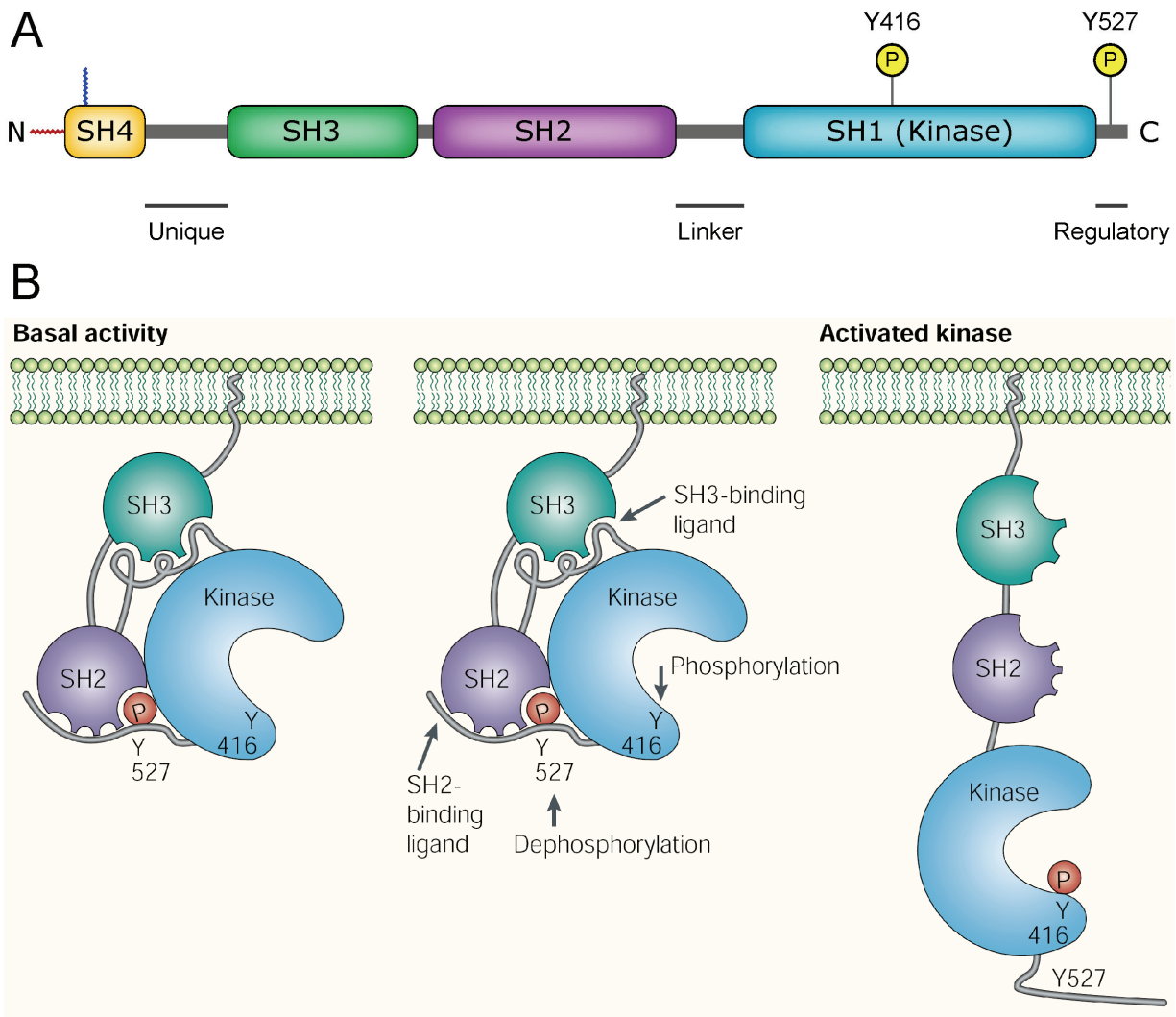

Figure 12: Organization and regulation of Src kinases.

(A) Schematic presentation of Src kinases. At the N-terminal end the SH4-domain is located which is often posttranslationally modified by myristoylation and palmitoylation for efficient membrane targeting. The Unique region represents a stretch of amino acids that are specific for the respective Src kinase. The SH3- and SH2-domains are required for protein-protein interactions. The SH1-domain is the kinase domain of the enzyme followed by the regulatory tail. Phosphorylation at amino acid residue Y416 inside the SH1-domain leads to full activation, whereas phosphorylation of Y527 in the regulatory domain results in deactivation of kinase activity. Organization and numbering system are based on chicken c-Src. **(B)** Regulation of Src kinases. Dormant Src kinases are phosphorylated in their regulatory tail as described in A resulting in an intramolecular binding to the SH2-domain. This autoinhibition is released by dephosphorylation of the tail making the SH2- and SH3-domains accessible for substrate interactions. This conformation is further stabilized by phosphorylation of amino acid Y416 in the kinase domain (Martin, 2001).

Additionally, the Unique-domain, that is distinct for each member is thought to mediate interactions with receptors or proteins that are specific for each Src kinase (Summy *et al.*, 2003).

The targeting of Src kinases and other proteins to cellular membranes is mediated by the SH4-domain.

5.3.1.3 SH4-Domains Mediate Membrane Targeting

In Src kinases, the N-terminal stretch of 18 amino acid residues is denoted as SH4-domain. These short sequences are sufficient to mediate membrane association and are also found in other cellular and pathogenic proteins: The α subunits of heterotrimeric G proteins as well as several retroviral Gag proteins and the HIV-1 Nef protein are targeted to the PM in this way (McCabe and Berthiaume, 1999, Resh, 1999). An SH4-domain is also found in the surface coat protein of *Leishmania* parasites, the hydrophilic acetylated surface protein B (HASPB) (Denny *et al.*, 2000, Nickel, 2005). Although the overall amino acid homology between these SH4-domains is less conserved, a common feature is the posttranslational modification by acetylation with fatty acids. All SH4-domains have a glycine at position 2 (G2) in common (fig. 13).

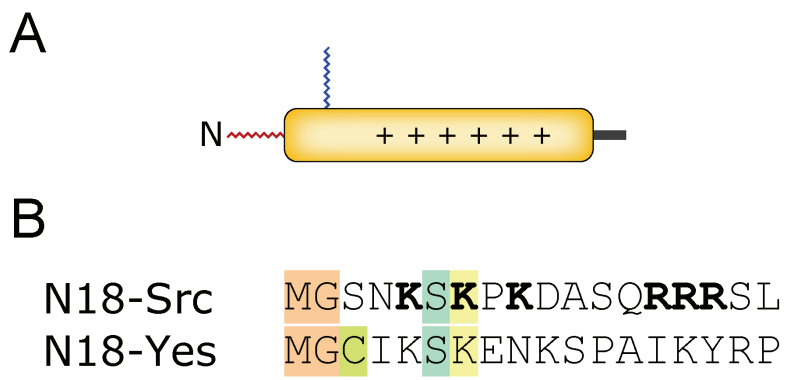

Figure 13: SH4-domains.

(A) Schematic presentation of SH4-domains. Located at the N-terminal end of various peripheral PM proteins, SH4-domains are myristoylated (red) and can be additionally palmitoylated (blue) or have a basic cluster (+ + +) of positively charged amino acid residues (Lys or Arg), respectively, to mediate PM targeting. **(B)** Examples of two SH4-domains. Depicted are the first 18 amino acid residues of the myristoylated Src kinases c-Src that furthermore conatin a basic cluster and Yes, that is palmitoylated as well. Selected residues are written in bold letters (basic cluster) or highlighted by light colors (red: myristoylated; green: palmitoylated; required for efficient myristoylation: Ser or Thr (cyan) and Arg or Lys (yellow)).

During translation of the protein, this specific glycine is myristoylated by N-myristoyl transferase (NMT), an enzyme catalyzing the transfer of myristate from myristoyl-CoA (coenzyme A) to its substrate. Since the glycine has to be located at the very N-terminal end to be recognized by NMT, the methionine at position 1 (M1) is initially removed by a methionine amino peptidase. The consensus sequence for efficient myristoylation is M-G-X-X-X-S/T-K/R/X-K/R/X (where G is glycine, K is lysine, M is methionine, R is arginine, S is serine, T is threonine and X is any amino acid) and can be found in almost all SH4-domains (Resh, 1999).

Myristate is a 14-carbon saturated fatty acid and is introduced hydrophobically into the lipid bilayer of a membrane. However, although myristoylation is required, it is not sufficient for stable membrane binding, since these interactions are relatively weak. A second signal is necessary and may be provided in two ways: first, the SH4-domain possesses a stretch of basic amino acids downstream the recognition site for myristoylation. These positively charged amino acid residues electrostatically interact with the headgroups of acidic phospholipids. These are primarily localized at the inner leaflet of the bilayer, causing a net negative charge to the cytoplasmic leaflet surface. Examples for myristoylated SH4-domains possessing a basic cluster are c-Src and the viral proteins HIV-1 Gag and HIV-1 Nef (Resh, 1999). The second possibility to assure efficient membrane binding includes an additional acetylation step. In SH4-domains, cysteins that follow the G2 are usually palmitoylated, most likely with the help of the enzyme palmitoyl acyl transferase (Bijlmakers and Marsh, 2003, Resh, 1999). In this reaction, which is performed after translation of the whole protein, a 16-carbon saturated fatty acid palmitate molecule is linked *via* a thioester linkage to the sulfhydryl group of a cysteine. Although the consensus sequence for palmitoylation M-G-C (where C is cysteine, G is glycine and M is methionine) is highly conserved and can be found in for instance the Src kinases Fyn, Lck and Yes. However, HASPB which shows a serine instead of a cysteine at position 3 (C3) is palmitoylated as well, but at position 5 (C5) (Denny *et al.*, 2000). Since palmitoyl acyl transferase localizes at membranes as well, palmitoylation is thought to occur directly at this site. Therefore, the first signal that is provided by myristic acid is required for membrane targeting of the SH4-domain, where its localization is than assured by the following palmitoylation step. Interestingly, for HASPB it is thought that palmitoylation of its SH4-domain at Golgi membranes is required to target the protein to the PM (Denny *et al.*, 2000, Stegmayer *et al.*, 2005). Since both myristate and palmitate possess a saturated hydrocarbon chain, SH4-domains show a high affinity to liquid-ordered domains inside the PM like lipid-rafts and in particular caveolae, which are small invaginations of the PM (Resh, 1999, Simons and Toomre, 2000). However, additional functions of SH4-domains beyond membrane targeting have not been described so far.

6 OBJECTIVES OF THE STUDY

The phenomenon of PM blebbing on animal cell surfaces describes a type of PM dynamization that results in the formation and retraction of large spherical protrusions with distinct kinetics. It is linked to various physiological processes such as apoptosis (Mills *et al.*, 1999, Zhang *et al.*, 1998), secretion (MacKenzie *et al.*, 2001, Mehul and Hughes, 1997), cytokinesis (Boss, 1955, Laster and Mackenzie, 1996) and tumor cell invasion (Sahai and Marshall, 2003, Wyckoff *et al.*, 2006), but has also been observed as a constant process in cell lines lacking distinct structural or regulatory proteins (Cunningham, 1995, Gadea *et al.*, 2007) or expressing SH4-domains (this study). Although cellular triggers for its induction are unique and might originate from different internal or external signals, the machinery required for PM blebbing is thought to be equal (Charras *et al.*, 2005, Sahai and Marshall, 2003). It is defined by a Rho-ROCK dependent contractility of the microfilament system as well as its dynamic reorganization. A ubiquitous family of regulated Rho-GTPase effector proteins actively reorganizing the actin cytoskeleton by nucleation of actin filament polymerization is represented by the diaphanous related formins (Drfs). This group of formin homology domain containing proteins plays a crucial role in cytokinesis, embryonal development, endocytosis and cell migration. Nevertheless, their individual function is thought to be unique (Faix and Grosse, 2006, Goode and Eck, 2007, Wallar and Alberts, 2003). A less characterized member of this family is the formin homology domain 2 containing 1 (FHOD1) protein. This Drf has been shown to interact with the Rho-GTPase Rac1 but functions in a ROCK dependent manner (Gasteier *et al.*, 2003, Westendorf, 2001). Thus, a direct interplay for FHOD1 and ROCK1 has been suggested linking the activity of the two different Rho-GTPases Rac1 and Rho that are responsible for distinct cellular functions (Gasteier *et al.*, 2003).

Several aspects concerning PM blebbing and characterization of possible key players were to be addressed in the course of this study:

1. *Is there a functional interaction of FHOD1 and ROCK1 in mammalian cells?* Therefore, co-expression studies should be performed, a possible phenotype characterized and this interaction functionally mapped in comparison with *in vitro* binding experiments.

2. *What is the physiological function of endogenous FHOD1?* Since the knowledge on FHOD1 was so far exclusively based on over-expression studies, the distribution and function of endogenous FHOD1 should be analyzed with the help of a specific antibody in combination with specific RNAi based knockdown of the protein.

3. *What is the mechanism that is required for PM blebbing?* Based on findings that have been obtained during this study regarding the induction of PM blebbing by SH4-domains and the role for FHOD1 in ROCK1 mediated PM blebbing, the functional interplay of Src kinases, ROCK proteins and FHOD1 had to be analyzed by addressing their individual contribution to different types of PM blebbing.

4. *Is there a physiological relevance for SH4-domain induced PM blebbing?* Since triggering of PM blebbing was a novel finding that had not been linked to SH4-domains before, its functional relevance for cellular processes had to be analyzed.

7 MATERIAL AND METHODS

7.1 Materials

7.1.1 Reagents

Reagents were purchased from the following companies: Metafectene (Biontex); (-) Blebbistatin, BrdU Cell Proliferation Assay, Cycloheximide, Cytochalasin D, immersion oil, Latrunculin B, Nocodazole, PP1-analog, Rho-Kinase inhibitor H-1152, SU6656, Y27632, zVAD-fmk (Calbiochem, Merck); [^{32}P]-γATP (Hartmann Analytic); Annexin V-Alexa-Fluor-568, dextran-Alexa-Fluor-568/647 (10 kDa), Lipofectamine 2000, Oligofectamine, phalloidin-Alexa-Fluor-350/660 (Invitrogen, Molecular Probes); Lin-Mount (Linaris); Nucleobond PC 500 (Machery-Nagel); ECL-solution, Micro BCA Protein Assay Kit (Pierce); rhTNFα (Promega); HiPerFect Transfection Reagent (Qiagen); Paraformaldehyde (Riedel de Haën); TUNEL = "*In situ* Cell Death Detection Kit, TMR red" (Roche); bovine serum albumin (Roth); BrefeldinA, Chlorpromazine, doxicycline, Etoposide, Hoechst 33268, myosin light chain, myelin basic protein, Naphtol blue black, phalloidin-TRITC/FITC, poly-L-lysine, protease inhibitor cocktail, sodium orthovanadate (Sigma).
Reagents and chemicals not specifically listed were purchased from the following companies: AppliChem, Riedel de Haën, Roche, Roth, Serva, Sigma, Zentrallager INF.

7.1.2 Consumables

Consumption items were purchased from the following companies: HiTrap NHS activated HP affinity column, Glutathione Sepharose 4B, ProteinA Sepharose CL-4B (Amersham Biosciences); plastic pipettes for cell culture (Costar); 8 µm ThinCert cell culture inserts (Greiner Bio-One); coverslips with a diameter of 12 mm, object slides (Marienfeld); PVDF membrane (Millipore); Lab-Tek chamber slides (Nunc), parafilm (Pechiney); CL-XPosure film, Clear Blue X-Ray film (Pierce); Protran nitrocellulose transfer membrane, Whatman paper (Schleicher & Schuell); plastic materials for cell culture (TPP).
Further consumption items were purchased from the following companies: Corning, Eppendorf, Greiner Bio-One, neoLab.

7.1.3 Sterilization

Media were autoclaved at 121°C and 1 bar positive pressure for 20 min. Other substances and solutions were either autoclaved or, if temperature sensitive, sterilized by filtration (pore width 0.22 µm).

7.1.4 Cell Culture Media and Solutions

- freezing medium: 90 % (v/v) heat inactivated fetal calve serum (FCS, Bio Whittaker, Invitrogen), 10 % (v/v) DMSO.
- phosphate buffered saline (PBS, see chapter 7.1.11).
- trypsin/EDTA: 10 % (v/v) trypsin/EDTA (10x, Biochrom), 90 % PBS.
- OptiMEM I: "Reduced Serum Medium" (Invitrogen).

The following media were usually supplemented with 10 % heat inactivated FCS, 2.0 mM glutamate (Invitrogen), 50 U/ml penicillin and 50 µg/ml streptomycin (Invitrogen). Furthermore,

if indicated, media were additionally supplemented with 0.1 mM non essential amino acids (NEA, Invitrogen) and 1 mM sodium pyruvate (Invitrogen):

- DMEM-high: "Dulbecco's Modified Eagle Medium", 4,500 mg/l glucose (Invitrogen).
- DMEM-low: "Dulbecco's Modified Eagle Medium", 1,000 mg/l glucose (Invitrogen).
- MEM-alpha: "Minimal Essential Medium alpha", 1,000 mg/l glucose (Invitrogen).

7.1.5 Bacterial Growth Media

- Luria Bertani (LB)-Medium:

bacto-tryptone	1.0 % (w/v)
yeast extract	0.5 % (w/v)
NaCl	170 mM
NaOH	5 mM
pH 7.5; autoclaved	

- LB agar plates: LB medium was supplemented with 12.5 g/l agar, autoclaved and appropriate amounts were added to 10 cm Petri dishes.
- Antibiotics for selection of resistant bacterial strains were prepared as concentrated stock solutions, sterilized by filtration and added to the medium after autoclavation (final concentrations: 100 µg/ml ampicillin, Roth; 50 µg/ml kanamycin, Roth).

7.1.6 Eukaryotic Cell Lines

- CHO-MCAT-TAM2:
  CHO cells with stably integrated cDNAs encoding the murine cation transporter MCAT-1, the doxicycline-sensitive transactivator rtTA2-M2 and a truncated version of the cell surface protein CD2 (Engling *et al.*, 2002).
  Origin: Chinese hamster ovary (Puck *et al.*, 1958).
  Morphology: epithelial-like cells, adherent monolayer.
  Cell culture medium: Alpha MEM.
  Passaging: 1:20.

- CHO-GFP:
  CHO-MCAT-TAM2 cells with stably integrated cDNA encoding for eGFP which was initially cloned into pREV-TRE2 vector (Clontech) containing a transactivator/doxicycline-responsive element for retroviral transduction (Engling *et al.*, 2002).
  Cell culture medium: Alpha MEM.
  Passaging: 1:20.

- CHO-N18-c-Src-GFP, CHO-N18-Fyn-GFP, CHO-N18-HASPB-GFP, CHO-N18-ΔMyr-HASPB-GFP, CHO-N18-ΔPal-HASPB-GFP, CHO-N18-Lck-GFP, CHO-N18-Yes-GFP:

  CHO-MCAT-TAM2 cells with stably integrated cDNA encoding for ProteinA linked SH4-domains of c-Src, Fyn, HASPB, Lck or Yes or the respective mutants which were initially cloned into pREV-TRE2 vector (Clontech) containing a transactivator/doxicycline-responsive element for retroviral transduction. These cell lines were generated by Stella Tournaviti (BZH, University of Heidelberg) similarly to CHO-GFP cells (Engling *et al.*, 2002).
  Cell culture medium: Alpha MEM.
  Passaging: 1:20.

- HeLa:
  Origin: human cervical adenocarcinoma (Scherer *et al.*, 1953).
  Morphology: epithelial-like cells, adherent monolayer.
  Cell culture medium: DMEM-high.
  Passaging: 1:10.

- HeLa-N18-HASPB-GFP, HeLa-N18-ΔMyr-HASPB-GFP, HeLa-N18-ΔPal-HASPB-GFP, HeLa-N18-Yes-GFP, HeLa-N18-ΔMyr-Yes-GFP, HeLa-N18-ΔPal-Yes-GFP:
  HeLa cells with stably integrated cDNA encoding for SH4-domains of HASPB or Yes or the respective mutants which were initially cloned into pREV-TRE2 vector (Clontech) containing a transactivator/doxicycline-responsive element for retroviral transduction. These cell lines were generated by Julia Ritzerfeld (BZH, University of Heidelberg) similarly to CHO-GFP cells (Engling *et al.*, 2002).
  Cell culture medium: DMEM-high.
  Passaging: 1:10.

- NIH3T3:
  Origin: contact-inhibited NIH Swiss mouse embryo (Aaronson and Todaro, 1968).
  Morphology: fibroblastic cells, adherent monolayer.
  Cell culture medium: DMEM-low.
  Passaging: 1:10.

- MEF:
  Origin: mouse embryo.
  Morphology: fibroblastic cells, adherent monolayer.
  Cell culture medium: DMEM-high.
  Passaging: 1:20.

- MDA-MB-435:
  These cells were kindly provided by Robert Grosse (Pharmacology, University Hospital Heidelberg).
  Origin: human breast carcinoma (Cailleau *et al.*, 1978).
  Morphology: epithelial-like cells, round, loosely attached monolayers.
  Cell culture medium: DMEM-high, supplemented with NEA and Na-pyruvate.
  Passaging: 1:10.

- SYF -/-:
  These cell lines were kindly provided by Klemens Rottner (HZI, Braunschweig).
  Origin: mouse embryo harboring functional null mutations in both alleles of the Src kinases c-Src, Yes, and Fyn. Cells were immortalized with SV40 large T antigen (Klinghoffer *et al.*, 1999).
  Morphology: fibroblastic cells, adherent monolayer.
  Cell culture medium: DMEM-high, 0.1 mM NEA and 1 mM Na-pyruvate.
  Selection medium: cell culture medium supplemented with 400 µg/ml hygromycin.
  Passaging: 1:10.

- SYF + c-Src:
  These cell lines were kindly provided by Klemens Rottner (HZI, Braunschweig).
  Origin: mouse embryo harboring functional null mutations in both alleles of the Src kinases c-Src, Yes, and Fyn. Cells were immortalized with SV40 large T antigen. Wild type c-Src

was stably reintroduced into SYF -/- cells *via* the retroviral vector pLXSH (Klinghoffer *et al.*, 1999).
Morphology: fibroblastic cells, adherent monolayer.
Cell culture medium: DMEM-high, 0.1 mM NEA and 1 mM Na-pyruvate.
Selection medium: cell culture medium supplemented with 400 µg/ml hygromycin.
Passaging: 1:20.

7.1.7 Bacterial Strains

For amplification of plasmid DNA the following bacterial strain was used:

- *Escherichia coli* DH5α (Invitrogen): F^- φ80*lac*ZΔM15 Δ(*lac*ZYA-*arg*F)U169 *rec*A1 *end*A1 *hsd*R17(r_k^-, m_k^+) *pho*A *sup*E44 *thi*-1 *gyr*A96 *rel*A1 λ^-.

7.1.8 siRNA Oligonucleotides

All siRNA oligonucleotides used in this work are listed in tab. 1 and were purchased at MWG Biotech.

Table 1: List of synthetic siRNA oligonucleotides.

Oligonucleotide	Target sequence (sense)	Specificity
Unspecific control (MWG)	5'-AGGUAGUGUAAUCGCCUUGUU-3'	–
FHOD1-specific P1	5'-UACCAGAGCUACAUCCUUAUU-3'	human, rodent
FHOD1-specific P2	5'-GGUCAACGCUAUCUUGGAAUU-3'	human

7.1.9 Plasmids

All plasmids used in this work are listed in tab. 2.

Table 2: List of plasmids for mammalian cells.

Plasmid	Description	Reference
Vectors:		
pEGFP-C1/N1	Vector for expression of enhanced green fluorescent protein (eGFP) in mammalian cells	Clontech
pMRFP-N1	Vector for expression of monomeric red fluorescent protein (mRFP) in mammalian cells	Michel *et al.*, 2006
pMCherry	Monomeric Cherry fluorescent protein	Shaner *et al.*, 2004
pEF-HA	Vector for expression of hemagglutinin (HA) epitope tag in mammalian cells	Alberts *et al.*, 1998
pRev-TRE2	MoMuLV derived retroviral vector for expression of a gene of interest from the tet-response element (TRE)	Clontech
Rho GTPase and related constructs:		
pGEX-RhoA-GFP	c-Myc-fusion protein of wildtype RhoA	A. Alberts, Van Andel Institute, Grand Rapids
pEGFP-C3ex	GFP-fusion protein of *Clostridium botulinum* TAT-C3 transferase	Watanabe *et al.*, 1999

pGEX-Rac1-GFP	c-Myc-fusion protein of wildtype Rac1	Moreau *et al.*, 2000
pGEX-Rac1-N17-GFP	GFP-fusion protein of a dominant negative form of Rac1 with a point mutation at aa residue 17 (Thr to Asn)	Moreau *et al.*, 2000
pGEX-Cdc42-GFP	c-Myc-fusion protein of wildtype Cdc42	Moreau *et al.*, 2000
pGEX-Cdc42-N17-GFP	GFP-fusion protein of a dominant negative form of Cdc42 with a point mutation at aa residue 17 (Thr to Asn)	Moreau *et al.*, 2000
pRK5-c-Myc-RhoA-wt	c-Myc-fusion protein of wildtype RhoA	A. Hall, Cancer Research UK, London
pRK5-c-Myc-RhoA-V14	c-Myc-fusion protein of a constitutively active form of RhoA with a point mutation at aa residue 14 (Gly to Val)	A. Hall, Cancer Research UK, London
pRK5-c-Myc-C3	c-Myc-fusion protein of *Clostridium botulinum* TAT-C3 transferase	S. Offermanns, Molecular Pharmacology, Heidelberg
pRK5-c-Myc-Rac1-wt	c-Myc-fusion protein of wildtype of Rac1	A. Hall, Cancer Research UK, London
pRK5-c-Myc-Rac1-L61	c-Myc-fusion protein of a constitutively active form of Rac1 with a point mutation at aa residue 61 (Gln to Leul)	A. Hall, Cancer Research UK, London
pRK5-c-Myc-Rac1-L61A37	c-Myc-fusion protein of a constitutively active form of Rac1 with point mutations at aa residues 61 (Gln to Leu) and 37 (Phe to Ala)	Lamarche *et al.*, 1996
pRK5-c-Myc-Rac1-L61C40	c-Myc-fusion protein of a constitutively active form of Rac1 with point mutations at aa residues 61 (Gln to Leu) and 37 (Tyr to Cys)	Lamarche *et al.*, 1996
pRK5-c-Myc-Rac1-N17	c-Myc-fusion protein of a dominant negative form of Rac1 with a point mutation at aa residue 17 (Thr to Asn)	A. Hall, Cancer Research UK, London
pRK5-c-Myc-Cdc42-wt	c-Myc-fusion protein of wildtype Cdc42	A. Hall, Cancer Research UK, London
pRK5-c-Myc-Cdc42-V14	c-Myc-fusion protein of a constitutively active form of Cdc42 with a point mutation at aa residue 12 (Gly to Val)	A. Hall, Cancer Research UK, London
pRK5-c-Myc-Cdc42-N17	c-Myc-fusion protein of a dominant negative form of Cdc42 with a point mutation at aa residue 17 (Thr to Asn)	A. Hall, Cancer Research UK, London
pCAG-c-Myc-ROCK1-wt	c-Myc-fusion protein of wildtype ROCK1	Ishizaki *et al.*, 1997
pCAG-c-Myc-ROCK1-Δ3	c-Myc-fusion protein of constitutively active ROCK1 that is C-terminally truncated (aa 1-727)	Ishizaki *et al.*, 1997
FHOD1 constructs:		
pCMV5-HA-1-FHOD1-wt	HA-fusion protein of wildtype FHOD1	Westendorf *et al.*, 1999
pCMV5-HA-1-FHOD1-ΔC	HA-fusion protein with constitutively active FHOD1 that is C-terminally truncated (Δ aa residues 1011-1164)	Westendorf *et al.*, 1999
pEF-HA-FHOD1-ΔFH1	HA-fusion protein with FHOD1 lacking its FH1-domain (Δ aa residues 570-611)	Gasteier *et al.*, 2003
pEF-HA-FHOD1-ΔFH1	HA-fusion protein with FHOD1 lacking its core	Gasteier *et al.*, 2003

	FH2-domain (Δ aa residues 807-866)	
pEF-HA-FHOD1-Δ4	HA-fusion protein with FHOD1 aa residues 486-1068	J. Gasteier
pEF-HA-FHOD1-Δ5	HA-fusion protein with FHOD1 aa residues 570-1068	J. Gasteier
SH4-domain constructs:		
pREV-TRE2-HASPB	The *Leishmania* HASPB surface coat protein	W. Nickel, BZH, Heidelberg
pREV-TRE2-HASPB-GFP	GFP-fusion protein of the *Leishmania* HASPB surface coat protein	W. Nickel, BZH, Heidelberg
pREV-TRE2-N18-HASPB-GFP-PA	GFP-ProteinA-fusion protein of the HASPB-SH4-domain including a TEV cleavage site	S. Tournaviti, BZH, Heidelberg
pREV-TRE2-N18-Δmyr-HASPB-GFP-PA	GFP-ProteinA-fusion protein of the non-myristoylated and non-palmitoylated HASPB-SH4-domain mutant including a TEV cleavage site	S. Tournaviti, BZH, Heidelberg
pREV-TRE2-N18-Δpal-HASPB-GFP-PA	GFP-ProteinA-fusion protein of the non-palmitoylated HASPB-SH4-domain mutant including a TEV cleavage site	S. Tournaviti, BZH, Heidelberg
pREV-TRE2-N18-HASPB-GFP	GFP-fusion protein of the HASPB-SH4-domain	J. Ritzerfeld, BZH, Heidelberg
pREV-TRE2-N18-Δmyr-HASPB-GFP	GFP-fusion protein of the non-myristoylated and non-palmitoylated HASPB-SH4-domain mutant	J. Ritzerfeld, BZH, Heidelberg
pREV-TRE2-N18-Δpal-HASPB-GFP	GFP-fusion protein of the non-palmitoylated HASPB-SH4-domain mutant	J. Ritzerfeld, BZH, Heidelberg
pREV-TRE2-N18-HASPB-MCherry	mCherry-fusion protein of the HASPB-SH4-domain	J. Ritzerfeld, BZH, Heidelberg
pREV-TRE2-N18-YES-GFP-PA	GFP-ProteinA-fusion protein of the YES-SH4-domain including a TEV cleavage site	S. Tournaviti, BZH, Heidelberg
pREV-TRE2-N18-Δmyr-YES-GFP-PA	GFP-ProteinA-fusion protein of the non-myristoylated and non-palmitoylated YES-SH4-domain mutant including a TEV cleavage site	S. Tournaviti, BZH, Heidelberg
pREV-TRE2-N18-Δpal-YES-GFP-PA	GFP-ProteinA-fusion protein of the non-palmitoylated YES-SH4-domain mutant including a TEV cleavage site	S. Tournaviti, BZH, Heidelberg
pREV-TRE2-N18-YES-GFP	GFP-fusion protein of the YES-SH4-domain	J. Ritzerfeld, BZH, Heidelberg
pREV-TRE2-N18-Δmyr-YES-GFP	GFP-fusion protein of the non-myristoylated and non-palmitoylated YES-SH4-domain mutant	J. Ritzerfeld, BZH, Heidelberg
pREV-TRE2-N18-Δpal-YES-GFP	GFP-fusion protein of the non-palmitoylated YES-SH4-domain mutant	J. Ritzerfeld, BZH, Heidelberg
pEGFP-Lck	GFP-fusion protein of the Src kinase Lck	C. Haller
pREV-TRE2-N18-Lck-GFP-PA	GFP-ProteinA-fusion protein of the Lck-SH4-domain including a TEV cleavage site	S. Tournaviti, BZH, Heidelberg
pREV-TRE2-N18-Fyn-GFP-PA	GFP-ProteinA-fusion protein of the Fyn-SH4-domain including a TEV cleavage site	S. Tournaviti, BZH, Heidelberg
pREV-TRE2-N18-Src-GFP-PA	GFP-ProteinA-fusion protein of the c-Src-SH4-domain including a TEV cleavage site	S. Tournaviti, BZH, Heidelberg
Miscellaneous constructs:		
pMRFP-β-Actin	mRFP-fusion protein with β-actin	Pacholsky *et al.*, 2004

pVSVG3-SP-FP-CFP	CFP-fusion protein of a temperature sensitive mutant of the vesicular stomatitis virus glycoprotein (ts-045-G-CFP)	Keller *et al.*, 2001
p3D.Afos	Reporter plasmid encoding for firefly luciferase (pGL3, Promega) controlled by 3D.ACAT promotor sequences	Geneste *et al.*, 2002
pRL-TK	Reporter plasmid encoding for *renilla* luciferase	Promega

aa = amino acid.

7.1.10 Antibodies

Specific detection of proteins *via* Western blot analysis or immuno-fluorescence was performed by usage of specific primary antibodies directed against endogenous proteins or protein tags (tab. 3) and secondary antibodies coupled to enzymes or fluorophores (tab. 4).

Table 3: List of primary antibodies.

Antibody	Source (catalog number)	Usage/Dilution
pc-rabbit-α-**14-3-3** (C-16)	Santa Cruz Biotechnology (sc-731)	WB 1:500
mc-mouse-α-CM1A10 (**coatomer**)	Wegmann *et al.*, 2004	IF 1:200
pc-goat-α-**EEA1**	Santa Cruz Biotechnology (sc-6414)	IF 1:500
pc-rabbit-α-**FHOD1** (aa1-14 & aa345-369)	Gasteier *et al.*, 2005; this work	IF 1:50; WB: 1:500; EM undiluted
mc-mouse-α-**FLNa** (PM6/317)	Santa Cruz Biotechnology (sc-58764)	WB 1:200
pc-rabbit-α-phospho-**FLNa**-S2152	Cell Signaling (#4761)	WB 1:1000
mc-mouse-α-**GFP** (GFP-20)	Sigma (G6539)	WB 2000
mc-mouse-α-**HA** (F-7)	Santa Cruz Biotechnology (sc-7392)	WB 1:200
pc-rabbit-α-**HA** (Y-11)	Santa Cruz Biotechnology (sc-805)	IF 1:200; WB 1:200
mc-mouse-α-**MLC** (MY-21)	Sigma (M4401)	WB 1:1000
pc-rabbit-α-**MLC2**	Cell Signaling (#3672)	IF 1:100; WB 1:1000
pc-rabbit-α-phospho-**MLC2**-Ser19	Cell Signaling (#3671)	IF 1:100; WB 1:1000
mc-mouse-α-CD63 (**MVB**)	BD Pharmingen (556019)	IF 250
mc-mouse-α-**c-Myc** (9E10)	Santa Cruz Biotechnology (sc-40)	IF 1:200; WB 1:500;
mc-mouse-α-**c-Myc-FITC**	Sigma (F2047)	IF 1:200
pc-rabbit-α-**c-Myc**	Sigma (C3956)	WB 1:1000
mc-mouse-α-**P115**/TAP	B. Brügger, BZH Heidelberg	IF 1000
mc-mouse-α-**ROCK1**	BD Pharmingen (611137)	WB 1:500
mc-mouse-α-**c-Src** (B-12)	Santa Cruz Biotechnology (sc-8056)	IF 1:100; WB 1:200
pc-rabbit-α-phospho-**c-Src**-Y418	Biosource, Invitrogen (44-660G)	IF 1:100; WB 1:1000
mc-mouse-α-**TfR** (H68.4)	Zymed, Invitrogen (13-6800)	IF 1:200; WB 1:500
pc-sheep-α-**TGN-46**	Serotec (AHP500G)	IF 1:300
mc-mouse-α-**ts-045-G**	Scales *et al.*, 1997	IF 1:100
mc-mouse-α-**α-tubulin** (B-5-1-2)	Sigma (T5168)	IF 1:500; WB 1:500

aa = amino acid residues, mc = monoclonal, pc = polyclonal, IF = immuno-fluorescence, EM = electron microscopy, WB = Western blot.

Table 4: List of secondary antibodies.

Antibody	Source	Usage/Dilution
pc-donkey-α-goat-Alexa-Fluor-488	Molecular Probes, Invitrogen (A11055)	IF: 1:2,000
pc-donkey-α-goat-Alexa-Fluor-568	Molecular Probes, Invitrogen (A11057)	IF: 1:2,000
pc-donkey-α-goat-Alexa-Fluor-680	Molecular Probes, Invitrogen (A21084)	WB: 1:20,000
pc-donkey-α-sheep-Alexa-Fluor-568	Molecular Probes, Invitrogen (A21099)	IF: 1:2,000
pc-goat-α-mouse-Alexa-Fluor-350	Molecular Probes, Invitrogen (A21049)	IF: 1:2,000
pc-goat-α-mouse-Alexa-Fluor-488	Molecular Probes, Invitrogen (A11011)	IF: 1:2,000
pc-goat-α-mouse-Alexa-Fluor-568	Molecular Probes, Invitrogen (A11004)	IF: 1:2,000
pc-goat-α-mouse-Alexa-Fluor-660	Molecular Probes, Invitrogen (A21054)	IF: 1:2,000
pc-goat-α-mouse-Alexa-Fluor-680	Molecular Probes, Invitrogen (A21057)	WB: 1:20,000
pc-goat-α-mouse-HRP	Jackson Immuno Research	WB: 1:5,000
pc-goat-α-rabbit-Alexa-Fluor-350	Molecular Probes, Invitrogen (A11069)	IF: 1:2,000
pc-goat-α-rabbit-Alexa-Fluor-488	Molecular Probes, Invitrogen (A11008)	IF: 1:2,000
pc-goat-α-rabbit-Alexa-Fluor-568	Molecular Probes, Invitrogen (A11036)	IF: 1:2,000
pc-goat-α-rabbit-Alexa-Fluor-660	Molecular Probes, Invitrogen (A21074)	IF: 1:2,000
pc-goat-α-rabbit-Alexa-Fluor-680	Molecular Probes, Invitrogen (A21076)	WB: 1:20,000
pc-goat-α-rabbit-HRP	Jackson Immuno Research	WB: 1:5,000
pc-rat-α-goat-HRP	Jackson Immuno Research	WB: 1:5,000

pc = polyclonal.

7.1.11 Standard Buffers

- **AB-buffer:**

HEPES	10.0 mM
NaCl	140.0 mM
$CaCl_2$	2.5 mM

- **Amido-black staining solution**

Amido-black 10B in H_2O	30 mg/ml

- **Destain-buffer**

Acetic acid	10 % (v/v)
Isopropanol	8 % (v/v)

- **DNA loading buffer:**

Tris-HCl, pH 7.5	50 mM
EDTA	50 mM
Glycerol	50 % (v/v)
Bromphenol blue	0.25 % (v/v)

- **EM-Fix I**

PHEM	100 mM
Paraformaldehyde	4 % (w/v)
Glutaraldehyde	0.1 % (w/v)
in PBS	

- **EM-Fix II**

PHEM	100 mM
Paraformaldehyde	4 % (w/v)
in PBS	

- **Endocytosis-Detachment (ED) buffer**

EDTA	50 mM
Trypsin	2 mg/ml
in PBS	

- **Endocytosis-FACS (E-FACS) buffer**

FCS	2 % (v/v)
in PBS	

- **Endocytosis-Stop (E-Stop) solution**

FCS	7 % (v/v)
in PBS	

- **Endocytosis-washing (EW) buffer**

Sodium acetate, pH 5.5	100 mM
NaCl	50 mM
in PBS	

- **Kinase-activation buffer (KAB):**

HEPES, pH 8.0	50 mM
EDTA	5 mM
NaCl	150 mM
$MgCl_2$	10 mM
Triton X-100	0.02 % (v/v)

- **P1-buffer:**

$NaHCO_3$, pH 8.3	200 mM
NaCl	500 mM

- **P2-buffer:**

HCl	1.0 mM

- **P3-buffer:**

Ethanolamine	500 mM
NaCl	500 mM
HCl, pH 8.3	

- **P4-buffer:**

Acetic acid	100 mM
NaCl	500 mM
NaOH, pH 4.0	

- **P5-buffer:**

Na_2HPO_4, pH 7.0	500 mM
NaN_3	0.1 %

- **Paraformaldehyde (PFA):**

Paraformaldehyde	3 % (w/v)
in PBS, pH 7.2	

- **PBS (Phosphate buffered saline):**

NaCl	96.0 mM
Na_2HPO_4 x $2H_2O$	10.0 mM
NaH_2PO_4 x H_2O	2.3 mM
pH 7.4	

- **PBS-T:**

NaCl	96.0 mM
Na_2HPO_4 x $2H_2O$	10.0 mM
NaH_2PO_4 x H_2O	2.3 mM
Tween 20	1.0 mM
pH 7.4	

- **PFA (Paraformaldehyde):**

Paraformaldehyde	3 % (w/v)
in PBS, pH 7.2	

- **R1-buffer:**

PBS	100 %

- **R2-buffer:**

Tris-HCl, pH 8.0	50 mM
NaCl	500 mM

- **R3-buffer:**

Tris-HCl, pH 9.0	50 mM
NaCl	500 mM

- **R4-buffer:**

Glycine-HCl, pH 2.5	50 mM
NaCl	150 mM

- **R5-buffer:**

Tris-HCl, pH 8.0	1 M

- **ROCK-Lysis buffer**

Tris-HCl, pH 7.5	10 mM
$Na_4P_2O_7$ x 10 H_2O	40 mM
EDTA	5 mM
NaCl	150 mM
NP-40	1 % (v/v)
Na-Deoxycholate	0.5 % (v/v)
SDS	0.025 % (v/v)
Na_3VO_4 (fresh)	1 mM
protease inhibitors (fresh)	1: 1000
filtration (0.45 µm)	

- **ROCK-Wash buffer**

Tris-HCl, pH 7.5	50 mM
$Na_4P_2O_7$ x 10 H_2O	40 mM
$MgCl_2$ x 6 H_2O	10 mM
NaCl	50 mM
Glycerole	10 % (v/v)
Brij-35	0.03 % (v/v)
DTT (fresh)	1 mM
Na_3VO_4 (fresh)	1 mM
protease inhibitors (fresh)	1: 1000
filtration (0.45 µm)	

- **SDS-PAGE-Running buffer:**

Tris-HCl, pH 6.8	250 mM
Glycine	200 mM
SDS	0.1 %

- **SDS-PAGE-Running gel stock-solution:**

Tris-HCl, pH 8.8	1.5 M
SDS	0.4 % (v/v)

- **SDS-PAGE-Stacking gel stock-solution:**

Tris-HCl, pH 6.8	0.6 M
SDS	0.4 % (v/v)

- **SDS-SB (SB, 2x):**

Tris-HCL, pH 6.8	130 mM
β-Mercaptoethanol	10 % (v/v)
Glycerol	10 % (v/v)
SDS	6 % (w/v)
Bromphenol blue	tip of a spatula

- **SDS-SB (6x):**

Tris-HCL, pH 6.8	390 mM
β-Mercaptoethanol	30 % (v/v)
Glycerol	30 % (v/v)
SDS	10 % (w/v)
Bromphenol blue	tip of a spatula

- **TAE-buffer (50x):**

Tris-acetic acid, pH 7.8	2 M
Sodium acetate	250 mM
EDTA	500 µM

- **TBS (Tris buffered saline)**

Tris-HCl, pH 7.6	20 mM
NaCl	140 mM

- **TBS-T**

Tris-HCl, pH 7.6	20 mM
NaCl	140 mM
Tween 20	1 mM

- **TE-buffer:**

Tris-HCl, pH 7.8	10 mM
EDTA	1 mM

- **TFB I:**

Sodium acetate, pH 5.8	30 mM
$MnCl_2$	50 mM
NaCl	100 mM
$CaCl_2$	10 mM
Glycerol	15 % (v/v)

- **TFB II:**

MOPS, pH 6.5	10 mM
$CaCl_2$	75 mM
NaCl	10 mM
Glycerol	15 % (v/v)

- **Transfer-buffer:**

Tris-HCl, pH 8.8	25 mM
Glycine	192 mM
Methanol	20 % (v/v)
SDS	0.05 % (w/v)

7.1.12 Software

The software used for this study is listed in tab. 5.

Table 5: Analytical and processing software.

Software	Version	Source
Adobe Photoshop CS2	9.0x211	Adobe Systems
CellQuestPro	4.0.2	BD Biosciences
analySIS	3.0	Soft Imaging System
ImageJ	1.36b	http://rsb.info.nih.gov/ij
Imaris	—	Bitplane
Leica Confocal Simulator	2.5.1227a	Leica
Leica FW4000	—	Leica
Odyssey Application Software	2.0.40	LI-COR Biosciences
Quantity One 1-D Analysis Software	4.4.1	http://www.bio-rad.com
VirtualDub	1.6.14	http://www.virtualdub.org
Zeiss LSM Image Browser	4.2	http://www.zeiss.de

7.2 Molecular Biology

7.2.1 Transformation of Bacteria

E. coli cells were grown aerobically in 500 ml autoclaved LB medium containing the required additives. When the culture reached an optical density OD_{578} of 0.6 cells were harvested by centrifugation (10 min at 6,000 x *g* and 4°C), suspended in 200 ml TFB1 and incubated on ice for 5 min. After subsequent centrifugation (5 min at 3,000 x *g* and 4°C) cells were suspended in two volumes of TFB2 (referring to the volume of the cell sediment), incubated on ice for 30 min and divided into 40 µl aliquots. These were either immediately used for transformation or stored at – 80°C
Transformation of chemo-competent cells was applied as standard transformation method. 40 µl of $CaCl_2$-competent cells were combined with 1-2 µl DNA solution (50 µg/ml) and subjected to a heat shock for 60 s at 42°C. Immediately after the transformation cells were cooled on ice for 2 min. Afterwards 1 ml of preheated antibiotic free LB medium was added and cells were incubated at 37°C for 30 min (ampicillin resistance) or 1 h (kanamycin resistance). Depending on the expected colony density, different volumes were streaked on agar plates containing the appropriate antibiotics and plates were incubated overnight at 37°C.

7.2.2 Preparation of Plasmid DNA

Plasmid DNA was purified *via* alkaline lysis in combination with anion exchange chromatography using the "NucleoBond PC 500 Kit" (Macherey-Nagel). Purification was performed according to the manufacturer's instructions. Briefly, 250 ml (Maxi preparation) of an overnight culture were harvested by centrifugation (20 min at 5,000 x *g* and 4°C) and bacterial cells suspended in 11 ml S1 buffer. Following addition of 11 ml S2 buffer, the sample was carefully mixed by inverting the tube and incubated at RT for 5 min. Next, 11 ml S3 buffer were added, the sample was again carefully mixed and further incubated on ice for 5 min. Following centrifugation (15 min at 15,000 x *g* and 4°C) and filtration for removal of cell debris, the supernatant was loaded on N2 buffer equilibrated anion exchange cartridges for further purification. Therefore, the cartridge was washed twice with 18 ml N3 buffer and plasmid DNA was eluted with 15 ml N5 buffer and precipitated by addition of 11 ml isopropanol at RT. Following centrifugation (20 min at 15,000 x *g* and -20°C), the DNA was washed in washed twice with 70 % (v/v) ethanol. After all traces of ethanol had evaporated, the DNA was solubilized in 200 µl TE buffer. Following a first determination of DNA concentration, the concentration was adjusted to 1.0 µg/µl by addition of respective amounts of TE buffer. Finally, quality of the DNA and identity of the clone were verified by digestion with restriction endonucleases and electrophoretic separation.

7.2.3 Determination of DNA Concentration

The concentration of a DNA solution was determined by measuring the absorbance at 260 nm and additionally at 280 nm in a photometer to account for protein impurities. For a pure DNA solution an OD_{260} of one corresponds to a dsDNA concentration of 50 ng/µl. The purity of the DNA solution can be deduced from the ratio of OD_{260} to OD_{280}: With an OD_{260}/OD_{280} ratio of 1.8-2.0 the DNA was considered as pure.

7.2.4 Digestion of DNA with Restriction Endonucleases

Restriction of plasmid-DNA was carried out using restriction endonucleases purchased from Fermentas. Reaction buffers as well as concentrations of enzymes and DNA were chosen

according to the manufacturer's instructions. The digestion was allowed to proceed for 2-3 h at 37°C or over night at RT and was, if possible, followed by heat inactivation of the restriction endonucleases (20 min at 65°C or 80°C, depending on the enzyme).

7.2.5 Electrophoretic Separation of DNA

For analytical separation of DNA fragments, agarose gels consisting of 1 % (w/v) agarose and 0.7 µg/ml ethidium bromide in TAE buffer were prepared. Depending on the gel size, a voltage of 80-100 V was applied. DNA fragments migrate towards the anode with a velocity that is proportional to the negative logarithm of their size. Prior to loading, DNA samples were mixed with DNA loading dye to facilitate loading and to indicate the progress of the samples in the gel. GeneRuler DNA Ladder Mix was used as size standard according to the manufacturer's instructions. After electrophoresis, DNA was detected *via* its fluorescence under UV light (λ = 254 nm).

7.3 Biochemistry

7.3.1 Production of Cell Lysates

For SDS-PAGE, Western blotting, IP and IVKA, adherent cells in cell culture dishes were washed with PBS and subjected to sufficient amounts of ice-cold ROCK-Lysis (Coleman *et al.*, 2001) buffer (6 well: 100 µl; 6 cm: 200 µl; 10 cm: 450 µl). Following detachment with a plastic cell scraper on ice, cells were thoroughly lysed by pipetting and lysates were subsequently transferred to a tube. After centrifugation (15 min at 13,000 rpm and 4°C) supernatants were transferred into a new tube, stored at -20°C or immediately subjected to IP, IVKA or determination of overall protein concentrations, respectively.

7.3.2 Determination of Overall Protein Concentration

Overall protein concentrations of cell lysates were determined using the "Micro BCA Protein Assay Kit" (Pierce) according to manufacturer's instructions. The bicinchoninic acid (BCA) protein assay combines the reduction of Cu^{2+} to Cu^{+} by protein in an alkaline medium with the highly sensitive and selective colorimetric detection of the cuprous cation (Cu^{+}) by bicinchoninic acid. The intensity of the color produced is proportional to the number of peptide bonds participating in the reaction. Briefly, 200 µl of BCA solution (BCA reagent A + 2 % (v/v) BCA reagent B) were added to 10 µl of at least two dilutions of cell lysates in a 96-well plate in a duplicate experiment. Following 30 min of incubation at 37°C, absorption at a wavelength of 540 nm was photometrically measured in an ELISA-reader (Labsystems Original Multiskan MS). Values were normalized to background levels obtained by lysis buffer only and protein concentrations were calculated relative to a standard curve obtained with bovine serum albumin (BSA).

7.3.3 Discontinuous SDS-PAGE

Proteins were analyzed by SDS-PAGE (sodium dodecyl sulfate polyacrylamide gel electrophoresis) as described by Laemmli (Laemmli, 1970) with modifications by Righetti (Righetti, 1990) for discontinuous SDS-PAGE. Cell lysates were denatured by heating to 95°C for 5 min in 6 x SDS sample buffer (SB). Equal amounts of overall protein were loaded onto the gel (tab. 6) which was run at 25 mA in SDS-PAGE-Running buffer. During electrophoresis, proteins were first focused in the stacking gel and subsequently separated according to their relative molecular mass in the running gel. The size standard employed was a broad range

prestained protein molecular weight marker (broad range prestained protein molecular weight marker, 6-175 kDa; New England Biolabs). Following SDS-PAGE, gels were subjected to Western blotting.

Table 6: Production of a SDS-PAGE gel.

Compound	Stacking gel	Running gel		
		8 %	10 %	14 %
MQ-water	0.8 ml	1.9 ml	1.7 ml	1.1 ml
SDS-PAGE-Stacking gel stock-solution	0.3 ml	–	–	–
SDS-PAGE-Running gel stock-solution	–	1.0 ml	1.0 ml	1.0 ml
Acrylamide/Bisacrylamide (30 %)	0.2 ml	1.1 ml	1.3 ml	1.8 ml
APS (10 %)	8.0 µl	13.0 µl	13.0 µl	13.0 µl
TEMED	3.0 µl	6.0 µl	6.0 µl	6.0 µl

APS = Ammonium persulfate, TEMED = N,N,N',N'-Tetramethylethylenediamine.

7.3.4 Western Blotting

Proteins separated by SDS-PAGE were transferred in a semi-dry process onto a nitrocellulose or polyvinylidenfluorid (PVDF)-membrane, which bind the proteins by polar interactions. Therefore, PVDF-membranes were additionally incubated in methanol for 10 min before they were incubated in transfer-buffer, similarly to the SDS-gel, the Whatman-blotting paper and the nitrocellulose-membrane. They were assembled in the following order on the blotting apparatus: Cathode, Whatman-blotting paper, membrane, SDS-gel, Whatman-blotting paper, anode. A current of 2 mA/cm^2 was applied for 90-120 min at 8 V. Nonspecific binding sites of the membrane were saturated in blocking-solution (5 % milk powder (w/v)) at RT for 20 min and slight shaking. Proteins immobilized on the membrane were specifically probed with primary antibodies (tab. 3) over night at 4°C in blocking solution and under slight shaking. Next, membranes were washed three times for 10 min with washing-buffer and incubated for 45 min at RT or over night at 4°C with the secondary antibody. Secondary antibodies were directed against the respective primary antibody and were either coupled to horse radish peroxidase for evaluation by enhanced chemiluminescence (ECL) or to Alexa Fluor-680 for evaluation with the LI-COR-System (tab. 4). After three additional washing steps with washing-buffer for 10 min, membranes were washed with PBS or TBS, respectively and were evaluated with the respective method: For ECL, membranes were incubated with SuperSignal West Pico reagent (Pierce) that was supplemented with SuperSignal West Femto reagent at low signals, subjected to a photosensitive film and subsequently developed. For evaluation with the LI-COR-System, membranes were scanned (LI-COR Odyssey) and analyzed with the LI-COR software.

7.3.5 Immunoprecipitation (IP) and *in vitro* Kinase Assay (IVKA)

To analyze the influence of FHOD1 expression on ROCK1 activity level, an IVKA was performed. Therefore, HeLa cells in a 6 well plate were transfected with combinations of expression plasmids encoding for vector only, Myc-ROCK-wt and HA-FHOD1-wt. At the following day and a 90 % cell confluency, medium was removed and cells carefully scraped with a cell scraper in 2 ml ice cold PBS. After centrifugation (5 min at 2,000 rpm and 4°C), pellet was lysed in 250 µl ice cold ROCK-Lysis buffer by thoroughly pipetting and subsequently incubation

on a rotator for 20 min at 4°C. Afterwards, the lysate was centrifuged (15 min at 13,000 rpm and 4°C) and 50 µl of the supernatant subjected to Western blotting (input control), whereas the rest residual amounts were transferred into a new 1.5 ml cup (safe lock. Next, 2.0 µl antibody (mc-mouse-α-c-Myc, 9E10) was added and the solution incubated on a rotator for 1 h at 4°C. Following addition of 20 µl thoroughly suspended ProteinA-sepharose beads, the solution was again incubated on a rotator for 2 h at 4°C. Subsequently, the beads were washed three times with 500 µl ice cold ROCK-Wash buffer and two times with 500 µl ice cold kinase-activation buffer (KAB). At the last step, 50 µl of the mixture were removed and subjected to Western blotting (IP control). Following centrifugation (5 min at 2,000 rpm and 4°C), supernatant was removed and beads were subjected to kinase reaction. Therefore, they were suspended in 30 µl KAB containing 4 µCi [^{32}P]-γATP, 10 mM ATP 1 µg substrate (myelin basic protein, Sigma) and either 5.5 µl MQ or 5.5 µl ROCK inhibitor (Y-27632, final concentration 900 µM) were added for specificity control. After 30 min shaking at 30°C, 7 µl 6xSDS-SB were added, the samples boiled for 5 min at 96°C and subsequently centrifuged (20 s at 13,000 rpm and RT). Samples were loaded on a SDS-PAGE (14 %) and after separation were transferred by Western blotting to a nitrocellulose membrane which was finally incubated for 24 h with a photosensitive film.

7.3.6 Purification of rabbit-α-FHOD1 Antibody

For production of polyclonal antiserum directed against FHOD1 protein, two synthetically produced peptides present in human and mouse FHOD1 protein (#20403: amino acid residues 1-14, MAGGEDRGDGEVSC; #20404: amino acid residues 356-370, KPSSEEGKKSRRSLEC; Peptide Specialty Laboratories) as previously described (Gasteier *et al.*, 2005). For purification of antibodies the final bleeding of immunized rabbits was subjected to affinity chromatography.

7.3.6.1 Preparation of the Affinity Column

For subsequent purification of antibodies an affinity column (HiTrap NHS activated HP Column, Amersham Biosciences) with a bed volume of 1 ml was initially loaded with FHOD1 derived synthetic peptides used for production of polyclonal antiserum. Therefore, the column was three times washed at a maximum speed of 1 drop/2 s with 2 ml of ice cold P2-buffer and subsequently incubated with 1 ml P1-buffer containing 10 mg synthetic peptides (5 mg #20403 + 5 mg #20404) for 30 min at RT. Afterwards, the column was washed three times with 2 ml P3-buffer, three times with 2 ml P4-buffer and three times with P3-buffer, incubated for 30 min at RT and washed again, three times with 2 ml P4-buffer, three times with 2 ml P3-buffer and finally three times with 2 ml P4-buffer. The column was stored in P6-buffer at 4°C.

7.3.6.2 Purification of FHOD1 Specific Antibodies by Affinity Chromatography

To affinity purify specific antibodies directed against FHOD1 from the final bleeding of an immunized rabbit (#1641) the prepared column was initially washed at a maximum speed of 1 drop/2 s with 10 ml R1-buffer, followed by washing with 5 ml R2-buffer, 5 ml R3-buffer and 10 ml R1-buffer. For specific interaction of antibodies with the column bound synthetic peptides, the column was loaded with rabbit serum and incubated for 1 h at RT. Subsequently, the column was rinsed with 6 ml R5-buffer while flow through (FT) was collected in three fractions (FT1-3). The bound antibodies were stripped by rinsing with 4 ml R4-buffer. Therefore, eluate was collected on ice in reaction cups containing either 200 µl (fraction #E1 + 800 µl eluate) or 400 µl ice cold R5-buffer (#E2, #E3, each with 1600 µl eluate). The column was washed again with 10 ml R1-buffer, 5 ml R2-buffer, 5 ml R3-buffer and 10 ml R1-buffer and was stored in P5-buffer at 4°C. To evaluate purification efficiency, 5 µl of each fraction (FT1, FT2, FT3, #E1,

#E2 and #E3) were spotted on a nitrocellulose membrane. To analyze total amounts of protein, the membranes were incubated by slow shaking for 10 min at RT with Amido-black staining solution, twice for 5 min at RT with destain-buffer and finally washed with water for 10 min. Eluate fractions containing protein (#E2 and #E3) were pooled and concentrated with a R1-buffer equilibrated spin concentrator (Vivaspin 2 ml, 10,000 MWCO, Vivascience) by centrifugation (10-15 min at 4,500 rpm and 4°C) to a volume of 400 µl (10 fold concentration). Antibody solution was aliquoted and stored at -20°C, whereby unfrozen samples were stored at 4°C for maximal two weeks.

7.3.6.3 Specificity Test of Purified Antibodies

To analyze the specificity of the affinity purified antibodies, 20 µl antibody solution were incubated on ice for 1 h with 32 µg synthetic peptides (16 µg #20403 + 16 µg #20404) used for rabbit immunization and affinity purification. Subsequently, either cellular lysates (Western blot) or cells (immuno fluorescence, EM), respectively, were then probed with the purified antibody or epitope inhibited antibody as described in the previous chapters.

7.4 Cell Biology

7.4.1 Cultivation of Adherent Cell Lines

Usually, adherent cell lines were cultivated in 75 cm^2 cell culture flasks, covered with approx. 15 ml half synthetic cell culture medium which contained vitamins, amino acids, salt, glucose and a pH indicator in combination with a fresh supplement of heat inactivated fetal calve serum (FCS), glutamate and antibiotics (see chapter 7.1.4). Cells were kept in an incubator at 37°C with a humid atmosphere containing 5 % CO_2. For subculturing every 2-3 days, adherent cells were washed with sterile PBS and treated with 2 ml trypsin/EDTA for approx. 5 min at RT or 37°C till cells were detached from the cell culture flask. Following addition of 5 ml medium, cells were carefully separated by repeated pipetting. Depending on the cell line, a defined amount of these cells was further cultivated in 15 ml fresh medium.

7.4.1.1 Cryo-Conservation of Cell Lines

For cryo-conservation, adherent cells were cultivated in a 150 cm^2 cell culture flask to approx. 75 % confluency with the appropriate cell culture medium. Following detachment with 4 ml trypsin/EDTA and addition of 9 ml medium, cells were centrifuged (5 min at 1,200 rpm and RT) and carefully suspended in 5 ml freezing medium by repeated pipetting. 1 ml cell suspension was transferred into cryo-conservation tubes, wrapped in tissue and subjected to refreezing at -80°C for 2 days. Finally, cells were stored under fluid nitrogen.
For further cultivation, cells were rapidly thawed at 37°C, washed with cell culture medium and usually transferred to a 25 cm^2 flask containing fresh medium.

7.4.2 Transient Transfection of Animal Cells

Plasmid DNA was transiently introduced into animal cells by lipofection. This method describes a form of transfection based on complexation of the negatively charged DNA by positively charged cationic lipids. These complexes can be internalized by the cells resulting in an expression of the encoded proteins when the plasmid DNA localizes inside the nucleus. In contrast to stable transfection, in which the genetic information is stably introduced into the host's genome, the introduced genetic information in transiently transfected cells is subsequently lost over time.

For lipofection, glass coverslips with cells seeded at the previous day at a density yielding to 50-70 % confluency for transfection, were transferred into a 24 well plate, washed with PBS and covered with 400 µl OptiMEM I. Afterwards, 100 µl OptiMEM I were combined with 1 µg plasmid DNA in a 1.5 ml test tube. For co-expression experiments of different proteins, equal amounts of the respective plasmids were used, whereupon the total amount of DNA did not exceed 1 µg. The solution was mixed by pipetting and incubated for 10 min at RT. Next, 2 µl Lipofectamine 2000 or 2.5 µl Metafectene were added and the solution again mixed by pipetting. Following incubation for 15 min at RT, the mixture was carefully added to the cells dropwise. The cells were incubated for 3 h at 37°C in the incubator. Next, the transfection mixture was removed, medium was added and the cells were incubated for additional 20-24 h for expression of the respective proteins.
The described amounts used for transfection are related to a 24 well format. For transfections in 6 well plates, 6 cm and 10 cm dishes please refer to tab. 7.

Table 7: Transient transfection of animal cells by lipofection.

Cells		**Transfection solution**			
Dish	**OptiMEM I** [ml]	**OptiMEM I** [µl]	**Plasmid DNA** [µg]	**Lipofectamine 2000** [µl]	or **Metafectene** [µl]
24 well	0.4	100	1.0	2.0	2.5
6 well	0.8	200	2.0	4.0	5.0
6 cm	2.0	500	5.0	10.0	12.5
10 cm	4.0	1000	10.0	15.0	20.0

7.4.3 RNAi Based Knockdown of Endogenous FHOD1

RNA interference (RNAi) describes a basic mechanism of eukaryotic cells for post-transcriptional regulation of gene expression and was identified in 1998 by C. C. Mello and A. Fire (Fire *et al.*, 1998). Mediated by the antisense strand of a short doublestranded RNA (dsRNA) oligonucleotide (19 to 21 nucleotides) termed small interfering RNA (siRNA) the complementary cellular messenger RNA (mRNA) encoding for a gene product is repressed or degraded, resulting in a reduced production or knockdown of the respective protein.
In this work, dsRNA oligonucleotides directed against FHOD1 were transfected into target cells by lipofection. Depending on the cell line, different transfection methods and reagents were used (tab. 8). For transfection, the indicated amounts of cells were seeded respective to the used dish format. On the following day, cells were washed twice with PBS before OptiMEM I was added as indicated. For transfection with Oligofectamine or Lipofectamine 2000, the transfection reagent and dsRNA were separately resolved in OptiMEM I, mixed, incubated for 10 min at RT, combined and incubated again for 15 min at RT. Finally, the mixture was carefully added to the cells dropwise. For transfection with HiPerfect, dsRNA fast first added to OptiMEM I, mixed and incubated for 10 min at RT. Afterwards, HiPerFect was added, the solution carefully mixed, incubated for 15 min at RT and finally added to the cells dropwise. After 3 h of incubation in the incubator, either twofold amounts of medium was added to the transfection solution (Oligofectamine, HiPerFect) or transfection solution was removed first before medium was added (Lipofectamine 2000).

Table 8: RNAi based knockdown of FHOD1 in different cell lines.

Cells			Transfection solution					
Cell line	**Dish**	**Seeding** [cells]	**OptiMEM I** [ml]	**OptiMEM I** [µl]	**dsRNA [5 µM]** [µl]		**Transfection reagent** [µl]	
CHO	6 well	1.5 x 10^5	1.0	100	P1	2.5	HiPerFect	6.0
CHO	6 cm	3.0 x 10^5	2.75	200	P1	6.25	HiPerFect	12.0
HeLa	6 well	3.0 x 10^5	1.0	2 x 100	P1, P2	2.5	Oligofectamine	4.0
HeLa	6 cm	6.0 x 10^5	2.5	2 x 250	P1, P2	6.25	Oligofectamine	10.0
HeLa	10 cm	2.0 x 10^6	5.0	2 x 500	P1, P2	18.75	Oligofectamine	20.0
MEF	6 well	1.5 x 10^5	1.0	2 x 100	P1	2.5	Lipofectamine 2000	2.0
NIH3T3	6 well	1.5 x 10^5	1.0	2 x 100	P1	2.5	Lipofectamine 2000	2.0
NIH3T3	6 cm	3.0 x 10^5	2.5	2 x 250	P1	6.25	Lipofectamine 2000	4.0
NIH3T3	10 cm	1.2 x 10^6	5.0	2 x 250	P1	12.5	Oligofectamine	24.0

P1, P2: see tab. 1

On the following day, cells were split and seeded on coverslips in the respective dish format. 48 h after the first transfection, cells were again transfected as described. Further transfections with plasmid DNA were subsequently performed as described (see chapter 7.4.2) or expression of SH4-domains was induced by addition of 1 µg/ml dox. On the following day, coverslips were fixed and cells were harvested for knockdown control *via* Western blotting.

7.4.4 Induction of Gene Expression

In this study, HeLa and CHO cell lines were employed that stably or transiently expressed SH4-domains controlled by a dox inducible promotor based on the Tet-on/off system (Gossen and Bujard, 1992). For induction of gene expression, 1 µg/ml dox was added to medium for at least 24 h.

7.4.5 Microscopy

7.4.5.1 Fixation, Permeabilization and Staining of Cells

For microscopical analysis of protein localizations in cells that were grown on coverslips, cells were fixed with 3 % PFA (w/v) for 10 min at 4°C. Subsequently they were washed with PBS and were stored for up to one week at 4 °C or were immediately processed. Therefore, coverslips were transferred to a sheet of parafilm and cells were covered for 60 s with a solution of 0.1 % Triton X-100 (v/v) in PBS for permeabilization. Following brief washing with PBS, cells were treated for 20 min with blocking solution consisting of 1 % BSA (w/v) in PBS. Thereafter, cells were exposed to 100 µl of staining solution containing 1 % BSA (v/v) in PBS and primary antibody as indicated in tab. 3 for 1 h at RT in darkness. Coverslips were carefully washed three times with PBS and were subsequently incubated with 100 µl staining solution containing PBS and the respective fluorescently labeled secondary antibody as outlined in tab. 4. After 1 h at RT in darkness, coverslips were carefully washed four times with PBS and once with MQ. For mounting, the carefully drained but not completely dry coverslips were placed upside down onto a drop of 15-25 µl mounting medium (Lin-Mount) spotted onto a glass slide.

For stain of F-actin or chromatin, fluorescently labeled Phalloidin or Hoechst 33258, respectively, was added, diluted in PBS as depicted in tab. 9 directly after permeabilization for 30 min at RT in darkness or in combination with the secondary antibody.

Table 9: Staining of F-actin filaments and chromatin.

Substance	Source (catalog number)	Usage/Dilution
Phalloidin-Alexa-Fluor-350	Molecular Probes, Invitrogen (A22281)	IF 1:600
Phalloidin-Alexa-Fluor-633	Molecular Probes, Invitrogen (A22284)	IF 1:600
Phalloidin-Alexa-Fluor-660	Molecular Probes, Invitrogen (A22285)	IF 1:600
Phalloidin-FITC	Sigma (P5282)	IF 1:1,000
Phalloidin-TRITC	Sigma (P1951)	IF 1:1,000
Hoechst 33258	Sigma (861405)	IF 1:10,000

IF = immuno-fluorescence

For phospho-specific stain, all solutions were prepared in TBS instead of PBS and treatment with primary antibodies occurred for at least 12 h at 4°C in darkness. Therefore, coverslips were placed upside down onto 75 µl staining solution spotted onto parafilm in a chamber supplemented with wet tissues for a humid atmosphere.

7.4.5.2 Microscopy of Fixed Cells

Cells fixed and stained on coverslips were analyzed either by fluorescence microscopy using an Olympus IX70 inverted microscope (UPlanApo 40x/1.00 oil ∞/-; PlanApo 60x/1.40 Oil ∞/0.17; UPlanFL 100x/1.30 Oil) or by confocal microscopy using a Zeiss LSM 410 confocal microscope.

7.4.5.3 Live Cell Microscopy for Real-Time Imaging

For live cell imaging, CHO cells were seeded in Lab-Tek chamber slides (Nunc) one day before analysis. Mid-cell z-sections of blebbing cells were obtained by usage of a Zeiss LSM 410 confocal microscope at RT. 2D and 3D real-time sequences were acquired using a PerkinElmer Life and Analytical Sciences Ultraview LCI spinning disc confocal (Boston) mounted on a Nikon Eclipse TE200 microscope stand equipped with a Nikon Plan Apo 60x 1,4NA oil objective. The microscope was kept at 37°C in a microscope incubator box (EMBL Heidelberg). Time-lapses of single sections were acquired for up to 10 min with 150 ms exposure time (6.6 fps) using binning 1x1.
4D series were acquired for up to 15 min with 50 ms exposure time per section and a step size of 0.5 µm between sections covering the whole cell body. Kymographs of the 2D real-time sequences were created using "ImageJ" plugins as described (Pepperkok *et al.*, 2005) employing only steps 6-8 in the section "Analyzing the Kinetics of Transport Carriers". Visualization of 4D data was perfomred using "Imaris" (Bitplane).

7.4.5.4 Electron Microscopy (EM)

For EM, 24 h after second RNAi treatment HeLa cells grown in a 6 well plate at a confluency of approx. 90 %, washed in PBS, treated for 3 min with 20 mM EDTA in PBS at 37°C and carefully scraped in PBS with a cell scraper. To determine knockdown efficiency, 50 % of the cells were subjected to Western blot analysis as described, whereas the rest was transferred to a 1.5 ml cup. Cells were centrifuged (5 min at 2,000 rpm and RT), suspended in 1 ml EM-Fix I

solution, centrifuged again and incubated for 90 min at RT without suspension. After additional centrifugation, EM-Fix I solution was substituted with 1 ml ice cold EM-Fix II solution and cells were stored at 4°C. Following embedding, sectioning and staining for endogenous FHOD1 (tab. 3) in combination with 5-10 nm ProteinA gold, sections were examined with a Zeiss EM10 microscope.

7.4.5.5 Scanning Electron Microscopy (SEM)

For SEM, stable CHO cells grown on a coverslip were induced for SH4-domain expression for 24 h and fixed with 2.5 % glutaraldehyde (v/v) in 100 mM PBS with 1 % sucrose (w/v), dehydrated in a graded series of ethanol and critical-point dried using carbon dioxide. Afterwards, cells were rotary-coated by electron beam evaporation using a BAF 300 freeze-etching device (Bal-Tec) with a single layer of platinum-carbon (coating thickness 3 nm). The samples were imaged in a Hitachi S-5200 in-lens field emission scanning electron microscope at an accelerating voltage of 4 kV using the secondary electron signal.

7.4.6 Inhibition of PM Blebbing by Drug-Treatment

To investigate the influence of cellular determinants on PM blebbing, cells grown on coverslips were treated with various inhibitory drugs. Initially for synchronization of PM bleb formation, PM blebbing was efficiently abrogated by treatment with 10-90 µM Y-27632 for 2 h. After extensive washing of the cells with PBS, *de novo* bleb formation was allowed for 3 hours in medium containing a solvent control or a specific drug in the indicated amounts as depicted in tab. 10. Cells stably expressing SH4-domains were drug treated in the presence of 1000 ng/ml dox during the whole procedure. Subsequently, the cells were fixed and stained for F-actin and α-tubulin, respectively.

Table 10: Drug-treatment for inhibition of PM blebbing.

Drug	Solvent	Source (catalog number)	Cell line	Final concentration [µM]
(-) Blebbistatin	DMSO	Calbiochem, Merck (203391)	CHO/Hela	100
Cytochalasin D	Ethanol	Calbiochem, Merck (250255)	CHO	1
Cytochalasin D	Ethanol		HeLa	2
Latrunculin B	DMSO	Calbiochem, Merck (428020)	HeLa	25
Nocodazole	DMSO	Calbiochem, Merck (487928)	CHO	100
Nocodazole	DMSO		HeLa	384
PP1	DMSO	Calbiochem, Merck (529579)	CHO	1
PP1	DMSO		CHO	10
PP1	DMSO		HeLa	50
SU-6656	DMSO	Calbiochem, Merck (572636)	CHO	1
SU-6656	DMSO		CHO	10
Y-27632	MQ	Calbiochem, Merck (688001)	CHO/HeLa	10
Y-27632	MQ		CHO/HeLa	90

7.4.7 Induction, Detection and Inhibition of Apoptosis

Apoptosis or programmed cell death is a highly regulated process resulting in cellular decease. For induction of apoptosis, HeLa cells grown on coverslips were treated for 3 h with a combination of 50 µg/ml recombinant human tumor necrosis factor-α (rhTNF-α) and 5 µg/ml Cycloheximide (Chx). Apoptotic HeLa cells were either determined by stain with Hoechst 33268 for detection of condensed chromatin or by an Annexin V mediated surface specific stain of externalized phosphatidyl-serine (PS). Therefore, living cells were carefully washed with AB-buffer and incubated with staining solution consisting of AB-buffer fluorescently labeled Annexin V-Alexa-Fluor-568 at a dilution of 1:50 (v/v) for 15 min at RT in darkness. Finally, cells were fixed and stained as already described.
CHO cells grown on coverslips were induced for apoptosis either by treatment with 4 % DMSO (v/v) in medium for 5 h or by treatment with 200 µg/ml Etoposide (Eto) in combination with 200 µg/ml Chx in medium for 12 h. For apoptosis detection, cells were either stained with Hoechst 33268 for identification of cells with condensed chromatin or apoptosis was evaluated by a transferase-dUTP nick end labeling (TUNEL) assay (Gavrieli *et al.*, 1992). During TUNEL reaction, the enzyme deoxynucleotidyl transferase (TdT) specifically binds to terminal 3'-OH ends of fragmented DNA and incorporates dUTP fluorescently labeled with tetramethyl rhodamine (TMR). Therefore, cells were fixed, permeabilized and subjected to TUNEL reaction by incubation with staining solution consisting of enzyme solution, label solution and PBS (1:10:20) for 1 h at RT in darkness (*In situ* Cell Death Detection Kit, TMR red, Roche). Finally, cells were stained for F-actin and chromatin.
For inhibition of caspase mediated apoptosis, cells were cultured in the presence of 100 µM zVAD-fmk.

7.4.8 VSV-G Transport Assay

The capacity for Golgi mediated protein transport can be evaluated by the usage of specific cargo proteins such as the temperature sensitive vesicular stomatitis virus (VSV) ts-045-G glycoprotein. At the non-permissive temperature of 39.5°C the cargo marker accumulates in the ER due to a reversible folding defect. When shifted to the permissive temperature of 31°C, correctly folded ts-045-G is rapidly transported from the ER through the Golgi apparatus to the cell surface, where its appearance can be monitored using an antibody against the lumenal domain of the glycoprotein (Pepperkok *et al.*, 1993). Therefore, 5 h after the second RNAi treatment for FHOD1 knockdown, HeLa cells were transformed with DNA encoding ts-045-G fused to CFP by infection with adenoviruses (MOI of 10) for 17 h at 39.5°C. At the following day, medium was supplemented with 1 M HEPES buffer (pH 7.5) to a final concentration of 25 mM HEPES and temperature was shifted to 31°C for up to 90 min. Cell were fixed and stained without permeabilization with mc-mouse-α-ts-045-G antibody (tab. 3). Following analysis of the cells by fluorescence microscopy, internal and external amounts of ts-045-G-CFP protein were determined by quantification of the respective mean grey values from single cells using the "Freehand selection" tool in combination with the "Measurement" tool of "ImageJ" software. The relative protein transport of single cells was calculated by the ratio of external to total signal.

7.4.9 Adhesion and Proliferation Assay

To determine cellular adherence capacity of FHOD1 knockdown cells, 1.0 x 10^4 HeLa cells/well were seeded 3 h after second RNAi treatment in 96 well plates either non-coated or coated with different matrix proteins. For coating, wells were previously covered either with 40 µg/ml fibronectin in PBS, 1 mg/ml collagen in PBS, or with 0.01 % (w/v) poly-L-lysine solution,

respectively, for 1 h at 37°C and finally washed with PBS. In parallel, 3 x 10^5 cells were seeded in 6-well plates for determination of knockdown efficiency on the following day. Adherence in 96-well plates was allowed for 2 h. Afterwards cells were fixed, stained for chromatin with Hoechst 33258 without permeabilization and bulk fluorescence was measured in a fluorimeter (356 nm/458 nm). The number of attached cells was calculated by normalization to a standard curve, the experiments were performed in triplicates for each condition.
Proliferation rate for control and FHOD1 knockdown cells was measured by an ELISA based assay (BrdU Cell Proliferation Assay, Calbiochem, Merck) with antibodies probing for Bromodeoxyuridine (BrdU), a thymidine analog which is internalized in newly synthesized DNA during mitosis. Following seeding of HeLa in 96-well plates as described for the adhesion assay, medium was replaced with 120 µl medium containing 20 % (v/v) BrdU labeling solution after 2 h. 24 h later, cells were fixed by addition of fixative/denaturing solution for 30 min and treated according to manufacturer's instructions. The measured signals were normalized to the results of adhesion assays performed in parallel to exclude a possible interference of different adhesion capacity. The experiments were performed in triplicates for each condition.

7.4.10 Measurement of Cell Size

For determination of cell size, HeLa cells grown on coverslips were fixed, permeabilized and stained for F-actin 2 d after second RNAi treatment for FHOD1 knockdown. Subsequently, they were analyzed by fluorescence microscopy and cell size was determined by measurement of the area captured by a single cell using the "Freehand selection" tool in combination with the "Measurement" tool of "ImageJ" software.

7.4.11 SRE Transcription Assay

To investigate the influence of FHOD1 on Rho-GTPase and ROCK1 mediated activation of SRE transcription, 3 h after second RNAi treatment 3.5 x 10^5 NIH3T3 cells were seeded in a 6 cm dish for knockdown control and 5 x 10^4 NIH3T3 cells were seeded in a 12 well for subsequent transfection on the following day. Therefore, 1 µg of plasmid DNA encoding the respective constructs was mixed with 24 ng p3D.Afos and 10 ng pRL-TK reporter plasmids. 3 h after transfection, cells were subjected to starving medium containing 0.5 % FCS. At the following day, knockdown control cells were harvested as described and transfected cells were lysed in 100 µl "Passive Lysis buffer" (Dual-Luciferase Reporter Assay System, Promega). Lysates were processed according to the manufactures instructions. For measurement, 50 µl supernatant was added to a 96 well plate (white, non-transparent) and was mixed with 50 µl "Luciferase Assay II" solution. Following detection of firefly luciferase activity at the luminometer (Luminoskan Ascent luminometer, Thermo Labsystems) for 1 s, 50 µl "Stop & Glow" buffer was added, carefully mixed and *renilla* luciferase activity was measured for 5 s. For calculation of SRE activity, background values obtained for untransfected cells were subtracted from the respective values obtained for firefly and *renilla* luciferase. Subsequently, firefly luciferase activity was normalized to *renilla* luciferase activity. The experiments were performed in triplicates for each condition. For comparison with further experiments, SRE activity was expressed relative to control RNAi treated FHOD1-ΔC transfected cells which were arbitrarily set to 100.

7.4.12 Wound Healing Assay for 2D-Motility

Due to cell-cell contact-inhibition, migration of animal cells on 2D planar surfaces is inhibited under cell culturing conditions which are characterized by high cell confluency. In a wound healing assay, a unilateral loss of this contact-inhibition is achieved by scratching a 100 % confluent layer of cells resulting in a distinct area without cells referred to as wound. This trigger

in combination with chemotactic orientation induces a directional migration of the adjacent cells into the wound.
To investigate the wound healing efficiency of FHOD1 knockdown cells (HeLa, MEF, NIH3T3) or SH4-domain expressing CHO cells, confluent layers of cells in 6-well plates either 24 h after second RNAi treatment or 24 h after addition of 1000 ng/ml dox, respectively, were scratched with a pipette tip to cause a cell layer wound of about 200-300 µm in distance. Wound closure was monitored over 24 h at 37°C in medium supplemented with 20 mM HEPES by live cell imaging which was performed immediately after wounding for 18 h at 37 °C using a Leica CTR MIC microscope. Pictures were acquired every 30 min with a motor-controlled Leica DC 350 FX camera using the Leica software "FW4000", which enables simultaneous recordings from multiple wells. Subsequently, single pictures were assembled to a movie using the "Import Image Sequence" tool of the "ImageJ" software.

7.4.13 Chemotaxis Assay

Chemotaxis defines a type of cell motility in which cells migrate towards a chemo-attractant stimulus. To investigate the role of FHOD1 in chemotaxis driven motility, NIH3T3 cells in a 6 cm dish were serum starved with medium containing 0.5 % FCS (v/v) immediately after second RNAi treatment. 24 h later, cells were treated for 5 min at 37°C with a solution of 5 mM EDTA in PBS. After detachment, 2.75 x 10^3 cells were seeded on the bottom of a transwell insert with a pore size of 8 µm (ThinCert cell culture insert for 24 well plates, Greiner Bio-One) for 1 h at 37°C and the rest was used for determination of knockdown efficiency. Subsequently, transwell inserts were transferred to a 24-well plate and cells were allowed to migrate along a gradient of FCS for 8 h. Therefore, 550 µl 0.5 % FCS (v/v) was added to an individual well and 100 µl 10 % FCS (v/v) for the gradient or 100 µl 0.5 % FCS (v/v) for control, respectively, were given to the a single transwell insert. To maintain the gradient of FCS, medium was exchanged in a frequency of 1 h. Thereafter, cells at the transwell membrane were fixed and stained for F-actin and chromatin. Finally, the number of cells at the transwell membrane was quantified at the confocal microscope (Leica TCS SP2) and the relative number of cells migrated across the membrane was calculated.

7.4.14 Invasion Assay for 3D-Motility

For determination of cell invasiveness, a transwell assay was performed as described by Hooper and colleges (Hooper *et al.*, 2006). Therefore, membranes of transwell inserts with a pore size of 8 µm (ThinCert cell culture insert for 24 well plates, Greiner Bio-One) were coated with 20 µl of undiluted growth factor reduced matrigel (BD Biosciences). For the analysis of inducible CHO cell lines, cells were kept in the presence of 1 µg/ml dox. Following 12 h dox induction in the presence of 10 % FCS, cells were starved for 12 h in medium containing 0.5 % FCS, harvested and counted. 10^6 cells were seeded in the upper chamber of the transwell insert in medium supplemented with 0.5 % FCS, whereas the lower chamber was filled with medium supplemented with 10 % FCS (fig. 14)

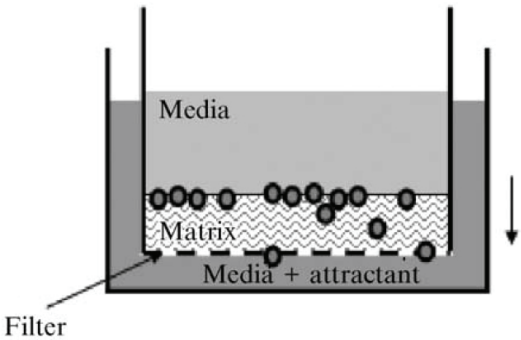

Figure 14: Invasion assay.

Serum starved cells were seeded on top of the matrigel and migrated along a gradient of FCS for 48 h. Following fixation, removal of the matrigel and stain with Hoechst 33258, cells appearing at the lower side of the transwell insert membrane (pore size 8 µm) were quantified (Hooper *et al.*, 2006).

After 48 h incubation at 37°C, cells in the upper chamber were carefully removed with a cotton swab and the cells that had traversed the membrane were fixed with 4 % PFA, stained with Hoechst 33258 and counted at the microscope (Leica DMIRE2). To account for potential differences in cell seeding and/or proliferation during the 48 hours invasion period, cells were also plated in parallel in culture plates without matrigel, fixed at the timepoint of harvest of the invasion samples and stained with Hoechst 33258. The number of nuclei in five representative areas was quantified and the number of invaded cells was normalized to the total number of cells. Maximum differences in cell numbers observed were 1.5 fold in parallel assays and increased cell proliferation observed in individual experiments was not correlated with the expression of any of the transgenes analyzed.

7.4.14.1 Confocal Microscopy and 3D Reconstructions

3D analyses were performed as described (Kitzing *et al.*, 2007). Briefly, CHO cells stably expressing N18-HASPB-GFP were transfected with an mRFP-actin expression plasmid. 24 h later cells were counted and seeded directly into Matrigel (BD Biosciences) and placed into µ-Slide VI chambers (ibidi). Cell morphologies were analyzed by taking z intervals of 1 µm with a 40x objective using confocal microscopy (Leica TCS SP2). 3D reconstructions and animations of the z-sections were performed using Leica "Confocal Simulator Software".

7.4.15 Golgi Disruption Assay

To analyze the localization of endogenous FHOD1 during disruption and reassembly of the Golgi apparatus, NIH3T3 cells grown for 1 d on coverslips were treated for either 10 min or 30 min with 5 µg/ml (+) Brefeldin A (BFA), respectively. Cells were immediately fixed or initially thoroughly washed three times with PBS and incubated for 1 h at 37°C for reassembly of the Golgi. Cells were permeabilized, stained for endogenous FHOD1 and coatomer (tab. 3) and were subjected to confocal microscopy.

7.4.16 Measurement of F-actin Content by Flow Cytometry

For evaluation of FHOD1s influence on intracellular steady state levels of polymerized F-actin, HeLa cells in a 10 cm dish at a confluency of approx. 75 % were detached 24 h after second RNAi treatment by trypsin/EDTA for 5 min. To determine knockdown efficiency, 20 % of the cells were subjected to Western blot analysis as described, whereas the rest was transferred to a 1.5 ml cup on ice, washed twice with PBS and finally suspended in 200 µl ice cold 3 % (w/v) PFA for fixation. After 30 min on ice, cells were centrifuged (5 min at 2,000 rpm and 4°C), subsequently resuspended in 1000 µl staining solution consisting of Phalloidin-Alexa-Fluor-633 (1:600) in ice cold PBS for F-actin stain and incubated for 45 min on ice in darkness. Following a final washing step in PBS, cells were suspended in 300 µl PBS and subjected to FACS analysis.

7.4.17 Endocytosis Assays

In order to investigate the influence of SH4-domains on different endocytotic pathways, the capacity of CHO cells for fluid-phase uptake as well as for clathrin mediated endocytosis was measured by microscopy and flow cytometry (FACS).

7.4.17.1 Analysis of Fluid-Phase Uptake by Microscopy

To qualitatively investigate fluid-phase uptake, stable CHO cells were seeded on coverslips and expression of respective proteins was either induced or not by addition of 1000 ng/ml dox for

24 h. Subsequently, cells were treated in a 24 well plate for up to 180 min at 37°C with 200 µl medium supplemented with 1 mg/ml fluorescently labeled dextran-TMR (10 kDa or 70 kDa). To evaluate the contribution of macropinocytosis, dextran-uptake was also measured in the presence of either 100 µM 5-(N-ethyl-N-isopropyl)-amiloride (EIPA) including a pretreatment for 1 h with the inhibitory drug or 200 nm phorbol myristate acetate (PMA) for induction of macropinocytosis, respectively. Cells were fixed, stained for F-actin and chromatin and were subjected to microscopy.

7.4.17.2 Quantification of Fluid-Phase Uptake by Flow Cytometry

To quantitatively investigate fluid-phase uptake, stable CHO cells were seeded in a density of 0.5 x 10^5 cells/well (24 well plate) and expression of respective proteins was either induced or not by addition of 1000 ng/ml dox for 24 h. Subsequently, cells were treated for up to 180 min at 37°C with 200 µl medium supplemented with 0.1 mg/ml fluorescently labeled dextran-Alexa-Fluor-647 (10 kD). As described above, control cells were treated either with EIPA or with PMA. To stop internalization, 24 well plates were transferred to ice and 800 µl ice cold PBS was added per well. Following three washing steps with ice cold PBS, cells were covered for 10 min with 200 µl ice cold EW buffer (Meier *et al.*, 2002) in darkness. After detachment with 300 µl ice cold ED buffer for 25 min in darkness, 700 µl E-Stop solution was added. The cells were carefully suspended by pipetting, transferred to a 1.5 ml cup and subsequently centrifuged (5 min at 2,000 rpm and 4°C). Following suspension in 300 µl E-FACS buffer, the cells were subjected to FACS analysis (flow cytometer FACSCalibur, Beckton Dickinson).

7.4.17.3 Quantification of Clathrin Mediated Endocytosis by Flow Cytometry

To quantitatively investigate clathrin mediated endocytosis, stable CHO cells were seeded in a density of 0.5 x 10^5 cells/well (24 well plate) and expression of respective proteins was either induced or not by addition of 1000 ng/ml dox for 24 h. Subsequently, cells were treated for up to 180 min at 37°C with 200 µl medium supplemented with 5 mg/ml fluorescently labeled transferrin-Alexa-Fluor-647. Finally, cells were treated and analyzed by FACS as described for fluid-phase uptake.

8 RESULTS

8.1 SH4-Domain Mediated PM Blebbing

SH4-domains represent the N-terminal membrane anchors of several membrane attached proteins including Src kinases as well as the *Leishmania* HASPB virulence factor, HIV-1 Nef and HIV-1 Gag proteins (Resh, 1993, Resh, 1994, Stegmayer *et al.*, 2005, Welker *et al.*, 1998). SH4-domains reveal no highly conserved amino acid sequence homology, but a common feature is posttranslationally modification by acetylation with myristoleic acid mediating their membrane targeting. They are additionally palmitoylated or possess a basic cluster consisting of positively charged residues like Lys or Arg (fig. 15) (McCabe and Berthiaume, 1999, Resh, 1994).

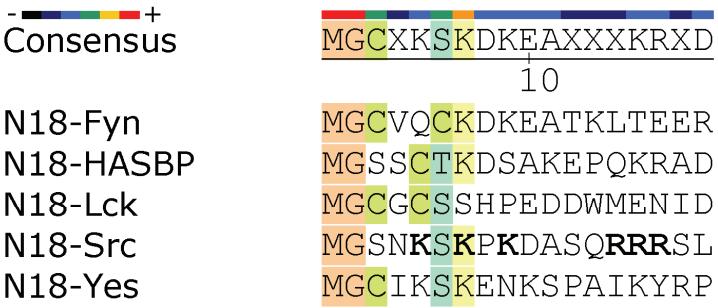

Figure 15: Alignment of SH4-domains investigated in this study.

Depicted are the first 18 residues of *Leishmania* HASPB as well as of the Src kinases Fyn, Lck, c-Src and Yes. The grades of homology are denoted by the shown color code (with "-" = minimal and "+" = maximal homogeneity). Selected residues are written in bold letters (basic cluster) or highlighted by light colors (red: myristoylated; green: palmitoylated; required for efficient myristoylation: Ser or Thr (cyan) and Arg or Lys (yellow)).

Appropriate subcellular localization and membrane attachment are prerequisites for the biological activity of Src kinases *e.g.* in oncogenic transformation (Kaplan *et al.*, 1988, Sigal *et al.*, 1994). Roles of SH4-domains beyond this targeting function, however, have not been described to date.

8.1.1 Generation of Stable SH4-Domain Cell Lines

To study the biology of SH4-domains, stable CHO cell lines (kindly provided by S. Tournaviti, group of W. Nickel, BZH, Heidelberg) and HeLa cell lines (kindly provided by J. Ritzerfeld, group of W. Nickel, BZH, Heidelberg) were generated as described previously (Engling *et al.*, 2002, Stegmayer *et al.*, 2005). In a doxicycline (dox) inducible manner, the CHO cell lines stably express eGFP fusion proteins of the 18 amino acid SH4-domain either from the HASPB protein or from the proto-oncogenic Src kinases c-Src, Fyn, Lck, Yes or their mutants

(Δmyr, Δpal), respectively, linked to a TEV cleavage site and a ProteinA tag for potential purification (fig. 16A).

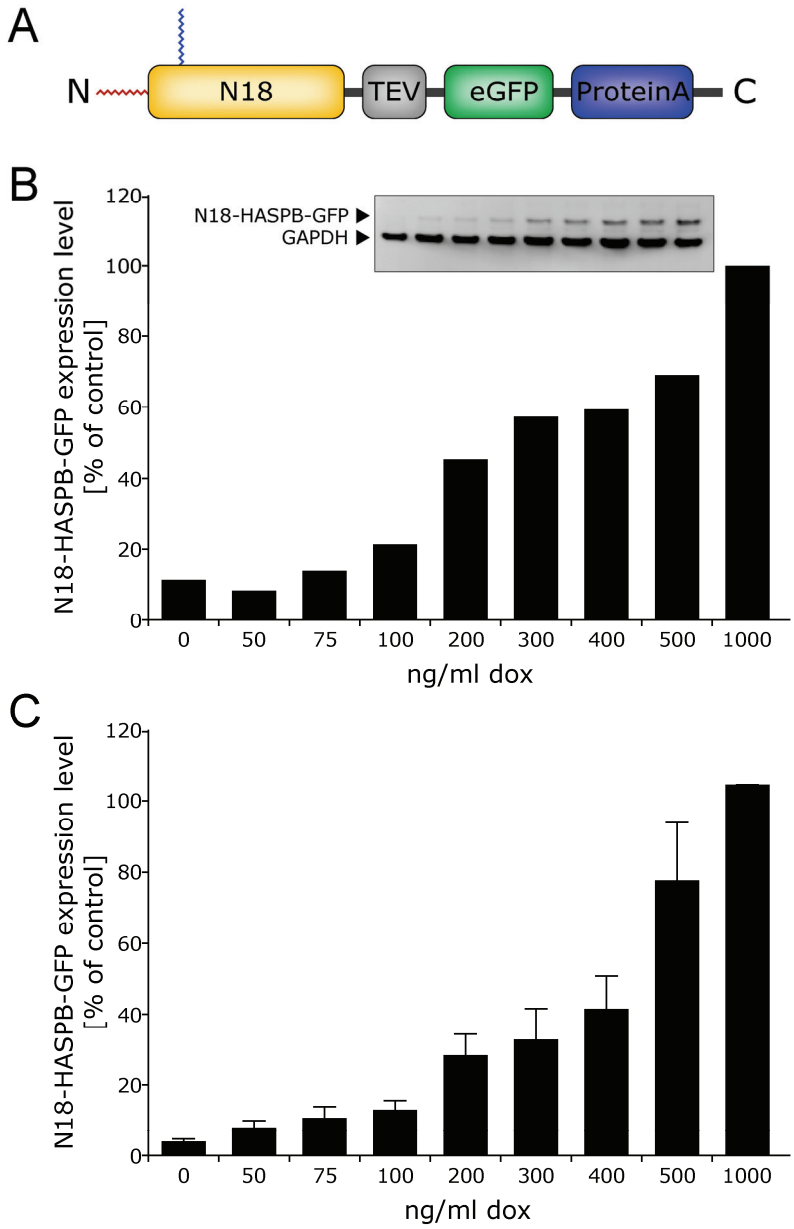

Figure 16: Generation of cell lines stably expressing SH4-domains.

(A) SH4-domain constructs. Expression cassettes encoding the first 18 residues of either the *Leishmania* HASPB protein or the Src kinases c-Src, Fyn, Lck or Yes, respectively, linked to a TEV cleavage site followed by GFP and ProteinA were cloned into a pREV-TRE2 vector containing a transactivator/doxicycline (dox)-responsive element and were stably integrated into the genome of CHO cells by viral transduction. GFP-positive cells were sorted by FACS. For HeLa cells, the integrated constructs are not linked to ProteinA. **(B+C)** Analysis of CHO cells induced for N18-HASPB-GFP expression with increasing amounts of dox for 24 h. **(B)** Western blot: The N18-HASPB-GFP signal (see insert) was normalized to the GAPDH loading control following quantification by the LI-COR Odyssey infrared imaging system. Relative expressions levels are depicted. **(C)** FACS: GFP fluorescence intensities of the cells were analyzed by flow cytometry and the relative expression levels presented are arithmetic means of three independent experiments + standard deviation (SD). Values for 1000 ng/ml dox were set to 100 % (kindly provided by S. Tournaviti).

As shown for N18-HASPB-GFP and investigated by Western blot and FACS analysis, induction of SH4-domain expression in stable CHO cell lines with increasing amounts of dox for 24 h resulted in rising protein production. Both methods revealed low background levels and low leakiness of the expression system without dox, but maximal expression by addition of 1000 ng/ml dox (fig. 16B/C). While these conditions yielded the most efficient SH4-domain production levels, they were applied for further experiments.

8.1.2 Expression of SH4-Domains Induces PM Blebbing

Since production of the generated GFP fusion proteins was successful, their cellular localization was analyzed by confocal microscopy on live CHO cells. According to the confocal micrographs, GFP linked to the HASPB-SH4-domain (N18-HASPB-GFP) was efficiently targeted to the PM as well as to cytoplasmic vesicular structures whereas GFP alone showed its typical cytoplasmic and nucleic distribution (fig. 17Aa-b).

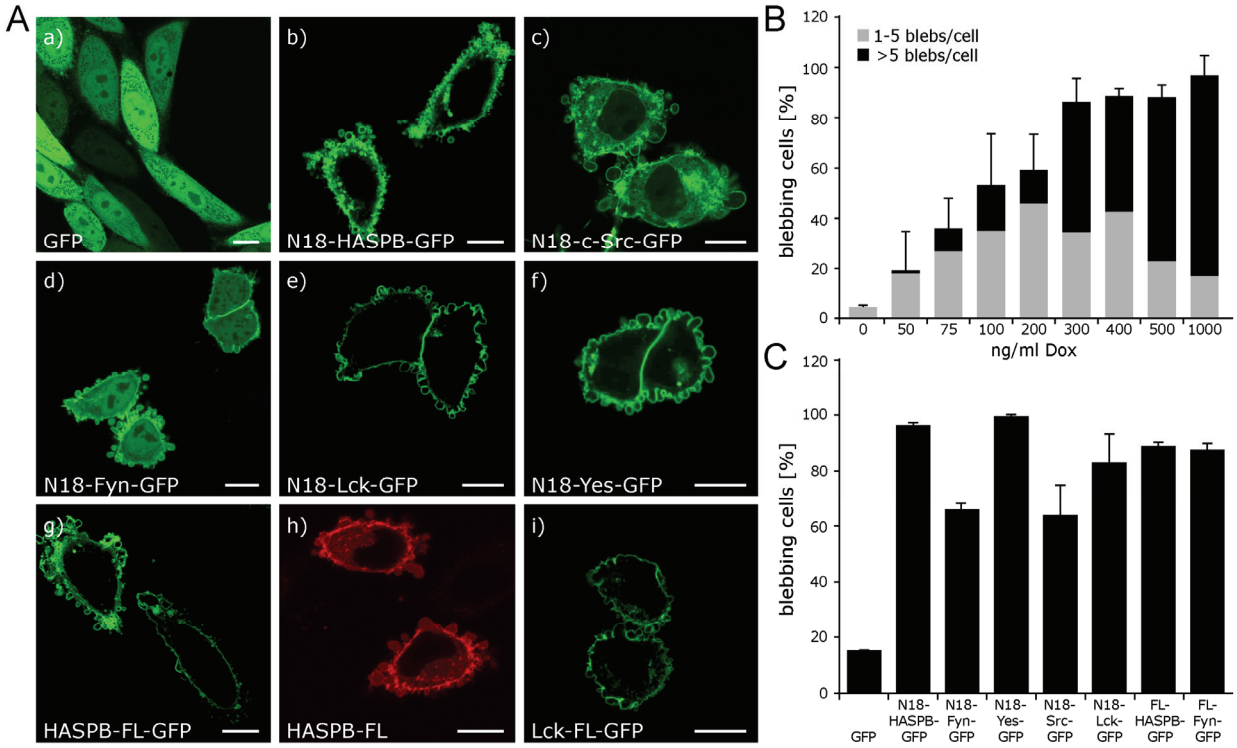

Figure 17: Expression of SH4-domains resulted in PM blebbing.

(A) Cellular localization of SH4-domains and triggering of PM blebbing. Live confocal microscopy of either CHO cell lines expressing GFP (a) or GFP fusion proteins of the SH4-domain of *Leishmania* HASPB (b) or the Src kinases c-Src (c), Fyn (d), Lck (e) or Yes (f), respectively, or CHO cells transfected with full length (FL) proteins of HASPB (g) or Lck (i) fused to GFP or not fused to GFP but co-transfected with mRFP-actin (h). Expression was induced with 1000 ng/ml dox for 24 h. Presented are representative mid-cell z-sections. Scale bars = 10 µm. **(B)** PM blebbing induction was correlated with expression levels of the HASPB-SH4-domain. To induce N18-HASPB-GFP expression, CHO cells were treated with the indicated concentrations of dox for 24 h. Following fixation, blebbing cells were quantified by confocal microscopy. Given is the overall percentage of cells displaying PM blebs. Black and grey columns indicate the fraction of blebbing cells with high (more than 5 blebs per cell) or low (less than 5 blebs per cell) blebbing activity, respectively (arithmetic means of at least three independent experiments + SD with > 100/condition). **(C)** Blebbing efficiency of cells depicted in selected panels of A. Percentage of cells displaying PM blebs (arithmetic means of at least three independent experiments + SD with > 100/condition; kindly provided by S. Tournaviti).

Surprisingly, the HASPB-SH4-domain drastically altered the PM morphology and caused extensive PM blebbing on the cellular surface. Although even low dox concentrations were sufficient to induce moderate PM blebbing by N18-HASPB-GFP, expression levels induced with at least 300 ng/ml dox resulted in efficient PM blebbing in over 80 % of the cells (fig. 17B). A

further increase up to 1000 ng/ml dox led to maximal protein production (fig. 16B/C) and enhanced PM blebbing per cell (fig. 17B). This PM blebbing was also observed in Hela cells, but was less pronounced which might be due to lower expression levels (data not shown). Similar results were obtained by expression of SH4-domains derived from the Src kinases c-Src, Fyn, Lck and Yes (fig. 17Ac-f). These SH4-domains efficiently targeted the coupled GFP to the PM and to other cytoplasmic membranes: Whereas N18-Lck-GFP and N18-Yes-GFP showed an internal distribution that was similar to N18-HASPB-GFP and reminded of Golgi related vesicles, N18-Fyn-GFP additionally revealed a more diffuse cytoplasmic dispersion. This also applied to N18-Src-GFP, although its vesicular localization appeared more outspread, which is in line with a previously described attachment to endocytotic vesicles like macropinosomes (Kasahara *et al.*, 2007). Nevertheless, all constructs potently induced PM blebbing with slight variations in morphology, size and bleb number per cell as well as in bleb induction efficiencies (fig. 17A/C and data not shown). Compared to the SH4-domains only, equally efficient PM blebbing combined with a similar cellular distribution was found upon transient expression of full length Lck or HASPB fused to GFP or co-transfection of mRFP-actin with a non-tagged version of full length HASPB, whereas expression of GFP alone had no such effect (fig. 17Ag-i/C).

In summary, by fusion of GFP to various SH4-domains, the protein was efficiently targeted to the PM. These SH4-domains were sufficient to potently induce PM blebbing by a mechanism depended on their expression level but not related to the GFP-ProteinA tag. Therefore, induction of PM blebbing is a conserved function of SH4-domains from different sources, including proto-oncogenic Src kinases.

8.1.3 Localization of the SH4-Domain to the PM is Required for Production of PM Blebs

Since a common feature of all of these SH4-domains was their targeting to the PM, the correlation between PM localization and bleb induction was investigated. PM targeting of SH4-domains mainly depends on acetylation of specific residues within this domain: The site for myristoylation is highly conserved in SH4-domain containing proteins and is located at position Gly2, whereas palmitoylation takes place on cysteins located in the amino acid residues three to seven (fig. 15B) (McCabe and Berthiaume, 1999, Resh, 1994). Therefore, two different mutants of N18-HASPB-GFP were used: N18-Δmyr-HASPB-GFP lacks both, its myristoylation and palmitoylation signal (Gly2 substituted by alanine: G2A) resulting in cytoplasmic and nucleic localization (fig. 18Ab).

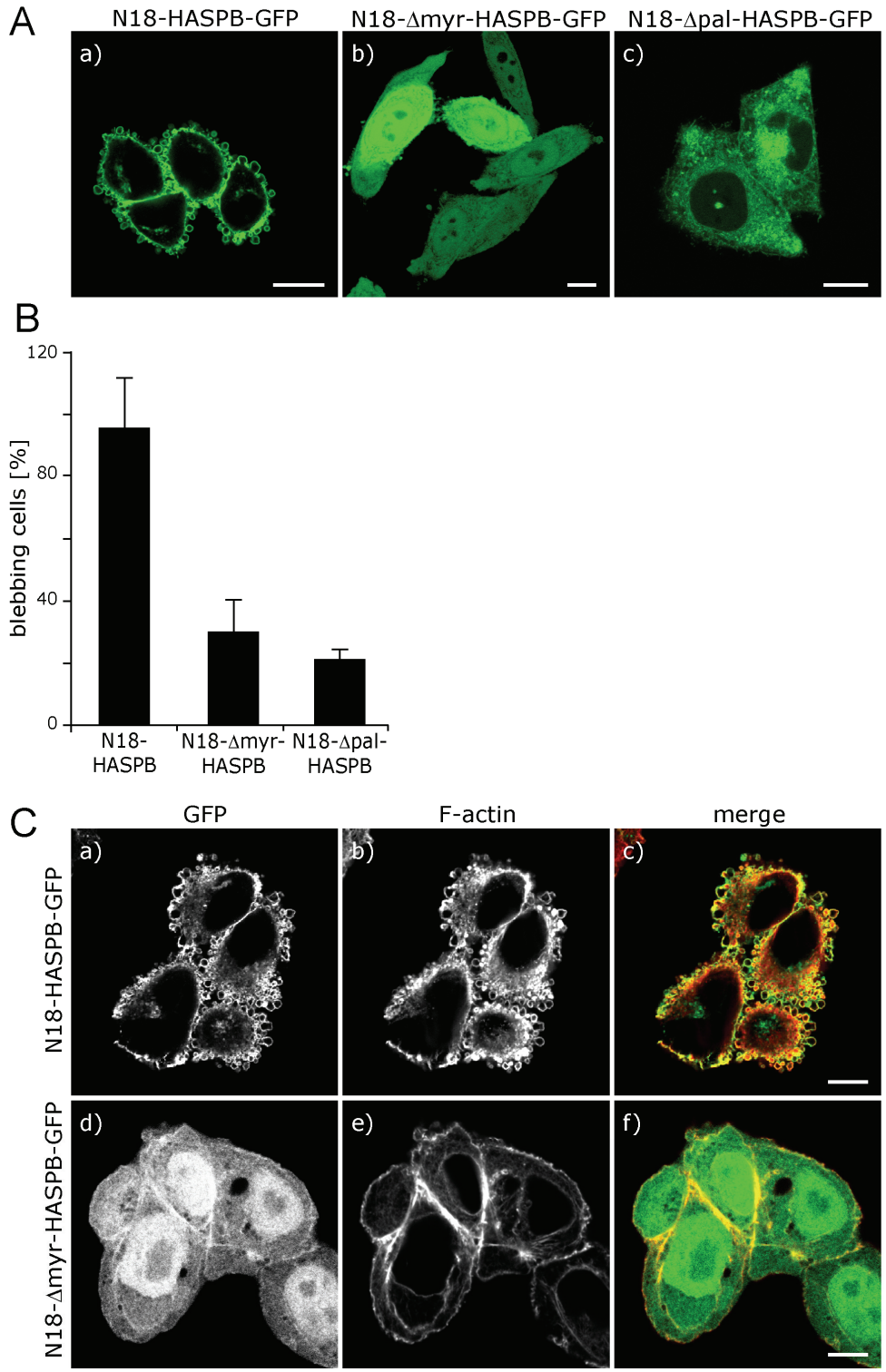

Figure 18: Induction of PM blebbing required PM targeting.

(A) Live confocal microscopy of CHO cell lines expressing GFP fusion proteins of the HASPB-SH4-domain (a: N18-HASPB-GFP) or mutants that are defective in PM targeting (b: N18-Δmyr-HASPB-GFP; c: N18-Δpal-HASPB-GFP). Depicted are representative mid-cell z-sections. Scale bars = 10 µm. **(B)** Blebbing efficiency of cells depicted in panel A (arithmetic means of at least three independent experiments + SD with > 100/condition). **(C)** Confocal microscopy of fixed CHO cell lines expressing GFP fused mutants of the HASPB-SH4-domain (a-c: N18-HASPB-GFP; d-f: N18-Δmyr-HASPB-GFP). Following fixation, cells were stained for F-actin with Phalloidin-TRITC (b/e). Depicted are representative mid-cell z-sections. Scale bars = 10 µm (kindly provided by S. Tournaviti: A/B).

N18-Δpal-HASPB-GFP lacks solely its palmitoylation signal (Cys5 substituted by serine: C5S) resulting in accumulation at perinuclear membranes (most likely the Golgi apparatus (Denny *et al.*, 2000, Stegmayer *et al.*, 2005) and exclusion from nuclei (fig. 18Ac). Interestingly, CHO cell lines expressing these mutants showed no PM blebbing in live cell imaging (fig. 18A/B). To further study this effect, cells were fixed and stained for F-actin (fig. 18C). Confocal microscopy again showed potent PM blebbing upon expression of N18-HASPB-GFP. The generated blebs were F-actin enriched at the limiting membrane and particularly at their neck (fig 18Cb). Again, no PM blebbing was found in cells expressing the acetylation deficient PM targeting mutants of the HASPB-SH4-domain (fig 18Cd-f). These results were confirmed by scanning electron micrographs (SEMs) of CHO cells transfected with the Yes-SH4-domain: Although all cells displayed peripheral membrane ruffling and microvilli like structures on their surface that are typical for these epithelial cells (Porter *et al.*, 1973), N18-Yes-GFP expressing cells showed an increased ruffling in combination with spherical structures on their surface resembling PM blebs in fluorescence microscopy (fig. 19BA). Consistent with the results obtained by confocal microscopy, these blebs were variable in size and number. Interestingly, they reminded of blebs that were previously described for G_1-phase CHO cells (Porter *et al.*, 1973). Nevertheless, these structures were absent in N18-Δmyr-Yes-GFP (G2A) producing cells that were indistinguishable from mock transfected cells (fig. 19B and data not shown).

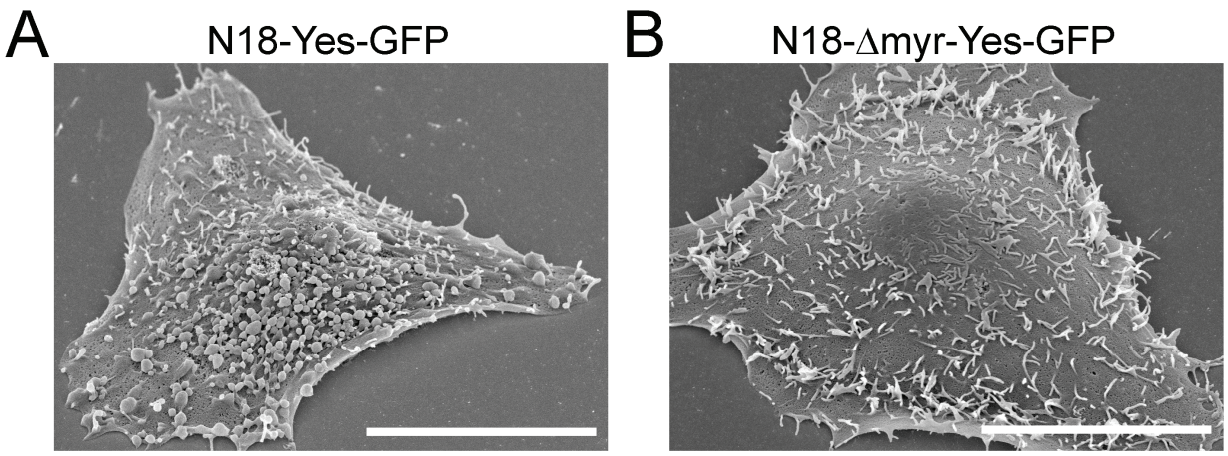

Figure 19: Expression of SH4-domains altered cellular surface morphology.

(A+B) Scanning electron micrographs (SEMs) of surfaces of fixed CHO cells transfected with either the PM blebbing inducing SH4-domain N18-Yes-GFP **(A)** or its myristoylation deficient mutant N18-Δmyr-Yes-GFP **(B)** that was not capable of PM blebbing induction. Scale bars = 10 µm (Pictures were generated with the help of P. Walther, Electron Microscopy Facility, University Ulm, Germany).

In summary, the potent induction of PM blebbing and formation of F-actin rich PM blebs by SH4-domains required their localization at the inner leaflet of the cell limiting PM.

8.1.4 N18-HASPB Induced PM Blebs are Highly Dynamic

PM blebbing is a highly dynamic process: M2 melanoma cells, for instance, that are deficient in the F-actin filament cross linking protein FLNa reveal constant PM blebbing with distinct kinetics due to local breakdowns of the cortical actin layer (Charras *et al.*, 2005, Cunningham, 1995). Similar behavior was observed for blebs of apoptotic cells that are also formed and retracted constantly in the beginning. Subsequently, they are shed as apoptotic bodies from the cell during late apoptotic phases (Barros *et al.*, 2003, Mills *et al.*, 1999, Zhang *et al.*, 1998). Furthermore, PM blebs that are induced during ATP induced secretion of IL-1ß, regularly pinch off from the cell surface (MacKenzie *et al.*, 2001). To characterize appearance and dynamics of SH4-domain induced PM blebs, N18-HASPB-GFP expressing CHO cells were analyzed by confocal real time imaging that was performed by S. Terjung (Advanced Light Microscopy Core Facility, EMBL, Heidelberg): A 4D surface reconstruction revealed that blebbing activity occurred at the whole surface, but was most pronounced at the edges of the cell (fig. 20A).

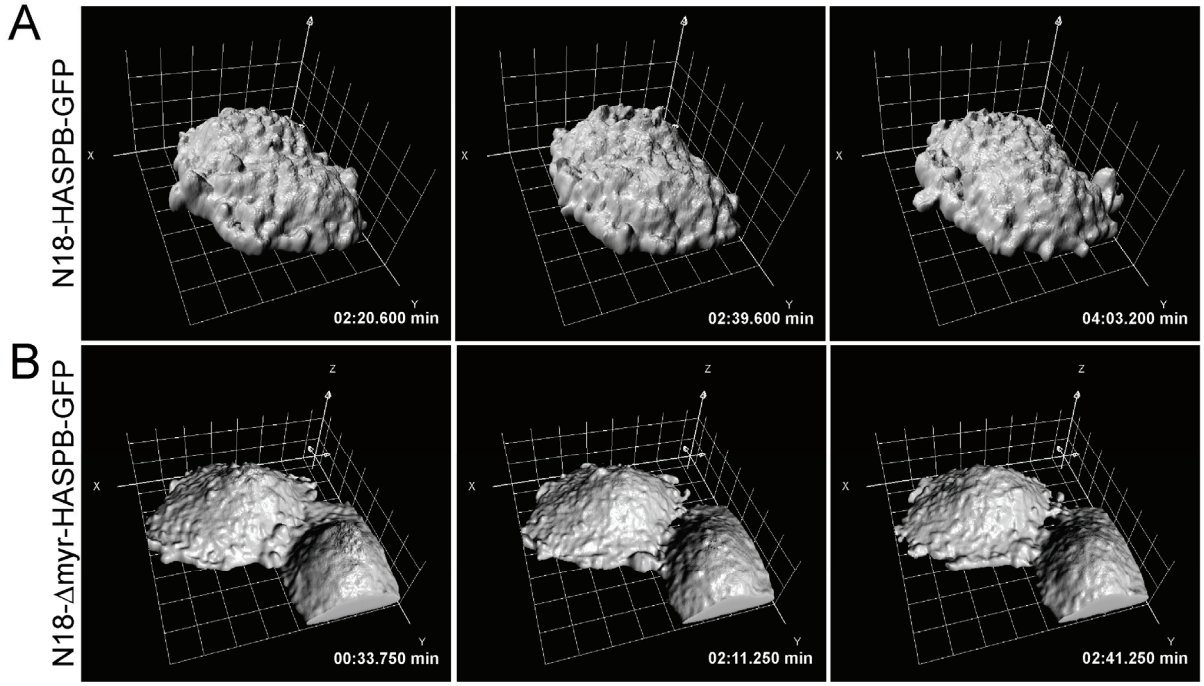

Figure 20: Expression of SH4-domains altered cellular surface dynamics.

(A+B) Representative image of a 4D time-lapse surface reconstruction of CHO cells expressing **(A)** N18-HASPB-GFP or **(B)** N18-Δmyr-HASPB-GFP. Over a time period confocal stacks (step size 0.5 µm) were taken and the raw data was filtered and visualized with Imaris (Bitplane) with a 3x3x3 median filter followed by an edge preserving filter (width = 0.140 µm). The PM is represented by iso surface rendering. Grid size = 5 µm (kindly provided by S. Terjung).

As a control N18-Δmyr-HASPB-GFP expressing cells revealed markedly reduced PM dynamics (fig. 20B). Consistently, a 2D confocal stack projection of stably N18-HASPB-GFP expressing CHO cells in a time lapse showed that PM blebbing occurred at the entire surface of the cells but

not at cell-cell or cell-substratum contacts (2D time-lapse, 10 minutes, 150 ms per frame; fig. 21A).

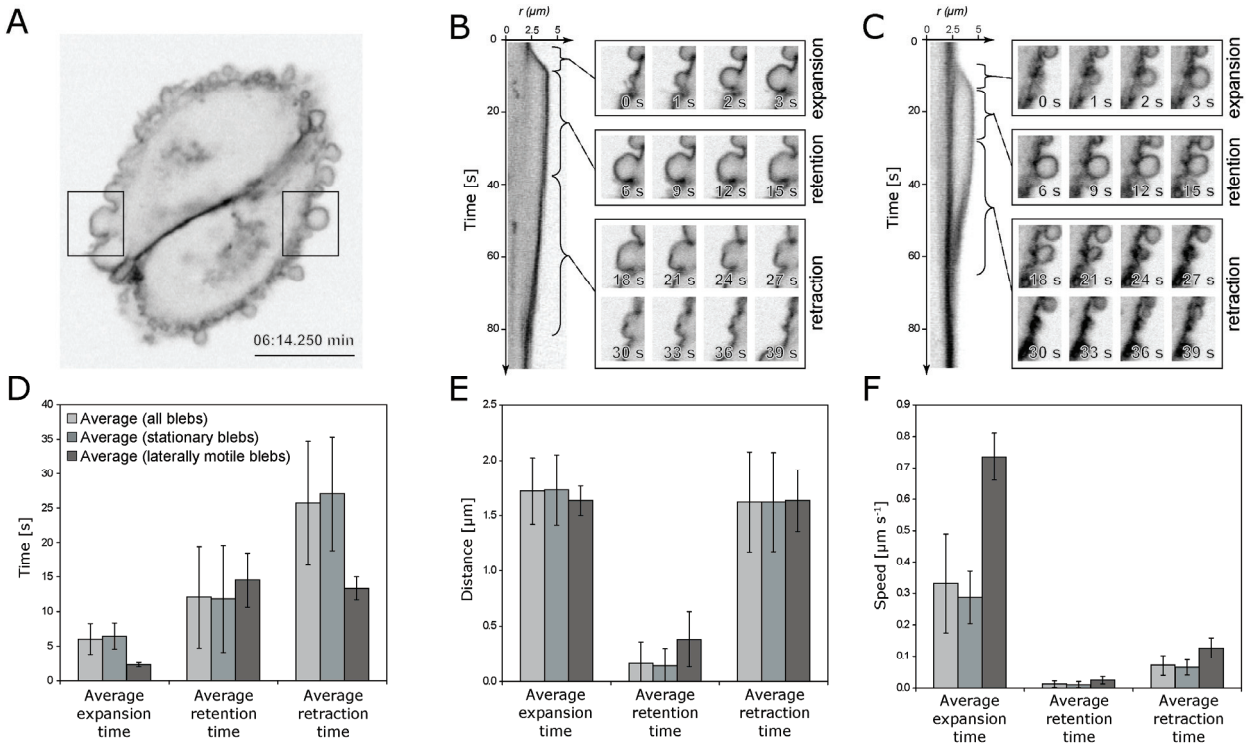

Figure 21: HASPB-SH4-domain induced PM blebbing was a highly dynamic and constantly performed process.

(A-C) HASBP-SH4-domain induced PM blebs were of different size and are constantly formed and retracted without shedding. **(A)** Representative confocal image of a fast 2D time-lapse (10 minutes, 150 ms per frame) of CHO cells stably expressing N18-HASPB-GFP. Scale bars = 10 µm. **(B+C)** Kymographs (time-space-plots) along the axis perpendicular to the bleb base and stills of two blebs framed by rectangles in A showed that PM blebbing is divided in three phases: expansion, retention and retraction. Note the different time intervals between the stills (formation: 1 s; retention and retraction: 3 s). **(D-F)** Kinetics of N18-HASPB-GFP induced PM blebbing revealed a fast expansion phase followed by a prolonged retention phase and a slow retraction phase. Average time **(D)**, average distance **(E)** bleb move and average speed **(F)** during expansion, retention and retraction phase of 40 individual blebs is plotted for all analyzed blebs (light gray), stationary blebs (medium gray) and laterally motile blebs (dark gray) + SD (kindly provided by S. Terjung).

According to kymographic tracing of individual blebs, their formation and retraction occurred on average within 44 s (fig. 21A-D). In line with previous characterizations of PM blebbing in M2 melanoma cells (Charras *et al.*, 2005, Cunningham, 1995), the life span of individual blebs consisted of three distinct steps: fast expansion (in average 6 s, 0.332 µm/s) followed by an extended retention phase (in average 12 s, 0.012 µm/s) and a subsequent slow retraction period (in average 26 s, 0.071 µm/s; fig. 21A-D/F). While most of the quantified blebs formed at and retracted to the identical position at the PM, a subpopulation of blebs displayed lateral mobility with accelerated apparent bleb expansion and retraction. Both types of blebs reached a similar size of approx. 1.7 µm in diameter at maximum extension and retracted completely (fig. 21A-C/E). During retraction, the previously round shape of the blebs typically turned into a

less homogenous, wave-like morphology. In contrast to blebbing observed during ATP-induced secretion of IL-1ß (MacKenzie *et al.*, 2001), real time microscopy analysis revealed that N18-HASPB-GFP mediated PM blebbing did not cause detectable shedding of SH4-domain positive vesicles into the cell culture supernatant.

Together, PM blebs induced by SH4-domains were highly dynamic: They were constantly formed and retracted and occurred at cell surfaces only but not at cell-cell or cell-surface contact sites. They also showed distinct kinetics and dimensions that were comparable to blebs constantly produced in M2 melanoma cells.

8.1.5 N18-HASPB Induced PM Blebs are Non-Apoptotic

Although PM blebs mediated by SH4-domain expression showed similar kinetics to M2 cells and PM blebbing was a constant process without any apparent damage of the cells, this phenotype reminded of apoptotic cells. Apoptosis or programmed cell death is a highly organized process. During apoptosis, cells round up and PM blebbing is induced. This process is thought to be involved in DNA fragmentation and initiation of immune responses (Fadeel, 2004, Martinez *et al.*, 2005). At late stages, apoptotic bodies are generated which pinch off the surface of apoptotic cells leading finally to their disruption (Mills *et al.*, 1999, Zhang *et al.*, 1998). Various different analyses were performed to test whether SH4-domain expressing cells were undergoing apoptosis. First, a transferase-dUTP nick end labeling (TUNEL) assay was performed (Gavrieli *et al.*, 1992), during which deoxynucleotidyl transferase (TdT) specifically binds to terminal 3'-OH ends of fragmented DNA and incorporates fluorescently labeled dUTP allowing microscopical examination of apoptotic cells (Huerta *et al.*, 2007). Cells expressing N18-HASPB-GFP for 24 h were strictly negative for TUNEL reaction, whereas treatment of these cells with 200 µg/ml Etoposide (Eto) in combination with 200 µg/ml Cycloheximide (Chx) for 12 h potently induced apoptosis (fig. 22A/B). Second, the viability of cultured cells was verified by a microscopic analysis of cellular DNA. Chromosomal DNA condensates during apoptosis and is fractionated during this process (Huerta *et al.*, 2007). As depicted in fig. 22, only DMSO treated (4 %, 5 h), but not untreated NI8-HASPB-GFP expressing CHO cells showed chromatin condensation after specific stain for DNA (fig. 22C/D).

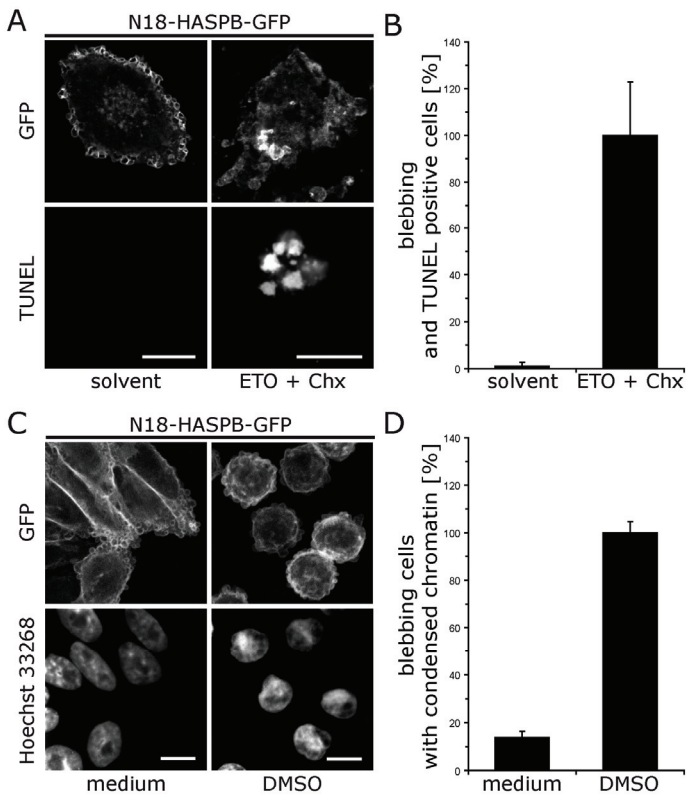

Figure 22: HASPB-SH4-domain expressing cells showed PM blebbing but are not apoptotic.

(A+B) SH4-blebbing cells showed no positive TUNEL signal. **(A)** CHO cells stably expressing N18-HASPB-GFP for 24 h were treated either with solvent or 200 µg/ml Etoposide (Eto) and 200 µg/ml Cycloheximide (Chx) for 12 h to induce apoptosis, fixed, subjected to TUNEL reaction and analyzed for apoptosis by confocal microscopy. Scale bars = 10 µm. **(B)** Percentage of blebbing and TUNEL positive cells depicted in A. Amounts of apoptotic cells following treatment with Eto/Chx was set to 100 % (arithmetic means of three independent experiments + SD with > 100/condition). **(C-D)** SH4 blebbing cells showed no chromatin condensation. **(C)** CHO cells stably expressing N18-HASPB-GFP for 24 h were treated either with solvent or 4 % DMSO for 5 h to induce apoptosis, fixed, stained with Hoechst 33268 for chromatin and analyzed for apoptosis by confocal microscopy. Scale bars = 10 µm. **(D)** Percentage of blebbing and cells with condensed chromatin as depicted in C. Amounts of apoptotic cells following treatment with DMSO was set to 100 % (arithmetic means of three independent experiments + SD with > 100/condition).

Finally, these cells were also negative for surface exposure of phosphatidyl serine (data not shown), which is externalized by cells in early stages of apoptosis presumably to attract phagocytotic cells (Fadok *et al.*, 1992, Huerta *et al.*, 2007). Thus, SH4-domain expressing cells were negative for apoptotic markers. In line with these findings, induction of PM blebbing by SH4-domains was also insensitive to treatment with zVAD-fmk (100 µM, 24 h, data not shown), a universal inhibitor for caspases. These regulatory proteases are activated during apoptosis where they play a central role in signaling events (Rupinder *et al.*, 2007).

Together, SH4-domain expressing cells showed PM blebbing but no detectable sign for enhanced apoptotic activity.

8.1.6 SH4-Domain Mediated PM Blebbing is a Rho Regulated Process

The above basal characterization of SH4-domain induced PM blebbing revealed a highly dynamic and structured process indicating an active control and regulation by intrinsic determinants. In eukaryotic cells, several basic processes such as cell polarity, adhesion and motility as well as membrane trafficking are regulated through the family of Rho-GTPases. By affecting the actin cytoskeleton, Rho-GTPases control the formation of cell protrusions like membrane ruffles, lamellipodia and filopodia which are important for cell motility (Ridley,

2006). They are also involved in F-actin dynamics that are critical for the formation of various types of PM blebs (Leverrier and Ridley, 2001, Sahai and Marshall, 2003, Verhoef *et al.*, 2004). To determine the role of small Rho-GTPases in SH4-domain mediated PM blebbing, their intracellular localization was analyzed. Expression of GFP fusion proteins of the wild type (wt) GTPases RhoA, Rac1 and Cdc42 in CHO cells revealed their partial PM attachment without the induction of PM blebbing (data not shown). However, PM blebbing was induced by co-expression of N18-Yes-GFP with a wt GTPase fused to a Myc-tag. Confocal microscopy of fixed cells revealed significant amounts of RhoA as well as Rac1 in the limiting membrane but not the lumen of the blebs. In contrast, Cdc42 could only be detected in marginal amounts in some of the analyzed blebs. Thus, all tested Rho GTPases were incorporated into SH4-domain induced blebs albeit with different efficiency (fig. 23A).

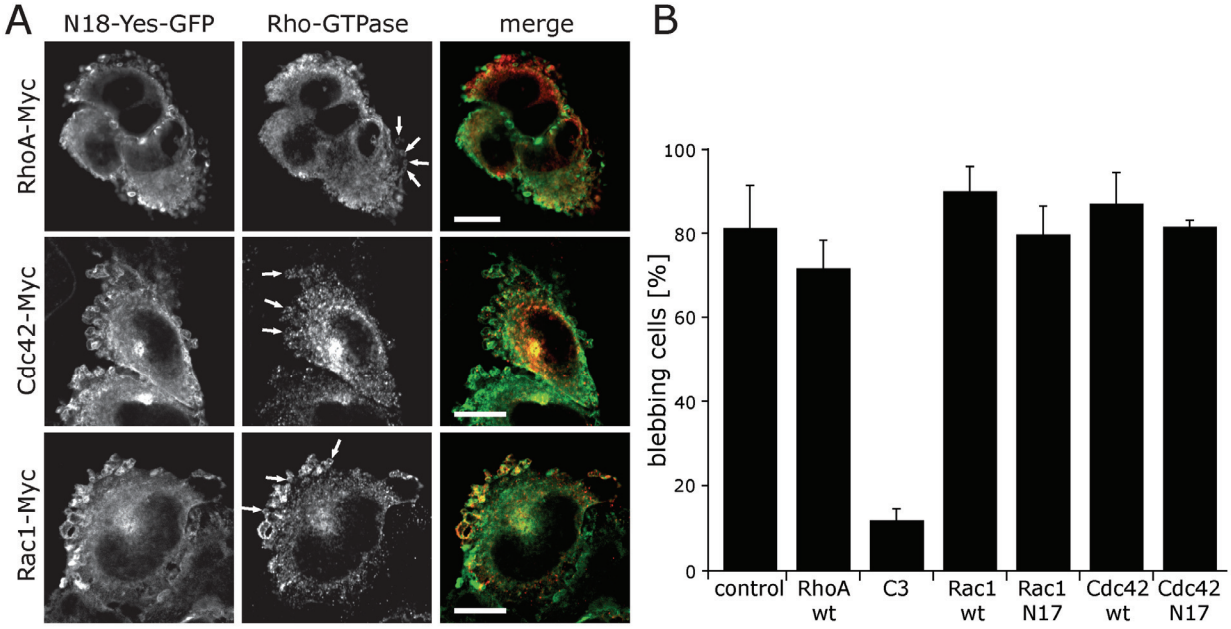

Figure 23: SH4-domain mediated PM blebbing was regulated by the Rho-GTPase Rho.

(A) Rho-GTPases were incorporated into Yes-SH4-domain blebs with different efficiency. Confocal micrographs of fixed and stained CHO cells transiently co-expressing N18-Yes-GFP and a Rho-GTPase as indicated fused to a Myc tag. Scale bars = 10 µm. **(B)** Rho activity was required for HASPB-SH4-domain induced PM blebbing. N18-HASPB fused to mCherry and the indicated GTPase or TAT-C3 transferase fused to GFP were co-expressed in CHO cells and analyzed by live cell confocal microscopy. Shown is the percentage of cells displaying pronounced PM blebbing. (arithmetic means of at least three independent experiments + SD with > 100/condition; kindly provided by S. Tournaviti: B).

To gain further insight into the cellular signal transduction pathway governing SH4-domain-mediated PM blebbing, the HASPB-SH4-domain fused to the fluorescent mCherry protein (N18-HASPB-mCherry) was co-expressed with GFP fusion proteins of wt GTPases, dominant negative (N17) Rac1 or Cdc42, or *Clostridium botulinum* TAT-C3 transferase to inhibit the activity of RhoA, RhoB and RhoC, respectively (Sahai and Olson, 2006). Although all GTPases

localized in SH4-domain induced PM blebs, only TAT-C3-mediated inhibition of Rho significantly reduced bleb formation (fig. 23B). Even though no blebbing was observed, N18-HASPB-mCherry still localized at the PM in the presence of TAT-C3 (data not shown). This indicated that SH4-domains were targeted to the PM in a Rho independent manner but utilized a signaling cascade downstream of Rho to trigger PM blebbing.

In summary, SH4-domain mediated PM blebbing but not targeting was shown to be exclusively regulated by the Rho-GTPase Rho, although RhoA, Rac1 as well as Cdc42 were present in these PM blebs.

8.1.7 Signaling Events Downstream of Rho are Involved in SH4-Domain Induced PM Blebbing

Since SH4-domain blebbing was regulated by the Rho-GTPase Rho, the regulation cascades downstream of this GTPase was analyzed in the following: Rho directly regulates the activity of the Rho effector kinase ROCK (Riento and Ridley, 2003). Active ROCK itself triggers the activity of its substrate the myosin II regulatory part MLC by direct phosphorylation as well as by phosphorylation mediated dissociation of MLCP. Myosin-activity then facilitates bundling of F-actin filaments and leads to contractility. For most types of PM blebbing it was shown that acto-myosin contractility is required for active bleb turnover (Leverrier and Ridley, 2001, Morelli *et al.*, 2003, Sahai and Marshall, 2003). Consequently, the involvement of several steps of the Rho-ROCK pathway in SH4-domain mediated PM blebbing was investigated. Therefore, cells expressing N18-HASPB-GFP for 24 h were treated for 2 h with 90 µM (or 10 µM, data not shown) of the ROCK-specific inhibitor Y-27632 (Davies *et al.*, 2000, Jacobs *et al.*, 2006) and were analyzed for PM blebbing. Blocking ROCK activity potently interfered with SH4-mediated PM blebbing, whereas wash out and additional incubation for 3 h with medium effectively retrieved PM blebbing (fig. 24A/C). Hence, a 2 h pretreatment with Y-27632 was used in the following to strip already formed blebs in order to investigate the formation of new ones. Treatment with 100 µM Blebbistatin (BS), a drug specifically interfering with the ATPase activity of the myosin II motor protein (Allingham *et al.*, 2005, Ramamurthy *et al.*, 2004, Straight *et al.*, 2003), efficiently blocked PM bleb formation, indicating a mechanistic role for myosin (fig. 24A/C). Myosins regulate the F-actin network for instance by facilitating bundling and contractility forces (Riento and Ridley, 2003). In fact, microscopical analysis demonstrated some enrichment of F-actin at the limiting membrane and in particular at the neck of SH4-domain induced PM blebs (fig. 18Cb and 24A). Consistently, disruption of F-actin filaments by treatment of the cells with 1 µM Cytochalasin D (CytoD) potently interfered with their formation

(fig. 24A/C). A second element of the cytoskeleton is represented by microtubules. Similarly to the results obtained for F-actin, depolymerization of microtubules with 100 µM Nocodazole efficiently inhibited SH4-domain mediated PM blebbing (fig. 24B/C).

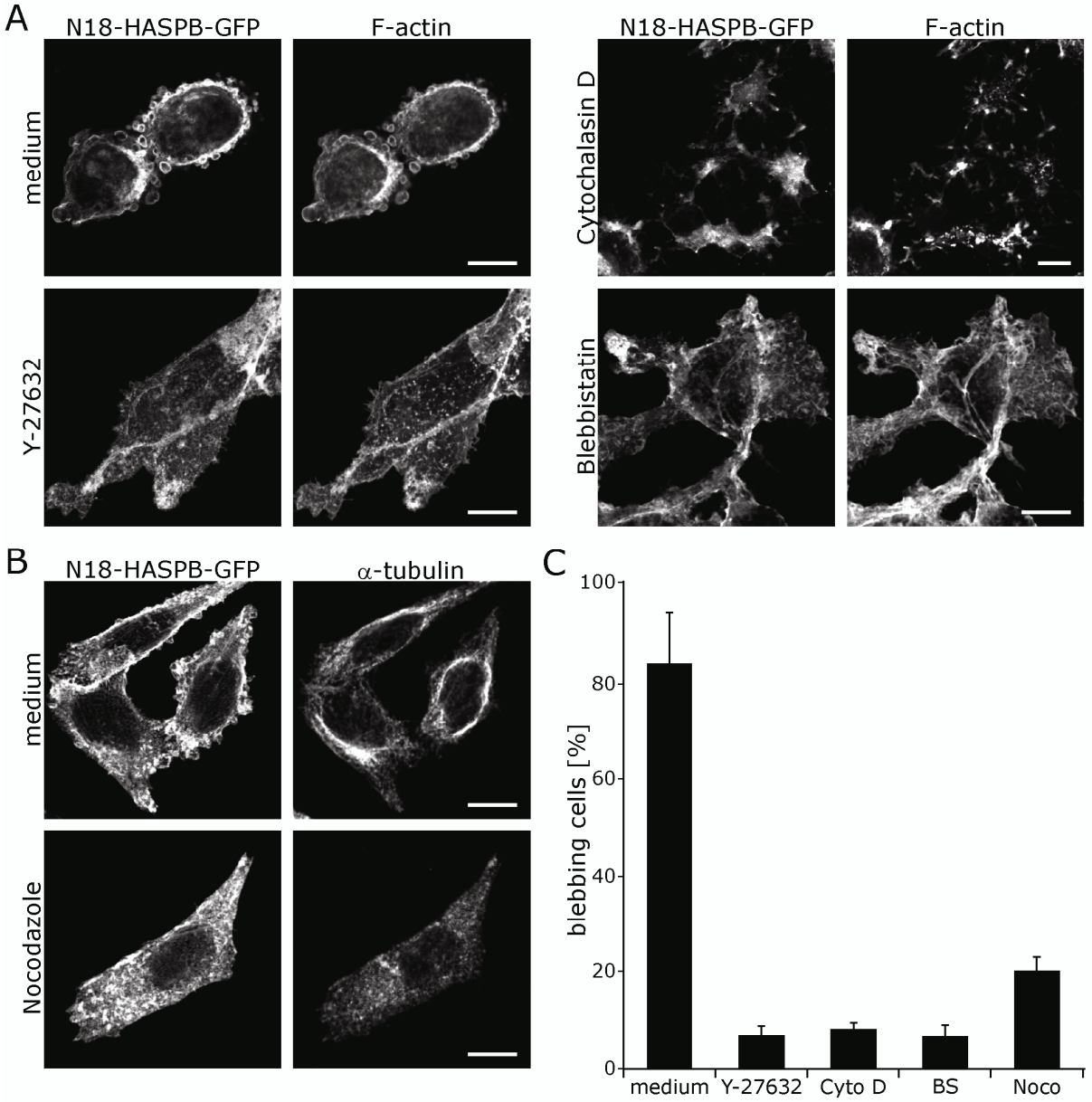

Figure 24: Functionality of the Rho pathway as well as F-actin and microtubule integrity was required for SH4-domain mediated PM blebbing.

(A) PM blebs were dependent on ROCK and myosin II activity as well as on an intact microfilament system. Confocal micrographs of CHO cells stably expressing N18-HASPB-GFP for 24 h were treated with Y-27632 for 2 h and subsequently with solvent or the indicated drugs for 3 h (90 µM Y27632, 1 µM Cytochalasin D, 100 µM Blebbistatin), fixed and stained for F-actin. Scale bars = 10 µm. **(B)** PM blebs were dependent on an intact microtubule architecture. Cells were treated and handled as described in A, but were treated with 100 µM Nocodazole and were additionally stained for α-tubulin. Scale bars = 10 µm. **(C)** Percentage of blebbing cells depicted in A and B (arithmetic means of at least three independent experiments + SD with > 100/condition).

Concordantly, a specific stain of β-tubulin showed perinuclear enrichment and cytoplasmic distribution of the filaments, but no localization at SH4-domain induced PM blebs (fig. 24B).

Together, induction of PM blebs by the HASPB-SH4-domain depended on the integrity of both F-actin and microtubule networks and required ROCK activity as well as myosin II functionality. These results revealed a novel link between Rho-ROCK activity and SH4-domains.

8.1.8 The Cortical Actin of SH4-Domain Induced PM Blebs is Enriched in Active MLC

The cortical actin is enriched in myosin II and directly linked to different kinds of PM blebbing (Eisenmann *et al.*, 2007, Huot *et al.*, 1998, Mills *et al.*, 1999). FLNa deficient M2 melanoma cells have a defect in F-actin filament cross linking. Therefore, local contractility of the acto-myosin system leads to a local destablization of the cortical actin meshwork and results in bleb formation due to intracellular pressure (Charras *et al.*, 2005). Furthermore, myosin activity is also required for bleb retraction in those cells (Charras *et al.*, 2006). Thus, the role of FLNa and myosin was investigated in the following. First of all, the effect of SH4-domain expression on bulk protein levels of FLNa and its active and phosphorylated form FLNa (S^{2151}) were evaluated (fig. 25). Lysates of HeLa cells which were either induced or not induced for expression of N18-Yes-GFP, N18-Δmyr-Yes-GFP or N18-Δpal-Yes-GFP were separated by SDS-PAGE and analyzed by Western blotting. Following probing with specific antibodies, no differences in the amounts of FLNa or FLNa (S^{2151}) were detected in any case. This indicated that SH4-domain mediated PM blebbing was not due to alterations in overall levels and activity of FLNa.

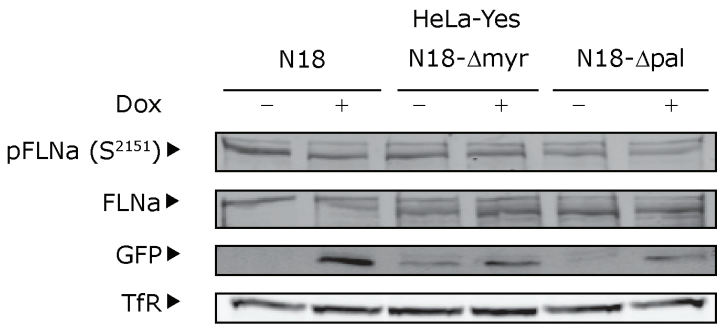

Figure 25: Overall expression levels of FLNa were not changed upon SH4-domain expression.

Expression of either N18-Yes-GFP, N18-Δmyr-Yes-GFP or N18-Δpal-Yes-GFP was induced (+) or not induced (-) in HeLa cells for 24 h. After lysis, equal amounts of total protein were separated by SDS-PAGE, subjected to Western blotting and probed with specific antibodies for total FLNa or pFLNa (S^{2151}), for endogenous transferrin receptor (Tfr, loading control) and GFP (expression control), respectively.

Besides FLNa, myosins also play a crucial role in cortical actin dynamics of M2 cells. These motor proteins are actin associated and directly facilitate contractility during cell motility and PM blebbing (Charras *et al.*, 2006, Mills *et al.*, 1998, Riento and Ridley, 2003). The necessity of active myosin and its regulatory kinase ROCK in SH4-domain mediated PM blebbing was shown in the previous chapter. To obtain further insight into the role of ROCK in this process, the intracellular localization of MLC and its active and phosphorylated form pMLC (S^{19}) was

investigated as an indicator for ROCK activity and localization. Confocal micrographs of CHO cells transiently expressing GFP, N18-Δmyr-Yes-GFP or N18-Yes-GFP showed a MLC and pMLC (S^{19}) association to F-actin stress fibers as well as to the cortical actin (fig. 26).

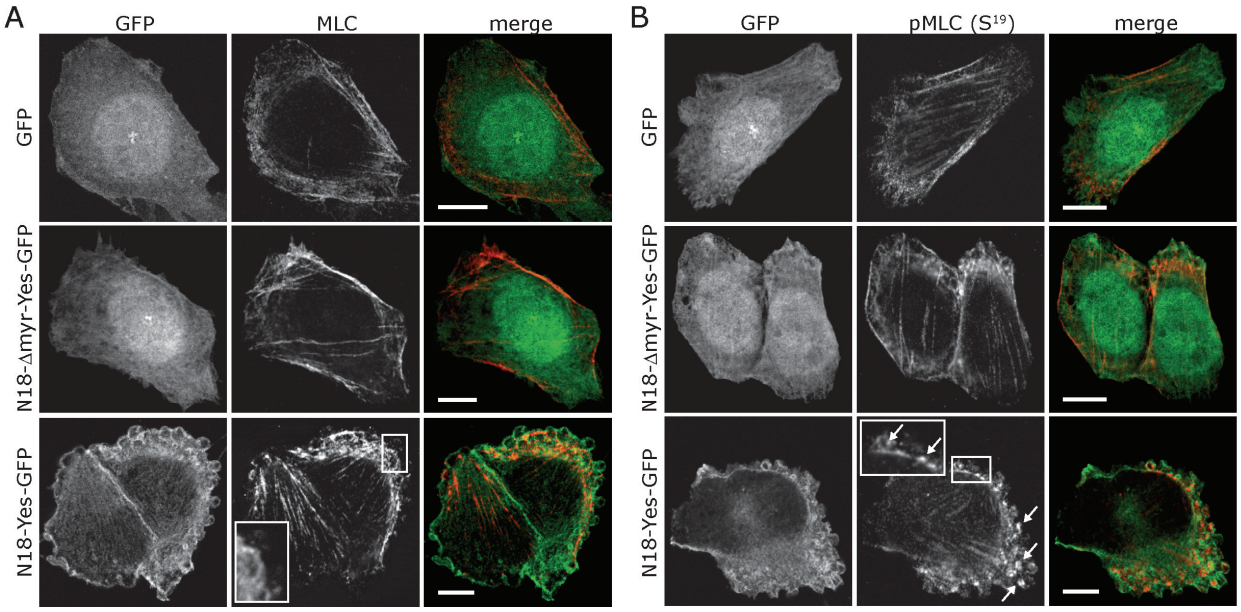

Figure 26: Total (MLC and active pMLC (S^{19}) localized in and at the basis of Yes-SH4-domain blebs.

(A+B) Confocal micrographs of fixed and stained CHO cells transiently expressing GFP, N18-Yes-Δmyr or N18-Yes-GFP, were fixed and stained for **(A)** endogenous MLC or **(B)** pMLC (S^{19}). Scale bars = 10 µm.

In blebbing cells, both, MLC and pMLC (S^{19}) additionally localized at the basis and the outer rim of the blebs, whereas the lumen of some blebs was also enriched with pMLC (S^{19}) (see arrows, fig. 26).

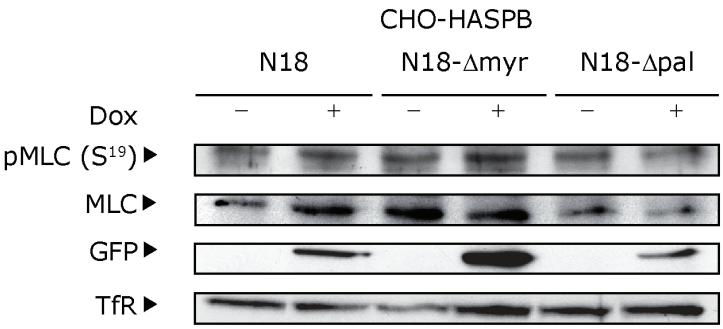

Figure 27: Overall expression levels of myosin light chain (MLC) were not changed upon SH4-domain expression.

Expression of either N18-HASPB-GFP, N18-Δmyr-HASPB-GFP or N18-Δpal-HASPB-GFP was induced (+) or not induced (-) in CHO cells for 24 h. After lysis, equal amounts of total protein were separated by SDS-PAGE, subjected to Western blotting and probed with specific antibodies for total MLC or pMLC (S^{19}), for endogenous transferrin receptor (Tfr, loading control) and GFP (expression control).

This suggested a local ROCK activity at the site of PM blebbing. To further investigate this activity, bulk levels of MLC and pMLC (S^{19}) were analyzed by western blot similar to FLNa and

pFLNa (S^{2151}) as described above. However, neither a change in MLC nor in pMLC (S^{19}) levels could be observed by induction of HASPB-SH4-domain expression in CHO cells (fig. 27).
In conclusion, induction of PM blebbing by SH4-domains did not alter bulk levels of active MLC or FLNa. Nevertheless, active MLC localized in the cortical actin beyond blebs and was enriched in their lumen, indicating either a local activation or a recruitment of active ROCK to the site of PM blebbing.

8.1.9 SH4-Domain Induced PM Blebbing Depends on Endogenous Src Activity

Next, the contribution of endogenous Src kinases was investigated. Src kinases were shown to play a key role in regulation of several intracellular signaling pathways involved in cell division, differentiation, survival, adhesion, motility and vesicular trafficking (Thomas and Brugge, 1997). So far, a contribution of Src kinases in any kind of PM blebbing was not suggested. However, some of the SH4-domains used in this work are the PM anchors for Src kinases such as c-Src, Fyn, Lck and Yes. Therefore, a role of endogenous Src kinase activity in SH4-domain mediated PM blebbing was hypothesized. To remove already formed PM blebs, CHO cells expressing N18-HASPB-GFP or N18-Fyn-GFP were treated with 10 µM Y-27632 for 2 h. Their reappearance was analyzed in the presence of the two well established, structurally distinct and specific Src kinase inhibitors PP1 and SU6656 (Bishop *et al.*, 1999, Blake *et al.*, 2000). Treatment with both inhibitors at 1 µM already markedly reduced PM blebbing (fig. 28A/B).

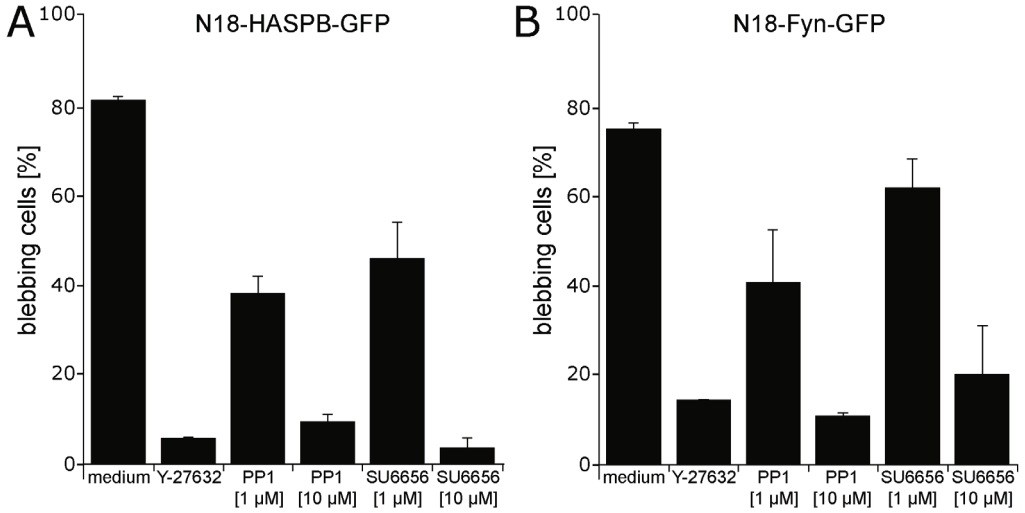

Figure 28: Induction of PM blebbing by SH4-domains required activity of endogenous Src kinases.

(A+B) CHO cells stably expressing either **(A)** N18-HASPB-GFP or **(B)** N18-Fyn-GFP were treated with 10 µM Y-27632 for 2 h to remove already formed blebs, washed and treated with medium or the indicated Src kinase inhibitors (PP1, SU6656) for additional 3 h. Cells were fixed, stained for F-actin and evaluated for newly formed blebs (arithmetic means of three independent experiments + SD with > 100/condition).

When 10 µM inhibitor was used, blebbing inhibition was well within the range of that observed with addition of the ROCK inhibitor Y-27632. Similar results were obtained for the SH4-domains of c-Src, Yes and Lck (data not shown).

These results could be verified by usage of SYF -/- mouse fibroblastic cells that are deficient in the Src kinases c-Src, Yes and Fyn (Klinghoffer *et al.*, 1999). In these cells expression of N18-Yes-GFP did not result in PM blebbing, whereas blebbing was readily observed in c-Src reconstituted SYF + c-Src cells (fig. 29A/B).

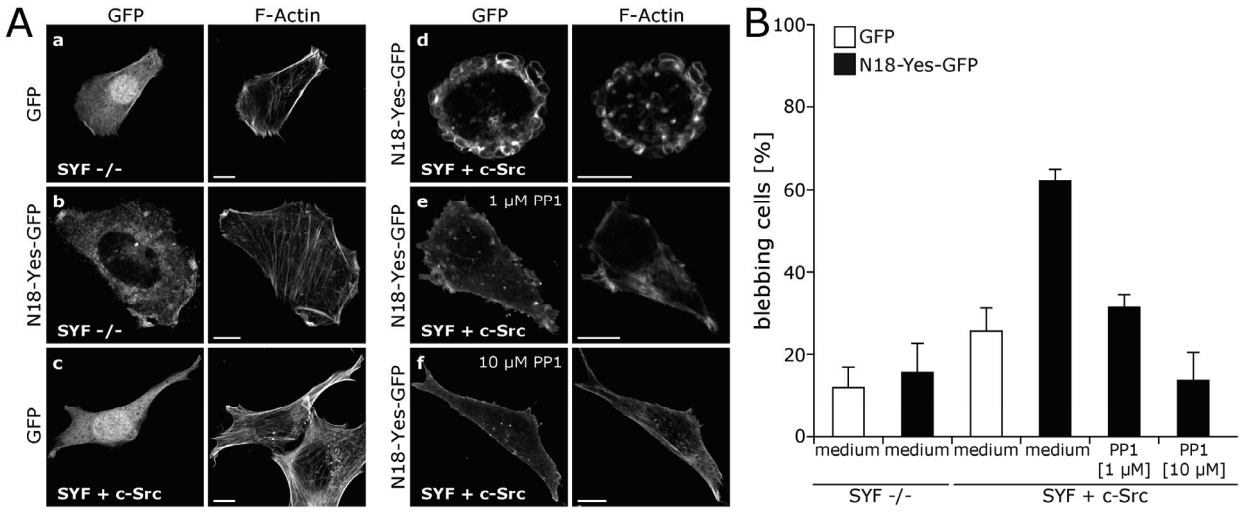

Figure 29: Endogenous Src kinases were necessary for SH4-domain mediated induction of PM blebbing.

(A) Confocal micrographs of either SYF -/- cells depleted for endogenous c-Src, Yes and Fyn (a-b) or SYF + c-Src cells reconstituted with c-Src (c-f) were transfected with GFP or N18-Yes-GFP and treated with solvent or the Src kinase inhibitor PP1 in the indicated amounts. Scale bars = 10 µm. **(B)** Percentage of blebbing cells depicted in A. Values for GFP transfected cells are shown in white bars, for N18-Yes-GFP cells in black bars (arithmetic means of three independent experiments + SD with > 100/condition).

Since this rescue was sensitive to PP1 treatment, not only presence but also activity of the reconstituted c-Src was required. These results demonstrated that endogenous Src activity was involved in the induction of SH4-domain mediated PM blebbing. To test whether endogenous Src kinases were activated during induction of PM blebbing, bulk levels of c-Src and pc-Src (Y^{418}) were analyzed by western blotting similar to FLNa and pFLNa (S^{2151}) as described above (fig. 30). Neither a change in Src nor in pSrc (Y^{418}) levels could be observed by induction of Yes-SH4-domain expression in HeLa cells. Note that varying signal intensities for c-Src in uninduced (-) and induced (+) N18-Yes-GFP cells were due to different amounts of loaded lysate as it is depicted in the loading control (TfR).

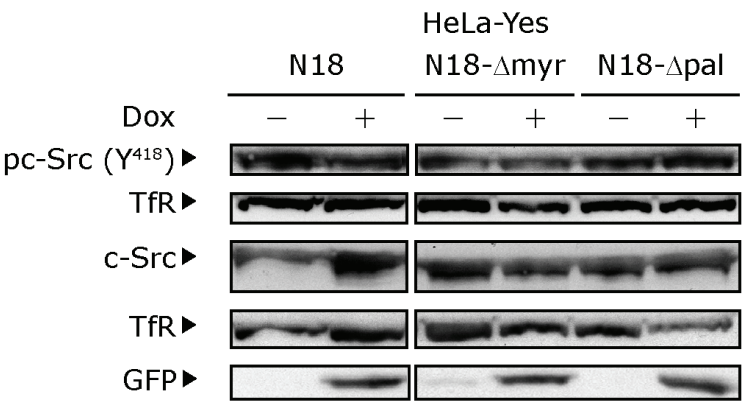

Figure 30: SH4-domains did not alter the overall activation levels of endogenous c-Src.

Expression of either N18-Yes-GFP, N18-Δmyr-Yes-GFP or N18-Δpal-Yes-GFP was induced (+) or not induced (-) in HeLa cells for 24 h. After lysis, equal amounts of total protein were separated by SDS-PAGE, subjected to Western blotting and probed with specific antibodies for total c-Src or pc-Src (Y^{418}), for endogenous transferrin receptor (Tfr, loading control) and GFP (expression control), respectively.

Nevertheless, analysis of the distribution of endogenous c-Src in CHO cells transiently expressing N18-Yes-GFP revealed a modest but significant localization of the kinase in the membrane of PM blebs (fig. 31A). No significant relocalization was observed upon expression of SH4-domains, suggesting that Src incorporation into blebs may reflect its genuine partial PM localization. This included the lack of displacement of c-Src from the PM upon SH4-domain over-expression which indicated that the expressed SH4-domain did not saturate PM docking sites of endogenous c-Src. In contrast and in line with the inhibitory effects on bleb formation of the Src inhibitors PP1 and SU6656, active pc-Src (Y^{418}) accumulated in the lumen of N18-Yes-GFP mediated blebs similarly to active pMLC (S^{19}) (fig. 26B and 31B).

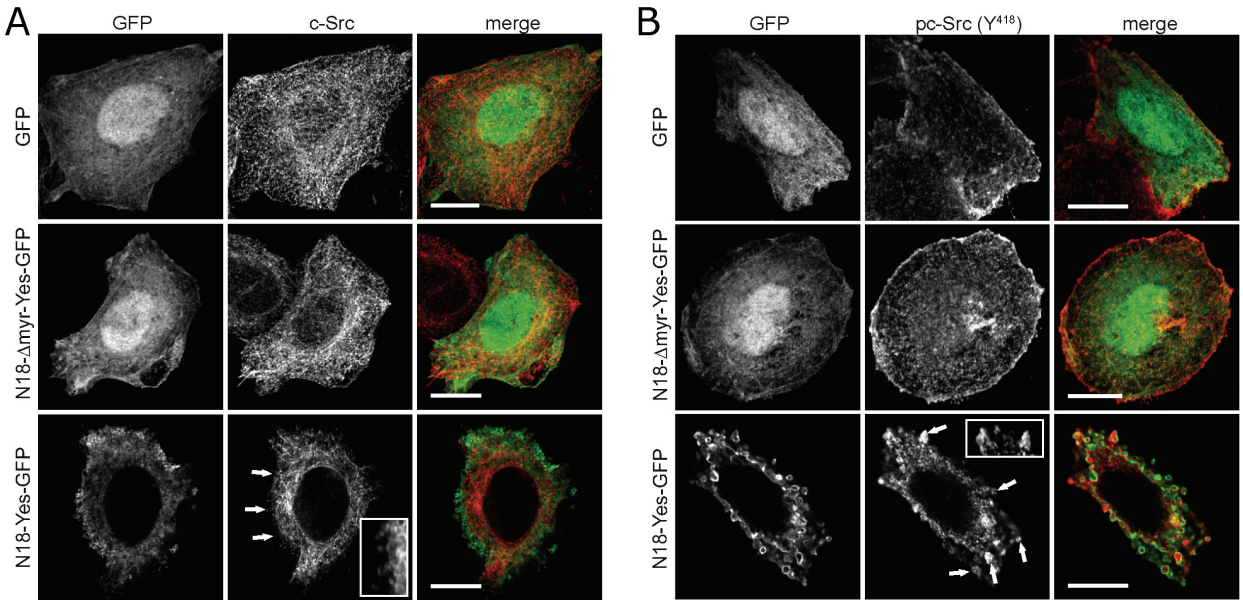

Figure 31: Active pc-Src (Y^{418}), but not total Src accumulated in Yes-SH4-domain blebs.

Confocal micrographs of fixed and stained CHO cells transiently expressing GFP, N18-Yes-Δmyr or N18-Yes-GFP, respectively, were fixed and stained for **(A)** endogenous Src or **(B)** pc-Src (Y^{418}). Scale bars = 10µm.

In summary, induction of PM blebbing by SH4-domains required the activity of endogenous Src kinases, although overall c-Src activation was not increased. Nevertheless, active c-Src was enriched in SH4-domain induced PM blebs suggesting a recruitment of active c-Src or a local activation of the kinase.

This initial characterization of SH4-domain PM blebbing is summarized in a manuscript (Tournaviti et al., in press) that was accepted for publishing during preparation of this thesis.

8.1.10 SH4-Domains Mediate Uptake of Dextran

Under physiological conditions, there are several situations in which PM blebbing is involved: As already discussed, during apoptosis PM blebbing is thought to support DNA fragmentation and initiation of immune responses (Fadeel, 2004, Martinez *et al.*, 2005). However, in this work it could be demonstrated that SH4-domain expressing cells were not apoptotic. Furthermore, PM blebbing also occurs during secretion of different proteins such as IL-1β and galectin 3 (MacKenzie *et al.*, 2001, Mehul and Hughes, 1997). Interestingly, the surface coat protein HASPB of the *Leishmania* parasite was shown to be secreted by mammalian cells (Denny *et al.*, 2000, Stegmayer *et al.*, 2005). Nevertheless, vesicle shedding from the surface was not observed for cells expressing the HASPB-SH4-domain. Additionally, block of PM blebbing by treatment of the cells with the ROCK inhibitor Y-27632 did not inhibit release of GFP fused to the HASPB-SH4-domain (C. Stegmayer, personal communication). However, PM blebbing was also observed during particle-uptake as well: Simultaneously to their own entry, Vaccinia viruses induce PM blebbing nearby the entry site (A. Helenius and J. Mercer: 58. Mosbacher Kolloquium 2007). Similarly, during clathrin-mediated endocytosis of Adenoviruses, they induce PM ruffling nearby the entry site in parallel which is correlated to enhanced macropinocytosis (Meier *et al.*, 2002, Meier and Greber, 2003). Both PM blebbing and endocytosis are processes that bear PM dynamization. In general, endocytosis describes a cellular process for specific or non-specific uptake of fluids, molecules or particles and is characteristic for all eukaryotic cells. One has to distinguish between several types of different endocytotic mechanisms that sometimes are cell type specific as well as stimulus dependent (Marsh and Helenius, 2006, Nichols and Lippincott-Schwartz, 2001). Clathrin independent macropinocytosis in particular allows actin-dependent, nonselective uptake of solute macromolecules from the fluid phase of the extra cellular milieu. During macropinocytosis large (> 1µm in diameter) vesicles of irregular size, called macropinosomes are developed on the cell surface presumably by merge of PM ruffles (Cardelli, 2001, Meier and Greber, 2003, Swanson and Watts, 1995). Their formation and trafficking depends on Src kinase activity (Kasahara *et*

al., 2007). Hence, the possible correlation between SH4-domain induced PM blebbing and macropinocytotic uptake was investigated.

Initially, the basal capacity of CHO cells for internalization of fluorescently labeled dextran (10 to 70 kDa) was analyzed. Fluorescence microscopy of CHO-GFP cells revealed incorporated dextran in a cytoplasmic distribution as well as localization in bright intracellular spots after 60 min (fig. 32A). This basal dextran-uptake was confirmed by FACS-analysis with Alexa Fluor-647 labeled dextran: After gating for the living cells in the SSC/FSC channel (fig. 32Ba), dot plots of GFP expressing cells showed a certain level of internalized dextran. Comparison of the mean fluorescence intensities (MFIs) of high (gate R4: MFI = 1078), low (gate R3: MFI = 622) or no (gate R2: MFI = 780) GFP expressing cells demonstrated that the uptake ability was uncoupled from GFP expression or if any, slightly reduced, indicating no effect for GFP itself. Consistent with this, internalization could be similarly blocked for cells of all expression levels by treatment with 100 µM 5-(N-ethyl-N-isopropyl)-amiloride (EIPA), a specific inhibitor for macropinocytosis (R3: 5.5 fold reduction; fig. 32Bb). In contrast, addition of a macropinocytosis stimulatory drug like phorbol myristate acetate (PMA, 200 nM), increased internalization for all expression levels by 1.9 fold (fig. 32Bb). Again, this enhanced uptake was sensitive to treatment with EIPA (data not shown). These results indicated that CHO cells themselves were able to perform macropinocytotic uptake of dextran. Next, the impact of SH4-domains on this internalization was investigated. CHO cells expressing N18-HASPB-GFP were analyzed by confocal microscopy. Interestingly, they showed a similar distribution of internalized dextran compared to GFP expressing cells (fig. 32C). Dextran also localized inside the lumen of PM blebs. Bleb specific accumulation of dextran in earlier time points representing bleb specific uptake, however, was not observed (fig. 32C and data not shown). Thus, a direct correlation of PM blebbing with dextran-uptake could not be verified by this method. Nevertheless, in order to investigate a possible effect of SH4-domains on dextran-uptake, a FACS analysis was performed for N18-HASPB-GFP expressing cells: The uptake-capacity for cells with no (gate R2: MFI = 857) or low (gate R3: MFI = 845) N18-HASPB-GFP expression was similar to GFP expressing cells (fig. 32Bd). In contrast, cells with high expression levels (gate R4: MFI = 1337) showed a specific increase in dextran-uptake. Quantification of the MFIs resulted in a 2.0-fold increased dextran internalization compared to GFP expressing cells (fig. 32B/D).

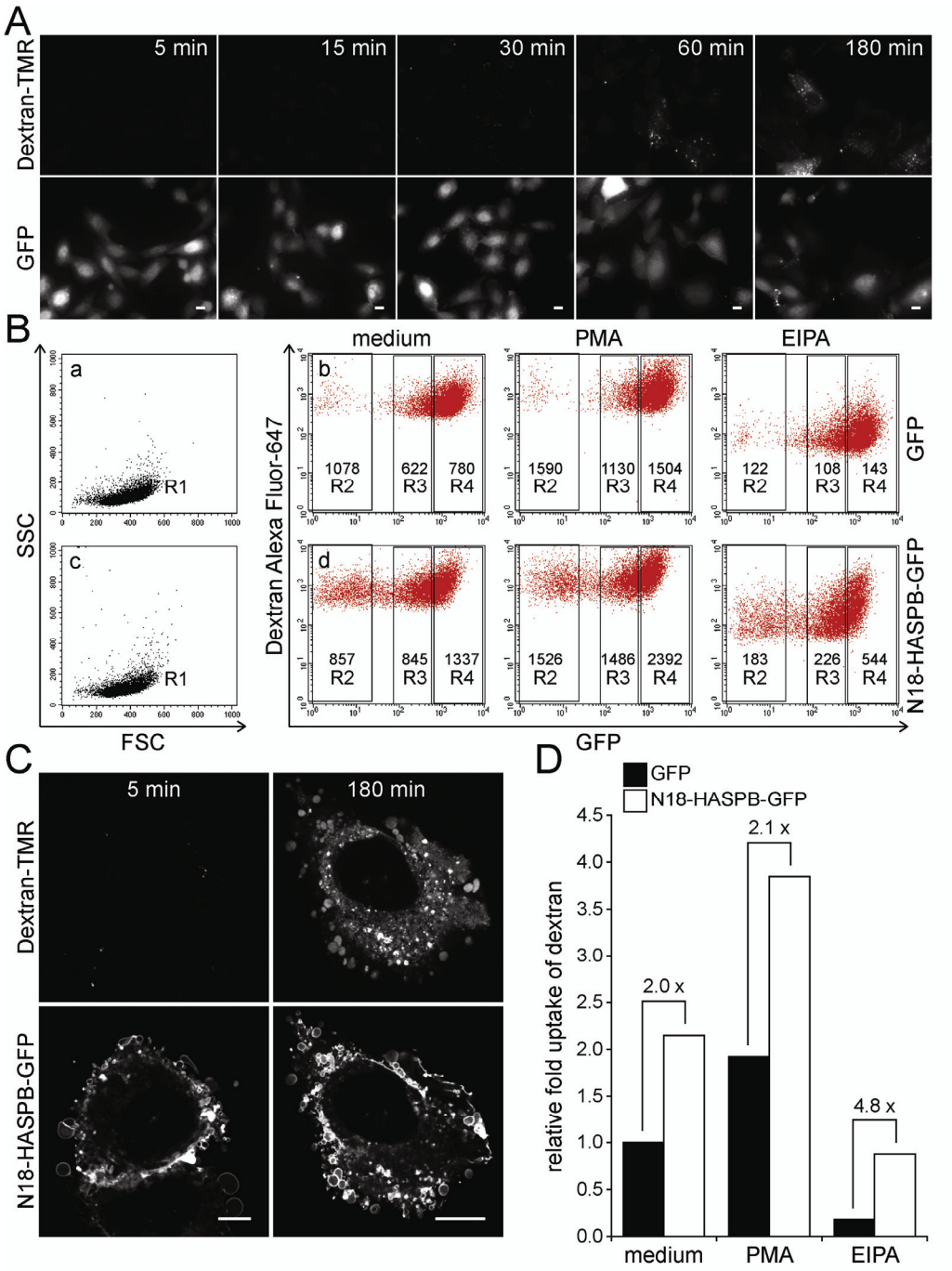

Figure 32: Uptake of dextran into CHO cells was increased upon expression of the HASPB-SH4-domain.

(A) CHO cells were capable of dextran-uptake. CHO cells stably expressing GFP were treated with TMR labeled dextran (70 kDa) for up to 180 min, fixed, and subjected to fluorescence microscopy. Scale bars = 10 µm. **(B)** HASPB-SH4-domains increased the ability for dextran-uptake. CHO cells stably expressing either GFP (a-b) or N18-HASPB-GFP (c-d) were treated with Alexa Fluor-647 labeled dextran (10 kDa) in the presence of the indicated macropinocytosis stimulatory (200 nM PMA) or inhibitory drugs (100 µM EIPA) for 180 min, washed with PBS and washing buffer (pH 5.5) and subjected to FACS analysis. Dot plots show side scatter (SSC) signals and forward scatter (FSC) signals of all cells (a+c) as well as signals obtained for internalized fluorescently labeled dextran and expressed GFP of gated living cells (b+d). Gates were set for non- (R2), low- (R3) and high- (R4) expressing cells and corresponding mean fluorescence intensities (MFIs) were indicated. **(C)** Dextran diffusely localized in the cytoplasm and in HASPB-SH4-domain blebs as well as in intracellular vesicle like structures. CHO cells stably expressing N18-HASPB-GFP for 24 h were treated as described in A but analyzed by confocal microscopy. Scale bars = 10 µm. **(D)** Relative mean values of cells gated for high expression levels (R4) as depicted in B (ratio of R4/(R2 of medium treated cells)) and fold differences.

Since two lasers were used for measurement, an artifact due to less compensation can be ruled out. Similar results were obtained with N18-Src-GFP and N18-Fyn-GFP (data not shown). Moreover, treatment with PMA enhanced (R3: 1.8 fold) and EIPA reduced (R3: 2.5 fold reduction) dextran-uptake for all expression levels. However, compared to GFP expressing cells, dextran-internalization of high N18-HASPB-GFP expressing cells was 4.8-fold increased in EIPA, but only 2.1-fold in PMA treated cells. This indicated that the SH4-domain mediated effect on dextran-uptake was not solely related to macropinocytosis (fig. 32B/D). To investigate whether other internalization pathways were involved as well, clathrin-dependent endocytosis was tested with fluorescently labeled transferrin analyzed by FACS (fig. 33A/B).

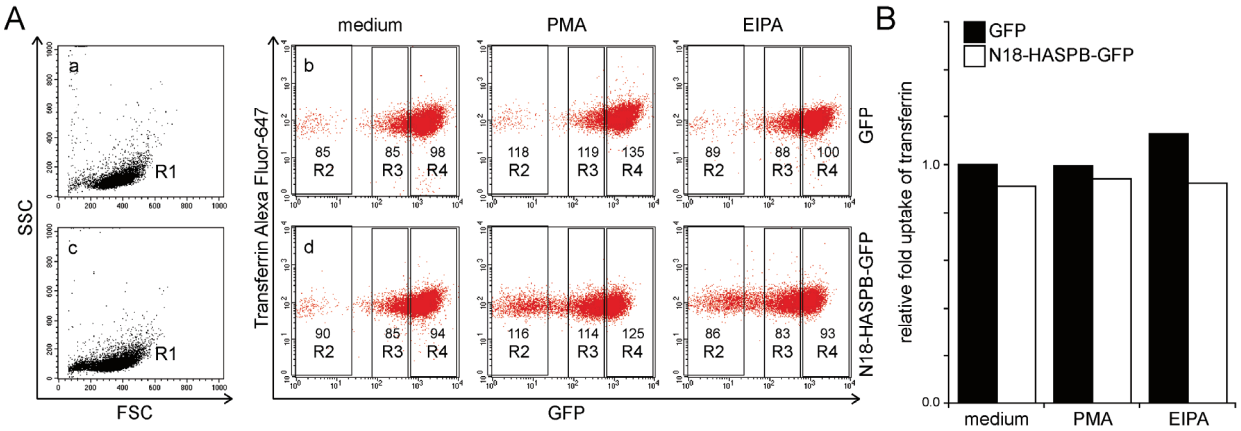

Figure 33: The HASPB-SH4-domain had no influence on transferrin-uptake.

(A) CHO cells stably expressing either GFP (a-b) or N18-HASPB-GFP (c-d) were treated with TMR labeled transferrin in the presence of the indicated drugs (200 nM PMA; 100 µM EIPA) for 180 min, washed with PBS and washing buffer (pH 5.5) and subjected to FACS analysis. Dot plots show side scatter (SSC) signals and forward scatter (FSC) signals of all cells (a+c) as well as signals obtained for internalized fluorescently labeled transferrin and expressed GFP of gated living cells (b+d). Gates were set for non- (R2), low- (R3) and high- (R4) expressing cells and corresponding MFIs were indicated. **(B)** Relative mean values of cells gated for high expression levels (R4) as depicted in C (ratio of R4/(R2 of medium treated cells)).

In a control experiment uptake of transferrin was neither stimulated by PMA nor inhibited by EIPA in CHO-GFP cells. Furthermore, expression of N18-HASPB-GFP did not alter transferrin-internalization at any expression level.

As shown in the previous part, expression of SH4-domains induced PM blebbing, but expression of non acetylated mutants that were deficient in PM targeting did not. To check whether PM blebbing is the driving force for increased dextran internalization the effect of the non-blebbing mutants N18-Δmyr-HASPB-GFP and N18-Δpal-HASPB-GFP were investigated. Fluorescence microscopy showed a reduced capacity of dextran-uptake for these mutants comparable to GFP expressing cells (fig. 34A).

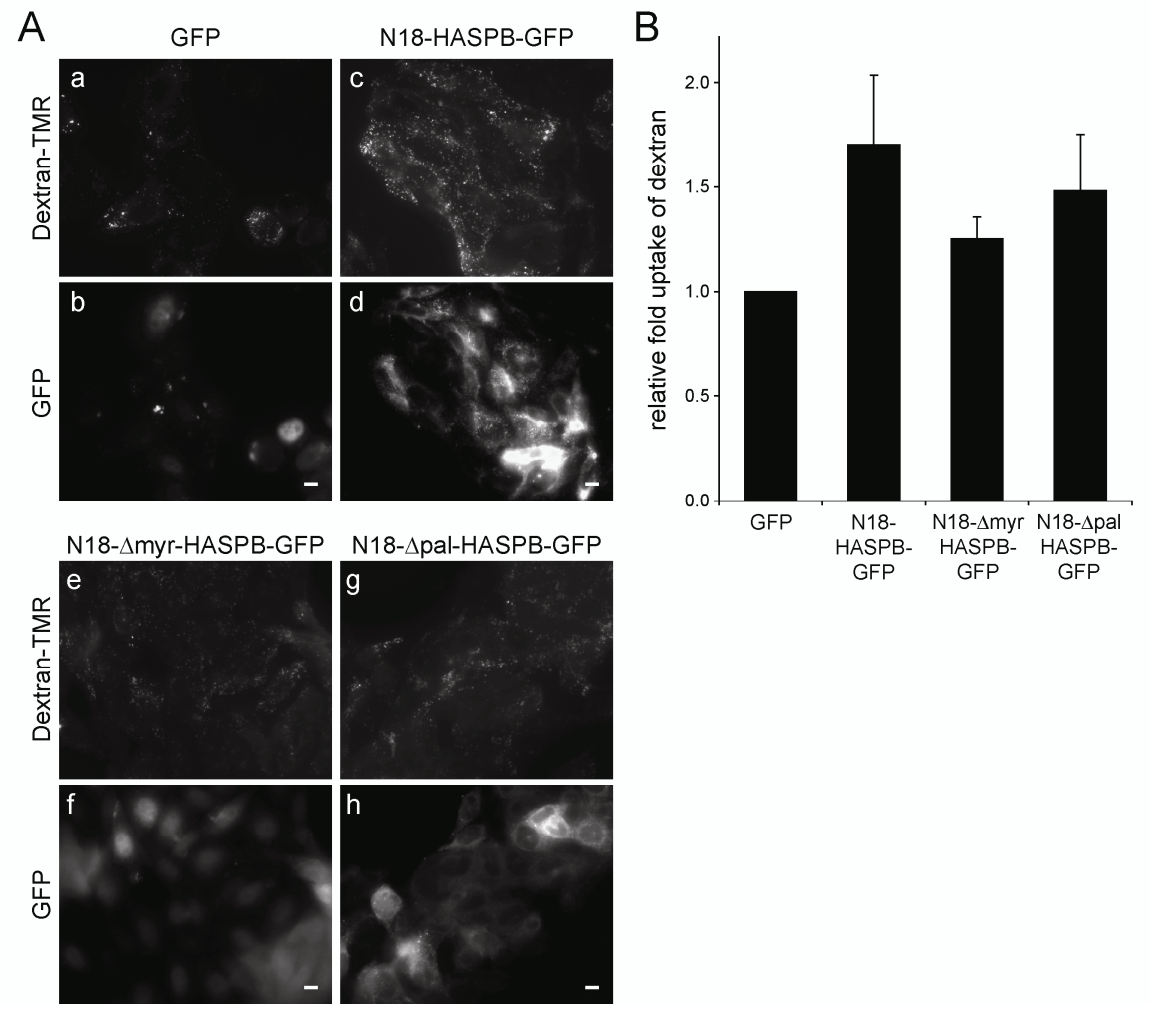

Figure 34: Uptake of dextran was reduced in HASPB-SH4-domain mutants not capable of PM blebbing induction.

(A) CHO cells stably expressing either GFP, N18-HASPB-GFP, N18-Δmyr-HASPB-GFP or N18-Δpal-HASPB-GFP for 24 h were treated with Alexa Fluor-568 labeled dextran (70 kDa) for up to 180 min, fixed, and subjected to fluorescence microscopy. Scale bars = 10 µm. **(B)** FACS analysis of CHO cells stably expressing either GFP, N18-HASPB-GFP, N18-Δmyr-HASPB-GFP or N18-Δpal-HASPB-GFP for 24 h. Cells were treated with Alexa Fluor-647 labeled dextran (10 kDa) for 180 min, washed with PBS and washing buffer (pH 5.5) and subjected to FACS analysis. Depicted are the relative mean values of cells gated for high expression levels (R4) (ratio of R4/R2; statistical analysis by Student's t-test: GFP to N18-HASPB-GFP: $p = 0.016$; N18-HASPB-GFP to N18-Δmyr-HASPB-GFP: $p = 0.076$; N18-HASPB-GFP to N18-Δpal-HASPB-GFP: $p = 0.338$).

This was confirmed by FACS analysis which shows an intermediate uptake capacity in CHO cells compared to GFP or N18-HASPB-GFP (fig. 34B). However, calculation of p-values by Sudent's t-test revealed no statistically significance (GFP to N18-HASPB-GFP: $p = 0.016$; N18-HASPB-GFP to N18-Δmyr-HASPB-GFP: $p = 0.076$; N18-HASPB-GFP to N18-Δpal-HASPB-GFP: $p = 0.338$) and indicated that PM blebbing and dextran-uptake could not be directly correlated.

Together, SH4-domains had the capacity to induce dextran-uptake by a clathrin-independent pathway that was not related to macropinocytosis. Furthermore, this effect on internalization

could not be directly correlated with their competence to induce PM blebbing indicating that other mechanisms might be involved.

8.1.11 N18-HASPB Mediated PM Blebbing Does not Alter Wound Healing Motility

PM blebbing on motile cells has long been described for cells during embryonic development and cells located at the leading edge of cellular sheets (Dipasquale, 1975, Trinkaus, 1973). To investigate whether SH4-domains had an influence on motility on planar surfaces, a wound healing assay was performed. Therefore, a confluent layer of CHO cells was scratched with a pipette tip to yield a wound of approx. 200-300 µm (fig. 35A).

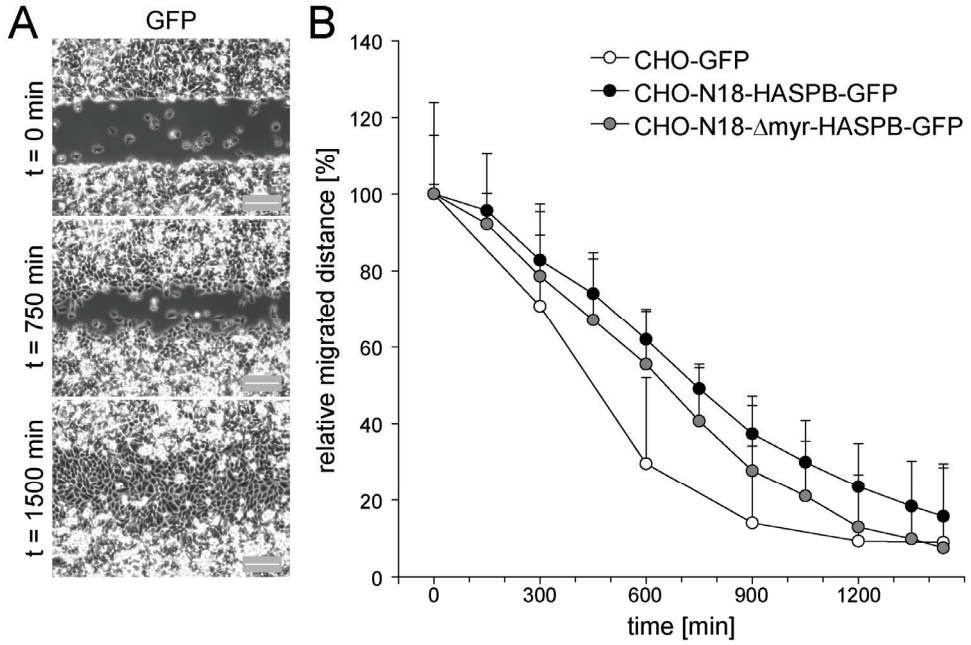

Figure 35: The SH4-domain of HASPB did not influence wound healing motility.

(A+B) The wound closure time was not altered in HASPB-SH4-domain expressing cells. **(A)** Representative images of a wound healing assay performed with GFP expressing CHO cells. A confluent cell layer was wounded and subsequently monitored by microscopy over time (24 h, 1 picture/30 min). Scale bars = 100 µm. **(B)** Quantification of wound closure time. Wound sizes of layers of cells expressing either GFP, N18-HASPB-GFP or N18-Δmyr-HASPB-GFP were measured with "ImageJ" software. Values are the arithmetic means of at least three wounds per condition + SD.

Cell migration was monitored for 24 h by a frequency of 1 picture/30 min and the distances were measured using ImageJ software (fig. 35B). Compared to GFP expressing cells, expression of blebbing N18-HASPB-GFP or not blebbing N18-Δmyr-HASPB-GFP had no influence on wound closure time.

Neither a function of SH4-domain mediated PM blebbing nor an intrinsic effect of SH4-domains on wound closure was detectable.

8.1.12 SH4-Domain Induced PM Blebbing Correlates with Enhanced Cell Invasion in 3D Matrices

Another form of bleb related cell motility occurs in tumor cells during the amoeboid mode of invasion into 3D environments like tissues or 3D matrices that consist of ECM proteins. (Sahai and Marshall, 2003, Wolf *et al.*, 2003, Wyckoff *et al.*, 2006). This amoeboid or rounded mode of invasion depends on the active generation of PM blebs by F-actin polymerization and is clearly distinct from the mesenchymal or elongated mode of invasion that is related to motility on planar surfaces, but depends on secretion of metalloproteases to disrupt the surrounding ECM. Interestingly, both invasion modes are stimulated by internalization of external signal peptides and growth factors (Sahai, 2005, Yamazaki *et al.*, 2005). To test the functional consequences of SH4-domain mediated PM blebbing on cell motility in 3D matrices a well-established matrigel transwell assay was used (Hooper *et al.*, 2006). Serum starved CHO-cells were seeded on top of undiluted growth factor reduced matrigel placed inside a transwell insert (pore size 8 µm). After 48 h incubation in a gradient of FCS (0.5–10 %) the percentage of cells that invaded the matrigel and crossed the transwell membrane was determined (fig. 14). Following induction of transgene expression, N18-HASPB-GFP (+ dox) cells migrated significantly faster in 3D than control cells expressing GFP (p = 0.019; Student's t-test) or N18-Δmyr-HASPB-GFP (p = 0.03; fig. 36A).

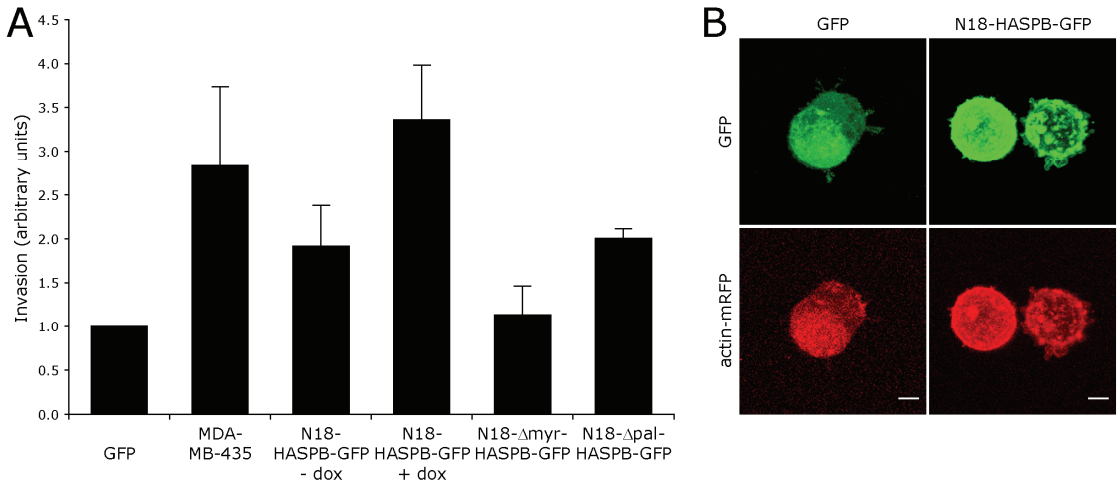

Figure 36: HASPB-SH4-domain induced PM blebbing correlated with enhanced 3D motility.

(A) Invasiveness of CHO cells was increased by expression of the bleb inducing SH4-domain of HASPB. Either serum starved CHO cells induced (+ dox) or not induced (- dox) for expression of GFP (+), N18-HASPB-GFP (+/-), N18-Δmyr-HASPB-GFP (+) or N18-Δpal-HASPB-GFP (+) or serum starved MDA-MB-435 breast cancer cells serving as positive control were assessed for cell migration across undiluted growth factor reduced matrigel coated transwells (pore size 8 µm) for 48 hours along a gradient of FCS (0.5-10 %). Invasiveness is given in relation to GFP expressing cells. Values are the arithmetic means of three independent experiments performed as duplicates with the indicated S.E.M. Statistical significance was evaluated by Student's t-test (relative to N18-HASPB-GFP (+): GFP p = 0.019, N18-Δmyr-HASPB p = 0.03, N18-HASPB-GFP (-) p = 0.14; relative to GFP: N18-HASPB-GFP (-) p = 0.12, N18-Δpal-HASPB p = 0.001). **(B)** HASPB-SH4-domain expressing cells showed PM blebbing in 3D matrices. 3D reconstruction of confocal stacks of serum starved CHO cells co-expressing actin-mRFP and GFP or N18-HASPB-GFP. Cells were seeded in 50 % growth factor reduced matrigel and migrated for 24 h along a gradient of FCS (0.5-10 %). Scale bars = 10 µm (with the help of T. Kitzing).

The invasiveness of N18-HASPB-GFP cells closely matched that of metastatic MDA-MB-435 human breast carcinoma cells that served as positive control. Uninduced N18-HASPB-GFP (- dox) cells showed intermediate invasiveness and could not statistically be separated from induced N18-HASPB-GFP cells (+ dox; $p = 0.14$; Student's t-test) or GFP expressing cells ($p = 0.12$). This might be due to a leakiness of the expression system without dox resulting in low background levels of N18-HASPB-GFP expression (fig. 16). Nevertheless, N18-Δpal-HASPB-GFP also significantly increased 3D motility compared to GFP cells ($p = 0.001$). Interestingly, most of N18-HASPB-GFP expressing cells seeded for 24 h in 50 % matrigel showed a blebbing morphology as well as filopodia surface structures. In contrast, CHO-GFP cells only revealed some filopodia like structures in 3D (fig. 36B).

These results indicated that SH4-domain induced PM blebbing correlated with induction of cell invasion. However, the non-blebbing variant N18-Δpal-HASPB-GFP also induced 3D invasion even though fewer cells were affected. Thus it is not clear, whether enhanced invasiveness is directly linked to SH4-domain induced PM blebbing or whether the SH4-domains had other effects on cellular signaling events. Interestingly, both invasion and PM blebbing of tumor cells in 3D matrices were shown to be related to ROCK activity (Sahai and Marshall, 2003) and were recently linked to the presence of Drfs (Kitzing *et al.*, 2007).

8.2 The Role of the Drf FHOD1 in PM Blebbing

In this work it was shown that SH4-domain mediated PM blebbing depended on several cellular determinants: Src and Rho are regulatory proteins, but also effector proteins like ROCK and myosin were necessary as well as the microfilament and the microtubule systems. A family of proteins that is capable of organizing the cytoskeleton are the formins and in particular the Drfs. As a surprising result of this study, the Drf FHOD1 was identified in knockdown experiments to be involved in SH4-domain related blebbing (see chapter 8.2.6). Therefore, a detailed analysis of its contribution to PM blebbing in combination with a further characterization of the Drf is addressed in the subsequent chapters.

8.2.1 FHOD1 Specifically Interacts with ROCK1

Drfs are thought to be partially regulated by Rho-GTPases. Even though Rac1 and not Rho have been identified to interact with FHOD1 (Westendorf, 2001), expression of the C-terminal truncated and therefore constitutively active form of FHOD1 (FHOD1-ΔC) causes F-actin cable formation in a ROCK dependent manner (Gasteier *et al.*, 2003). Thus, to investigate a direct

binding of FHOD1 and ROCK proteins, a Yeast-two-hybrid screen was performed by J. Bouchet (group of S. Benichou, Institut Cochin, Paris). Therefore, mutants of FHOD1 as bait (LexA) and mutants of ROCK1 or ROCK2 as prey (Gal4AD), respectively, were expressed in the L40 yeast strain which was analyzed for histidine auxotrophy as readout for a direct interaction (fig. 37).

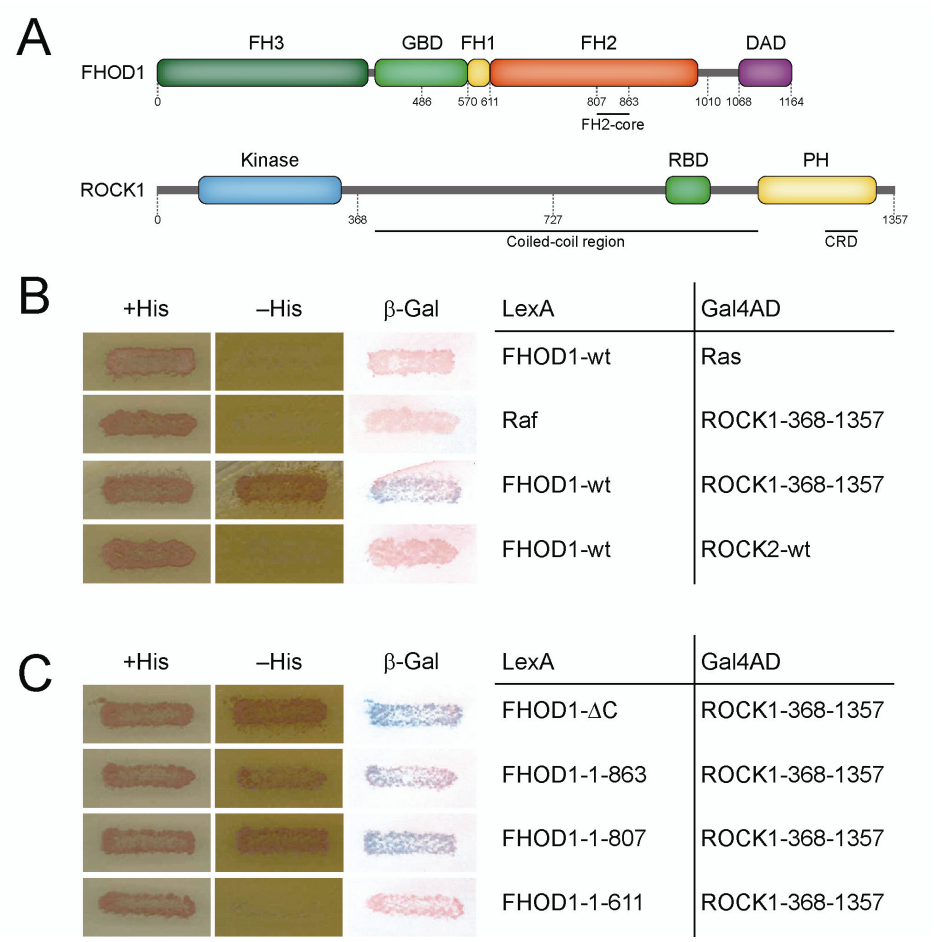

Figure 37: FHOD1 specifically interacted with ROCK1, but not with ROCK 2.

(A) Scheme of the employed constructs. Depicted are described domains and features of the protein. Residues are highlighted by their position-number. **(B)** FHOD1 interacted with ROCK1, but not with ROCK2. Yeast-two-hybrid screens in the L40 yeast strain expressing the indicated pairs of FHOD1 and ROCK constructs fused to LexA (left column) or Gal4AD (right column) were analyzed for histidine auxotrophy and β-gal activity. Double transformants were patched on selective medium with histidine (+His) and were replica plated on medium without histidine (-His) and on Whatman filters for subsequent β-gal assays. Growth in the absence of histidine and expression of β-gal activity indicated interaction between hybrid proteins. The specificity of the binding was verified by the absence of respective reporter gene activation in cells expressing LexA-FHOD1 in combination with the Gal4AD-Raf hybrid. **(C)** Parts of the FH2 domain of FHOD1 are important for its interaction with ROCK1. Shown is a Yeast to hybrid analysis as described in B but with different FHOD1 constructs for mapping its interaction to ROCK1 (kindly provided by J. Bouchet, group of S. Benichou, Institut Cochin, Paris).

Interestingly, FHOD1 was found to interact with full length ROCK1 as well as with a mutant consisting of the region located downstream its kinase domain (residues 368-1357), but not with its homolog ROCK2 (fig. 37B and data not shown).

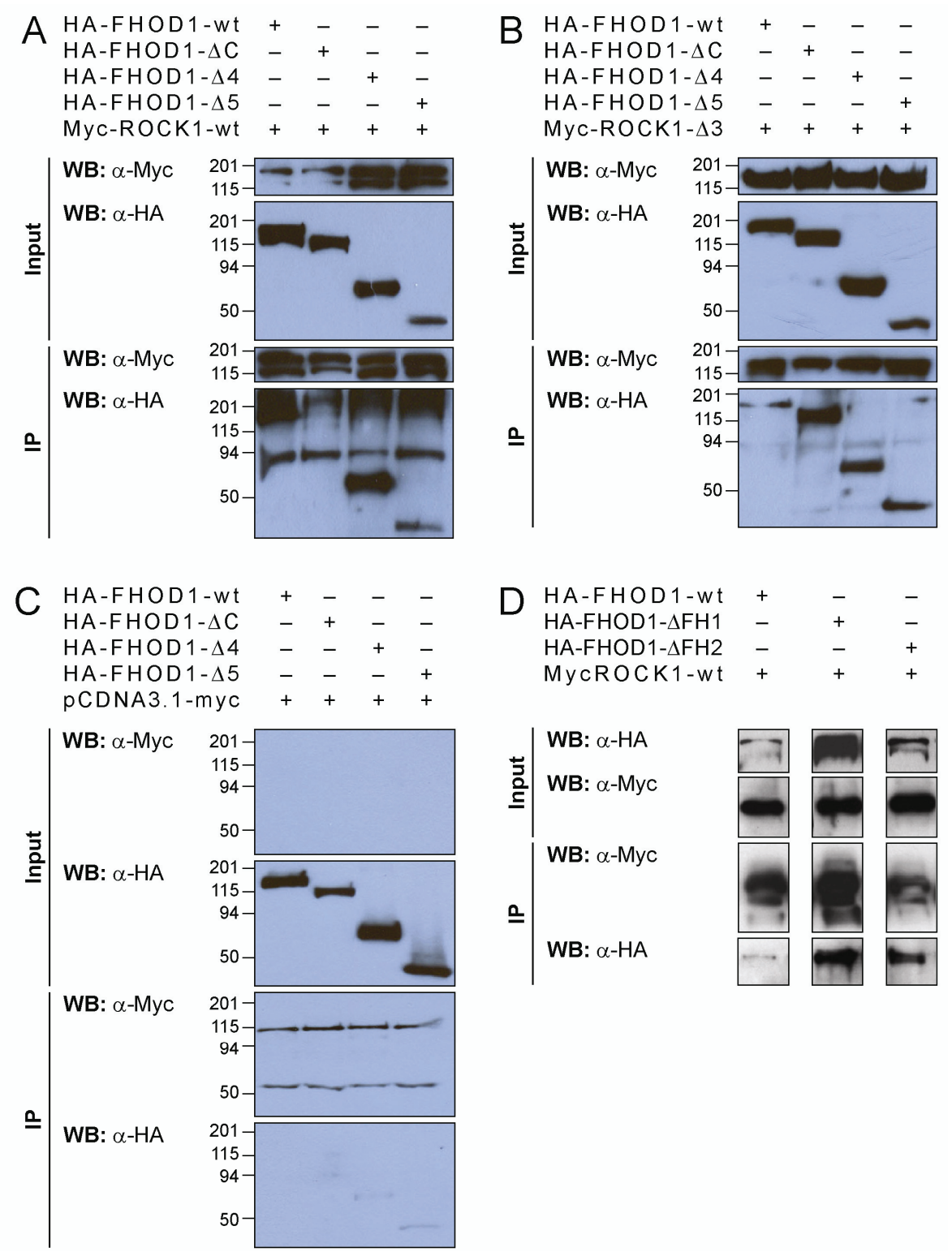

Figure 38: FHOD1 directly interacted with ROCK1.

(A-C) Direct interaction of FHOD1 and ROCK1. Lysates (Input) from COS cells expressing the indicated HA tagged FHOD1 (wt: 1-1164; Δ4: 486-1068; Δ5: 570-1068; ΔC: 1-1010, see also fig. 37) and Myc tagged ROCK1 constructs were subjected to immunoprecipitation (IP) with an anti-Myc antibody. Cell lysates and immunoprecipitates were separated by SDS–PAGE and analyzed by Western blotting with either anti-HA or anti-Myc antibodies. **(A)** IP of ROCK1-wt. **(B)** IP of ROCK1-Δ3 (1-727). **(C)** IP of empty vector. **(D)** FHOD1s FH1 and FH2 domains were not required for direct interaction with ROCK1. IP performed as described in A but with the indicated HA tagged constructs of FHOD1 (wt: 1-1164; ΔFH1 = Δ570-611; ΔFH2 = Δ807-866) and Myc tagged ROCK1-wt (kindly provided by R. Madrid, group of S. Benichou, Institut Cochin, Paris).

Further mapping also showed a potent binding for the C-terminal truncated mutant FHOD1-ΔC to ROCK1 and roughly narrowed the interacting region down to FHOD1s amino acid residues 611 to 807 (fig. 37C), located in the supposed N-terminal region of its FH2 domain (Schonichen *et al.*, 2006). The FHOD1-ROCK1 interaction was confirmed by co-immunoprecipitation (co-IP) experiments that were performed by R. Madrid (group of S. Benichou, Institut Cochin, Paris). An IP of either Myc-ROCK1-wt or a C-terminally truncated version Myc-ROCK1-Δ3 (1-727) that was shown to induce stress fiber and F-actin star formation (Ishizaki *et al.*, 1997) expressed in COS cells co-precipitated co-expressed HA-FHOD1-wt, whereas a control with empty vector did not (fig. 38A-C). This narrowed the interaction site of ROCK1 down to amino acid residues 368-727. However, co-precipitation of HA-FHOD1-ΔC was not observed by ROCK1-wt, but in some experiments by ROCK1-Δ3 (fig. 38A-C and data not shown). Additionally, Myc-ROCK1-wt and Myc-ROCK1-Δ3 also co-precipitated mutants of HA-FHOD1 either including the FH1 and FH2 domains (FHOD1-Δ4, 486-1068; FHOD1-Δ5, 570-1068) or lacking its FH1 domain (ΔFH1 = Δ570-611) or parts of its FH2 domain (ΔFH2 = Δ807-866), respectively (fig. 38A-D and data not shown). Presumably due to stability problems, transient expression of HA-FHOD1-1-611 in NIH3T3 or HeLa cells was not successful.
Together, FHOD1 specifically interacted with ROCK1 but not ROCK2. An interaction site could be roughly mapped to residues 368-727 in ROCK1 and 612-806 in FHOD1.

8.2.2 FHOD1 Increased ROCK1 Induced Non-Apoptotic PM Blebbing

It has previously been shown, that constitutively active FHOD1-ΔC induced the formation of stress fibers and F-actin bundles that were decorated by the Drf, whereas expression of FHOD1 had no detectable effect on the cells appearance and the Drfs localization (Gasteier *et al.*, 2003). Since FHOD1 specifically bound to ROCK1 *in vitro* this interaction might have an *in vivo* consequence for the cell as well as for FHOD1s localization. Therefore, expression plasmids encoding HA tagged FHOD1 and Myc tagged ROCK1 were co-transfected in HeLa cells for 24 h. After fixation and stain for F-actin and the over-expressed proteins the cells were analyzed by fluorescence or confocal microscopy. About 62 % of solely ROCK1 expressing cells showed PM blebbing as it has been published before (Coleman *et al.*, 2001, Sebbagh *et al.*, 2001). The PM blebs revealed a pronounced F-actin localization at the basis as well at the outer rim. ROCK1 was similarly distributed and was furthermore found in the lumen of some blebs (fig. 39Ab-e/B).

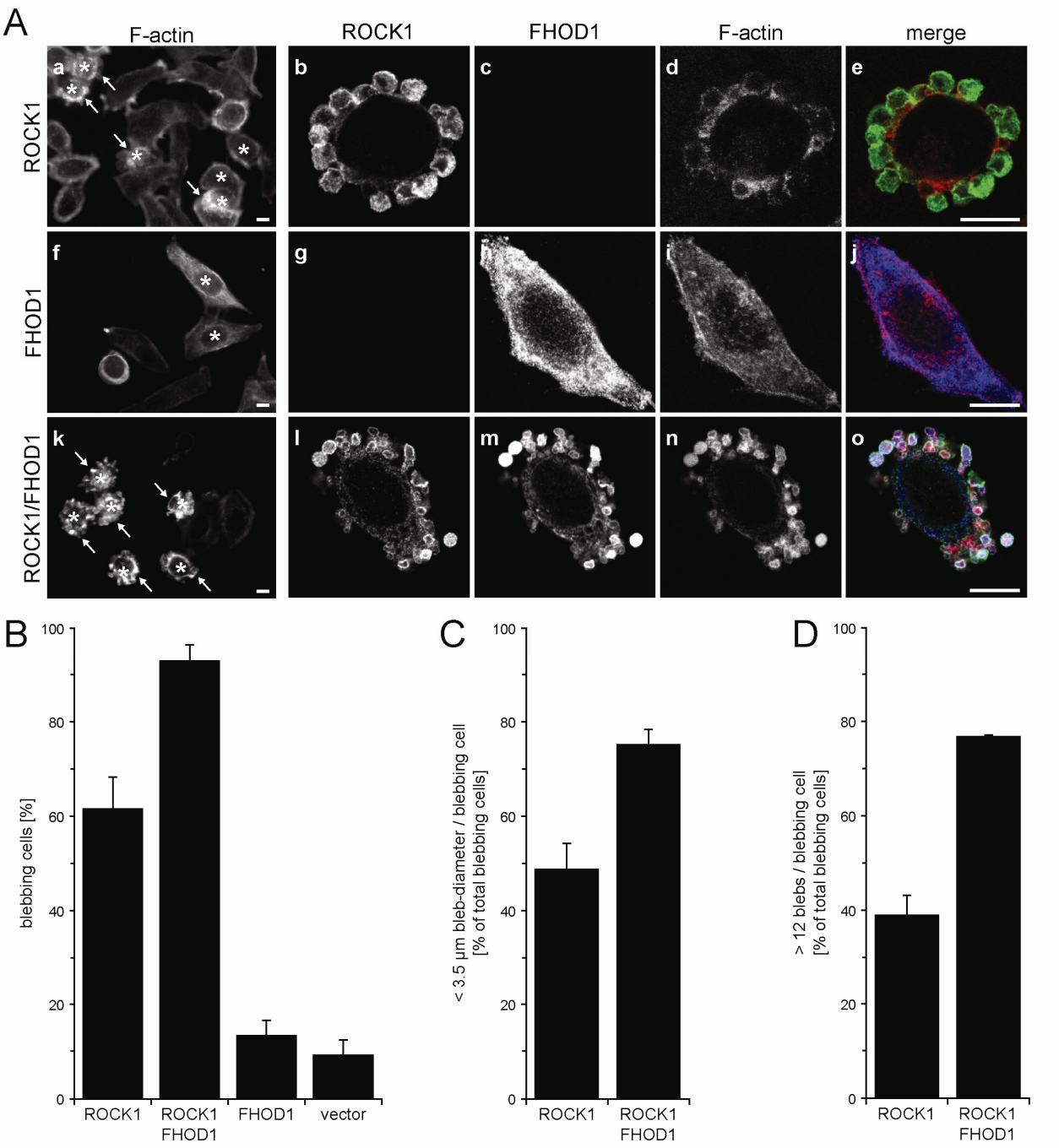

Figure 39: FHOD1 enhanced ROCK1 induced PM blebbing.

(A-B) FHOD1 increased the number of blebbing cells induced by ROCK1. **(A)** HeLa cells were transfected with the indicated Myc tagged ROCK1 and HA tagged FHOD1 constructs, fixed, stained for F-actin and the transiently expressed proteins and analyzed by fluorescence (a/f/k) or confocal microscopy (b-e/g-j/l-o). **(B)** Percentage of transfected cells revealing PM blebbing as described in A (arithmetic means of at least three independent experiments + SD with > 100/condition). Values for ROCK1 alone and ROCK1/FHOD1 together were statistically different (p = 0,00018, Student's t-test). **(C-D)** FHOD1 induced PM blebs are **(C)** reduced in size but **(D)** increased in number. Size and number of blebs on HeLa cells quantified in B were estimated (less than 3.5 µm or more than 12 blebs/cell; arithmetic means of at least three independent experiments + SD with > 100/condition).

Surprisingly, nearly all cells (93 %) that were positive for ROCK1 and FHOD1 also showed PM blebbing demonstrating a significant increase in PM blebbing induction (p = 0.00018, Student's

t-test, fig. 39Ak-o/B), whereas expression of FHOD1 or vector alone did not induce PM blebbing (9-13 % blebbing cells, fig. 39Af-j/B). In contrast to the ROCK1 distribution, most of these PM blebs were enriched with FHOD1 and F-actin (fig. 39Al-n). They were very similar to SH4-domain induced PM blebs (see chapter 8.1): In average, most of the cells showed more than 12 blebs per cell (approx. 75 % compared to 40 % of ROCK1 expressing cells, fig. 39D) and the size of an individual PM bleb tended to be smaller than 3.5 µm in diameter (approx. 75 % compared to 50 % in ROCK1 expressing cells, fig. 39C).

Interestingly, this FHOD1 mediated increase in PM blebbing depended on a functional FHOD1 protein: Co-expression of ROCK1 in combination with FHOD1 mutants that either lack their FH1-domain (FHOD1-ΔFH1) or their FH2-domain (FHOD1-ΔFH2) did not increase PM blebbing like the wt FHOD1 protein (fig. 40). Since these mutants lost their nucleation ability (Gasteier *et al.*, 2003), they served as a proper negative control and also indicated that F-actin polymerization was involved in PM blebbing.

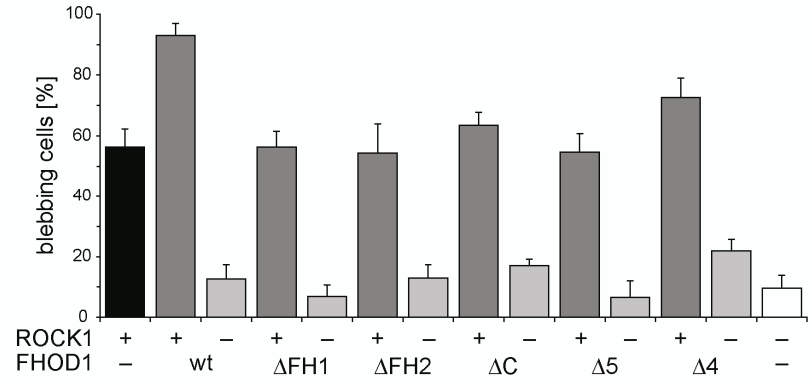

Figure 40: FHOD1 required a functional FH1 and FH2 domain as well as additional residues for efficient enhancement of PM blebbing.

HeLa cells were transfected with the indicated constructs of FHOD1 (wt, ΔFH1, ΔFH2, Δ4, Δ5 and ΔC see also fig. 37) and ROCK1. After 24 h, cells were fixed, stained for transiently expressed proteins and F-actin and analyzed by fluorescence microscopy. Depicted are the percentages of blebbing cells (arithmetic means of at least three independent experiments + SD with > 100/condition). As calculated by Student's t-test only values for ROCK1/FHOD1-Δ4 were statistical different to values of ROCK1 ($p = 0.0008$) and ROCK1/FHOD1-wt ($p = 0.00019$).

However, this increase in PM blebbing was also blocked with the constitutively active FHOD1-ΔC that still potently induced stress fiber formation, what might have influenced the bleb phenotype (fig. 40 and data not shown). A similar result was obtained for FHOD1-Δ5, which also did not enhanced bleb formation, although it bound to ROCK1, possessed the FH1 and FH2 domain and did not induce F-actin stress fibers (fig. 40 and data not shown). In contrast, FHOD1-Δ4 increased ROCK1 mediated PM blebbing to intermediate levels of approx. 73 % that were statistically different as calculated by Student's t-test to values obtained by ROCK1 alone (56 %, $p = 0.0008$) or by ROCK1/FHOD1-wt co-expression (93 %, $p = 0.00019$;

fig. 40). This indicated that parts of the Rac1 binding region that localized between FHOD1s residue 486 and its FH1-domain (Gasteier *et al.*, 2003, Westendorf, 2001) were involved in PM blebbing. This region either contributed to ROCK1 association by stabilization of the protein fragment or it was required for activation of ROCK1 or FHOD1, respectively.

During apoptosis, ROCK1 is directly involved in PM blebbing due to its caspase-3 mediated cleavage and therefore constitutive activation. Anyway, neither expression of ROCK1 nor its C-terminally truncated version (ROCK1-G1114*opa* or ROCK1-Δ1) are capable to induce apoptosis on their own (Coleman *et al.*, 2001, Sebbagh *et al.*, 2001). To test whether this held true for ROCK1/FHOD1 induced PM blebbing as well, cells were analyzed for apoptosis either by stain with Hoechst 33268 for chromatin fragmentation (fig. 41A) or with fluorescently labeled Annexin V for visualization of externalized phosphatidyl serine (PS, fig. 41B-C).

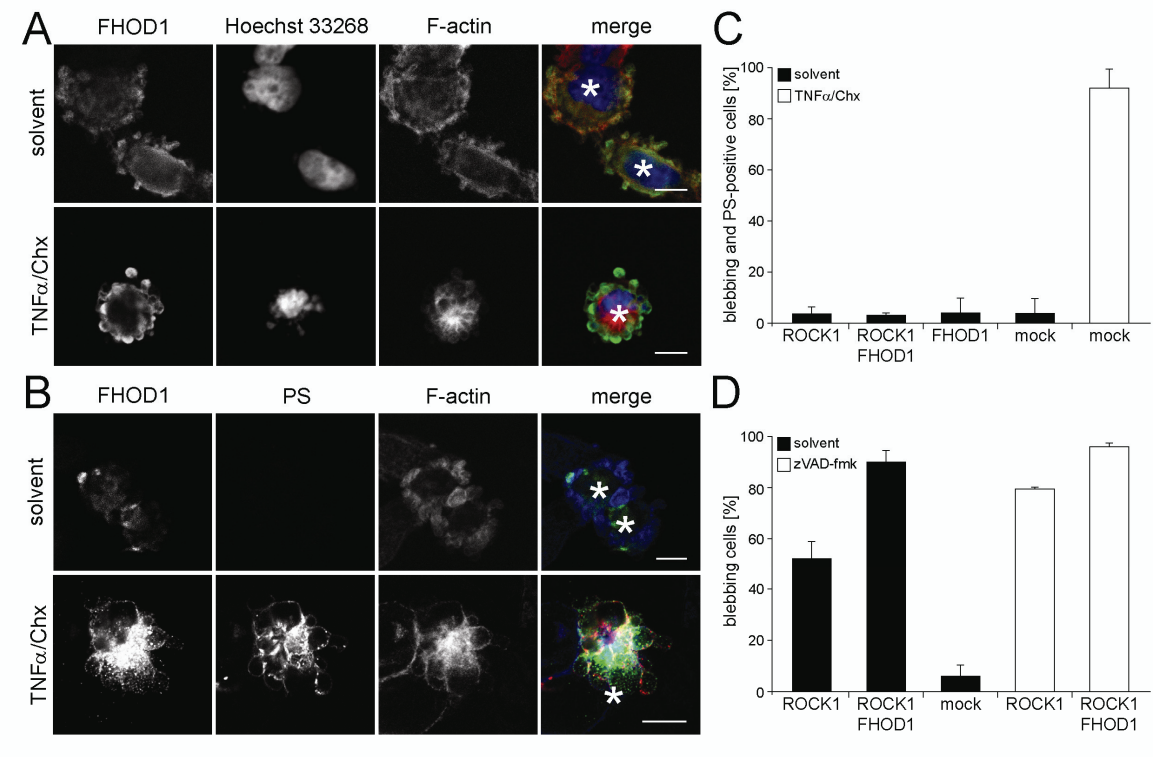

Figure 41: FHOD1 enhanced PM blebbing was not related to apoptosis.

(A-C) FHOD1 and ROCK1 co-expressing cells were not apoptotic. **(A)** HeLa cells were transiently co-transfected with plasmids encoding FHOD1 and ROCK1. Following growth for 24 h they were treated for 3 h either with solvent or TNFα/Chx (50 µg/ml and 5 µg/ml) for induction of apoptosis, fixed, stained for the transiently expressed proteins, F-actin and chromatin (Hoechst 33268) and analyzed by confocal microscopy. FHOD1 and ROCK1 co-expressing cells are highlighted (*), scale bars = 10 µm. **(B)** HeLa cells were similarly treated as described in A, but were stained for externalized phosphatidyl serine (PS) by Alexa Fluor-568 labeled Annexin V first, than fixed, stained for the transiently expressed proteins and F-actin and finally analyzed by fluorescence microscopy. FHOD1 and ROCK1 co-expressing cells are highlighted (*), scale bars = 10 µm. **(C)** Percentage of blebbing and PS positive HeLa cells treated and handled as described in B (arithmetic means of at least three independent experiments + SD with > 100/condition). **(D)** PM blebbing induced by FHOD1 and ROCK1 was not reduced by inhibition of apoptosis. HeLa cells were transiently co-transfected with plasmids encoding FHOD1 and ROCK1. Following growth in the presence of zVAD-fmk (100 µM) cells were fixed, stained for the transiently expressed proteins and F-actin and were analyzed by fluorescence microscopy. Depicted is the percentage of blebbing cells (arithmetic means of three independent experiments + SD with > 100/condition).

Although induction of apoptosis with TNFα (50 µg/ml) and Cycloheximide (Chx, 5 µg/ml for 3 h) was still possible in ROCK1/FHOD1 expressing HeLa cells, they showed no increased apoptotic behavior without apoptosis induction like the SH4-domain expressing cells (fig. 41A-C and data not shown). Furthermore, treatment of these cells with the apoptosis inhibitory drug zVAD-fmk (100 µM for 24h) did not reduce the amount of PM blebbing cells (fig. 41D).
Thus, FHOD1 increased ROCK1s capability to induce non apoptotic PM blebbing suggesting positive contribution of FHOD1. Therefore, FHOD1s F-actin nucleation ability was required as well as parts of its Rac1 binding region. These results supported the hypothesis of interplay between ROCK1 and FHOD1 (Gasteier *et al.*, 2003).

8.2.3 Regulation of FHOD1/ROCK1 PM Blebbing Depends on Rho Signaling

To obtain a more detailed picture of the signaling pathway that controls FHOD1/ROCK1 stimulated PM blebbing, the activity requirements of different Rho-GTPases were analyzed analogous to SH4-domain induced PM-blebbing (see chapter 8.1.6). Therefore FHOD1 was co-expressed in combination with ROCK1 and a GFP fusion protein of either dominant negative Rac1 (Rac1-N17) or Cdc42 (Cdc42-N17) or the *Clostridium botulinum* TAT-C3 transferase for inactivation of the Rho-pathway, respectively.

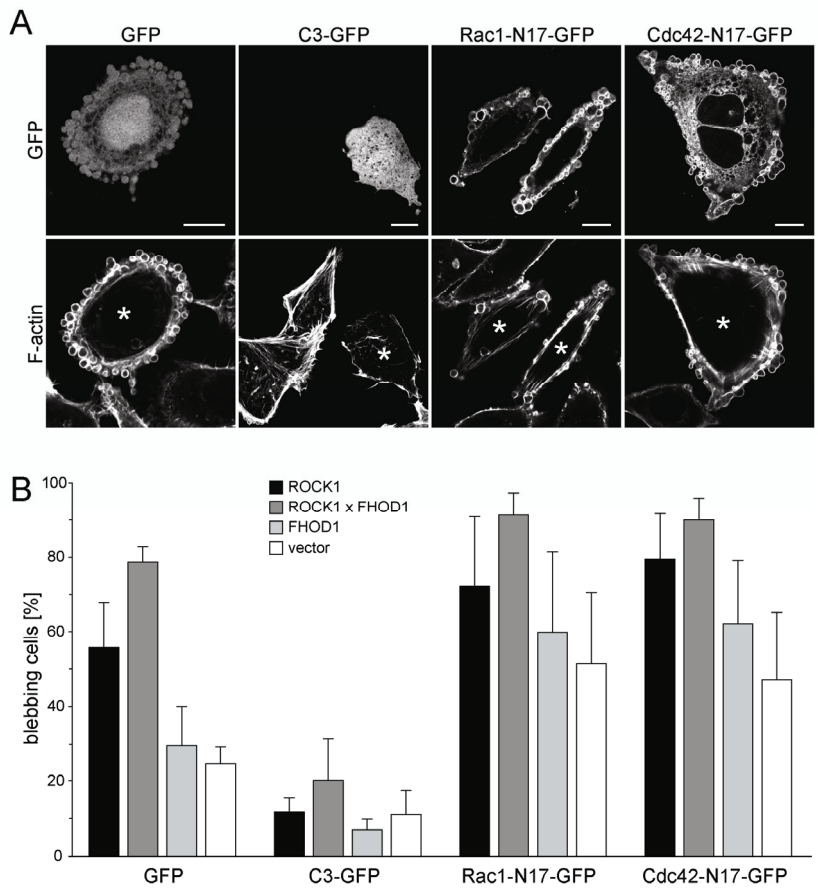

Figure 42: Rho activity was required for FHOD1 enhanced PM blebbing.

(A) HeLa cells were co-transfected with expression plasmids of ROCK1 and FHOD1 together with expression plasmids of either GFP or dominant negative forms of GTPases (Rac1-N17, Cdc42-N17) fused to GFP or GFP tagged TAT-C3 transferase from *Clostridium botulinum* for inhibition of Rho activity. After 24 h cells were fixed, stained for transiently expressed proteins and F-actin and analyzed for PM blebbing by confocal microscopy. Triple transfected cells are highlighted (*), scale bars = 10 µm. **(B)** Percentages of blebbing HeLa cells treated and processed as described in A (black bars: ROCK1; dark grey bars: ROCK1 and FHOD1; light grey bars: FHOD1; white bars: empty vector; (arithmetic means of at least three independent experiments + SD with > 100/condition).

Comparable to SH4-domain induced PM blebs, only inhibition of Rho activity significantly decreased the amount of blebbing HeLa cells to background levels obtained in parallel with GFP. In fact, neither expression of ROCK1 alone nor together with FHOD1 induced PM blebbing (fig. 42). Inhibition of Rac1 or Cdc42 drastically increased the amounts of blebbing cells even in cells expressing vector only (fig. 42). This might be due to a regulatory crosstalk between the single Rho-GTPases, as it was suggested for several physiological situations (Burridge and Wennerberg, 2004). These results were also in line with previously described findings in Rac1 deficient cells, which start blebbing in certain situations (Imamura *et al.*, 1999, Vidali *et al.*, 2006).

In order to gain further insight into the signaling events during FHOD1 enhancement of PM blebbing, several downstream steps of the Rho activation cascade were investigated by specific inhibition. Similar to SH4-domain expressing cells the generation of new PM blebs was studied in HeLa cells following pretreatment with the ROCK inhibitor Y27632 (90 µM or 10 µM, 2 h, see chapter 8.1.7). As it was observed for SH4-domain induced PM blebbing, its addition potently abolished PM blebbing in HeLa cells expressing solely ROCK1 or in combination with FHOD1 (fig. 43Acd/B and data not shown).

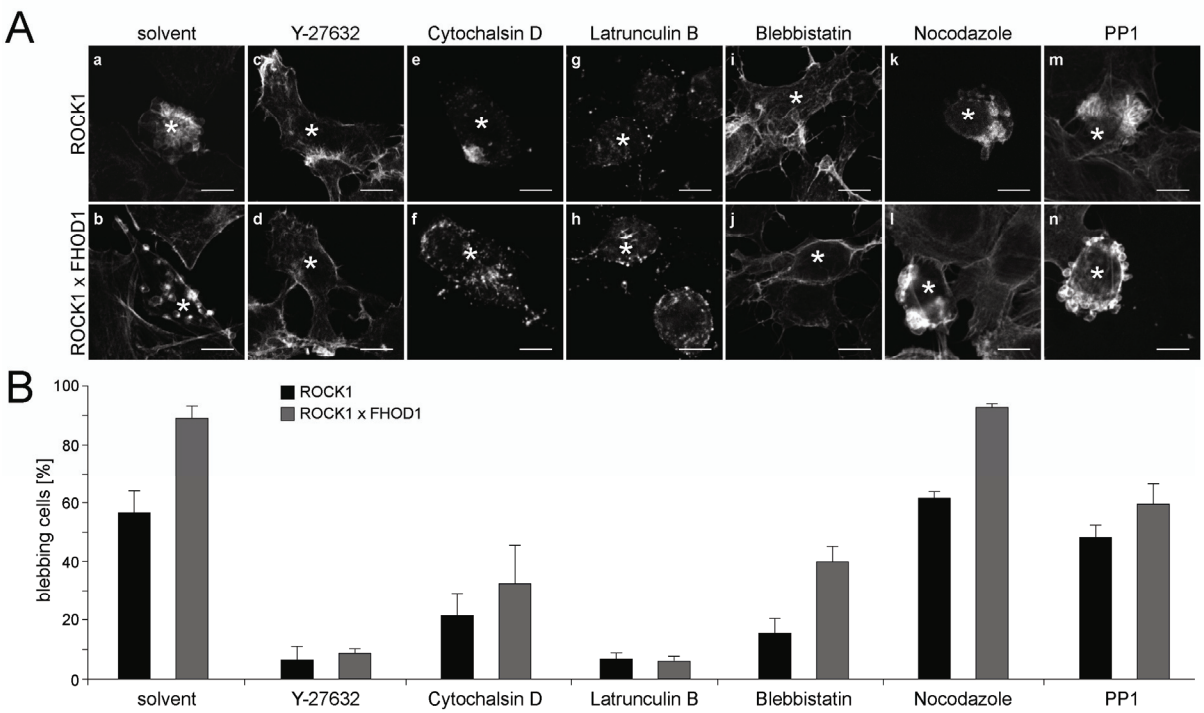

Figure 43: Activity of Rho-ROCK pathway proteins and activity of Src kinases were required but not microtubule integrity for FHOD1 mediated increase of PM blebbing.

(A) HeLa cells were transfected with plasmids encoding ROCK1 and FHOD1 as indicated, pretreated with 90 µM Y-27632 for 2 h to remove already formed PM blebs, washed and incubated in the presence of the denoted drugs for additional 3 h (90 µM Y-27632; 2 µM Cytochalasin D; 25 µM Latrunculin B; 100 µM Blebbistatin; 384 µM Nocodazole; 50 µM PP1). Finally, cells were fixed, stained for the transiently expressed proteins and F-actin and analyzed for PM blebbing by confocal microscopy. Transfected cells are highlighted (*), scale bars = 10 µm. **(B)** Percentages of blebbing HeLa cells treated and handled as described in A (black bars: ROCK1; dark grey bars: ROCK1 and FHOD1; arithmetic means of at least three independent experiments + SD with > 100/condition).

These results were in line with the necessity of Rho and ROCK activity for induction of F-actin cables by FHOD1-ΔC (Gasteier *et al.*, 2003, Westendorf, 2001). To examine the role of the cytoskeleton, cells were treated either with F-actin (2 µM Cytochalasin D or 25 µM Latrunculin B) or microtubule (384 µM Nocodazole) disrupting drugs. As a result both, ROCK1 and ROCK1/FHOD1 induced PM blebs required microfilament integrity (fig. 43Ae-h/B), but in contrast to SH4-domain induced PM blebs, they were independent of microtubule disassembly (fig. 43Ak-l/B). Second, the need for myosin mediated contractility was determined. As mentioned before, ROCK proteins activate myosins by phosphorylation. To test the requirement of myosin activity, the myosin II motor protein was specifically inhibited by treatment of the cells with 100 µM Blebbistatin (BS). In presence of this drug, the number of blebbing cells expressing ROCK1 was decreased from 58 % to 16 %, but in combination with FHOD1 the level of blebbing cells remained at 40 % in comparison to 93 % (fig. 43Ai-j/B). However, in both cases the amount of blebbing cells was reduced (ROCK1: 3.8 fold; ROCK1/FHOD1: 2.2 fold). As it was described in the previous chapters, SH4-domain induced PM blebbing required the activity of endogenous Src kinases (see chapter 8.1.9). To check whether this held true for ROCK1 mediated PM blebbing as well, transfected cells were treated with the Src kinase inhibitor PP1 (50 µM). This drug had almost no effect on ROCK1 blebs (1.2 fold reduction), but reduced the amount of PM blebbing cells transfected with ROCK1/FHOD1 to the amount of blebbing cells achieved by ROCK1 only (1.5 fold reduction, fig. 43Aa/m-n/B).

Collectively, these results showed that enhancement of ROCK1 mediated PM blebbing by FHOD1 required the activity of the Rho-ROCK pathway and the integrity of the microfilament system. This was in line with the characteristics of SH4-domain induced PM blebs described above (chapter 8.1.6). In contrast, ROCK1 induced and FHOD1 enhanced PM blebbing did not depend on microtubule supply. However, the FHOD1 mediated increase in PM blebbing required Src kinase activity similar to SH4 blebs (chapter 8.1.9). The basal level of ROCK1 induced PM blebbing was independent of Src kinase activity.

8.2.4 Activation of ROCK1 and the Role of Src

As it was shown in the previous chapters the Rac1 binding protein FHOD1 specifically interacted with ROCK1 (fig. 37 and 38) and positively affected ROCK1 induced non-apoptotic PM blebbing (fig. 39 and 41). This effect depended on the Rho pathway as well as on ROCK activity (fig. 42 and 43) and was affected by inhibition of the ROCK substrate myosin II as well as of Src kinase activity. Therefore, the intracellular localization of endogenous c-Src was determined in HeLa cells by confocal microscopy (fig. 44). A specific stain revealed that

endogenous c-Src was located at the basis as well as in the outer rim of the blebs. Activated pc-Src (Y^{418}) localized in the lumen of ROCK1 induced blebs. In contrast but similar to N18-Yes-GFP induced blebs (see chapter 8.1.9), ROCK1/FHOD1 blebs were enriched in pc-Src (Y^{418}) (fig. 44A/B). Nevertheless, these experiments have been performed only once and need future examination. Thereafter, the cellular distribution of MLC as marker for ROCK activity was explored. MLC and its activated and phosphorylated form pMLC (S^{19}) specifically localized at the basis of PM blebs (fig. 44C/D).

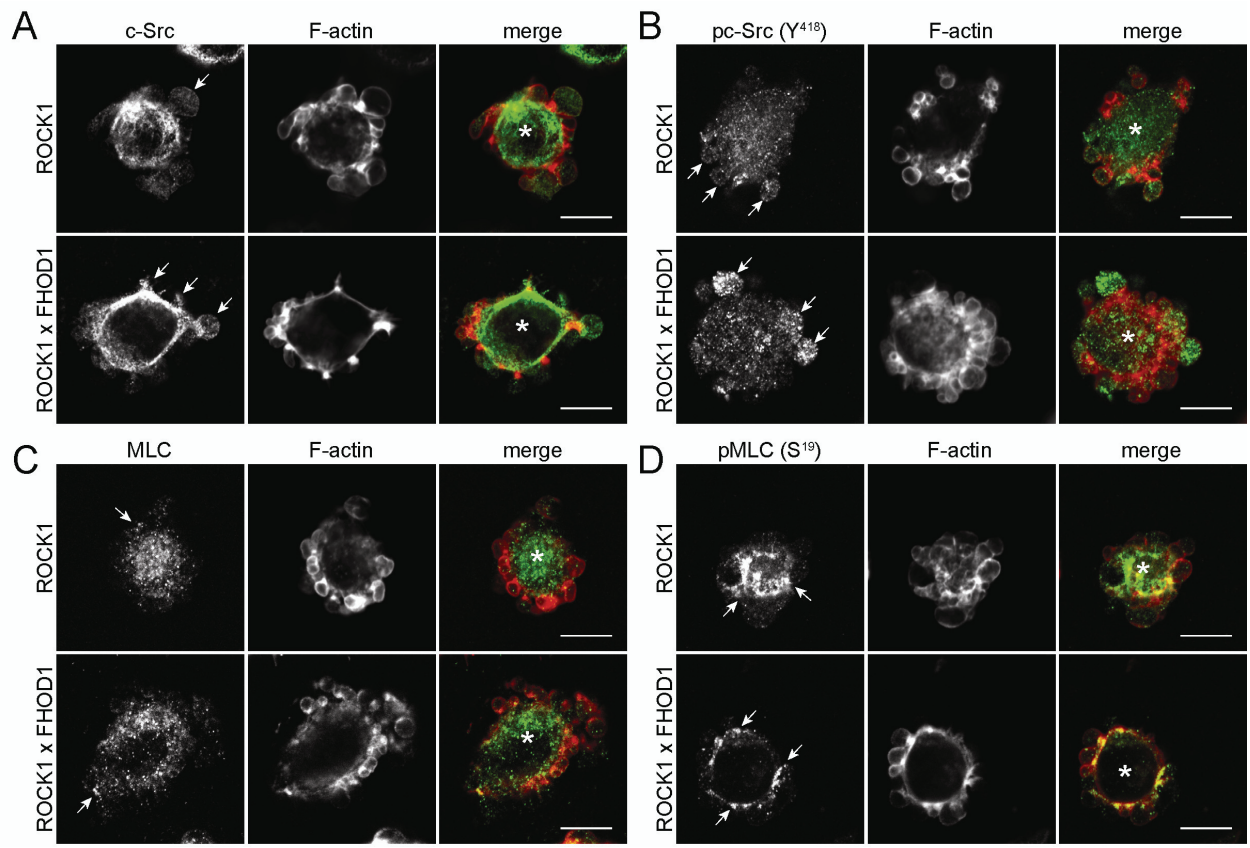

Figure 44: c-Src MLC localized in PM blebs.

(A-B) Activated pc-Src (Y^{418}) but not total Src was enriched in PM blebs. HeLa cells were co-transfected with FHOD1 and ROCK1. After 24 h cells were stained for the transiently expressed proteins as well as for F-actin and endogenous **(A)** c-Src or activated **(B)** pc-Src (Y^{418}), respectively. Depicted are confocal micrographs in which transfected cells are highlighted (*), scale bars = 10 µm. **(C-D)** MLC as well as activated pMLC (S^{19}) localize in PM blebs. HeLa cells were co-transfected with FHOD1 and ROCK1. After 24 h cells were stained for the transiently expressed proteins as well as for F-actin and endogenous **(C)** MLC or activated **(D)** pMLC (S^{19}), respectively. Depicted are confocal micrographs in which transfected cells are highlighted (*), scale bars = 10 µm.

The obtained results were comparable to SH4-domain induced PM blebs and confirmed that ROCK activity is essential. To test whether ROCK1 activity was induced by interaction with FHOD1, two strategies were pursued: The first approach based on the observation that during apoptosis ROCK1 is C-terminally cleaved at residue 1113 by caspase-3 and thus constitutively activated leading to bleb formation (Coleman *et al.*, 2001, Sebbagh *et al.*, 2005). To investigate

this possibility, cell lysates of transiently transfected HeLa cells were probed in a Western blot analysis for the two derivates of ROCK1 fused to a Myc tag. While induction of apoptosis with TNFα/Chx (50 µg/ml and 5 µg/ml for 3 h) clearly increased the amount of the cleaved and therefore smaller form, the cleavage was completely blocked by addition of 100 µM caspase inhibitor zVAD-fmk directly after transfection (fig. 45A, lanes 1, 3 and 4). However, co-expression of FHOD1 did not alter ROCK1 cleavage *per se* or following induction of apoptosis, respectively. It also did not interfere with the block of ROCK1 cleavage that was mediated by zVAD-fmk (fig. 45A, lanes 6, 8 and 9).

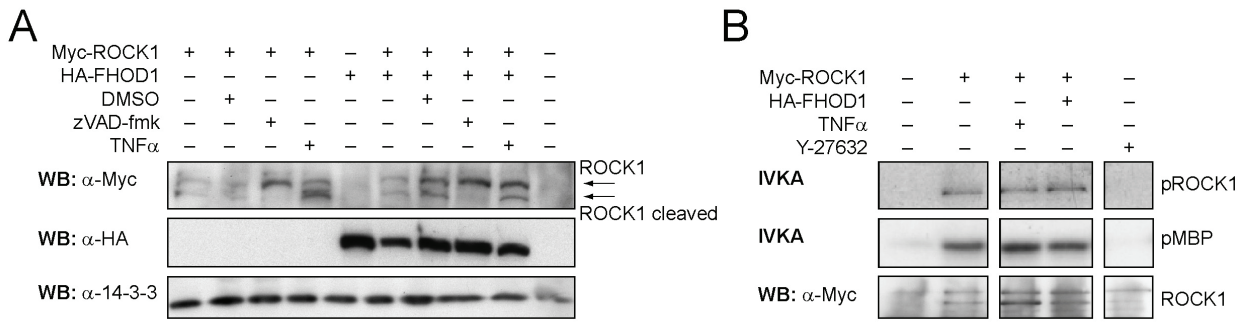

Figure 45: FHOD1 did not alter overall activation levels of ROCK1.

(A) FHOD1 did not activate ROCK1 by C-terminal truncation. HeLa cells transiently expressing either HA tagged FHOD1 or N-terminally Myc tagged ROCK1 alone or in combination either in the presence of zVAD-fmk (100 µM) or treated with TNFα/Chx (50 µg/ml and 5 µg/ml) for 3 h, respectively, were harvested and lysed. Equal amounts of total protein were separated by SDS-PAGE, subjected to Western blotting and probed with an antibody against Myc for expression levels and protein cleavage, against HA for expression levels or against 14-3-3 as loading control. The cleaved and therefore constitutively active form of ROCK1 is reduced in size and separates from the uncleaved protein during SDS-PAGE. **(B)** FHOD1 did not increase ROCK1-activity. *In vitro* kinase assay (IVKA) of immunoprecipitated Myc tagged ROCK1 transiently expressed alone or in combination with HA-tag fused FHOD1. 3 h before harvest, cells were either treated with solvent or TNFα/Chx (50 µg/ml and 5 µg/ml) to induce apoptosis as a positive control. Kinase reaction was started by addition of the immunoprecipitates to kinase activation buffer containing 4 µCi/30 µl [^{32}P]-γATP and 1 µg/30 µl myelin basic protein (MBP) as a substrate together with either solvent or Y-27632 (900 µM). After 30 min at 30°C, the kinase reaction was stopped by addition of 6 x SDS sample buffer, proteins were separated by SDS-PAGE and transferred to a nitrocellulose membrane that was exposed to a photosensitive film for 24 h. Depicted are the input levels of Myc-ROCK1 and the signals obtained from the radioactively labeled MBP and radioactively labeled uncleaved Myc-ROCK1.

The second employed strategy was a direct visualization of ROCK1-activity by an *in vitro* kinase assay (IVKA). Immunoprecipitated Myc-ROCK1 proteins from HeLa cell lysate were added to the kinase reaction containing [^{32}P]-ATP and myelin basic protein (MBP) as a substrate. As judged by a photosensitive film, MBP was specifically phosphorylated in the presence of Myc-ROCK1 as well as the kinase itself presumably by autophosphorylation but not in its absence (fig. 45B, lanes 1 and 2). Addition of the ROCK inhibitor Y-27632 (900 µM) to the reaction completely abolished kinase activity (fig. 45B, lane 5). However, the kinase activity was neither increased after induction of apoptosis by TNFα and Chx nor by co-expression of HA-FHOD1, respectively (fig. 45B, lanes 3 and 4). Nevertheless, these experiments bore some

intrinsic errors complicating interpretation: First, neither the immunoprecipitated Myc-ROCK1 nor the HA-FHOD1 could be probed by antibodies in the depicted experiment. Second, MBP is not a substrate specific for ROCK1 only and finally, the amounts of Y-27632 used were about 90 fold in excess to the specific concentration of 10 µM (Davies *et al.*, 2000).

Together, an enrichment of Src kinase activity was found in blebs generated by ROCK1 and FHOD1 as it was shown for SH4-domain induced blebs. Similarly, active MLC and therefore ROCK1 activity specifically localized at these blebs, but an activation of bulk levels of ROCK1 was not observed, which was also in line with the findings for SH4-doamins.

8.2.5 FHOD1 is not Required for PM Blebbing Induced by ROCK1, Rac1 and Apoptosis

Co-expression of FHOD1 increased the amount of ROCK1 induced PM blebbing in a way that required the activity of the Rho-ROCK cascade. As a Drf, FHOD1 is thought to have the potential for cytoskeletal rearrangements. Since the integrity of the microfilament system is required for formation of PM blebs, FHOD1 could be a central player in the development of PM blebbing. To investigate this hypothesis, the requirement of endogenous FHOD1 for several kinds of PM blebbing was investigated. Therefore, a specific RNAi mediated knockdown for FHOD1 was established. Depending on the cell line, cells were transfected with different methods but always twice (day 1 and day 3) with one of two different RNA-oligonucleotides directed against target sequences located in the N-terminus of FHOD1 or with unrelated control-oligonucleotides, respectively (for detailed information please refer to material and methods). The efficiencies of FHOD1 downregulation varied from 50-80 % after 4-5 d incubation as judged by western-blot analysis with an FHOD1 specific antibody (Gasteier *et al.*, 2005) and a following evaluation by BIO RAD "Quantity One" or LI-COR "Odyssey" software. First, the role of FHOD1 was analyzed for PM blebbing in apoptotic cells. Treatment of HeLa cells with TNFα/Chx (50 µg/ml and 5 µg/ml) for 3 h potently induced apoptosis and PM blebbing (fig. 41 and fig. 45). However, this held also true in FHOD1 reduced cells (fig. 46).

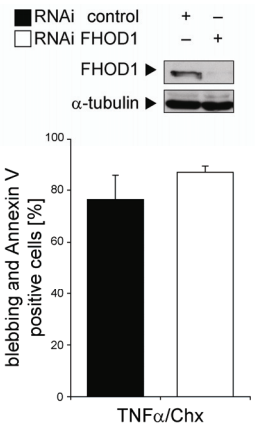

Figure 46: Reduction of FHOD1 had no influence on apoptotic PM blebbing.

Following RNAi treatment with either control no-target siRNA oligonucleotides or FHOD1 specific siRNA oligonucleotides (knockdown efficiency see insert), HeLa cells were treated with TNFα/Chx (50 µg/ml and 5 µg/ml) for 3 h to induce apoptosis, stained for externalized phosphatidyl serine (PS) with Alexa Fluor-568 labeled Annexin V, fixed, additionally stained for F-actin and chromatin and analyzed by fluorescence microscopy. Depicted are the percentages of blebbing and PS positive cells (arithmetic means of two independent experiments + SD with > 100/condition).

In line with the fact that ROCK1/FHOD1 blebs are not apoptotic, FHOD1 had no detectable influence on apoptotic PM blebbing.

A second approach addressed PM blebbing that was directly induced by ROCK1 expression. HeLa cells treated with siRNA oligonucleotides were transfected with expression plasmids encoding ROCK1. After fixation and stain the cells were analyzed for PM blebbing. FHOD1 knockdown in this case showed no decrease (fig. 47Acd/B). However, ROCK1 (75 %) as well as vector (29 %) transfected cells revealed an unusual high bleb affinity (fig. 47B and data not shown), which might be due to the demanding transfection protocol or to a possible upregulation of other Drfs like FHOD2 to compensate for the lack of FHOD1 (see Material and Methods).

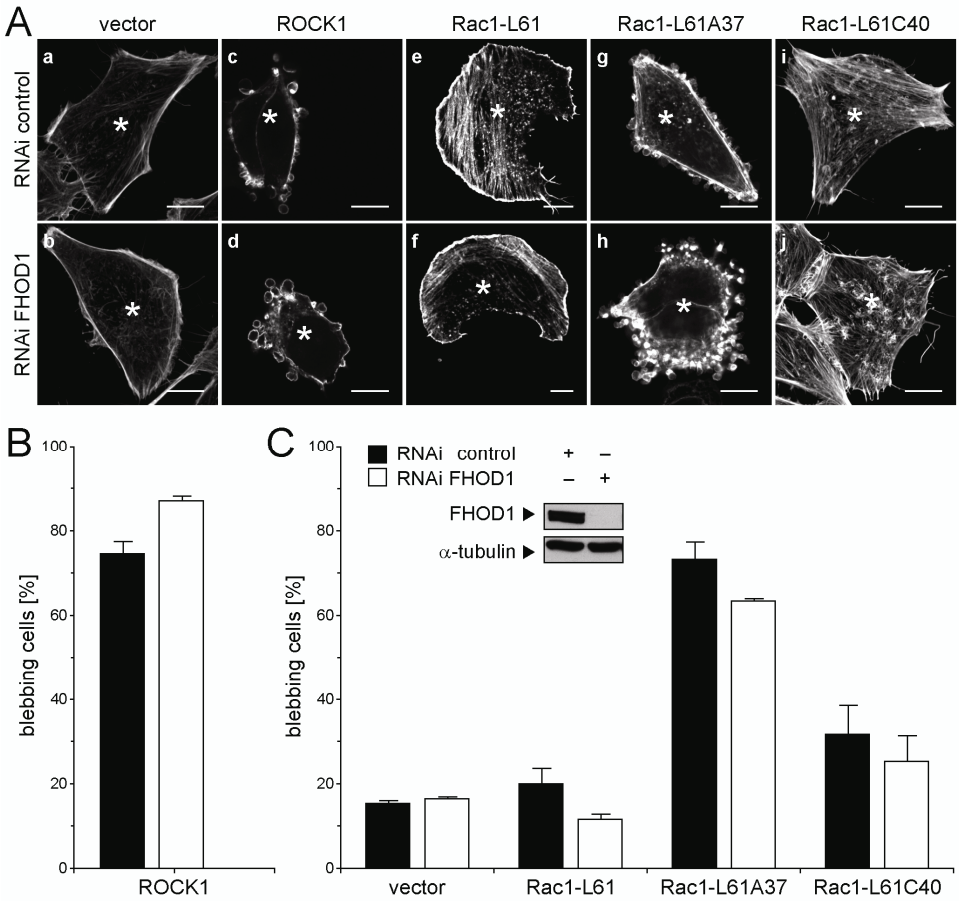

Figure 47: PM blebbing induced by ROCK1 or Rac1 was not influenced by RNAi mediated knockdown of FHOD1.

(A) Reduced levels of FHOD1 did not change cellular appearance of ROCK or Rac1 expressing cells. After a second RNAi treatment (knockdown efficiencies are depicted in insert of C), HeLa cells were either transfected with vector (a-b), plasmids encoding Myc-tagged ROCK1-wt (c-d) or constitutively active mutants of Rac1 (Rac1-L61: e-f; Rac1-L61A37: g-h; Rac1-L61C40: i-j). After 24 h, cells were fixed, stained for the transiently expressed proteins and F-actin and analyzed by confocal microscopy. Transfected cells are highlighted (*), scale bars = 10 µm. **(B)** Reduction of FHOD1 had no influence on ROCK1 induced PM blebbing. HeLa cells depicted in A transiently expressing ROCK1-wt were evaluated for PM blebbing. Depicted are the percentages of blebbing cells (arithmetic means of three independent experiments + SD with > 100/condition). **(C)** Reduction of FHOD1 had no influence on Rac1 induced PM blebbing. HeLa cells depicted in A transiently expressing either vector, Rac1-L61, Rac1-L61A37 or Rac1-L61C40 were evaluated for PM blebbing. Depicted are the percentages of blebbing cells (arithmetic means of three independent experiments + SD with > 100/condition).

As mentioned before, the FHOD1 protein binds to the Rho-GTPase Rac1 (Gasteier *et al.*, 2003, Westendorf, 2001). Interestingly, expression of a constitutively active form of Rac1 with two residue exchanges (Rac1-L61A37: Gln61 to leucine and Phe37 to alanine) had been described to induce PM blebbing (> 50 % after 7 h) in NIH3T3 cells. Two other Rac1 variants (Rac1-L61 and Rac1-L61C40: Gln61 to leucine and Tyr40 to cysteine) failed to induce PM blebbing (Schwartz *et al.*, 1998). To test the influence of FHOD1 on formation of these blebs, Myc fusion proteins of the Rac1 mutants were expressed in HeLa cells for 24 h and assayed for PM blebbing by confocal microscopy (fig. 47Ae-j/C). In line with the published data, Rac1-L61A37 induced PM blebbing in approx. 73 % of the transiently transfected cells whereas Rac1-L61 and the vector control did not. Rac1-L61C40, however, also slightly induced PM blebbing (32 %). Nevertheless, RNAi mediated reduction of FHOD1 had no quantifiable effect on PM blebbing, neither in Rac1-L61A37 nor in Rac1-L61C40 expressing cells (fig. 47Ag-j/C). These results were in agreement with the findings described in the previous chapters that FHOD1 mediated enhancement of ROCK1 induced PM blebbing did not required Rac1 activity (chapter 8.2.3).
In summary, PM blebbing induced by Rac1, ROCK1 or apoptosis was not affected by reduction of intracellular FHOD1 levels. Therefore, FHOD1 might be relevant in conjugation with ROCK1 after specific triggering.

8.2.6 FHOD1 Contributes to SH4 Mediated PM Blebbing

As described in the first part of this work, PM blebbing was also inducible by expression of SH4-domains (chapter 8.1). Although these blebs required the integrity of microtubules, they also showed remarkable similarities to FHOD1 enhanced ROCK1 blebs concerning size and number, their non apoptotic nature as well as their dependency on the Rho-ROCK pathway, on localization and activity of Src kinases and the integrity of the microfilament system in general. This suggested a possible role of the FHOD1 protein in SH4 mediated PM blebbing. To test this hypothesis, RNAi mediated knockdown of FHOD1 was performed in CHO cells stably expressing N18-HASPB-GFP. Indeed, compared to cells treated with control oligonucleotide, PM blebbing was reduced up to twofold ($p = 0.0004$) in FHOD1 knockdown cells (fig. 48). Of note, this reduction occurred although FHOD1 expression levels were only moderately diminished. Interestingly, a further decrease of FHOD1 levels caused no additional reduction of PM blebbing (data not shown) indicating that FHOD1 may represent one of several factors that synergistically mediate SH4-domain induced PM blebbing.

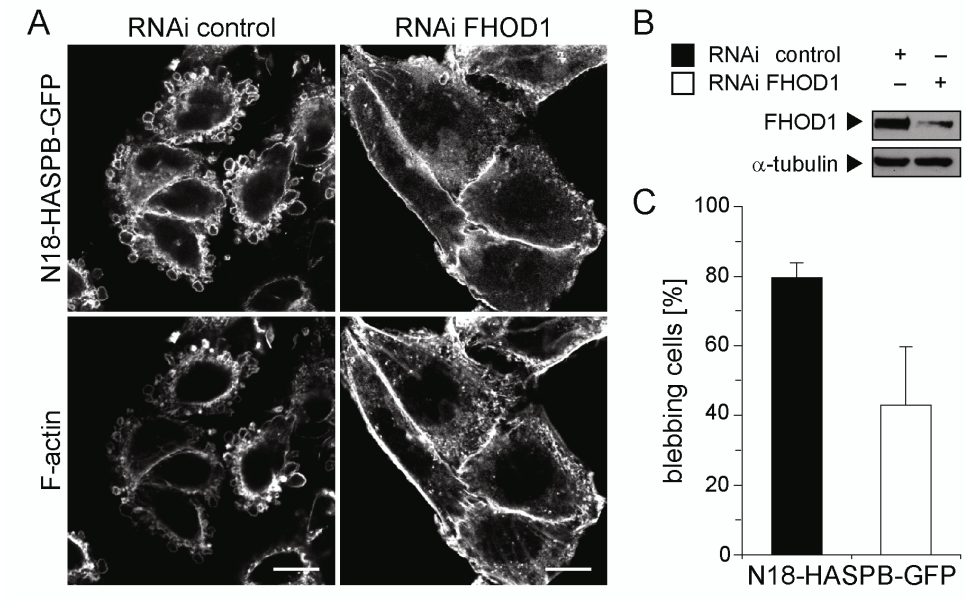

Figure 48: FHOD1 was involved in HASPB-SH4-domain induced PM blebbing.

(A-C) Reduction of FHOD1 resulted in decrease of HASPB-SH4-domain induced PM blebbing. **(A)** Following RNAi treatment (knockdown efficiency shown in B), N18-HASPB-GFP expression was induced for 24 h by addition of 1000 µg/ml dox in CHO cells. They were fixed and stained for F-actin to evaluate blebbing efficiency. Shown are confocal micrographs of control and FHOD1 knockdown cells. Scale bars = 10 µm. **(B)** Knockdown efficiency for CHO cells treated with either control no-target siRNA oligonucleotides or FHOD1 specific siRNA oligonucleotides. **(C)** Quantification of the blebbing efficiency of cells depicted in A. N18-HASPB-GFP expressing cells treated as described in A were evaluated for F-actin positive PM blebs by fluorescence microscopy. Values represent the arithmetic means of at least six independent experiments + SD in which over 100 cells were counted per condition. As calculated by Student's t-test values are statistical different (p = 0.0004).

The involvement of other Drfs like the Dia proteins or FHOD2 and the confirmation of FHOD1s role in SH4-domain PM blebbing is part of current investigations. Since SH4-domain mediated PM blebbing also correlated with enhanced invasiveness in 3D matrices, FHOD1s contribution to this is of special interest as well and has to be further investigated. Nevertheless, besides its contribution to PM blebbing, there might be additional functions of FHOD1 which were addressed in the following chapter.

8.3 The Role of FHOD1 in Intracellular Organization

8.3.1 Characterization of Cells Reduced in FHOD1

Drfs play a critical role in cytoskeletal reorganization. By nucleation of F-actin they control various cellular functions such as establishment of cell shape, cytokinesis or cell motility (Faix and Grosse, 2006, Wallar and Alberts, 2003). Although a common feature of Drfs is their highly conserved FH1- and FH2-domain which are required for interactions with cellular ligands, their individual function is thought to be unique. FHOD1s physiological functions remain elusive, although there have been many attempts for characterization. Besides its contribution to

PM blebbing as described in the previous chapters, it was shown that expression of FHOD1-ΔC leads to F-actin polymerization and formation of thick F-actin cables decorated by the Drf (Gasteier *et al.*, 2003, Koka *et al.*, 2003). Furthermore, it coordinates F-actin filaments and microtubules to induce cell elongation (Gasteier *et al.*, 2005), an effect that was assigned to its ability to stimulate cell migration in an integrin-independent manner (Koka *et al.*, 2003). However, all these functions have been deduced from over-expression experiments and might not display its natural physiological function. For more reliable characterization studies of FHOD1 that circumvent these limitations, a siRNA mediated knockdown of FHOD1 was employed as described in chapter 8.2.5. For a first approximation, the impact of an FHOD1 knockdown on general cellular functions linked to the cytoskeleton was investigated. Since the cytoskeleton determines the cellular shape, the impact on of cell size was addressed. HeLa cells were seeded on coverslips for two days, fixed and stained for F-actin. Following fluorescence microscopy, the size of individual cells was manually measured with "ImageJ" software (fig. 49A/B). Compared to cells treated with control siRNA, only a slight reduction in cell size was observed. Nevertheless, the two populations could statistically be separated by Student's t-test ($p < 0.001$). Next, the F-actin content was analyzed: Confocal micrographs of Phalloidin-TRITC stained adherent HeLa cells showed no obvious differences in F-actin levels (fig. 49A/C1-2). Similar results were obtained by FACS analysis. RNAi treated HeLa cells grown for 24 h on culture dishes at approx. 75 % confluency were fixed, stained for F-actin with Alexa-Fluor-660 labeled Phalloidin and measured for F-actin content. In these experiments a slight but significant ($p = 0.01$, Student's t-test) decrease in F-actin levels could be detected in FHOD1 knockdown cells (fig. 49A/C3-4). These results demonstrated only a minor contribution of FHOD1 to overall F-actin levels. Third, the impact of FHOD1 reduction in cell proliferation was analyzed. Former studies showed no influence of FHOD1 over-expression in cytokinesis (Gasteier *et al.*, 2005). In line with these results, a reduction of FHOD1 levels had no effect on proliferation of HeLa cells within 24 h ($p = 0.2$, Student's t-test) as it was measured by an incorporated thymidine analog (BrdU) in newly generated DNA (fig. 49A/D2).

In 2003, Koka and coworkers could show that over-expression of FHOD1 enhanced cell migration in an integrin- and cell-surface adhesion-independent manner (Koka *et al.*, 2003). Consequently, the adhesion capacity of siRNA treated HeLa cells to surfaces was determined. The amount of cells that were attached to different surfaces like uncoated wells or fibronectin, collagen or poly-L-lysine coated cell culture dishes, respectively, was quantified. In line with these studies no differences could be detected (fig. 49A/D1 and data not shown).

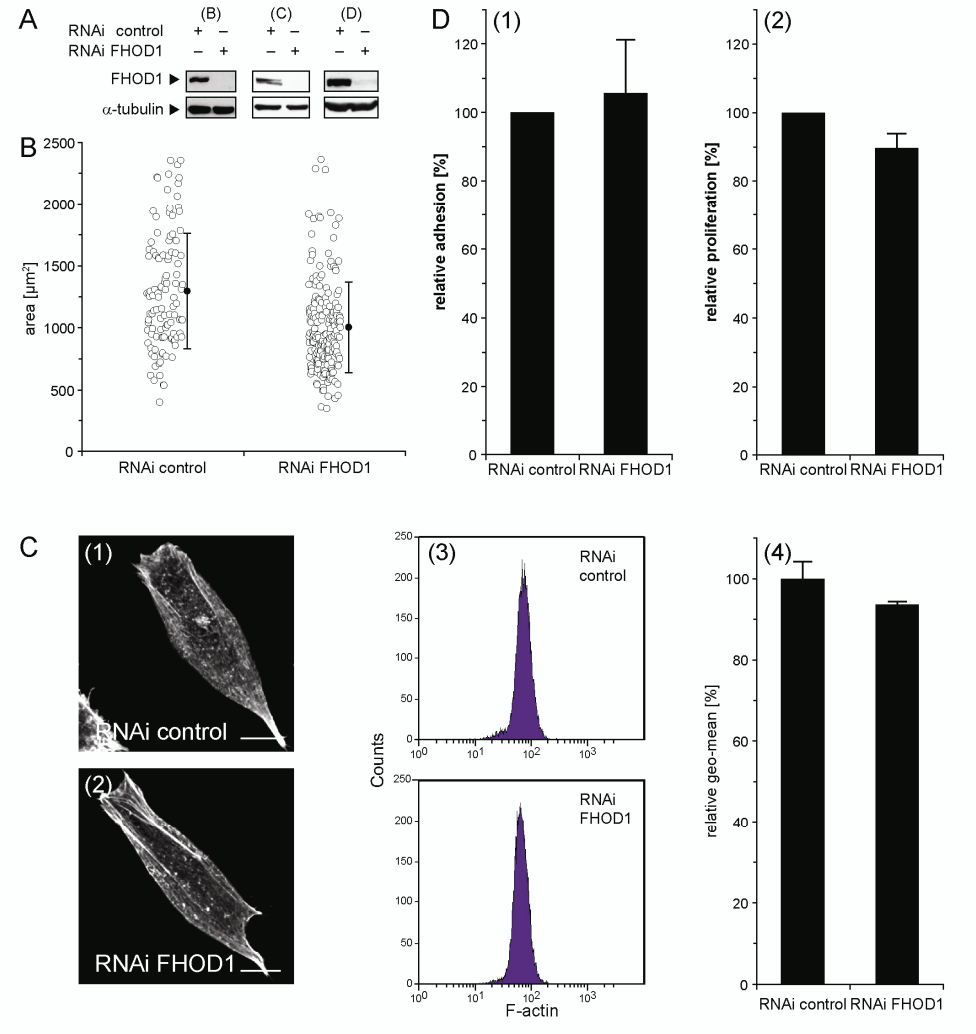

Figure 49: RNAi mediated knockdown of FHOD1 had minimal effects on cell size, F-actin levels, cell-surface adhesion and proliferation.

(A) Levels of endogenous FHOD1 were reduced by a specific RNAi mediated knockdown. HeLa cells were transfected either with unrelated control siRNA oligonucleotides or FHOD1 specific siRNA oligonucleotides on day 1 and on day 3 as described in material and methods and harvested on day 5. Equal amounts of total protein were separated by SDS-PAGE, subjected to Western blotting and probed with a specific antibody against FHOD1 (Gasteier *et al.*, 2005) for knockdown efficiencies or against α-tubulin serving as loading control. **(B)** FHOD1 reduction had minimal influence on cell size. RNAi treated HeLa cells with a knockdown efficiency as depicted in A were seeded on glass coverslips for 2 days. Cells were fixed, stained for F-actin and individual cell sizes were manually analyzed by perimeter measurement with "ImageJ" software (arithmetic means of three independent experiments + SD with > 100/condition; $p < 0.001$, Student's t-test). **(C)** FHOD1 reduction had minimal influence on F-actin levels. RNAi treated HeLa cells with a knockdown efficiency as depicted in A were grown on coverslips, fixed, stained for F-actin and subjected to confocal microscopy (1+2). In parallel, cells grown for 24 h on a culture dish by a confluency of approx. 75 % were detached by trypsin/EDTA, fixed, stained for F-actin with Alexa-Fluor-660 labeled Phalloidin and analyzed by FACS. Shown are the geo-mean values of gated cells (3) and arithmetic means (4) of three independent experiments + SD ($p = 0.01$, Student's t-test). Scale bars = 10 µm **(D)** FHOD1 reduction had minimal influence on cell-surface adhesion and proliferation. RNAi treated HeLa cells with a knockdown efficiency as depicted in A were seeded as triplicates in 96 well plates for 2 h. For evaluation of adhesion efficiencies, relative numbers of fixed cells were measured after chromatin stain (Hoechst 33268) with a fluorimeter (356 nm/458 nm) and normalized to a standard curve. Depicted are the percentages of the measured signals relative to control cells (1). For determination of proliferation rates, after adhesion newly generated DNA was labeled by addition of BrdU reagent for 24 h. Cells were fixed and analyzed by ELISA. Depicted are the percentages of the measured signals normalized to adhesion rates and relative to control cells (2) (arithmetic means of three independent experiments + SD with > 100/condition; Student's t-test: adhesion $p = 0.7$; proliferation $p = 0.2$).

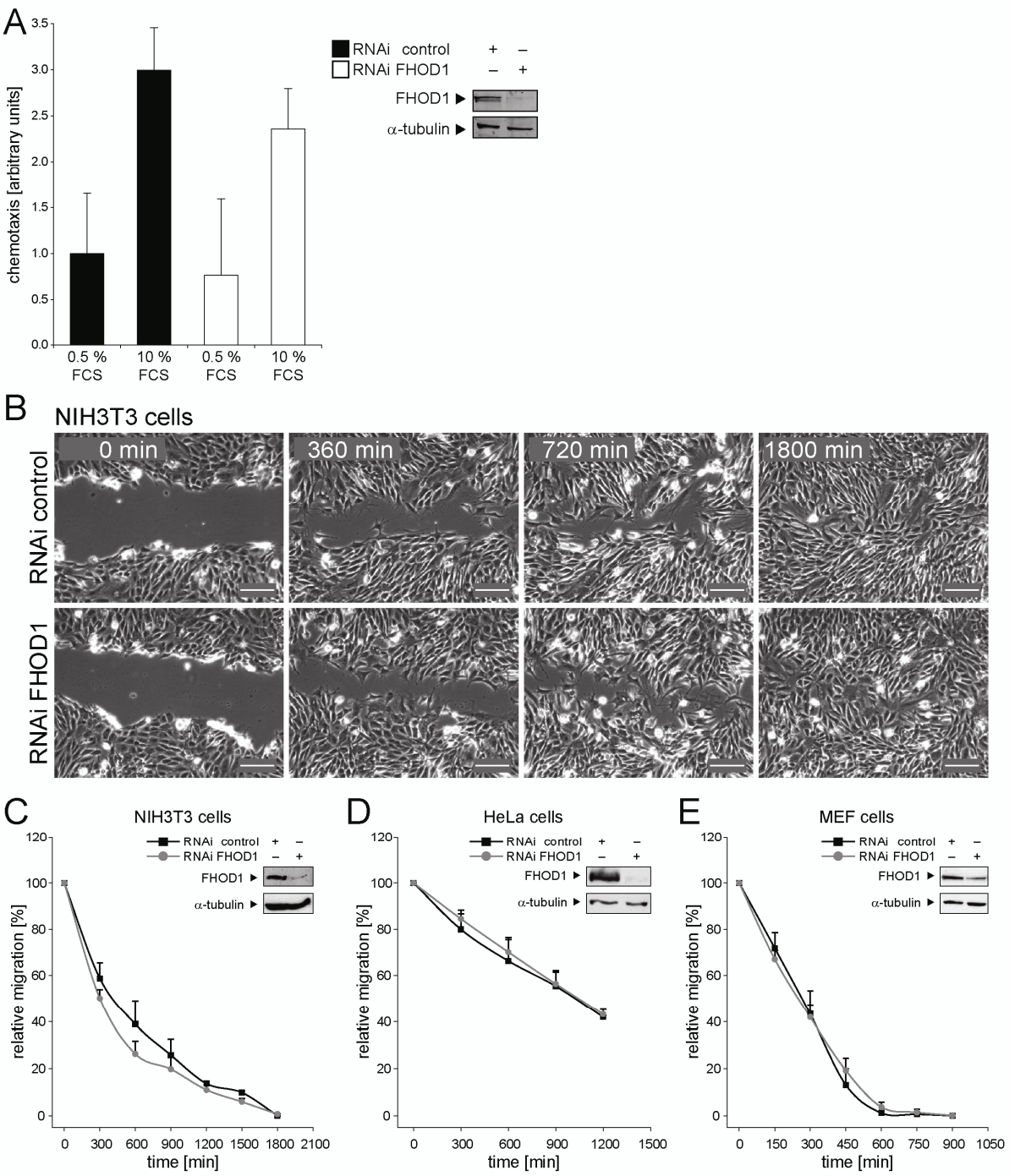

Figure 50: Reduction of endogenous FHOD1 had no effect on chemotaxis and motility on planar surfaces.

(A) FHOD1 reduction had no influence on chemotaxis. NIH3T3 cells were transfected either with unrelated control siRNA oligonucleotides or FHOD1 specific siRNA oligonucleotides (knockdown efficiency is depicted in insert). Serum starved cells were seeded onto a transwell insert grid (pore size 8 µm) for 1 h and were exposed to a gradient of FCS (0.5-0.5 % or 0.5-10 %) for 8 h. They were fixed and stained for F-actin and chromatin and amounts of migrated and not migrated cells were counted. Depicted are the relative amounts of migrated cells. Values are the arithmetic means of five microscopy fields + SD. **(B-E)** FHOD1 reduction has no influence on motility on planar surfaces. Cells were transfected either with unrelated control siRNA oligonucleotides or FHOD1 specific siRNA oligonucleotides (knockdown efficiency is depicted in insert). **(B)** Representative images of wound healing assays performed with NIH3T3 cells. Confluent cell layers were wounded and monitored by microscopy over time (24 h, 1 picture/30 min). Scale bars = 100 µm. **(C-E)** Quantification of wound closure time. Wound sizes of cell layers as described in B were measured by "ImageJ" software for **(C)** NIH3T3 cells, **(D)** HeLa cells and **(E)** MEFs. Values are the arithmetic means of at least three wounds + SD.

Additionally, cell migration in 2D was measured by two distinct methods: In a chemotaxis assay, the capacity of serum starved NIH3T3 cells was measured to migrate along a gradient of FCS (0.5-10 %). Therefore, siRNA treated cells were seeded at the bottom of a transwell insert and were monitored for 8-24 h. The relative amount of migrated cells was quantified after fixation and stain for chromatin and F-actin. In contrast to the results that had been described for over-expressed FHOD1 (Koka *et al.*, 2003), knockdown of FHOD1 did not yield significant difference in chemotaxis (fig. 50A and data not shown). Similar results were obtained in wound healing assays performed as described earlier for SH4-domain expressing cells (see chapter 8.1.11). Neither a reduction of FHOD1 in NIH3T3 nor in HeLa cells or MEFs revealed a detectable defect in motility on planar surfaces (fig. 50B-D).

In summary, reduction of FHOD1 had no pronounced effect on cell size, F-actin content, cell proliferation, cell-surface adhesion, chemotaxis or cell migration. However, it cannot be excluded that other Drfs compensate for FHOD1s reduction. Furthermore, residual amounts of FHOD1 in knockdown cells might have been sufficient to facilitate the investigated functions.

8.3.2 Interference of FHOD1 with Rho-GTPases

The activity of Drfs is at least partially regulated by Rho-GTPases. Their interaction is mediated by the mostly N-terminally located GTPase binding domain (GBD) of Drfs (Faix and Grosse, 2006, Wallar and Alberts, 2003). FHOD1 was shown to specifically interact with Rac1, but not with RhoA or Cdc42, and colocalizes with co-expressed constitutively active Rac1 at the PM of lamellipodia (Gasteier *et al.*, 2003, Westendorf, 2001), but it has not been verified whether FHOD1 is a Rac1 effector. Interestingly, the already mentioned stress fiber formation by active FHOD1-ΔC depends on the activity of Rho and its effector kinase ROCK (Gasteier *et al.*, 2003). Thus, RNAi mediated knockdown of FHOD1 was used to investigate a specific function of FHOD1 as Rho-GTPase effector in actin remodeling. HeLa cells treated with FHOD1 specific siRNA for efficient knockdown were transfected with expression plasmids of constitutively active Myc-tagged mutants of Rho-GTPases. Following fixation and staining, the cells were analyzed by confocal microscopy for the formation of F-actin phenotypes that are typically induced by Rho-GTPases (Allen *et al.*, 1997). Quantification of at least 100 cells per experiment revealed neither a difference in development of stress fibers initiated by Rho-V14 or its effector ROCK1-Δ3 nor in formation of lamellipodia or filopodia induced by Rac1-L61 or Cdc42-L61, respectively (fig. 51A-F). If anything, the latter one was slightly increased.

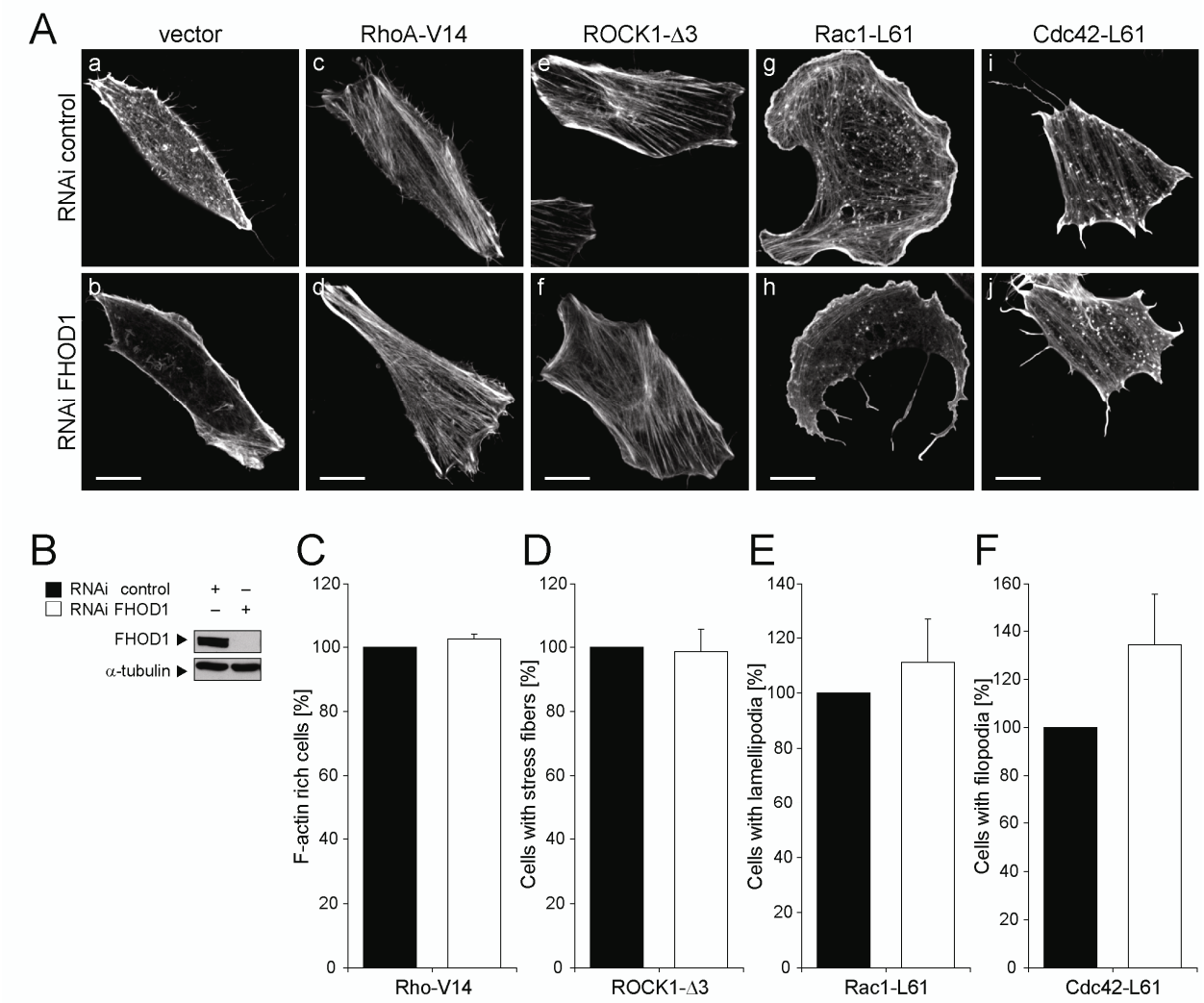

Figure 51: FHOD1 reduction has no influence on GTPase mediated cytoskeletal rearrangements.

(A) After RNAi treatment, HeLa cells were transfected with expression plasmids for the indicated constitutively active Rho-GTPases fused to GFP or GFP alone. Following 24 h of incubation the cells were fixed and stained for F-actin. Scale bars = 10 µm. **(B)** Knockdown efficiency for HeLa cells treated twice with either control no-target siRNA oligonucleotides or FHOD1 specific siRNA oligonucleotides. **(C-E)** HeLa cells as depicted in A were microscopically quantified for a specific phenotype: **(C)** Evaluation of RhoA-V14 expressing cells (see also Ac-d) for formation of F-actin fibers. **(D)** Evaluation of ROCK1-Δ3 expressing cells (see also Ae-f) for formation of F-actin fibers. **(E)** Evaluation of Rac1-L61 expressing cells (see also Ag-h) for lamellipodia formation. **(F)** Evaluation of Cdc42-L61 expressing cells (see also i-j) for filopodia formation. RNAi control values are set to 100 % (arithmetic means of three independent experiments + SD with > 100/condition).

Via increase of actin treadmilling, Rho-GTPases also regulate transcription from the SRE (Hill *et al.*, 1995). The SRE is a common regulatory element of many promotors of genes whose transcription is linked to growth factor or mitogen stimulation (Treisman, 1992). To investigate the influence of FHOD1 in Rho-GTPase mediated SRE activation, FHOD1 reduced NIH3T3 cells were co-transfected with expression plasmids of constitutively active Myc tagged GTPases in combination with a SRE reporter construct fused to luciferase (fig. 52). For evaluation, the fluorescently detected substrate turnover was normalized to the values obtained for FHOD1-ΔC

which have been shown to induce SRE activation as well (Gasteier *et al.*, 2003, Westendorf, 2001). No differences between control and FHOD1 knockdown cells were observed for any GTPase or for ROCK1-Δ3 (fig. 52).

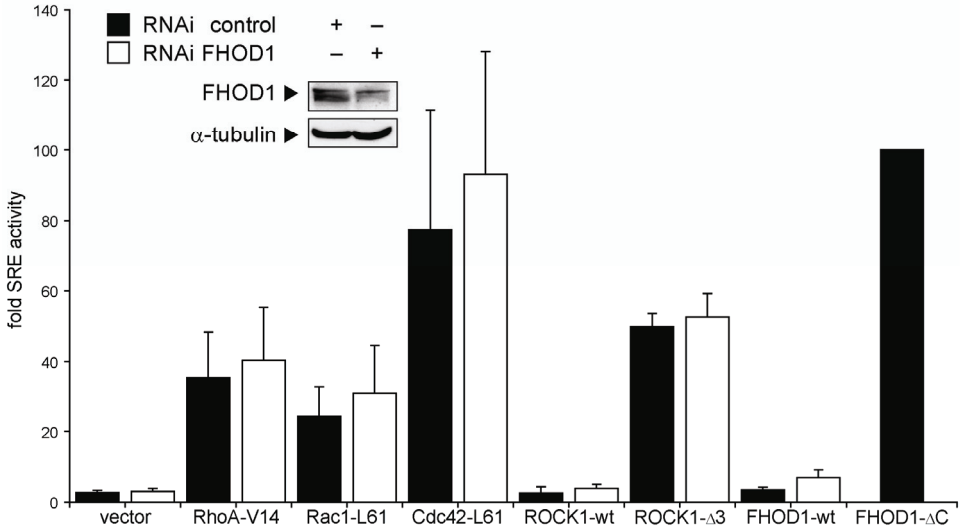

Figure 52: FHOD1 reduction had no influence on GTPase mediated SRE activation.

After second RNAi treatment with either control no-target siRNA oligonucleotides or FHOD1 specific siRNA oligonucleotides (knockdown efficiency see insert), NIH3T3 cells were co-transfected with SRE reporter constructs and an expression plasmid encoding the indicated protein in triplicate experiments. After 24 h serum starvation cells were harvested and SRE activity luminiscently detected with a luminometer. Depicted are the fold activities normalized to the control FHOD1-ΔC signal (set to 100 % in each experiment) and relative to vector control. Values are the arithmetic means of three independent experiments + S.E.M.

In summary, FHOD1 was not limiting for Rho-GTPase or ROCK1 mediated F-actin remodeling or SRE activation. These results were in contrast to described associations of FHOD1 with Rac1 and Rho pathways. However, they also did not disprove this theory due to possible residual amounts of FHOD1 after siRNA treatment.

8.3.3 Endogenous FHOD1 is Localized at to Golgi Structures

Since studies of general and specific cytoskeletal phenotypes revealed no obvious contribution of the FHOD1 protein, another approach to investigate its intracellular distribution was chosen. As already mentioned, exogenous FHOD1 localizes at the PM of lamellipodia if co-expressed with the constitutively active form of the Rho-GTPase Rac1. Additionally, the constitutively active form FHOD1-ΔC decorates F-actin bundles, but FHOD1 alone shows an unspecific cytoplasmatic distribution (Gasteier *et al.*, 2003, Westendorf, 2001). To investigate the intrinsic localization of FHOD1, the endogenous protein was detected with a specific polyclonal antibody directed against two FHOD1 peptide sequences in its N-terminal part (Gasteier *et al.*, 2005). This revealed a certain perinuclear localization of FHOD1 in NIH3T3 cells that was not detectable by

usage of peptide saturated antibodies or the secondary antibody alone, respectively (fig. 53A and data not shown). However, these studies were only successful in rodent cell lines as mouse NIH3T3, hamster CHO or rat Rat2 cells, but not in human cell lines like HeLa, Huh-7 or Jurkat T-cells (fig. 53A/B and data not shown). In contrast, immuno-electron micrographs as described later were obtained from HeLa cells, only, but not from rodent cells (fig. 53C and data not shown).

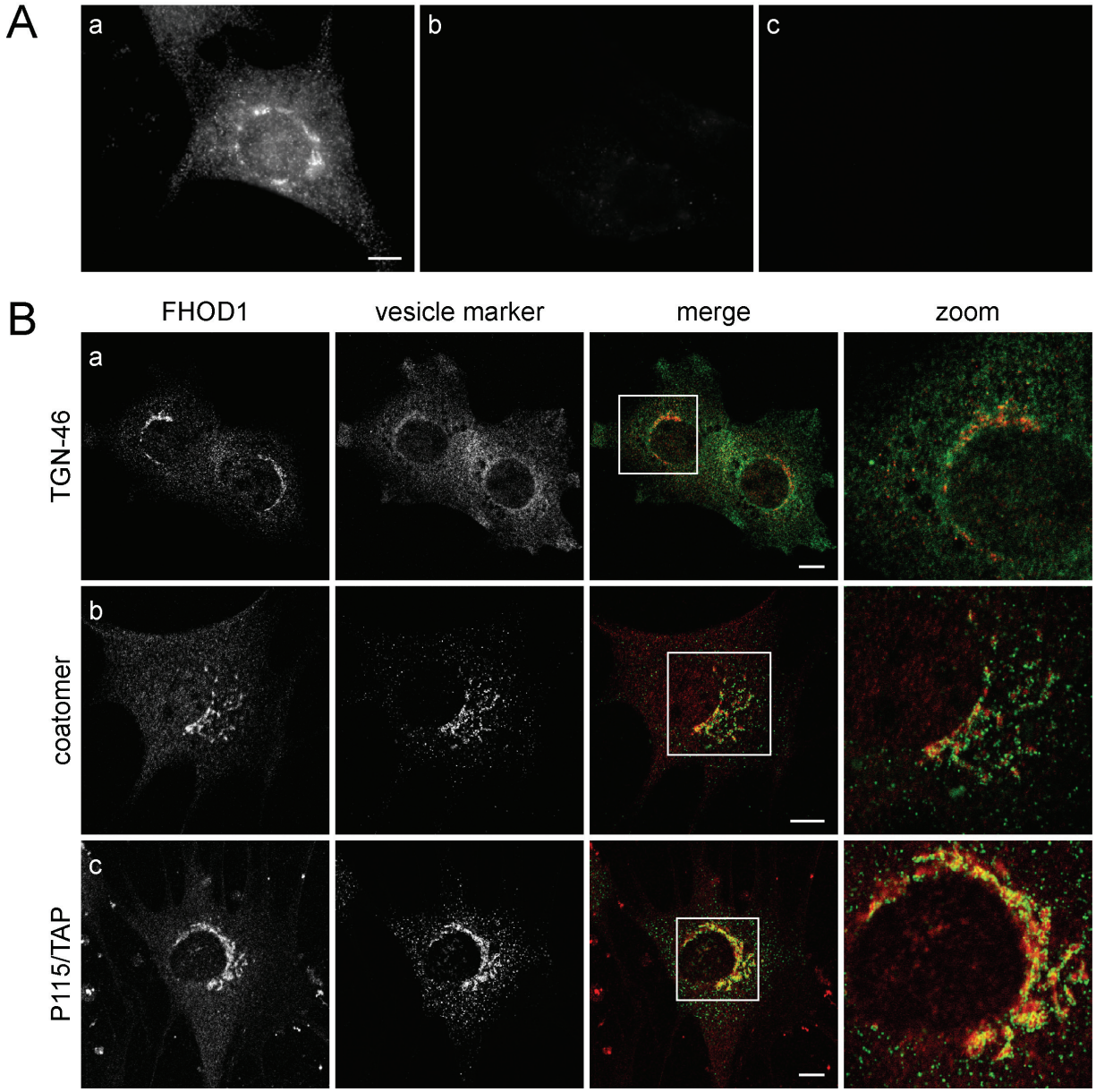

Figure 53: Endogenous FHOD1 was found in perinuclear regions and localized at Golgi structures.

(A) Endogenous FHOD1 specifically localized in a perinuclear region. NIH3T3 cells grown on a coverslip were fixed and stained with (a) an antibody against FHOD1 (Gasteier *et al.*, 2005) together with a fluorescently labeled secondary antibody. For specificity control cells were stained with (b) FHOD1 antibody saturated with its target peptides or (c) fluorescently labeled secondary antibody alone. Scale bars = 10 µm. **(B)** Endogenous FHOD1 is associated with Golgi proteins. Confocal micrographs of NIH3T3 cells grown on glass coverslips. They were fixed and stained for endogenous FHOD1 in combination with the indicated Golgi proteins. Squares in the "merge" panel indicate the zoomed regions depicted in the right panel. Scale bars = 10 µm.

The reason for this discrepancy is unclear. Possibly due to distinct posttranslational modifications such as species or cell type specific phosphorylations or variable complexation with other proteins the accessibility of the epitopes for the antibody was altered differently. Anyway, detection of endogenous FHOD1 in western blot analysis has been shown to be species independent (Gasteier *et al.*, 2005) which was also proven in this work (fig. 50). In order to further define these perinuclear structures, co-localization studies with endogenous marker proteins were performed. As a result, FHOD1 localized in close proximity to Golgi marker proteins like TGN-46, coatomer or P115/TAP, but not with other vesicular markers like EEA1, LAMP1 or TfR (fig. 53B and data not shown). Endogenous FHOD1 localized very pronounced in between vesicles that were positive for P115/TAP, a protein that is involved in fusion of ER-derived COP-II vesicles and their binding to Golgi membranes (Allan *et al.*, 2000, Alvarez *et al.*, 2001). To get further insight into this distribution, immuno-electron microscopy of negative stained HeLa cells was performed by S. Welsch (group of G. Griffiths, EMBL, Heidelberg) (fig. 54A):

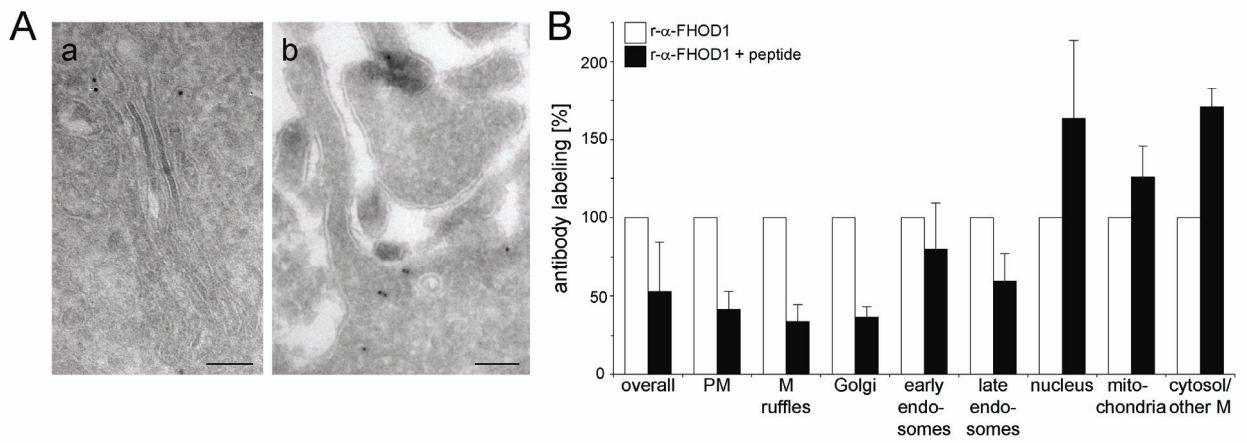

Figure 54: Endogenous FHOD1 localized at Golgi structures and PM ruffles.

(A) Electron micrographs of HeLa cells stained for endogenous FHOD1 (10 nm gold) showed (a) Golgi related localization and (b) localization in ruffles at the PM. Scale bars = 100 nm **(B)** For specificity control cells were stained with antibody against endogenous FHOD1 untreated or treated with its target peptide for compensation. Values are the relative amounts of gold particles counted for each compound and are the arithmetic means of three independent labeling experiments + SD in which 100-200 particles were counted per grid (2 grids/experiment). Compensation values are set to 100 % . (kindly provided by S. Welsch from the group of G. Griffiths, EMBL, Heidelberg).

Although the overall antibody affinity to the used samples in general was very low and, as judged by peptide compensation studies, the unspecific background relatively high (early or late endosomes, nucleus, mitochondria or other cellular components: fig. 54B), the signals for some cellular compartments were specific: Endogenous FHOD1 mainly localized at the lateral sites or in between some Golgi stacks and was also associated to PM ruffles (fig. 54C).

Assuming a specific role for FHOD1 in Golgi organization, variations in FHOD1 levels should possibly change the appearance of Golgi stacks. However, neither transiently expressed HA-FHOD1-wt for 24 h nor its active mutant HA-FHOD1-ΔC that potently induced F-actin cable formation changed the distribution of the Golgi marker p115/TAP (fig. 55).

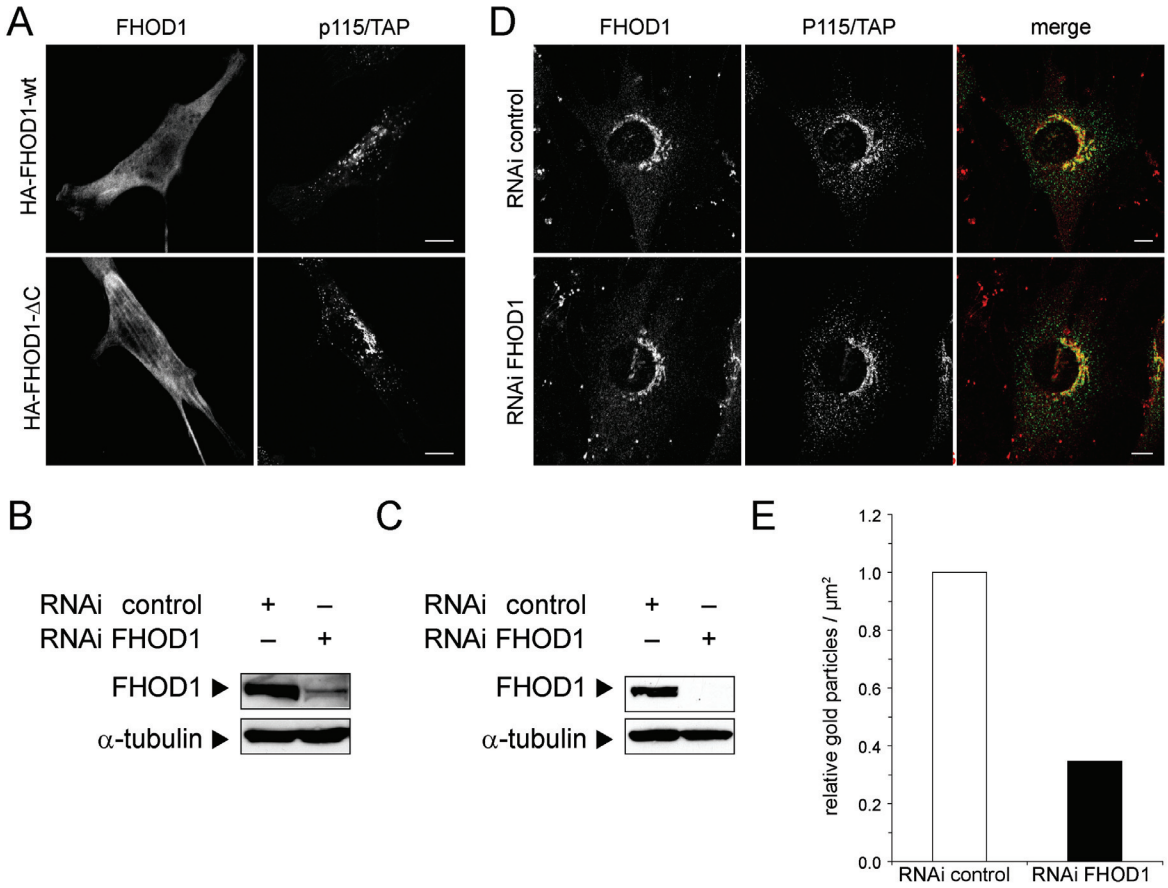

Figure 55: Protein level variations of FHOD1 had no influence on Golgi organization.

(A) Over-expression of FHOD1 did not alter Golgi organization. Confocal micrographs of NIH3T3 cells that were transfected either with HA tagged FHOD1 or its constitutively active form FHOD1-ΔC. Cells were fixed and stained for the expressed proteins as well as for endogenous P115/TAP as a Golgi marker. **(B-C)** Knockdown efficiencies for NIH3T3 cells **(B)** or HeLa cells **(C)** treated either with unrelated control siRNA oligonucleotides or FHOD1 specific siRNA oligonucleotides. **(D)** Reduced FHOD1 expression had no influence on Golgi organization and perinuclear FHOD1 stain. Confocal micrographs of RNAi treated NIH3T3 cells (knockdown efficiency see B) grown on a coverslip. Cells were fixed and stained for endogenous FHOD1 and for endogenous p115/TAP as a Golgi marker. **(E)** RNAi mediated FHOD1 reduction decreased signals in immuno-electron micrographs. Hela cells were subjected to FHOD1 knockdown as described in C, stained for endogenous FHOD1 and the number of gold particles was counted on electron micrographs. Data are exclusive mitochondrial signals. Values are the relative amounts of gold paritcles/μm^2 that were counted on randomly taken images (100/condition) where RNAi control values were set to 100 % (kindly provided by S. Welsch: E).

Similar results were obtained by siRNA mediated reduction of FHOD1 in NIH3T3 cells. Although the overall amounts of endogenous FHOD1 were drastically reduced in a western blot analysis, the signal intensity of the perinuclear stain was not obviously decreased (fig. 55D). This might indicate that a Golgi associated population of FHOD1 is more stable than the diffusely distributed cytoplasmic protein and was not affected by four days siRNA treatment. However, a

specific reduction could be observed in FHOD1 knockdown cells during immuno-electron microscopy: upon exclusion of signals obtained for mitochondria that usually show a high background level (S. Welsch, personal communication), quantification of gold particles/μm^2 cell area in FHOD1 stained cells revealed a fourfold reduction of the overall cellular signal (inclusive mitochondria: 1.7 fold reduction) but without any apparent morphological changes (fig. 55E and data not shown).

Since a strong association of endogenous FHOD1 with the Golgi apparatus could be demonstrated its functional relevance was investigated in the following. The Golgi complex consists of vesicles and cisternae that are thought to be organized by microtubules and F-actin dynamics (Egea *et al.*, 2006, Vaughan, 2005). To investigate FHOD1s role in these organization processes, disassembly and reassembly of Golgi structures was analyzed. Therefore the Arf GEF inhibitor Brefeldin A (BFA) was employed. This drug specifically and reversibly blocks translocation of proteins from the endoplasmic reticulum to the Golgi apparatus without affecting endocytosis or lysosome function and furthermore causes disassembly of the Golgi apparatus (Dinter and Berger, 1998, Jackson and Casanova, 2000). Treatment of NIH3T3 cells with 5 µg/ml BFA potently disrupted the Golgi apparatus as shown in fig. 56 for the coatomer protein. After 10 min the perinuclear coatomer distribution completely dissolved and the protein strongly localized at distal areas of the cell. Interestingly, endogenous FHOD1 was still in close proximity to the coatomer protein (fig. 56, 10 min BFA, left insert), whereas most of the signal in the perinuclear region had disappeared (fig. 56, 10 min BFA, right insert). After 30 min of treatment the distribution of coatomer as well as of endogenous FHOD1 was observed to be more homogenously dispersed over the whole cell, although some distal accumulations were still detectable (fig. 56, 30 min BFA, insert). After removal of BFA from the cells the typical stack like structure of the Golgi reappeared within 1 h (fig. 56, 1h wash out). Of note, during microscopical observation of the Golgi redistribution the impression evolved that in some cells parts of the coatomer pool still distributed over the whole cell area, but the accumulation of endogenous FHOD1 seemed to proceed somehow faster (data not shown). Nevertheless, this effect was not quantified and requires further investigation. Moreover, siRNA mediated knockdown did not alter the reappearance of the Golgi after BFA treatment (data not shown). Thus, FHOD1 played no role in steady state organization and reorganization of the Golgi after disruption.

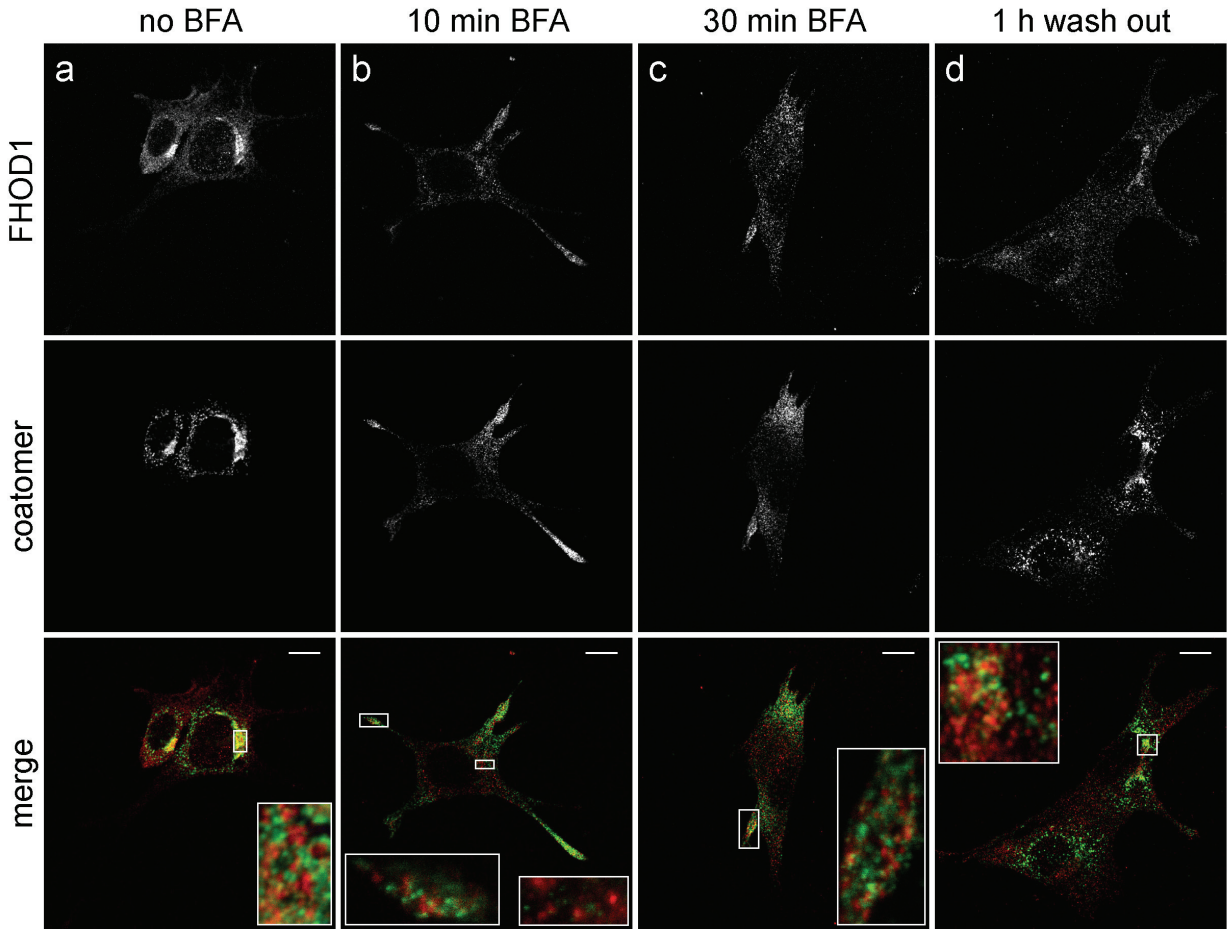

Figure 56: Brefeldin A (BFA) mediated disruption of the Golgi apparatus also disrupts perinuclear FHOD1 distribution.

Confocal micrographs of NIH3T3 cells that were treated with 5 µg/ml BFA for up to 30 min (b-c) or additionally with medium without BFA for 1 h (d). Cells were fixed and stained for endogenous FHOD1 and coatomer as Golgi marker. Squares indicate the zoomed regions depicted in the images. Scale bars = 10 µm.

Since FHOD1 had no obvious effect in Golgi organization its contribution to vesicular transport was analyzed next. The Golgi apparatus of eukaryotic cells is the central organelle of the classical ER/Golgi dependent secretory pathway. Herein, vesicular transport is directed from the ER *via* the Golgi to the cell surface. Lumenal proteins are finally released into the extracellular space by fusion of Golgi-derived secretory vesicles with the PM (Mogelsvang and Howell, 2006, Nickel, 2003). The secretory capacity of this pathway can easily be quantified by tracking of cargo proteins such as the temperature sensitive vesicular stomatitis virus (VSV) ts-045-G glycoprotein fused to CFP. At the non-permissive temperature of 39.5°C the cargo marker accumulates in the ER due to a reversible folding defect. When shifted to the permissive temperature of 31°C, correctly folded ts-045-G is rapidly transported from the ER through the Golgi apparatus to the cell surface, where its appearance can be monitored using an antibody against the lumenal domain of the glycoprotein (Pepperkok *et al.*, 1993). However, in a

fluorescence microscopy based analysis of ts-045-G-CFP transformed HeLa cells (adenovirus, MOI of 10; performed with the help of J. Simpson from the group of R. Pepperkok, EMBL, Heidelberg), the relative amounts of externalized ts-045-G (ratio antibody signal/CFP signal) were similar in control and FHOD1 knockdown cells over the monitored period of 90 min (fig. 57).

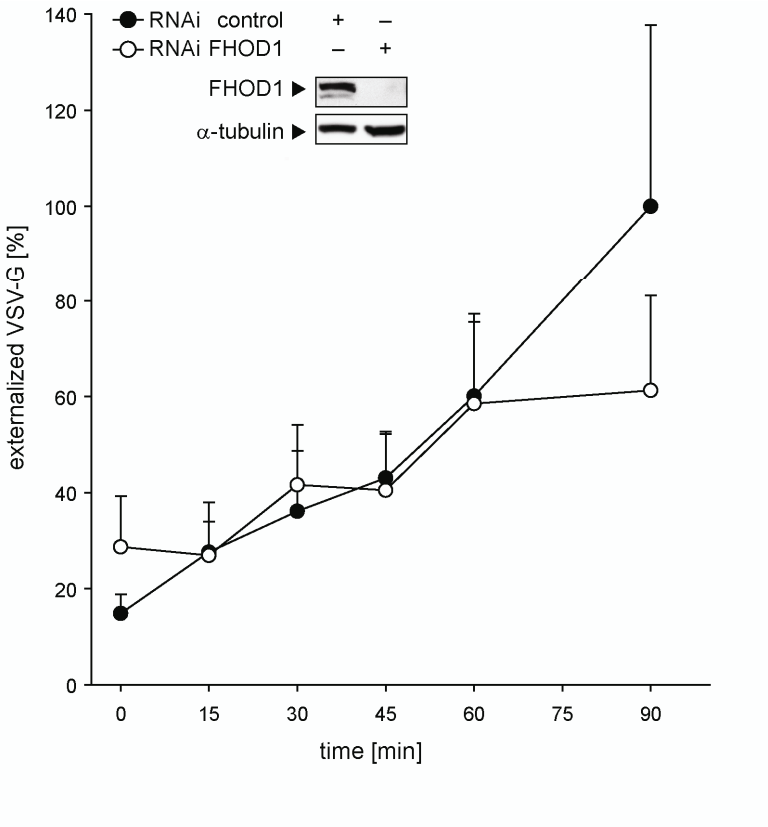

Figure 57: FHOD1 knockdown had no influence on Golgi mediated transport of VSV-G cargo proteins.

Following RNAi treatment with either control no-target siRNA oligonucleotides or FHOD1 specific siRNA oligonucleotides (knockdown efficiency see insert), HeLa cells were infected with adenoviruses (MOI of 10, 17 h) carrying genetic information for a CFP fused temperature sensitive mutant of the vesicle stomatitis virus (VSV) G-protein (ts-045-G-CFP). Cells were grown at 39.5°C for accumulation of the protein in the ER and were shifted for up to 90 min to 31°C allowing Golgi mediated VSV-G transport. After fixation, surface bound VSV-G was stained. Cells were evaluated by fluorescence microscopy. Signal intensities (mean grey values) of total and externalized VSV-G were measured with "ImageJ" software. Depicted are the ratios of external signal to total signal, relative to RNAi control at 90 min. Values are the arithmetic means of at least 100 cells per condition and time point + SD, with the help of J. Simpson).

In summary, endogenous FHOD1 was specifically found in perinuclear regions and closely localized nearby several Golgi marker proteins. Although variations of FHOD1 levels did not change the typical Golgi stack like structure, it is potently reorganized in these structures after removal of Golgi disrupting drugs. This indicated that FHOD1 might be a protein located at the Golgi periphery or the Golgi matrix. Since reduction of FHOD1 production had no detectable influence on ts-045-G cargo protein secretion or Golgi organization, its physiological role in processes other than PM blebbing remains unclear.

9 DISCUSSION

PM blebbing describes a dynamic process at cellular surfaces that occurs under various circumstances, including apoptosis, secretion, virus entry and cell motility. It is thought to be mediated by common mechanisms. This work deals with the induction and regulation of PM blebbing by factors that have not been linked to this process before: PM blebbing was specifically induced by SH4-domains of various proteins. Formation of these blebs was related to the local activity of regulatory proteins like ROCK and Src kinases. In knockdown experiments, an additional factor, the Drf FHOD1 could be identified as a functional player in this process of PM dynamization. Expression of FHOD1 in combination with its binding partner ROCK1 also induced PM blebbing very similar to SH4-domains, again in a Src dependent manner. These results suggest a functional interplay of these factors.

In the following, the individual regulation, activities and mechanistical functions of these proteins in PM blebbing and related phenotypes like cell motility will be discussed on the basis of experimental results that have been obtained during this work.

9.1 The Induction and Regulation of PM Blebbing

9.1.1 Induction of PM Blebbing by SH4-Domains

The biological function of SH4-domains is described by their capacity to target proteins like proto-oncogenic Src kinases to cellular membranes where these subsequently perform many of their specific activities (Resh, 1999). A surprising and unexpected result of this work revealed that expression of SH4-domains from different proteins potently induced highly dynamic PM blebbing on cellular surfaces describing a phenomenon that has not been linked to these membrane anchoring domains before. In general, PM blebbing is not fully understood, but has been connected to a variety of physiological conditions such as apoptosis (Mills *et al.*, 1999, Zhang *et al.*, 1998), vesicle shedding during secretion (MacKenzie *et al.*, 2001, Mehul and Hughes, 1997), cytokinesis (Boss, 1955, Laster and Mackenzie, 1996) and cell migration (Sahai and Marshall, 2003, Trinkaus, 1973).

In order to evaluate SH4-domain induced PM blebbing, as a first approach the characteristics of PM blebs and blebbing cells were analyzed. CHO cells expressing SH4-domains were constantly blebbing over an extended period without any detectable vesicular shedding. Although the SH4-domain of HASPB has been reported to be released into the medium (Stegmayer *et al.*, 2005), a bleb related secretion was not observed (C. Stegmayer, personal communication). Vesicular

shedding from blebbing cells has been reported for galactins and ATP-induced secretion of IL-1β MacKenzie *et al.*, 2001, Mehul and Hughes, 1997), even though it was suggested that IL-1β secretion is uncoupled of PM blebbing (Verhoef *et al.*, 2003). Release of cellular compartments occurs in the late phases of apoptosis as well. In this case, these apoptotic bodies bud from the cell leading to its disruption (Mills *et al.*, 1999, Zhang *et al.*, 1998). During this work, pronounced cell fractionation has not been observed for SH4-domain expressing cells. Furthermore, these cells were negative for TUNEL reaction, PS externalization or chromatin condensation. Together, this clearly indicated that SH4-domain expressing cells were not in an apoptotic stage (Huerta *et al.*, 2007) and inhibition of caspase dependent apoptosis did not influence blebbing.

Interestingly, a prerequisite for bleb induction by SH4-domains was their presence at the PM, since PM blebbing was absent upon expression of myristoylation or palmitoylation defective mutants of the HASPB- or Yes-SH4-domains. Consistently, the number of blebs per cell was related to SH4-domain expression levels indicating that high amounts of SH4-domains are required for induction of PM blebbing. A comparison of amino acid sequences from various SH4-domains, however, did not yield a common consensus sequence providing hints for specificity. Since the PM is the site for a variety of signaling events that require a definite interplay and localization of distinct determinants, these results might indicate that SH4-domain induced PM blebbing was caused by artificial effects due to their abundant presence at the PM. In this scenario, SH4-domains would alter the organization of the PM thereby disturbing subsequent signaling events required for its maintenance. Indeed, it has been shown that the myristoylated protein MARCKS which localizes at the PM upon activation of a myristoyl-electrostatic switch, is also capable of PM blebbing induction if a palmitoylated mutant is expressed in fibroblasts (Myat *et al.*, 1997). Nevertheless, as shown in this work the mode of acetylation does not determine blebbing activity, since non palmitoylated SH4-domains like the one of c-Src potently induced PM blebbing as well. Furthermore, endogenous c-Src was still found at the PM of Yes-SH4-domain expressing cells. Thus, the binding sites for this protein at the PM were not saturated by the presence of SH4-domains indicating that the PM is at least not overloaded with SH4-domains and a more specific process is involved.

Together, SH4-domain induced PM blebbing was not related to secretion or apoptotic behavior. An artificial effect caused by the abundant presence of SH4-domains at the PM is unlikely as well, but cannot be excluded at the moment. To address this issue, a PM targeted SH4-domain lacking the capacity for PM blebbing induction will have to be identified in future experiments.

9.1.2 Identification of Central Factors in PM Blebbing

A further microscopical analysis of SH4-domain induced PM blebbing revealed a well organized process that can be subdivided into three distinct phases: A fast bleb expansion, in which a newly formed bleb inflates very rapidly, always followed by an extended retention phase characterized by a stable distance of the distal bleb membrane relative to the PM. Finally, the blebs are retrieved to PM levels in a slow process termed retraction phase. Together with the observed bleb size and morphology, these characteristics were very similar to PM blebs described for M2 melanoma cells (Charras *et al.*, 2005, Cunningham, 1995). Detailed investigations of these constantly blebbing cells had contributed to the model of poroelastic bleb formation: Herein it is thought that local contractility of the cortical actin meshwork which is tethered to the PM, causes a local hydrostatic pressure of the cytoplasm in this particular area. In combination with a destabilization of the cortical actin the cytosol squeezes out, resulting in detachment of the PM and thereby in bleb expansion (Charras *et al.*, 2005). Subsequently, this enlargement is stopped by *de novo* polymerization of F-actin generating a new actin cortex that stabilizes the bleb membrane. The bleb is finally retracted in an active process based on acto-myosin contractility (Charras *et al.*, 2006, Cunningham, 1995, Paluch *et al.*, 2005, Wyckoff *et al.*, 2006).

Consistent with this model, SH4-domain mediated formation of PM blebs required acto-myosin contractility: Disruption of the microfilament system potently blocked PM blebbing which indicated that its integrity as well as active actin turnover were important prerequisites. Similar results have been obtained by bulk inhibition of myosin II mediated contractility or its activating kinase ROCK. In fact, ROCK proteins, being effectors of the Rho-GTPase Rho, are key regulators of contractility and play a central role during apoptotic PM blebbing (Coleman *et al.*, 2001, Riento and Ridley, 2003, Sebbagh *et al.*, 2005, Sebbagh *et al.*, 2001). In line with this, SH4-domain mediated PM blebbing was specifically regulated by the activity of Rho and not by other Rho-GTPases such as Rac or Cdc42, although all of them were found at the outer rim of a bleb membrane. Since PM localization of the SH4-domain was not impaired by inhibition of GTPase activity, Rho regulation of PM blebbing is likely to occur downstream of SH4-domain PM targeting and indicates that bleb induction is triggered by the presence of SH4-domains at the site of action. Whether Rho-GTPase activity can be found at the site of PM blebbing in particular and if it is deregulated in SH4-domain expressing cells will have to be addressed in future experiments.

Nevertheless, a local activity of its effector ROCK was discovered at the bleb basis and inside the bleb lumen as demonstrated by specific staining of endogenous phosphorylated ROCK substrate MLC. Since no general MLC activation was detected upon SH4-domain expression by

Western blot analysis, the acto-myosin contractility is limited to local areas only. This is consistent with the model of poroelastic bleb formation, in which a delimited contraction of the cortical actin meshwork leads to PM blebbing as it occurs in M2 cells. Due to their FLNa deficiency, M2 cells possess a reduced integrity of the cortical actin meshwork triggering PM blebbing (Charras *et al.*, 2006, Cunningham, 1995, Stossel *et al.*, 2001). However, expression of SH4-domains had no obvious effects on overall FLNa expression levels or its serine phosphorylation, suggesting that SH4-domains either induce PM blebbing by a distinct trigger or cause only local variations of FLNa. Whether this is the case could not be demonstrated by immuno-fluorescence with the used antibodies.

Another group of factors contributing to SH4-domain PM blebbing was identified in this study: Src kinases had not been linked to any kind of PM blebbing before. Inhibition of overall Src kinase activity potently reduced PM blebbing. Additionally, the Yes-SH4-domain failed to induce PM blebbing in fibroblasts depleted of the Src kinases c-Src, Yes and Fyn (SYF -/-), but succeeded in c-Src reconstituted cells (SYF + c-Src) again in a manner that required Src activity. These experiments clearly suggest that presence as well as activity of Src kinases is necessary for PM blebbing, which is highly interesting since they itself are attached to the PM by SH4-domains (Resh, 1999). In line with this, endogenous c-Src was found at the PM and at the membrane of SH4-domain induced PM blebs. Thereby, its general distribution did not change upon expression of SH4-domains. In contrast to this, tyrosine phosphorylated and active c-Src accumulated in the bleb lumen similar to phosphorylated MLC. Since a change in bulk levels of active c-Src upon expression of SH4-domains was not detected, a local activation or most likely a specific recruitment of active c-Src can be suggested. This implies a novel biological function for SH4-domains that has not been described yet.

In addition to ROCK and Src kinases, the Drf FHOD1 was found to play a role in PM blebbing as well: Co-expression of FHOD1 and ROCK1, but not of FHOD1 alone resulted in an apoptosis independent increase of ROCK1 mediated PM blebbing. Drfs are F-actin organizing proteins which have the ability to nucleate F-actin polymerization. Consistently, FHOD1/ROCK1 blebs were filled with F-actin, whereas co-expression of ROCK1 with FHOD1 variants lacking their capacity for G-actin recruitment or F-actin nucleation (ΔFH1, ΔFH2; (Gasteier *et al.*, 2003) failed to increase PM blebbing. Interestingly, most of the parameters characterizing FHOD1/ROCK1 blebs are highly similar to SH4-domain induced blebs concerning bleb number and size, dependency on F-actin integrity, myosin II contractility, Rho and ROCK activity as well as localization of ROCK activity at the site of PM blebbing. Furthermore, the contribution

of FHOD1 to the formation of FHOD1/ROCK induced PM blebs was sensitive to inhibition of Src kinase activity, which was also enriched in the bleb lumen.

In line with this, knockdown experiments of FHOD1 showed that SH4-domain induced PM blebbing was not simply depended on Src kinase or ROCK activity, but also involved the presence of FHOD1. Moderate reduction of endogenous FHOD1 levels decreased the amount of PM blebbing cells indicating a functional role for the Drf. Interestingly, this effect was not enhanced by a more efficient knockdown of FHOD1 suggesting that the Drf is not absolutely essential for PM blebbing. Thus, it might act in combination with other factors that do not require FHOD1. For example other Drfs such as mDia1, mDia2 or FHOD2 might compensate FHOD1 reduction simply by their presence or by an upregulation of their expression. This has not been tested yet, but would explain the slight increase in PM blebbing of ROCK1 expressing FHOD1 knockdown HeLa cells. Furthermore, FHOD1 might be of minor importance in endothelial cells such as CHO or HeLa cells. Although FHOD1 is ubiquitously expressed to some levels in human tissues, it had been predominantly detected in spleen cells, suggesting a tissue specific physiological role for the formin (Westendorf *et al.*, 1999). In fact, two recent studies in mDia1 knockout mice have clearly demonstrated that various physiological processes are affected in T-cells only, but not in closely related B lymphocytes which are additionally enriched in mDia2 that presumably adopts functions of mDia1 (Eisenmann *et al.*, 2007, Sakata *et al.*, 2007). This also means that the key player for maintenance of the cortical actin in HeLa cells and possibly in CHO cells might be another Drf. Indeed, mDia1 is required for PM blebbing related invasion of MDA-MB-435 breast cancer cells (Kitzing *et al.*, 2007). Furthermore, a role for mDia2 in PM blebbing had been suggested as well, even though knockdown of the Drf had not been sufficient to induce PM blebbing *per se* (Eisenmann *et al.*, 2007). Consistently, potent reduction of endogenous FHOD1 which localized in the cortical actin of PM ruffles neither induced PM blebbing nor had a negative effect on PM blebbing of ROCK1 or Rac-L61A37 expressing or apoptotic HeLa cells, respectively. This might indicate that specific Drfs are employed trigger dependently to mediate PM blebbing and are redundant in other blebbing situations. Thus, FHOD1 may represent one of several factors that synergistically mediate PM blebbing possibly cell type and trigger dependent.

In summary, the three cellular determinants ROCK1, FHOD1 and c-Src were identified as potential regulatory proteins being involved in PM blebbing which is related to their presence at the blebbing site. While c-Src and ROCK1 are most likely recruited in their active forms, FHOD1 that to not induce PM blebbing when it is solely expressed may be activated during this process as discussed in the following chapter.

9.1.3 Synergistic Interplay Between ROCK1, FHOD1 and c-Src in PM Blebbing

Although the Drf FHOD1 had been shown to interact with the Rho-GTPase Rac1 but not with RhoA (Westendorf, 2001), expression of a constitutively active variant lacking its C-terminal DAD results in formation of F-actin stress fibers and cables which are decorated with the Drf (Gasteier *et al.*, 2003). This phenotype is dependent on the Rho-ROCK pathway but does not require Rac1 activity, suggesting a functional interaction between FHOD1 and ROCK. Indeed, Yeast two hybrid and Co-IP experiments revealed a physiological interaction of FHOD1 and ROCK1, but not ROCK2. The interacting regions could be roughly mapped to amino acid residues 368-727 in ROCK1 and 612-806 in FHOD1. In ROCK proteins this region is thought to be required for protein-protein interactions since it is part of a general coiled-coil structure (Nakagawa *et al.*, 1996). The coiled-coil regions of ROCK proteins share 55 % identity in their amino acid sequences and are proposed to interact with α-helical structures of further proteins (Liao *et al.*, 2007, Riento and Ridley, 2003). Such a 3-helix-bundle has been found at the C-terminal end of the FHOD1 region that binds to ROCK1 (Madrid *et al.*, 2005). The 3-helix-bundle is integrated into a predicted knob domain which provides structure and formation of the FH2-hemidimer in combination with the lasso region of a second FH2-monomer (Xu *et al.*, 2004). This predicted FHOD1 lasso-linker region is also part of the ROCK1 binding region. Since lasso-linker and knob without its 3-helix-bundle are mainly constructed of non-helical regions, only the 3-helix-bundle provides the required structure for an interaction. This interaction might be involved in a ROCK1 mediated activation of the autoinhibited FHOD1, a process that is not fully understood, yet. Drfs are thought to be regulated by the activity of Rho GTPases and additional factors (Faix and Grosse, 2006). Thus, ROCK1 may represent one of these factors for regulation of FHOD1. Therefore, the 3-helix-bundle in non-activated FHOD1 has to be accessible to ROCK1, which is very likely since an interaction was detected with full-length FHOD1 as well.

This interaction, however, might be dependent on the presence of further cellular proteins as well. *In vitro* experiments demonstrated that FHOD1 co-precipitated with ROCK1 in the presence of active Src only, but not in PP2 treated cells (R. Madrid, personal communication). Consistently, SRE-activity mediated by constitutively active FHOD1-ΔC requires Src kinase activity (Koka *et al.*, 2005). This is in line with the findings obtained in this work revealing that Src kinases are involved in FHOD1/ROCK1 mediated PM blebbing. Thus, a functional and physical interaction of these proteins might be suggested, although a direct c-Src binding to FHOD1 or ROCK1 was not investigated so far and will be addressed in future experiments.

Nevertheless, other Drfs like mDia1 and mDia2 directly interact with the c-Src SH3-domain presumably *via* proline rich regions of their FH1-domain suggesting this possibility for FHOD1 as well (Tominaga *et al.*, 2000, Yamana *et al.*, 2006).

Together, a hypothetical ternary regulatory complex of ROCK1, FHOD1 and c-Src is a likely option and might be constantly or transiently formed during induction and maintenance of PM blebbing. Whether for its assembly FHOD1 binds to c-Src first, followed by a subsequent recruitment of ROCK1 or a complex formation of FHOD1 and ROCK1 is required as the initially step, is not clear. Since over-expressed FHOD1 alone did not induce PM blebbing and predominately showed a cytoplasmic location, the latter possibility is more likely. In fact, activation of ROCK1 by additional factors seems to be a prerequisite for PM blebbing. During apoptosis, ROCK1 is C-terminally cleaved by caspase-3 and therefore constitutively activated (Coleman *et al.*, 2001, Sebbagh *et al.*, 2001). Furthermore, ROCK1/FHOD1 as well as SH4-domain induced PM blebbing were dependent on Rho activity which directly activates ROCK1. This had been shown for other PM blebbing cells as well (Charras *et al.*, 2006, Gadea *et al.*, 2007, Riento and Ridley, 2003, Sahai and Marshall, 2003). Interestingly, in p53 deficient MEF cells (p53 -/- MEF) Rho is activated and recruited to the PM of blebbing cells (Gadea *et al.*, 2007). Since Rho also localizes at the PM of SH4-domain induced blebbing cells a direct contribution to the complex formation is possible. Thus, active ROCK1 may be the seed which subsequently bind to FHOD1 mediated by additional factors like c-Src. One of these factors might be the Rho-GTPase Rac1 as well, which could be found at the membrane of SH4-domain blebbing cells. FHOD1 co-localizes with co-expressed constitutively active Rac1-L61 at the cortical actin (Gasteier *et al.*, 2003) and interacts with Rac1-GTP as well as with its diphosphate variant *in vitro* (Westendorf, 2001). This suggests a contribution of the physical presence of Rac1 independent of its activity state to FHOD1 regulation. In fact, this would explain why dominant negative Rac1-N17 had no effect on PM blebbing. Interestingly, ROCK1/FHOD1 PM blebbing was supported by parts of the upstream region adjacent to the FH1-domain (FHOD1-Δ4). This region participates in FHOD1s interaction with Rac1 (Gasteier *et al.*, 2003, Westendorf, 2001). In contrast to Rac1, proteins like DIP/WISH can bridge the interaction of Drfs and Src kinases. They interact directly and functionally with c-Src (Meng *et al.*, 2004) as well as with Drfs such as mDia1, mDia2 and most importantly with FHOD1 (Eisenmann *et al.*, 2007, Satoh and Tominaga, 2001, Westendorf and Koka, 2004). Thereby, the N-terminal SH3-domain of DIP/WISH binds to the FH1-domain and N-terminal region of FHOD1. Interestingly, DIP/WISH proteins also regulate ROCK activity in a Src dependent manner by phosphorylation of p190RhoGAP facilitating hydrolysis of Rho-GTP to Rho-GDP, and further

Rho regulating proteins such as MEK and RhoGDI (DerMardirossian *et al.*, 2006, Meng *et al.*, 2004, Pawlak and Helfman, 2002).

Together, a combinatory binding of active ROCK1 together with Rac1, c-Src and DIP/WISH might synergistically regulate the activity of FHOD1 presumably by conformational changes and thereby interferes with its intramolecular autoinhibition. Since c-Src and ROCK1 are kinases, phosphorylation of FHOD1 might contribute to this regulation. Indeed, FHOD1 had been shown to be a target of GMP-dependent protein kinase 1 (PGK1), a serine/threonine kinase that phosphorylates the C-terminal DAD at amino acid residue Ser1131 in vascular smooth muscle cells (Wang *et al.*, 2004). Phosphorylation of the DAD might impair its binding to the N-terminal end to release FHOD1 autoinhibition. So far, such a mechanism has not been described for other formins, even though it had been postulated (Wallar and Alberts, 2003). According to the consensus sequences for ROCK phosphorylation (R/K-X-S/T or R/K-X-X-S/T), a prediction of FHOD1 phosphorylation sites resulted in about 15 serine and 11 threonine residues which are distributed across the whole protein (NetPhos 2.0: http://www.cbs.dtu.dk/services/NetPhos (Blom *et al.*, 1999). Interestingly, Ser1131, Ser1137 and Thr1141 are located in the basic cluster of the DAD, whereas Ser138, Ser357, Ser358, Ser364 and Ser367 lay within the predicted DAD-interacting FH3-domain (Schonichen *et al.*, 2006) that basically consists of a cluster of armadillo repeats (A. Schulte, submitted). Consistently, a phosphorylation at these sites might release FHOD1s autoinhibition or contribute to a stabilization of the open conformation. In fact, Ser367 had been found to be phosphorylated in HeLa cells (Beausoleil *et al.*, 2004). In addition to the amino acid residues located in the armadillo repeat, Thr42 represents a potential target for ROCK1 phosphorylation and Tyr99 is predicted to be phosphorylated by c-Src (NetPhos 2.0: http://www.cbs.dtu.dk/services/NetPhosK (Blom *et al.*, 2004). These amino acid residues are located in a novel GTPase-domain that has been identified at the very N-terminus of FHOD1 (amino acid residues 1-135) and is placed upstream of the armadillo repeat within the FH3-domain (A. Schulte, submitted). This GTPase-domain is unique to Drfs, although a similar N-terminal domain lacking the very first 70 amino acid residues has been described for mDia1 as well (Nezami *et al.*, 2006, Rose *et al.*, 2005). The FHOD1 N-terminal domain displays an ubiquitin-superfold which is thought to bind to the Ras family of GTPases. Functional studies with various GTPases which are supposed to interact with this domain are currently under investigation and may reveal a new regulatory pathway for FHOD1, which might be regulated by ROCK1 or c-Src mediated phosphorylation.

Interestingly, PM blebbing induced by SH4-domains or FHOD1/ROCK1 is inhibited upon co-expression of the HIV-1 Nef protein (B. Stolp, unpublished data). In infected cells this viral

pathogenicity factor shows a variety of functions that are related to downmodulation of cell-surface receptors such as CD4, MHC-I, CXCR4 and CCR5 (Garcia and Miller, 1991, Michel *et al.*, 2005, Schwartz *et al.*, 1996, Venzke *et al.*, 2006) as well as to F-actin organization (Fackler *et al.*, 1999). In fact, the HIV-1 Nef protein had been shown to interact *in vitro* with the DAD of FHOD1 in Yeast two hybrid (S. Benichou, Institut Cochin, Paris, unpublished data) and GST-pulldown experiments (J. Gasteier, unpublished data). Additionally to inhibition of PM blebbing, a significant amount of co-expressed SH4-domains and HIV-1 Nef highly co-localized in a not yet identified perinuclear region. Similar results had been described in T-cells in which HIV-1 Nef caused the relocalization of the Src kinase Lck from the immunological synapse to an intracellular compound, thereby altering signaling events at the site of cell-cell contact and inhibiting cytoskeletal rearrangements (Haller *et al.*, 2006, Thoulouze *et al.*, 2006 and C. Haller, unpublished data). Of note, the inhibitory effect on PM blebbing was not detected by co-expression of SH4-domains in combination with HIV-1 Nef mutants lacking either their PM targeting signal (Nef-G2A, non-myristoylated) or their P-X-X-P motif (Nef-AxxA) which is required for binding to SH3-domains such as of Src kinases. Together, HIV-1 Nef has the capacity to interfere with processes that involve the postulated c-Src-FHOD1-ROCK1 complex at the PM and may thus serve as a tool to identify the associated blebbing machinery.

Additionally to its function in complex assembly and regulation, c-Src might be involved in PM targeting of the complex. Src kinases preferentially localize *via* their SH4-domain in lipid-ordered areas of the PM termed lipid-rafts (Resh, 1999). These microdomains are hallmarked by a higher packing of the saturated hydrocarbon chains (Rajendran and Simons, 2005) and are proposed to be very dynamic and float freely within the disordered bilayer. They are thought to represent a site for enhanced cell signaling. According to a current model, lipid-rafts are formed and stabilized by the presence of PM associated peripheric proteins such as glycolphosphatidyl-inositol (GPI)-anchored proteins, cholesterol-binding proteins like caveolin or double acetylated proteins like Src kinases (Hancock, 2006, Simons and Toomre, 2000). This indicates that the expressed SH4-domains preferentially localize at these lipid-ordered areas and might contribute to local clustering and enrichment of lipid-rafts. As a result, Src kinases and therewith the postulated c-Src-FHOD1-ROCK1 complex might then be recruited and concentrated at such sites leading to an increased net activity and thus bleb formation. Consistently, lipid-rafts are enriched in arachidonic acid (Pike *et al.*, 2002), which regulate ROCK activity by direct interaction with its PH-domain and would therefore contribute to PM blebbing (Riento and Ridley, 2003).

In addition to their intrinsic dynamics, PMs are in continuous turnover. For fibroblasts with a surface area of about 3600 μm^2, a PM endocytosis rate of 1-3 $\mu m^2/s$ was measured suggesting a very rapid process (Sheetz *et al.*, 2006). Interestingly, cultivation of SH4-domain expressing cells at 20°C markedly reduced PM blebbing (S. Tournaviti, personal communication) indicating that an active vesicular transport providing the PM with cellular determinants is necessary. In fact, at least the HASPB-SH4-domain binds to vesicles in anterograde or retrograde transport which mostly occurs along microtubule tracks (Musch, 2004, Nickel, 2005). Since the components of the c-Src-FHOD1-ROCK1 complex might be transported to the PM in a similar way possibly following recruitment by SH4-domains, a destruction of microtubules would abolish SH4-domain mediated PM blebbing which was indeed demonstrated in this study. However, PM blebbing induced by co-expression of FHOD1 and ROCK1 was independent of microtubule integrity. This may be due to their abundant presence in the cytoplasm that does not require an active PM directed transport. Nevertheless, this model provides a simple mechanism of how SH4-domains recruit cellular components to the PM.

Finally, the enrichment of SH4-domains at the PM might have further effects on its molecular composition which may contribute to induction of PM blebbing. In *in vitro* experiments it had been shown that alterations in the lipid composition directly influence the curvature of a monolayer membrane (Bacia *et al.*, 2005). In SH4-domain expressing cells, this alteration may either be caused by the high proportion of integrated myristoyl and palmitoyl hydrocarbon chains itself or due to a selective recruitment of certain lipid species, but would have to be restricted to only one leaflet of the PM bilayer (Zimmerberg and Kozlov, 2006). However, SH4-domains were not enriched in PM blebs. An asymmetric distribution of the SH4-domains is also unlikely, since the SH4-domain of HASPB is present at both sides of the PM bilayer (Denny *et al.*, 2000). Nevertheless, further experiments addressing the lipid and the protein composition of the bleb membrane are required to determine the direct contribution of the PM consistence in PM blebbing and to visualize a possible clustering of the lipid-ordered areas.

Although there is no final prove for the formation of a ternary complex, the assimilation of the three central factors c-Src, FHOD1 and ROCK1 to form a functional PM blebbing machinery which is regulated by additional triggers appears likely based on obtained results.

9.1.4 A Hypothetical Model for SH4-Domain Induced PM Blebbing

Assuming formation of a ternary regulatory complex of ROCK1, FHOD1 and c-Src, the following hypothetical model on SH4-domain induced PM blebbing is proposed. Consistent with the poroelastic model of PM blebbing, the elements of this complex may orchestrate various

steps of this dynamic process. At the onset of bleb formation, the complex is formed and recruited by SH4-domains to the PM (fig. 58A). There, ROCK1 contributes in combination with c-Src to the regulation of FHOD1 (fig. 58B). Active FHOD1 catalyzes *de novo* polymerization of F-actin filaments thereby disturbing the organization of the cortical F-actin meshwork resulting in pore formation. This would be a simple explanation for FHOD1s effect in PM blebbing upon co-expression with ROCK1, since a further activation of ROCK1 by FHOD1 was not detected in IVKAs or Western blot analysis.

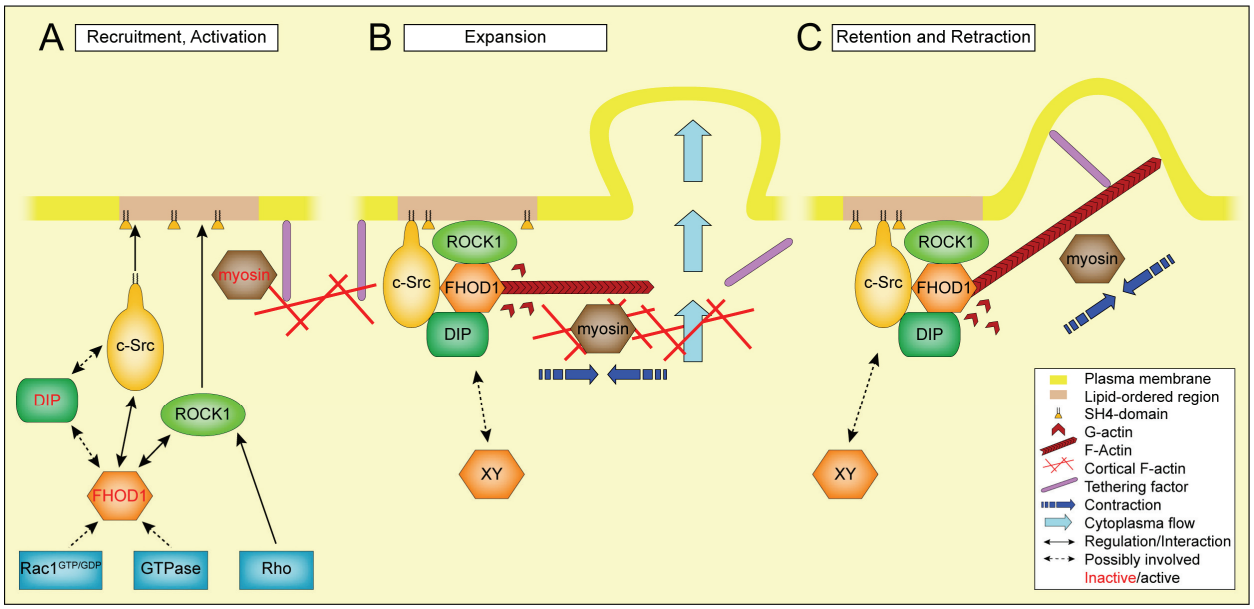

Figure 58: Hypothetical model of the machinery orchestrating dynamic SH4-domain induced PM blebbing.

(A) Recruitment and activation phase: Driven by SH4-domains as a specific trigger, a ternary complex consisting of the Drf FHOD1, the Ser/Thr kinase ROCK1 and the Tyr kinase c-Src is formed in the presence of active Rho and is in parallel recruited to lipid ordered regions at the PM. Adaptor proteins such as DIP/WISH may contribute to this complex since they bind to both Src kinases and FHOD1 and may be required for an intrinsic regulation of the complex. Furthermore, the Rho GTPase Rac1 interacts irrespectively of its activation state with FHOD1 and may help to release its intramolecular binding. Further, yet unidentified GTPases might be involved in this process as well. **(B)** Expansion phase: Activity of the ternary c-Src-FHOD1-ROCK1 complex at the PM results in F-actin polymerization and myosin II dependent contraction. Upon this activity and in line with the model of poroelastic bleb formation, the integrity of the cortical F-actin meshwork is disrupted and local hydrostatic pressure is affected to the cytoplasm resulting in its flow towards the PM. Combined with a c-Src-FHOD1-ROCK1 complex mediated regulation of tethering factors like ERM-proteins a PM bleb is formed. **(C)** Retention and retraction phase: Activity of the ternary c-Src-FHOD1-ROCK1 complex also facilitates generation of a new cortical F-actin meshwork which is linked to the bleb membrane by recruited tethering proteins and thereby stabilizes the newly formed bleb. Subsequently, ROCK1 activity mediates myosin II dependent contraction of the new filaments which results in bleb retraction. Additional, so far unidentified factors (XY) may be required for further regulation of the complex activity.

However, pore formation might include additional factors as well. At least for the Src kinase Lck a phosphorylation mediated regulation of FLNa has been shown and FLNa deficiency triggers PM blebbing in M2 cells (Cunningham, 1995, Goldmann, 2002, Pal Sharma and Goldmann, 2004). Since only serine phosphorylation was tested in this study, effects of SH4-domain expression on tyrosine phosphorylation by Src kinases cannot be excluded. Thus, this regulated

process would generate a situation very similar to that in M2 cells. Mediated by ROCK1 activity, contraction of the actin cortex by phosphorylation of myosin II is initiated and forces a cytoplasmic flow toward the PM where a bleb is formed. This process might be supported by a local variation of PM tethering to the cortical actin again by the activity of c-Src and ROCK1. Indeed, it has been shown, that both kinases phosphorylate members of the family of ERM proteins (Bretscher *et al.*, 2002, Elliott *et al.*, 2004, Riento and Ridley, 2003, Srivastava *et al.*, 2005). However, since phosphorylation of ERM proteins was linked to their activation only, a contribution in bleb stabilization during retention phase is more likely (fig. 58C). In fact, ezrin had been shown to play a role in regeneration of the cortical actin meshwork during retention and retraction phase of blebs generated in M2 cells (Charras *et al.*, 2006). There it facilitates the connection of newly formed F-actin fibers to the bleb membrane. Thus, actin polymerization activity is required in these phases of PM blebbing (Charras *et al.*, 2006, Paluch *et al.*, 2005) and could be catalyzed by FHOD1. In this way, a new scaffold is organized which is subsequently retracted by ROCK1 mediated contractility through phosphorylation of MLC.

In summary, the postulated ternary complex of c-Src, ROCK1 and FHOD1 may constitute a basic component of a prevalent blebbing machinery. However, depending on the trigger and the cellular environment, its elements might be replaceable with ROCK2, other Drfs or Src kinases. Nevertheless, the described hypothetical model of PM blebbing can be used as a working hypothesis for future studies. Whether this machinery represents a general mechanism for PM blebbing will have to be addressed in future experiments.

9.2 Functional Relevance

9.2.1 Functions of SH4-Domain Induced PM Blebbing

Physiological PM blebbing occurring on animal cells is usually linked to certain situations in which specific signals presumably trigger a common machinery. Tumor cells show no PM blebbing when cultured on planar surfaces, but activate blebbing motility in 3D environments consisting of ECM determinants (Sahai and Marshall, 2003, Wolf *et al.*, 2003). During this amoeboid or rounded mode of motility, blebs are formed in the direction of movement and are thought to provide the basic structure that enables the cell to squeeze through the matrix pores (Sahai, 2005, Yamazaki *et al.*, 2005). Interestingly, upon expression of SH4-domains but not of GFP alone, CHO cells were able to invade into such 3D environments in which they showed PM blebbing as well. In fact, the invasiveness closely matched that of MDA-MB-435 human breast carcinoma cells that were used as a control. Furthermore, this motility seems to be related to the

capability of SH4-domains to induce PM blebbing, since expression of the myristoylation mutant of the HASPB-SH4-domain did not mediate invasiveness. This implies that SH4-domain induced PM blebbing in 2D represents the constitutive activation of a cellular pathway which is required for 3D motility of tumor cells. Interestingly, the palmitoylation deficient mutant of the HASPB-SH4-domain, that failed to induce PM blebbing in 2D, still slightly enhanced invasiveness of CHO cells. Thus, SH4-domains may have additional effects on cell signaling events that are independent of PM blebbing but influence 3D motility. Since the N18-Δpal-HASPB-GFP is enriched at intracellular membranes that are most likely Golgi associated vesicles (Denny *et al.*, 2000, Stegmayer *et al.*, 2005), SH4-domains may contribute to events that are required for directed cell motility such as cell polarization (Nabi, 1999, Nobes and Hall, 1999). To obtain a further insight into this phenomenon, additional SH4-domains will have to be investigated for induction of invasiveness by an approach allowing analysis of single cell behavior during migration. Of note, Src kinase activity which is required for the formation of SH4-domain induced blebs contributes to the mesenchymal or elongated mode of motility that depends on the formation of invadopodia or podosomes which are distinct from PM blebs (Linder and Aepfelbacher, 2003). This type of 3D invasion is based on secretion of metalloproteases that disrupt the ECM in order to form a passage for the cell (Sahai, 2005, Yamaguchi and Condeelis, 2007). Whether SH4-domain mediated invasiveness depends on Src activity has to be analyzed in future experiments as well. However, first experiments demonstrated that SH4-domain mediated 3D motility was dependent on ROCK activity which is not required for the mesenchymal but necessary for the amoeboid mode (Sahai and Marshall, 2003, Wyckoff *et al.*, 2006).

Motility in 3D environments is usually investigated in combination with a gradient of FCS to provide a directional movement (Hooper *et al.*, 2006), which was applied in this study as well. This implicates that chemotactic factors bind to specific receptors at cellular surfaces or have to be internalized into the cell in order to induce an internal signaling asymmetry that leads to cytoskeletal rearrangements and polarization of the cell (Yamazaki *et al.*, 2005). Since PM blebbing had been observed during the entry process of *Vaccinia* viruses (A. Helenius and J. Mercer: 58. Mosbacher Kolloquium 2007) a possible role of SH4-domain induced PM blebbing in internalization of extracellular fluid was investigated. Indeed, SH4-domain expressing cells showed an increased ability for non-specific fluid-phase uptake of dextran from the extracellular space. This additional internalization was insensitive to EIPA, an inhibitory drug mainly interfering with macropinocytosis but also with other endocytotic pathways (Norbury, 2006). Although a contribution of clathrin mediated uptake of dextran was considered

as well, SH4-domain expression did not influence the internalization of transferrin. Further experiments with specific inhibitory drugs are required to address this issue. Additionally, other endocytotic mechanisms principally facilitate fluid-phase uptake, especially over a long time range. Interestingly both caveolae and lipid-raft mediated endocytosis depend on lipid-ordered areas where SH4-domains are predominantly localized (Johannes and Lamaze, 2002, Resh, 1999). Assuming an influence of abundant SH4-domains on the characteristics of such microdomains as discussed above, these internalization pathways are indeed possible candidates to facilitate SH4-domain mediated fluid-phase uptake. These possibilities will have to be addressed in future experiments. Nevertheless, this uptake does not seem to be solely dependent on PM blebbing induction since the myristoylation and palmitoylation defective mutants of the HASPB-SH4-domain were able to induce this uptake as well, though with reduced efficiency. This again indicates possible additional effects of SH4-domains in cellular signaling as it was suggested for 3D motility. Thus it is not clear whether mediation of fluid-phase uptake of chemotactic factors can account for increased motility in 3D. However, in a 2D wounding assay where cellular motility is triggered by chemotactic orientation in combination with a unilateral loss of cell-cell contact-inhibition (Nobes and Hall, 1999), expression of SH4-domains had no detectable influence on cell migration.

In summary, it was shown that SH4-domains are the triggers for induction of 2D PM blebbing, 3D invasion and fluid-phase uptake. Although 2D PM blebbing is highly dependent on their PM localization, additional signaling events may be involved in 3D invasion and fluid-phase uptake, mediated by the presence of SH4-domains *e.g.* on internal membranes. Whether these signaling events are interconnected and require the activity of the postulated c-Src-FHOD1-ROCK1 ternary complex will have to be addressed in future experiments. Nevertheless, all these results claim novel functions for SH4-domains that had not been described before and exceed their function as simple membrane anchors.

9.2.2 The Role of FHOD1 in Intracellular Organization

Another aim of this study was the investigation of endogenous FHOD1. In over-expression experiments, FHOD1 exclusively shows a diffuse cytoplasmic distribution. To investigate cellular functions and localization of the endogenous protein, a polyclonal rabbit antibody directed against two peptides in the N-terminus of the protein has been generated (Gasteier *et al.*, 2005). Interestingly, in immuno-fluorescence experiments, a specific signal in perinuclear regions was obtained with this antibody. This could be confirmed by immuno-electron microscopy, in which it was shown that the protein mainly localized at the lateral sites but not in

the lumen of Golgi vesicles as well as in close proximity to PM ruffles. The specificity of the antibody was verified in both methods *via* blocking experiments with the target peptides. However, examination of immuno-fluorescence experiments was possible in rodent cell lines only, whereas electron-microscopy yielded specific signals in human HeLa cells. Detection of FHOD1 by Western blotting was possible with lysates from cells of both phylae. The reasons for this discrepancy are unclear but might be due to a different accessibility of the protein. For Western blotting, the proteins are initially denaturated during SDS-PAGE for a homologous separation. They are thought to be partially refolded after transfer to the nitrocellulose membrane due to a change of buffer conditions. Thereby, initially hidden epitopes might be exposed under these circumstances. This is supported by destruction of intracellular protein complexes and removal of posttranslational modifications, which might be specific for diverse cell types and phylae. However, the signals confirm a role for FHOD1 at the PM in which it is involved in PM blebbing as shown in this study. Furthermore, these findings were in line with FRET experiments with co-expressed FHOD1 and constitutively active Rac1-L61 (A. Alberts, unpublished data). In these experiments a specific FRET signal distribution was found that indicated a localization of FHOD1 in similar perinuclear regions as well as in membrane ruffle like structures. Of note, a comparable distribution of over-expressed FHOD1 in lamellipodia upon co-expression with constitutively active Rac1-L61 had been shown as well (Gasteier *et al.*, 2003). Furthermore, FHOD1 has been demonstrated to co-localize with the multifunctional cell surface protein CD21 at the PM following binding to EBV (Gill *et al.*, 2004). In fact, in the same study the authors have also described that over-expressed FHOD1 fused to GFP can be found in a perinuclear region of some cells *per se*, which is in contrast to other studies (Gasteier *et al.*, 2003, Koka *et al.*, 2003, Takeya and Sumimoto, 2003) and the results obtained in this work. Finally and most interestingly, FHOD1 had been shown to be phosphorylated by PGK1 at the DAD and to co-localize with the kinase at perinuclear regions of vascular smooth muscle cells (Wang *et al.*, 2004). However, this localization was not observed by co-expression of FHOD1 in combination with ROCK1 or with the constitutively active ROCK1-Δ3, even though endogenous ROCK1 has been shown to localize at Golgi stacks (Percival *et al.*, 2004, Riento *et al.*, 2003). Unfortunately, staining of endogenous ROCK1 in order to investigate the co-localization with FHOD1 at the Golgi failed with the employed antibodies.

Interestingly, the microfilament system is required to determine Golgi shape and regulate vesicle transport (DePina and Langford, 1999). Thus, a role for FHOD1 in combination with its binding partner ROCK1 in Golgi specific F-actin organization could be envisioned. For identification of relevant Golgi compartments, immuno-fluorescence studies with marker proteins were

performed: Endogenous FHOD1 localized distinct to endosome marker proteins (EEA1, LAMP1, TfR), but in close proximity to the *cis*- and *trans*-Golgi proteins TGN-46 or coatomer and most pronounced in between p115/TAP positive vesicles. This protein is involved in fusion of ER-derived COP-II vesicles and their binding to Golgi membranes (Allan *et al.*, 2000). However, neither over-expression nor knockdown of FHOD1 altered the appearance of these vesicles. Of note, the FHOD1 specific perinuclear stain was not altered as expected from reduced protein amounts detectable in a Western blot analysis. The reason for this observation is unclear, but Golgi associated FHOD1 might comprise of subpopulations with evaluated half life as compared to cytosolic protein pools. Increased incubation times in knockdown experiments might then be necessary to remove these proteins as well. Indeed, in HeLa cells in which the knockdown efficiency had been improved, the specific signal was clearly diminished in immuno-electron microscopy, however, without any apparent effect on Golgi organization. Nevertheless, this might be due to sufficient residual amounts of FHOD1 or substitutive effects of other Drfs as already discussed in the previous chapters. Even so, after BFA mediated disruption of the Golgi, distinct amounts of FHOD1 were still associated with the coatomer protein at distal regions of the cell. Both proteins were similarly redistributed to a stack like structure upon wash out of the inhibitory drug. By microscopical observation the impression was obtained that FHOD1 assembled faster to the perinuclear region, but this has yet to be quantified. However, knockdown of FHOD1 had no effect on reorganization of the Golgi (data not shown). Similarly, a cargo transport assay with VSV-G protein did not show any defect in Golgi dependent secretion.

Since FHOD1 was not involved in the functionality of the Golgi, further Golgi related functions were analyzed by an FHOD1 specific knockdown: During mitosis, the Golgi disperses in the cytoplasm and reorganizes following completed cytokinesis (Colanzi and Corda, 2007). However, FHOD1 had no detectable influence on the proliferation rate. Furthermore, in various cells, a polarization of the Golgi and the MTOC towards the direction of movement is required for cell migration (Nabi, 1999). Reduction of FHOD1 neither affected these active processes (data not shown) nor impaired cell migration in wound healing assays or chemotaxis along a gradient of FCS, which stays in conflict with published data obtained with over-expressed FHOD1 (Koka *et al.*, 2003). Next, knockdown of FHOD1 did not affect cell adhesion to various surfaces, nor had a detectable influence on F-actin content or cell size. Consistently, reduction of FHOD1 levels had no detectable effects on Rho, Rac1 or Cdc42 mediated microfilament reorganization or SRE activation.

In summary, endogenous FHOD1 localized at Golgi structures which was in line with several studies. The role of the protein at this cellular compartment remains elusive although a contribution to Golgi organization cannot be ruled out by the knockdown experiments. Since all these experiments have been performed in HeLa cells or fibroblasts, future experiments should include cells of spleen origin. Therefore, a more advanced screen than the published one (Westendorf *et al.*, 1999) should be performed that distinguishes between different cell types as it has been evaluated in other studies for mDia proteins (Eisenmann *et al.*, 2007, Sakata *et al.*, 2007). Since FHOD1 is involved in SH4-domain mediated PM-blebbing and SH4-domains such as that of HASPB are palmitoylated in association to the Golgi apparatus, FHOD1 might have the capacity to affect transport and posttranslational modifications of these proteins. Whether this link can be deduced will have to be addressed in future studies.

10 OUTLOOK

In this study, SH4-domains have been identified as a new trigger for cell invasion, fluid-phase uptake and PM blebbing. Following detailed analysis of intrinsic signaling pathways required for PM blebbing, a novel mechanism is proposed which includes Src kinases as novel key players, ROCK proteins and the Drf FHOD1 as actin remodeling and regulatory components. Furthermore, this study adds new knowledge to the activation of FHOD1 and provides a first view on cellular localization and function of the endogenous FHOD1 protein. However, various additional experiments will be necessary to answer open questions and to complete the hypothetical model of a synergistic interplay between Src kinases, ROCK proteins and FHOD1:

1. *What are the physiological roles and specificities of SH4-domain induced PM blebbing, cell invasion and fluid-phase uptake and is there evidence for the influence of lipid-ordered microdomains on these functions?* The most important issue will be the identification of a PM targeted SH4-domain, that fails to induce PM blebbing. To investigate the physiological relevance, Src kinases that are linked to this artificial SH4-domain have to be constructed followed by a detailed study evaluating a variety of endogenous functions *e.g.* by transient expression in SYF -/- cells. Additionally, a detailed analysis of the lipid and protein composition of bleb membranes is required as well as an artificial change of this composition and its influence on the described phenotypes.

2. *Is there a biochemical and functional proof for the here postulated ternary complex of c-Src, FHOD1 and ROCK1 and does it have a physiological relevance?* Detailed interaction studies and systematic modifications of the interaction partners should be addressed in the background of PM blebbing, cell invasion and fluid-phase uptake. First approaches include the investigation of the influence of inhibitory drugs that target Src kinase and ROCK activity.

3. *Is FHOD1 the only Drf that is involved in SH4-mediated PM blebbing, fluid-phase uptake and cell invasion and other forms of PM blebbing or are further Drfs involved as well?* Therefore, a detailed analysis of the protein and expression levels of FHOD1 knockdown cells as well as knockdown of further Drfs like Dia1, Dia2, Dia3, FHOD2,

FRL and others, singularly or in combination with each other is necessary. In line with this, the knockdown efficiency of FHOD1 will have to be further improved, *e.g.* by further methods based on shRNA. The final goal must be a rescue of obtained phenotypes with expression of RNAi insensitive constructs.

4. *What is the exact mechanism for regulation of the Drf FHOD1?* To answer this question, functional interaction partners with the N-terminal GTPase domain are under current investigation. Furthermore, the role of ROCK1 will have to be examined, particularly by a more detailed mapping of the regions necessary for interaction. In line with this, the role of Src kinases for this interaction and other proteins like DIP/WISH must be addressed as well.

5. *What is the functional relevance of FHOD1 localization at Golgi structures and is there a link to other functions like PM blebbing?* Localization studies of endogenous FHOD1 in SH4-domain expressing cells and cells that are treated with inhibitory drugs against Src kinases or ROCK will be necessary to address this question. Since Drfs are postulated to function in specific tissues, a detailed analysis of FHOD1 expression patterns in several cells especially in those derived from spleen is required to narrow down FHOD1s functions.

11 REFERENCES

Aaronson, S. A. and Todaro, G. J. 1968. Development of 3T3-like lines from Balb-c mouse embryo cultures: transformation susceptibility to SV40. J Cell Physiol **72:**141-8.

Adamson, P., Marshall, C. J., Hall, A. and Tilbrook, P. A. 1992. Post-translational modifications of p21rho proteins. J Biol Chem **267:**20033-8.

Alberts, A. S. 2001. Identification of a carboxyl-terminal diaphanous-related formin homology protein autoregulatory domain. J Biol Chem **276:**2824-30.

Alberts, A. S., Bouquin, N., Johnston, L. H. and Treisman, R. 1998. Analysis of RhoA-binding proteins reveals an interaction domain conserved in heterotrimeric G protein beta subunits and the yeast response regulator protein Skn7. J Biol Chem **273:**8616-22.

Allan, B. B., Moyer, B. D. and Balch, W. E. 2000. Rab1 recruitment of p115 into a cis-SNARE complex: programming budding COPII vesicles for fusion. Science **289:**444-8.

Allen, W. E., Jones, G. E., Pollard, J. W. and Ridley, A. J. 1997. Rho, Rac and Cdc42 regulate actin organization and cell adhesion in macrophages. J Cell Sci **110 (Pt 6):**707-20.

Allingham, J. S., Smith, R. and Rayment, I. 2005. The structural basis of blebbistatin inhibition and specificity for myosin II. Nat Struct Mol Biol **12:**378-9.

Alvarez, C., Garcia-Mata, R., Hauri, H. P. and Sztul, E. 2001. The p115-interactive proteins GM130 and giantin participate in endoplasmic reticulum-Golgi traffic. J Biol Chem **276:**2693-700.

Amano, T., Tanabe, K., Eto, T., Narumiya, S. and Mizuno, K. 2001. LIM-kinase 2 induces formation of stress fibres, focal adhesions and membrane blebs, dependent on its activation by Rho-associated kinase-catalysed phosphorylation at threonine-505. Biochem J **354:**149-59.

Aspenstrom, P., Fransson, A. and Saras, J. 2004. Rho GTPases have diverse effects on the organization of the actin filament system. Biochem J **377:**327-37.

Aspenstrom, P., Richnau, N. and Johansson, A. S. 2006. The diaphanous-related formin DAAM1 collaborates with the Rho GTPases RhoA and Cdc42, CIP4 and Src in regulating cell morphogenesis and actin dynamics. Exp Cell Res **312:**2180-94.

Bacia, K., Schwille, P. and Kurzchalia, T. 2005. Sterol structure determines the separation of phases and the curvature of the liquid-ordered phase in model membranes. Proc Natl Acad Sci U S A **102:**3272-7.

Barros, L. F., Kanaseki, T., Sabirov, R., Morishima, S., Castro, J., Bittner, C. X., Maeno, E., Ando-Akatsuka, Y. and Okada, Y. 2003. Apoptotic and necrotic blebs in epithelial cells display similar neck diameters but different kinase dependency. Cell Death Differ **10:**687-97.

Baum, B. and Kunda, P. 2005. Actin nucleation: spire - actin nucleator in a class of its own. Curr Biol **15:**R305-8.

Beausoleil, S. A., Jedrychowski, M., Schwartz, D., Elias, J. E., Villen, J., Li, J., Cohn, M. A., Cantley, L. C. and Gygi, S. P. 2004. Large-scale characterization of HeLa cell nuclear phosphoproteins. Proc Natl Acad Sci U S A **101:**12130-5.

Bedford, M. T., Chan, D. C. and Leder, P. 1997. FBP WW domains and the Abl SH3 domain bind to a specific class of proline-rich ligands. Embo J **16:**2376-83.

Bennett, J. P., Zaner, K. S. and Stossel, T. P. 1984. Isolation and some properties of macrophage alpha-actinin: evidence that it is not an actin gelling protein. Biochemistry **23:**5081-6.

Berdeaux, R. L., Diaz, B., Kim, L. and Martin, G. S. 2004. Active Rho is localized to podosomes induced by oncogenic Src and is required for their assembly and function. J Cell Biol **166:**317-23.

Bereiter-Hahn, J., Luck, M., Miebach, T., Stelzer, H. K. and Voth, M. 1990. Spreading of trypsinized cells: cytoskeletal dynamics and energy requirements. J Cell Sci **96 (Pt 1):**171-88.

Bijlmakers, M. J. and Marsh, M. 2003. The on-off story of protein palmitoylation. Trends Cell Biol **13:**32-42.

Bishop, A. C., Kung, C. y., Shah, K., Witucki, L., Shokat, K. M. and Liu, Y. 1999. Generation of Monospecific Nanomolar Tyrosine Kinase Inhibitors via a Chemical Genetic Approach. J. Am. Chem. Soc. **121:**627-631.

Bishop, A. L. and Hall, A. 2000. Rho GTPases and their effector proteins. Biochem J **348 Pt 2:**241-55.

Blake, R. A., Broome, M. A., Liu, X., Wu, J., Gishizky, M., Sun, L. and Courtneidge, S. A. 2000. SU6656, a selective src family kinase inhibitor, used to probe growth factor signaling. Mol Cell Biol **20:**9018-27.

Blanchoin, L., Amann, K. J., Higgs, H. N., Marchand, J. B., Kaiser, D. A. and Pollard, T. D. 2000. Direct observation of dendritic actin filament networks nucleated by Arp2/3 complex and WASP/Scar proteins. Nature **404:**1007-11.

Blom, N., Gammeltoft, S. and Brunak, S. 1999. Sequence and structure-based prediction of eukaryotic protein phosphorylation sites. J Mol Biol **294:**1351-62.

Blom, N., Sicheritz-Ponten, T., Gupta, R., Gammeltoft, S. and Brunak, S. 2004. Prediction of post-translational glycosylation and phosphorylation of proteins from the amino acid sequence. Proteomics **4:**1633-49.

Boehm, M. B., Milius, T. J., Zhou, Y., Westendorf, J. J. and Koka, S. 2005. The mammalian formin FHOD1 interacts with the ERK MAP kinase pathway. Biochem Biophys Res Commun **335:**1090-4.

Boss, J. 1955. Mitosis in cultures of newt tissues. IV. The cell surface in late anaphase and the movements of ribonucleoprotein. Exp Cell Res **8:**181-7.

Brandt, D. T., Marion, S., Griffiths, G., Watanabe, T., Kaibuchi, K. and Grosse, R. 2007. Dia1 and IQGAP1 interact in cell migration and phagocytic cup formation. J Cell Biol **178:**193-200.

Bray, D. and White, J. G. 1988. Cortical flow in animal cells. Science **239:**883-8.

Bretscher, A., Chambers, D., Nguyen, R. and Reczek, D. 2000. ERM-Merlin and EBP50 protein families in plasma membrane organization and function. Annu Rev Cell Dev Biol **16:**113-43.

Bretscher, A., Edwards, K. and Fehon, R. G. 2002. ERM proteins and merlin: integrators at the cell cortex. Nat Rev Mol Cell Biol **3:**586-99.

Brinkley, W. 1997. Microtubules: a brief historical perspective. J Struct Biol **118:**84-6.

Brotschi, E. A., Hartwig, J. H. and Stossel, T. P. 1978. The gelation of actin by actin-binding protein. J Biol Chem **253:**8988-93.

Burridge, K. and Wennerberg, K. 2004. Rho and Rac take center stage. Cell **116:**167-79.

Byers, H. R., Etoh, T., Doherty, J. R., Sober, A. J. and Mihm, M. C., Jr. 1991. Cell migration and actin organization in cultured human primary, recurrent cutaneous and metastatic melanoma. Time-lapse and image analysis. Am J Pathol **139:**423-35.

Cailleau, R., Olive, M. and Cruciger, Q. V. 1978. Long-term human breast carcinoma cell lines of metastatic origin: preliminary characterization. In Vitro **14:**911-5.

Campbell, P. M. and Der, C. J. 2004. Oncogenic Ras and its role in tumor cell invasion and metastasis. Semin Cancer Biol **14:**105-14.

Cardelli, J. 2001. Phagocytosis and macropinocytosis in *Dictyostelium*: phosphoinositide-based processes, biochemically distinct. Traffic **2:**311-20.

Castrillon, D. H. and Wasserman, S. A. 1994. Diaphanous is required for cytokinesis in *Drosophila* and shares domains of similarity with the products of the limb deformity gene. Development **120:**3367-77.

Chang, F., Drubin, D. and Nurse, P. 1997. cdc12p, a protein required for cytokinesis in fission yeast, is a component of the cell division ring and interacts with profilin. J Cell Biol **137:**169-82.

Charras, G. T., Hu, C. K., Coughlin, M. and Mitchison, T. J. 2006. Reassembly of contractile actin cortex in cell blebs. J Cell Biol **175:**477-90.

Charras, G. T., Yarrow, J. C., Horton, M. A., Mahadevan, L. and Mitchison, T. J. 2005. Non-equilibration of hydrostatic pressure in blebbing cells. Nature **435:**365-9.

Chen, X. Q., Tan, I., Ng, C. H., Hall, C., Lim, L. and Leung, T. 2002. Characterization of RhoA-binding kinase ROKalpha implication of the pleckstrin homology domain in ROKalpha function using region-specific antibodies. J Biol Chem **277:**12680-8.

Colanzi, A. and Corda, D. 2007. Mitosis controls the Golgi and the Golgi controls mitosis. Curr Opin Cell Biol **19:**386-93.

Coleman, M. L., Sahai, E. A., Yeo, M., Bosch, M., Dewar, A. and Olson, M. F. 2001. Membrane blebbing during apoptosis results from caspase-mediated activation of ROCK I. Nat Cell Biol **3:**339-45.

Cunningham, C. C. 1995. Actin polymerization and intracellular solvent flow in cell surface blebbing. J Cell Biol **129:**1589-99.

Cunningham, C. C., Gorlin, J. B., Kwiatkowski, D. J., Hartwig, J. H., Janmey, P. A., Byers, H. R. and Stossel, T. P. 1992. Actin-binding protein requirement for cortical stability and efficient locomotion. Science **255:**325-7.

Daly, R. J. 2004. Cortactin signalling and dynamic actin networks. Biochem J **382:**13-25.

Davies, S. P., Reddy, H., Caivano, M. and Cohen, P. 2000. Specificity and mechanism of action of some commonly used protein kinase inhibitors. Biochem J **351:**95-105.

del Pozo, M. A., Alderson, N. B., Kiosses, W. B., Chiang, H. H., Anderson, R. G. and Schwartz, M. A. 2004. Integrins regulate Rac targeting by internalization of membrane domains. Science **303:**839-42.

Denny, P. W., Gokool, S., Russell, D. G., Field, M. C. and Smith, D. F. 2000. Acylation-dependent protein export in *Leishmania*. J Biol Chem **275:**11017-25.

DePina, A. S. and Langford, G. M. 1999. Vesicle transport: the role of actin filaments and myosin motors. Microsc Res Tech **47:**93-106.

DerMardirossian, C., Rocklin, G., Seo, J. Y. and Bokoch, G. M. 2006. Phosphorylation of RhoGDI by Src regulates Rho GTPase binding and cytosol-membrane cycling. Mol Biol Cell **17:**4760-8.

Dinter, A. and Berger, E. G. 1998. Golgi-disturbing agents. Histochem Cell Biol **109:**571-90.

Dipasquale, A. 1975. Locomotory activity of epithelial cells in culture. Exp Cell Res **94:**191-215.

Dvorsky, R., Blumenstein, L., Vetter, I. R. and Ahmadian, M. R. 2004. Structural insights into the interaction of ROCKI with the switch regions of RhoA. J Biol Chem **279:**7098-104.

Egea, G., Lazaro-Dieguez, F. and Vilella, M. 2006. Actin dynamics at the Golgi complex in mammalian cells. Curr Opin Cell Biol **18:**168-78.

Eisenmann, K. M., Harris, E. S., Kitchen, S. M., Holman, H. A., Higgs, H. N. and Alberts, A. S. 2007. Dia-interacting protein modulates formin-mediated actin assembly at the cell cortex. Curr Biol **17:**579-91.

Eisenmann, K. M., West, R. A., Hildebrand, D., Kitchen, S. M., Peng, J., Sigler, R., Zhang, J., Siminovitch, K. A. and Alberts, A. S. 2007. T cell responses in mammalian diaphanous-related formin mDia1 knockout mice. J Biol Chem.

Elliott, B. E., Qiao, H., Louvard, D. and Arpin, M. 2004. Co-operative effect of c-Src and ezrin in deregulation of cell-cell contacts and scattering of mammary carcinoma cells. J Cell Biochem **92:**16-28.

Engling, A., Backhaus, R., Stegmayer, C., Zehe, C., Seelenmeyer, C., Kehlenbach, A., Schwappach, B., Wegehingel, S. and Nickel, W. 2002. Biosynthetic FGF-2 is targeted to non-lipid raft microdomains following translocation to the extracellular surface of CHO cells. J Cell Sci **115:**3619-31.

Erickson, C. A. and Trinkaus, J. P. 1976. Microvilli and blebs as sources of reserve surface membrane during cell spreading. Exp Cell Res **99:**375-84.

Evangelista, M., Blundell, K., Longtine, M. S., Chow, C. J., Adames, N., Pringle, J. R., Peter, M. and Boone, C. 1997. Bni1p, a yeast formin linking cdc42p and the actin cytoskeleton during polarized morphogenesis. Science **276:**118-22.

Evangelista, M., Pruyne, D., Amberg, D. C., Boone, C. and Bretscher, A. 2002. Formins direct Arp2/3-independent actin filament assembly to polarize cell growth in yeast. Nat Cell Biol **4:**32-41.

Evangelista, M., Zigmond, S. and Boone, C. 2003. Formins: signaling effectors for assembly and polarization of actin filaments. J Cell Sci **116:**2603-11.

Fackler, O. T., Luo, W., Geyer, M., Alberts, A. S. and Peterlin, B. M. 1999. Activation of Vav by Nef induces cytoskeletal rearrangements and downstream effector functions. Mol Cell **3:**729-39.

Fadeel, B. 2004. Plasma membrane alterations during apoptosis: role in corpse clearance. Antioxid Redox Signal **6:**269-75.

Fadok, V. A., Voelker, D. R., Campbell, P. A., Cohen, J. J., Bratton, D. L. and Henson, P. M. 1992. Exposure of phosphatidylserine on the surface of apoptotic lymphocytes triggers specific recognition and removal by macrophages. J Immunol **148:**2207-16.

Faix, J. and Grosse, R. 2006. Staying in shape with formins. Dev Cell **10:**693-706.

Faix, J. and Rottner, K. 2006. The making of filopodia. Curr Opin Cell Biol **18:**18-25.

Fire, A., Xu, S., Montgomery, M. K., Kostas, S. A., Driver, S. E. and Mello, C. C. 1998. Potent and specific genetic interference by double-stranded RNA in *Caenorhabditis elegans*. Nature **391:**806-11.

Frame, M. C. 2004. Newest findings on the oldest oncogene; how activated src does it. J Cell Sci **117:**989-98.

Frazier, J. A. and Field, C. M. 1997. Actin cytoskeleton: are FH proteins local organizers? Curr Biol **7:**R414-7.

Gadea, G., de Toledo, M., Anguille, C. and Roux, P. 2007. Loss of p53 promotes RhoA-ROCK-dependent cell migration and invasion in 3D matrices. J Cell Biol **178:**23-30.

Garcia, J. V. and Miller, A. D. 1991. Serine phosphorylation-independent downregulation of cell-surface CD4 by nef. Nature **350:**508-11.

Gasman, S., Kalaidzidis, Y. and Zerial, M. 2003. RhoD regulates endosome dynamics through Diaphanous-related Formin and Src tyrosine kinase. Nat Cell Biol **5:**195-204.

Gasteier, J. E., Madrid, R., Krautkramer, E., Schroder, S., Muranyi, W., Benichou, S. and Fackler, O. T. 2003. Activation of the Rac-binding partner FHOD1 induces actin stress fibers via a ROCK-dependent mechanism. J Biol Chem **278:**38902-12.

Gasteier, J. E., Schroeder, S., Muranyi, W., Madrid, R., Benichou, S. and Fackler, O. T. 2005. FHOD1 coordinates actin filament and microtubule alignment to mediate cell elongation. Exp Cell Res **306:**192-202.

Gavrieli, Y., Sherman, Y. and Ben-Sasson, S. A. 1992. Identification of programmed cell death *in situ* via specific labeling of nuclear DNA fragmentation. J Cell Biol **119:**493-501.

Geeves, M. A. and Holmes, K. C. 1999. Structural mechanism of muscle contraction. Annu Rev Biochem **68:**687-728.

Geneste, O., Copeland, J. W. and Treisman, R. 2002. LIM kinase and Diaphanous cooperate to regulate serum response factor and actin dynamics. J Cell Biol **157:**831-8.

Gill, M. B., Roecklein-Canfield, J., Sage, D. R., Zambela-Soediono, M., Longtine, N., Uknis, M. and Fingeroth, J. D. 2004. EBV attachment stimulates FHOS/FHOD1 redistribution and co-aggregation with CD21: formin interactions with the cytoplasmic domain of human CD21. J Cell Sci **117:**2709-20.

Goethe, J. W. 1808. Faust. Gotta'sche Buchhandlung, Tübingen.

Goldmann, W. H. 2002. p56(lck) Controls phosphorylation of filamin (ABP-280) and regulates focal adhesion kinase (pp125(FAK)). Cell Biol Int **26:**567-71.

Goode, B. L. and Eck, M. J. 2007. Mechanism and Function of Formins in Control of Actin Assembly. Annu Rev Biochem.

Gossen, M. and Bujard, H. 1992. Tight control of gene expression in mammalian cells by tetracycline-responsive promoters. Proc Natl Acad Sci U S A **89:**5547-51.

Goulimari, P., Kitzing, T. M., Knieling, H., Brandt, D. T., Offermanns, S. and Grosse, R. 2005. Galpha12/13 is essential for directed cell migration and localized Rho-Dia1 function. J Biol Chem **280:**42242-51.

Gundersen, G. G., Gomes, E. R. and Wen, Y. 2004. Cortical control of microtubule stability and polarization. Curr Opin Cell Biol **16:**106-12.

Habas, R., Kato, Y. and He, X. 2001. Wnt/Frizzled activation of Rho regulates vertebrate gastrulation and requires a novel Formin homology protein Daam1. Cell **107:**843-54.

Hall, A. 1998. Rho GTPases and the actin cytoskeleton. Science **279:**509-14.

Haller, C., Rauch, S., Michel, N., Hannemann, S., Lehmann, M. J., Keppler, O. T. and Fackler, O. T. 2006. The HIV-1 pathogenicity factor Nef interferes with maturation of stimulatory T-lymphocyte contacts by modulation of N-Wasp activity. J Biol Chem **281:**19618-30.

Hancock, J. F. 2006. Lipid rafts: contentious only from simplistic standpoints. Nat Rev Mol Cell Biol **7:**456-62.

Harris, E. S. and Higgs, H. N. 2004. Actin cytoskeleton: formins lead the way. Curr Biol **14:**R520-2.

Harris, E. S., Li, F. and Higgs, H. N. 2004. The mouse formin, FRLalpha, slows actin filament barbed end elongation, competes with capping protein, accelerates polymerization from monomers, and severs filaments. J Biol Chem **279:**20076-87.

Harris, E. S., Rouiller, I., Hanein, D. and Higgs, H. N. 2006. Mechanistic differences in actin bundling activity of two mammalian formins, FRL1 and mDia2. J Biol Chem **281:**14383-92.

Higashida, C., Miyoshi, T., Fujita, A., Oceguera-Yanez, F., Monypenny, J., Andou, Y., Narumiya, S. and Watanabe, N. 2004. Actin polymerization-driven molecular movement of mDia1 in living cells. Science **303:**2007-10.

Higgs, H. N. 2005. Formin proteins: a domain-based approach. Trends Biochem Sci **30:**342-53.

Higgs, H. N. and Peterson, K. J. 2004. Phylogenetic Analysis of the Formin Homology 2 (FH2) Domain. Mol Biol Cell **27:**27.

Higgs, H. N. and Pollard, T. D. 2001. Regulation of actin filament network formation through ARP2/3 complex: activation by a diverse array of proteins. Annu Rev Biochem **70:**649-76.

Hill, C. S., Wynne, J. and Treisman, R. 1995. The Rho family GTPases RhoA, Rac1, and CDC42Hs regulate transcriptional activation by SRF. Cell **81:**1159-70.

Hooper, S., Marshall, J. F. and Sahai, E. 2006. Tumor cell migration in three dimensions. Methods Enzymol **406:**625-43.

Huerta, S., Goulet, E. J., Huerta-Yepez, S. and Livingston, E. H. 2007. Screening and detection of apoptosis. J Surg Res **139:**143-56.

Huot, J., Houle, F., Rousseau, S., Deschesnes, R. G., Shah, G. M. and Landry, J. 1998. SAPK2/p38-dependent F-actin reorganization regulates early membrane blebbing during stress-induced apoptosis. J Cell Biol **143:**1361-73.

Imamura, F., Mukai, M., Ayaki, M., Takemura, K., Horai, T., Shinkai, K., Nakamura, H. and Akedo, H. 1999. Involvement of small GTPases Rho and Rac in the invasion of rat ascites hepatoma cells. Clin Exp Metastasis **17:**141-8.

Ishizaki, T., Naito, M., Fujisawa, K., Maekawa, M., Watanabe, N., Saito, Y. and Narumiya, S. 1997. p160ROCK, a Rho-associated coiled-coil forming protein kinase, works downstream of Rho and induces focal adhesions. FEBS Lett **404:**118-24.

Jackson, C. L. and Casanova, J. E. 2000. Turning on ARF: the Sec7 family of guanine-nucleotide-exchange factors. Trends Cell Biol **10:**60-7.

Jacobs, M., Hayakawa, K., Swenson, L., Bellon, S., Fleming, M., Taslimi, P. and Doran, J. 2006. The structure of dimeric ROCK I reveals the mechanism for ligand selectivity. J Biol Chem **281:**260-8.

Jaffe, A. B. and Hall, A. 2005. RHO GTPASES: Biochemistry and Biology. Annu Rev Cell Dev Biol **21:**247-269.

Johannes, L. and Lamaze, C. 2002. Clathrin-dependent or not: is it still the question? Traffic **3:**443-51.

Kanaya, H., Takeya, R., Takeuchi, K., Watanabe, N., Jing, N. and Sumimoto, H. 2005. Fhos2, a novel formin-related actin-organizing protein, probably associates with the nestin intermediate filament. Genes Cells **10:**665-78.

Kaplan, J. M., Mardon, G., Bishop, J. M. and Varmus, H. E. 1988. The first seven amino acids encoded by the v-src oncogene act as a myristylation signal: lysine 7 is a critical determinant. Mol Cell Biol **8:**2435-41.

Kasahara, K., Nakayama, Y., Sato, I., Ikeda, K., Hoshino, M., Endo, T. and Yamaguchi, N. 2007. Role of Src-family kinases in formation and trafficking of macropinosomes. J Cell Physiol **211:**220-32.

Kater, S. B. and Rehder, V. 1995. The sensory-motor role of growth cone filopodia. Curr Opin Neurobiol **5:**68-74.

Kato, T., Watanabe, N., Morishima, Y., Fujita, A., Ishizaki, T. and Narumiya, S. 2001. Localization of a mammalian homolog of diaphanous, mDia1, to the mitotic spindle in HeLa cells. J Cell Sci **114:**775-84.

Keller, H. and Eggli, P. 1998. Protrusive activity, cytoplasmic compartmentalization, and restriction rings in locomoting blebbing Walker carcinosarcoma cells are related to detachment of cortical actin from the plasma membrane. Cell Motil Cytoskeleton **41:**181-93.

Keller, H., Rentsch, P. and Hagmann, J. 2002. Differences in cortical actin structure and dynamics document that different types of blebs are formed by distinct mechanisms. Exp Cell Res **277:**161-72.

Keller, P., Toomre, D., Diaz, E., White, J. and Simons, K. 2001. Multicolour imaging of post-Golgi sorting and trafficking in live cells. Nat Cell Biol **3:**140-9.

Kerkhoff, E. 2006. Cellular functions of the Spir actin-nucleation factors. Trends Cell Biol **16:**477-83.

Kerkhoff, E., Simpson, J. C., Leberfinger, C. B., Otto, I. M., Doerks, T., Bork, P., Rapp, U. R., Raabe, T. and Pepperkok, R. 2001. The Spir actin organizers are involved in vesicle transport processes. Curr Biol **11:**1963-8.

Kim, S. and Coulombe, P. A. 2007. Intermediate filament scaffolds fulfill mechanical, organizational, and signaling functions in the cytoplasm. Genes Dev **21:**1581-97.

Kitayama, C. and Uyeda, T. Q. 2003. ForC, a novel type of formin family protein lacking an FH1 domain, is involved in multicellular development in *Dictyostelium discoideum*. J Cell Sci **116:**711-23.

Kitzing, T. M., Sahadevan, A. S., Brandt, D. T., Knieling, H., Hannemann, S., Fackler, O. T., Grosshans, J. and Grosse, R. 2007. Positive feedback between Dia1, LARG, and RhoA regulates cell morphology and invasion. Genes Dev **21:**1478-1483.

Klinghoffer, R. A., Sachsenmaier, C., Cooper, J. A. and Soriano, P. 1999. Src family kinases are required for integrin but not PDGFR signal transduction. Embo J **18:**2459-71.

Kobielak, A., Pasolli, H. A. and Fuchs, E. 2004. Mammalian formin-1 participates in adherens junctions and polymerization of linear actin cables. Nat Cell Biol **6:**21-30.

Koka, S., Minick, G. T., Zhou, Y., Westendorf, J. J. and Boehm, M. B. 2005. Src regulates the activity of the mammalian formin protein FHOD1. Biochem Biophys Res Commun **336:**1285-91.

Koka, S., Neudauer, C. L., Li, X., Lewis, R. E., McCarthy, J. B. and Westendorf, J. J. 2003. The formin-homology-domain-containing protein FHOD1 enhances cell migration. J Cell Sci **116:**1745-55.

Kovar, D. R., Kuhn, J. R., Tichy, A. L. and Pollard, T. D. 2003. The fission yeast cytokinesis formin Cdc12p is a barbed end actin filament capping protein gated by profilin. J Cell Biol **161:**875-87.

Kovar, D. R. and Pollard, T. D. 2004. Insertional assembly of actin filament barbed ends in association with formins produces piconewton forces. Proc Natl Acad Sci U S A **101:**14725-30. Epub 2004 Sep 17.

Kunda, P., Craig, G., Dominguez, V. and Baum, B. 2003. Abi, Sra1, and Kette control the stability and localization of SCAR/WAVE to regulate the formation of actin-based protrusions. Curr Biol **13:**1867-75.

Laemmli, U. K. 1970. Cleavage of structural proteins during the assembly of the head of bacteriophage T4. Nature **227:**680-5.

Laki, K., Bowen, W. J. and Clark, A. 1950. The polymerization of proteins; adenosine triphosphate and the polymerization of actin. J Gen Physiol **33:**437-43.

Lamarche, N., Tapon, N., Stowers, L., Burbelo, P. D., Aspenstrom, P., Bridges, T., Chant, J. and Hall, A. 1996. Rac and Cdc42 induce actin polymerization and G1 cell cycle progression independently of p65PAK and the JNK/SAPK MAP kinase cascade. Cell **87:**519-29.

Lammers, M., Rose, R., Scrima, A. and Wittinghofer, A. 2005. The regulation of mDia1 by autoinhibition and its release by Rho*GTP. Embo J **24:**4176-87.

Lassing, I. and Lindberg, U. 1985. Specific interaction between phosphatidylinositol 4,5-bisphosphate and profilactin. Nature **314:**472-4.

Laster, S. M. and Mackenzie, J. M., Jr. 1996. Bleb formation and F-actin distribution during mitosis and tumor necrosis factor-induced apoptosis. Microsc Res Tech **34:**272-80.

Leverrier, Y. and Ridley, A. J. 2001. Apoptosis: caspases orchestrate the ROCK 'n' bleb. Nat Cell Biol **3:**E91-3.

Li, F. and Higgs, H. N. 2003. The mouse Formin mDia1 is a potent actin nucleation factor regulated by autoinhibition. Curr Biol **13:**1335-40.

Li, F. and Higgs, H. N. 2005. Dissecting requirements for auto-inhibition of actin nucleation by the formin, mDia1. J Biol Chem **280:**6986-92.

Liao, J. K., Seto, M. and Noma, K. 2007. Rho kinase (ROCK) inhibitors. J Cardiovasc Pharmacol **50:**17-24.

Linder, S. and Aepfelbacher, M. 2003. Podosomes: adhesion hot-spots of invasive cells. Trends Cell Biol **13:**376-85.

Lodish, H., Berk, A., Zipursky, S. L., Matsudaira, P., Baltimore, D. and Darnell, J. E. 2000. Molecular Cell Biology, 4th edition ed. W.H. Freeman and Company, New York.

Lu, J. and Pollard, T. D. 2001. Profilin binding to poly-L-proline and actin monomers along with ability to catalyze actin nucleotide exchange is required for viability of fission yeast. Mol Biol Cell **12:**1161-75.

Machesky, L. M. and Insall, R. H. 1998. Scar1 and the related Wiskott-Aldrich syndrome protein, WASP, regulate the actin cytoskeleton through the Arp2/3 complex. Curr Biol **8:**1347-56.

Machesky, L. M., Mullins, R. D., Higgs, H. N., Kaiser, D. A., Blanchoin, L., May, R. C., Hall, M. E. and Pollard, T. D. 1999. Scar, a WASp-related protein, activates nucleation of actin filaments by the Arp2/3 complex. Proc Natl Acad Sci U S A **96:**3739-44.

MacKenzie, A., Wilson, H. L., Kiss-Toth, E., Dower, S. K., North, R. A. and Surprenant, A. 2001. Rapid secretion of interleukin-1beta by microvesicle shedding. Immunity **15:**825-35.

Madrid, R., Gasteier, J. E., Bouchet, J., Schroder, S., Geyer, M., Benichou, S. and Fackler, O. T. 2005. Oligomerization of the diaphanous-related formin FHOD1 requires a coiled-coil motif critical for its cytoskeletal and transcriptional activities. FEBS Lett **579:**441-8.

Manseau, L. J. and Schupbach, T. 1989. cappuccino and spire: two unique maternal-effect loci required for both the anteroposterior and dorsoventral patterns of the *Drosophila* embryo. Genes Dev **3:**1437-52.

Marsh, M. and Helenius, A. 2006. Virus entry: open sesame. Cell **124:**729-40.

Marshall, C. J. 1993. Protein prenylation: a mediator of protein-protein interactions. Science **259:**1865-6.

Martin, G. S. 2001. The hunting of the Src. Nat Rev Mol Cell Biol **2:**467-75.

Martinez, M. C., Tesse, A., Zobairi, F. and Andriantsitohaina, R. 2005. Shed membrane microparticles from circulating and vascular cells in regulating vascular function. Am J Physiol Heart Circ Physiol **288:**H1004-9.

Mass, R. L., Zeller, R., Woychik, R. P., Vogt, T. F. and Leder, P. 1990. Disruption of formin-encoding transcripts in two mutant limb deformity alleles. Nature **346:**853-5.

Matsumura, F. 2005. Regulation of myosin II during cytokinesis in higher eukaryotes. Trends Cell Biol.

Matusek, T., Djiane, A., Jankovics, F., Brunner, D., Mlodzik, M. and Mihaly, J. 2006. The *Drosophila* formin DAAM regulates the tracheal cuticle pattern through organizing the actin cytoskeleton. Development **133:**957-66.

McCabe, J. B. and Berthiaume, L. G. 1999. Functional roles for fatty acylated amino-terminal domains in subcellular localization. Mol Biol Cell **10:**3771-86.

Mehul, B. and Hughes, R. C. 1997. Plasma membrane targetting, vesicular budding and release of galectin 3 from the cytoplasm of mammalian cells during secretion. J Cell Sci **110:**1169-78.

Meier, O., Boucke, K., Hammer, S. V., Keller, S., Stidwill, R. P., Hemmi, S. and Greber, U. F. 2002. Adenovirus triggers macropinocytosis and endosomal leakage together with its clathrin-mediated uptake. J Cell Biol **158:**1119-31.

Meier, O. and Greber, U. F. 2003. Adenovirus endocytosis. J Gene Med **5:**451-62.

Meng, W., Numazaki, M., Takeuchi, K., Uchibori, Y., Ando-Akatsuka, Y., Tominaga, M. and Tominaga, T. 2004. DIP (mDia interacting protein) is a key molecule regulating Rho and Rac in a Src-dependent manner. Embo J **23:**760-71.

Michel, N., Allespach, I., Venzke, S., Fackler, O. T. and Keppler, O. T. 2005. The Nef protein of human immunodeficiency virus establishes superinfection immunity by a dual strategy to downregulate cell-surface CCR5 and CD4. Curr Biol **15:**714-23.

Michel, N., Ganter, K., Venzke, S., Bitzegeio, J., Fackler, O. T. and Keppler, O. T. 2006. The Nef protein of human immunodeficiency virus is a broad-spectrum modulator of chemokine receptor cell surface levels that acts independently of classical motifs for receptor endocytosis and Galphai signaling. Mol Biol Cell **17:**3578-90.

Miki, H., Yamaguchi, H., Suetsugu, S. and Takenawa, T. 2000. IRSp53 is an essential intermediate between Rac and WAVE in the regulation of membrane ruffling. Nature **408:**732-5.

Millard, T. H., Sharp, S. J. and Machesky, L. M. 2004. Signalling to actin assembly via the WASP (Wiskott-Aldrich syndrome protein)-family proteins and the Arp2/3 complex. Biochem J **380:**1-17.

Mills, J. C., Stone, N. L., Erhardt, J. and Pittman, R. N. 1998. Apoptotic membrane blebbing is regulated by myosin light chain phosphorylation. J Cell Biol **140:**627-36.

Mills, J. C., Stone, N. L. and Pittman, R. N. 1999. Extranuclear apoptosis. The role of the cytoplasm in the execution phase. J Cell Biol **146:**703-8.

Miralles, F., Posern, G., Zaromytidou, A. I. and Treisman, R. 2003. Actin dynamics control SRF activity by regulation of its coactivator MAL. Cell **113:**329-42.

Mogelsvang, S. and Howell, K. E. 2006. Global approaches to study Golgi function. Curr Opin Cell Biol **18:**438-43.

Moreau, V., Frischknecht, F., Reckmann, I., Vincentelli, R., Rabut, G., Stewart, D. and Way, M. 2000. A complex of N-WASP and WIP integrates signalling cascades that lead to actin polymerization. Nat Cell Biol **2:**441-8.

Morelli, A., Chiozzi, P., Chiesa, A., Ferrari, D., Sanz, J. M., Falzoni, S., Pinton, P., Rizzuto, R., Olson, M. F. and Di Virgilio, F. 2003. Extracellular ATP causes ROCK I-dependent bleb formation in P2X7-transfected HEK293 cells. Mol Biol Cell **14:**2655-64.

Moseley, J. B., Sagot, I., Manning, A. L., Xu, Y., Eck, M. J., Pellman, D. and Goode, B. L. 2004. A conserved mechanism for Bni1- and mDia1-induced actin assembly and dual regulation of Bni1 by Bud6 and profilin. Mol Biol Cell **15:**896-907. Epub 2003 Dec 2.

Mosquera, J. A., Hernandez, J. P., Valero, N., Espina, L. M. and Anez, G. J. 2005. Ultrastructural studies on dengue virus type 2 infection of cultured human monocytes. Virol J **2:**26.

Mullins, R. D., Heuser, J. A. and Pollard, T. D. 1998. The interaction of Arp2/3 complex with actin: nucleation, high affinity pointed end capping, and formation of branching networks of filaments. Proc Natl Acad Sci U S A **95:**6181-6.

Musch, A. 2004. Microtubule organization and function in epithelial cells. Traffic **5:**1-9.

Myat, M. M., Anderson, S., Allen, L. A. and Aderem, A. 1997. MARCKS regulates membrane ruffling and cell spreading. Curr Biol **7:**611-4.

Nabi, I. R. 1999. The polarization of the motile cell. J Cell Sci **112 (Pt 12):**1803-11.

Nakagawa, O., Fujisawa, K., Ishizaki, T., Saito, Y., Nakao, K. and Narumiya, S. 1996. ROCK-I and ROCK-II, two isoforms of Rho-associated coiled-coil forming protein serine/threonine kinase in mice. FEBS Lett **392:**189-93.

Nezami, A. G., Poy, F. and Eck, M. J. 2006. Structure of the autoinhibitory switch in formin mDia1. Structure **14:**257-63.

Nichols, B. J. and Lippincott-Schwartz, J. 2001. Endocytosis without clathrin coats. Trends Cell Biol **11:**406-12.

Nickel, W. 2003. The mystery of nonclassical protein secretion. A current view on cargo proteins and potential export routes. Eur J Biochem **270:**2109-19.

Nickel, W. 2005. Unconventional secretory routes: direct protein export across the plasma membrane of mammalian cells. Traffic **6:**607-14.

Nobes, C. D. and Hall, A. 1999. Rho GTPases control polarity, protrusion, and adhesion during cell movement. J Cell Biol **144:**1235-44.

Noguchi, T. and Mabuchi, I. 2001. Reorganization of actin cytoskeleton at the growing end of the cleavage furrow of *Xenopus* egg during cytokinesis. J Cell Sci **114:**401-12.

Norbury, C. C. 2006. Drinking a lot is good for dendritic cells. Immunology **117:**443-51.

Orlando, K. A., Stone, N. L. and Pittman, R. N. 2006. Rho kinase regulates fragmentation and phagocytosis of apoptotic cells. Exp Cell Res **312:**5-15.

Otomo, T., Otomo, C., Tomchick, D. R., Machius, M. and Rosen, M. K. 2005. Structural basis of Rho GTPase-mediated activation of the formin mDia1. Mol Cell **18:**273-81.

Otomo, T., Tomchick, D. R., Otomo, C., Panchal, S. C., Machius, M. and Rosen, M. K. 2005. Structural basis of actin filament nucleation and processive capping by a formin homology 2 domain. Nature **433:**488-94.

Pacholsky, D., Vakeel, P., Himmel, M., Lowe, T., Stradal, T., Rottner, K., Furst, D. O. and van der Ven, P. F. 2004. Xin repeats define a novel actin-binding motif. J Cell Sci **117:**5257-68.

Pal Sharma, C. and Goldmann, W. H. 2004. Phosphorylation of actin-binding protein (ABP-280; filamin) by tyrosine kinase p56lck modulates actin filament cross-linking. Cell Biol Int **28:**935-41.

Palazzo, A. F., Cook, T. A., Alberts, A. S. and Gundersen, G. G. 2001. mDia mediates Rho-regulated formation and orientation of stable microtubules. Nat Cell Biol **3:**723-9.

Palazzo, A. F., Eng, C. H., Schlaepfer, D. D., Marcantonio, E. E. and Gundersen, G. G. 2004. Localized stabilization of microtubules by integrin- and FAK-facilitated Rho signaling. Science **303:**836-9.

Paluch, E., Piel, M., Prost, J., Bornens, M. and Sykes, C. 2005. Cortical actomyosin breakage triggers shape oscillations in cells and cell fragments. Biophys J **89:**724-33.

Pawlak, G. and Helfman, D. M. 2002. MEK mediates v-Src-induced disruption of the actin cytoskeleton via inactivation of the Rho-ROCK-LIM kinase pathway. J Biol Chem **277:**26927-33.

Pederson, T. and Aebi, U. 2005. Nuclear actin extends, with no contraction in sight. Mol Biol Cell **16:**5055-60.

Pellegrini, F. and Budman, D. R. 2005. Review: tubulin function, action of antitubulin drugs, and new drug development. Cancer Invest **23:**264-73.

Pepperkok, R., Scheel, J., Horstmann, H., Hauri, H. P., Griffiths, G. and Kreis, T. E. 1993. Beta-COP is essential for biosynthetic membrane transport from the endoplasmic reticulum to the Golgi complex *in vivo*. Cell **74:**71-82.

Pepperkok, R., Simpson, J. C., Rietdorf, J., Cetin, C., Liebel, U., Terjung, S. and Zimmermann, T. 2005. Imaging platforms for measurement of membrane trafficking. Methods Enzymol **404:**8-18.

Percival, J. M., Hughes, J. A., Brown, D. L., Schevzov, G., Heimann, K., Vrhovski, B., Bryce, N., Stow, J. L. and Gunning, P. W. 2004. Targeting of a tropomyosin isoform to short microfilaments associated with the Golgi complex. Mol Biol Cell **15:**268-80.

Pike, L. J., Han, X., Chung, K. N. and Gross, R. W. 2002. Lipid rafts are enriched in arachidonic acid and plasmenylethanolamine and their composition is independent of caveolin-1 expression: a quantitative electrospray ionization/mass spectrometric analysis. Biochemistry **41:**2075-88.

Pollard, T. D., Blanchoin, L. and Mullins, R. D. 2000. Molecular mechanisms controlling actin filament dynamics in nonmuscle cells. Annu Rev Biophys Biomol Struct **29:**545-76.

Pollard, T. D. and Borisy, G. G. 2003. Cellular motility driven by assembly and disassembly of actin filaments. Cell **112:**453-65.

Pollard, T. D. and Earnshaw, W. C. 2004. Cell Biology. Saunders, Philadelphia.

Porter, K., Prescott, D. and Frye, J. 1973. Changes in surface morphology of Chinese hamster ovary cells during the cell cycle. J Cell Biol **57:**815-36.

Pring, M., Evangelista, M., Boone, C., Yang, C. and Zigmond, S. H. 2003. Mechanism of formin-induced nucleation of actin filaments. Biochemistry **42:**486-96.

Pruyne, D., Evangelista, M., Yang, C., Bi, E., Zigmond, S., Bretscher, A. and Boone, C. 2002. Role of formins in actin assembly: nucleation and barbed-end association. Science **297:**612-5.

Puck, T. T., Cieciura, S. J. and Robinson, A. 1958. Genetics of somatic mammalian cells. III. Long-term cultivation of euploid cells from human and animal subjects. J Exp Med **108:**945-56.

Qualmann, B. and Mellor, H. 2003. Regulation of endocytic traffic by Rho GTPases. Biochem J **371:**233-41.

Quinlan, M. E., Heuser, J. E., Kerkhoff, E. and Dyche Mullins, R. 2005. *Drosophila* Spire is an actin nucleation factor. Nature **433:**382-8.

Raftopoulou, M. and Hall, A. 2004. Cell migration: Rho GTPases lead the way. Dev Biol **265:**23-32.

Rajendran, L. and Simons, K. 2005. Lipid rafts and membrane dynamics. J Cell Sci **118:**1099-102.

Ramamurthy, B., Yengo, C. M., Straight, A. F., Mitchison, T. J. and Sweeney, H. L. 2004. Kinetic mechanism of blebbistatin inhibition of nonmuscle myosin IIb. Biochemistry **43:**14832-9.

Rentsch, P. S. and Keller, H. 2000. Suction pressure can induce uncoupling of the plasma membrane from cortical actin. Eur J Cell Biol **79:**975-81.

Resh, M. D. 1993. Interaction of tyrosine kinase oncoproteins with cellular membranes. Biochim Biophys Acta **1155:**307-22.

Resh, M. D. 1994. Myristylation and palmitylation of Src family members: the fats of the matter. Cell **76:**411-3.

Resh, M. D. 1999. Fatty acylation of proteins: new insights into membrane targeting of myristoylated and palmitoylated proteins. Biochim Biophys Acta **1451:**1-16.

Ridley, A. J. 2006. Rho GTPases and actin dynamics in membrane protrusions and vesicle trafficking. Trends Cell Biol **16:**522-9.

Riento, K., Guasch, R. M., Garg, R., Jin, B. and Ridley, A. J. 2003. RhoE binds to ROCK I and inhibits downstream signaling. Mol Cell Biol **23:**4219-29.

Riento, K. and Ridley, A. J. 2003. Rocks: multifunctional kinases in cell behaviour. Nat Rev Mol Cell Biol **4:**446-56.

Righetti, P. G. 1990. Recent developments in electrophoretic methods. J Chromatogr **516:**3-22.

Riveline, D., Zamir, E., Balaban, N. Q., Schwarz, U. S., Ishizaki, T., Narumiya, S., Kam, Z., Geiger, B. and Bershadsky, A. D. 2001. Focal contacts as mechanosensors: externally

applied local mechanical force induces growth of focal contacts by an mDia1-dependent and ROCK-independent mechanism. J Cell Biol **153:**1175-86.

Romero, S., Le Clainche, C., Didry, D., Egile, C., Pantaloni, D. and Carlier, M. F. 2004. Formin Is a Processive Motor that Requires Profilin to Accelerate Actin Assembly and Associated ATP Hydrolysis. Cell **119:**419-429.

Rose, R., Weyand, M., Lammers, M., Ishizaki, T., Ahmadian, M. R. and Wittinghofer, A. 2005. Structural and mechanistic insights into the interaction between Rho and mammalian Dia. Nature **435:**513-28.

Roskoski, R., Jr. 2004. Src protein-tyrosine kinase structure and regulation. Biochem Biophys Res Commun **324:**1155-64.

Ruegg, C., Veigel, C., Molloy, J. E., Schmitz, S., Sparrow, J. C. and Fink, R. H. 2002. Molecular motors: force and movement generated by single myosin II molecules. News Physiol Sci **17:**213-8.

Rupinder, S. K., Gurpreet, A. K. and Manjeet, S. 2007. Cell suicide and caspases. Vascul Pharmacol **46:**383-93.

Sagot, I., Rodal, A. A., Moseley, J., Goode, B. L. and Pellman, D. 2002. An actin nucleation mechanism mediated by Bni1 and profilin. Nat Cell Biol **4:**626-31.

Sahai, E. 2005. Mechanisms of cancer cell invasion. Curr Opin Genet Dev **15:**87-96.

Sahai, E. and Marshall, C. J. 2002. ROCK and Dia have opposing effects on adherens junctions downstream of Rho. Nat Cell Biol **4:**408-15.

Sahai, E. and Marshall, C. J. 2003. Differing modes of tumour cell invasion have distinct requirements for Rho/ROCK signalling and extracellular proteolysis. Nat Cell Biol **5:**711-9.

Sahai, E. and Olson, M. F. 2006. Purification of TAT-C3 exoenzyme. Methods Enzymol **406:**128-40.

Sakata, D., Taniguchi, H., Yasuda, S., Adachi-Morishima, A., Hamazaki, Y., Nakayama, R., Miki, T., Minato, N. and Narumiya, S. 2007. Impaired T lymphocyte trafficking in mice deficient in an actin-nucleating protein, mDia1. J Exp Med **204:**2031-8.

Satoh, S. and Tominaga, T. 2001. mDia-interacting protein acts downstream of Rho-mDia and modifies Src activation and stress fiber formation. J Biol Chem **276:**39290-4.

Scales, S. J., Pepperkok, R. and Kreis, T. E. 1997. Visualization of ER-to-Golgi transport in living cells reveals a sequential mode of action for COPII and COPI. Cell **90:**1137-48.

Scherer, W. F., Syverton, J. T. and Gey, G. O. 1953. Studies on the propagation *in vitro* of poliomyelitis viruses. IV. Viral multiplication in a stable strain of human malignant epithelial cells (strain HeLa) derived from an epidermoid carcinoma of the cervix. J Exp Med **97:**695-710.

Schonichen, A., Alexander, M., Gasteier, J. E., Cuesta, F. E., Fackler, O. T. and Geyer, M. 2006. Biochemical characterization of the diaphanous autoregulatory interaction in the formin homology protein FHOD1. J Biol Chem **281:**5084-93.

Schulze-Osthoff, K., Walczak, H., Droge, W. and Krammer, P. H. 1994. Cell nucleus and DNA fragmentation are not required for apoptosis. J Cell Biol **127:**15-20.

Schwartz, M. A., Meredith, J. E. and Kiosses, W. B. 1998. An activated Rac mutant functions as a dominant negative for membrane ruffling. Oncogene **17:**625-9.

Schwartz, O., Marechal, V., Le Gall, S., Lemonnier, F. and Heard, J. M. 1996. Endocytosis of major histocompatibility complex class I molecules is induced by the HIV-1 Nef protein. Nat Med **2:**338-42.

Sebbagh, M., Hamelin, J., Bertoglio, J., Solary, E. and Breard, J. 2005. Direct cleavage of ROCK II by granzyme B induces target cell membrane blebbing in a caspase-independent manner. J Exp Med **201:**465-71.

Sebbagh, M., Renvoize, C., Hamelin, J., Riche, N., Bertoglio, J. and Breard, J. 2001. Caspase-3-mediated cleavage of ROCK I induces MLC phosphorylation and apoptotic membrane blebbing. Nat Cell Biol **3:**346-52.

Shaner, N. C., Campbell, R. E., Steinbach, P. A., Giepmans, B. N., Palmer, A. E. and Tsien, R. Y. 2004. Improved monomeric red, orange and yellow fluorescent proteins derived from *Discosoma sp*. red fluorescent protein. Nat Biotechnol **22:**1567-72.

Sheetz, M. P., Sable, J. E. and Dobereiner, H. G. 2006. Continuous Membrane-Cytoskeleton Adhesion Requires Continuous Accommodation to Lipid and Cytoskeleton Dynamics. Annu Rev Biophys Biomol Struct **35:**417-34.

Shiratsuchi, A., Mori, T. and Nakanishi, Y. 2002. Independence of plasma membrane blebbing from other biochemical and biological characteristics of apoptotic cells. J Biochem (Tokyo) **132:**381-6.

Sigal, C. T., Zhou, W., Buser, C. A., McLaughlin, S. and Resh, M. D. 1994. Amino-terminal basic residues of Src mediate membrane binding through electrostatic interaction with acidic phospholipids. Proc Natl Acad Sci U S A **91:**12253-7.

Simons, K. and Toomre, D. 2000. Lipid rafts and signal transduction. Nat Rev Mol Cell Biol **1:**31-9.

Siripala, A. D. and Welch, M. D. 2007. SnapShot: actin regulators I. Cell **128:**626.

Siripala, A. D. and Welch, M. D. 2007. SnapShot: actin regulators II. Cell **128:**1014.

Song, Y., Hoang, B. Q. and Chang, D. D. 2002. ROCK-II-induced membrane blebbing and chromatin condensation require actin cytoskeleton. Exp Cell Res **278:**45-52.

Srivastava, J., Elliott, B. E., Louvard, D. and Arpin, M. 2005. Src-dependent ezrin phosphorylation in adhesion-mediated signaling. Mol Biol Cell **16:**1481-90.

Stegmayer, C., Kehlenbach, A., Tournaviti, S., Wegehingel, S., Zehe, C., Denny, P., Smith, D. F., Schwappach, B. and Nickel, W. 2005. Direct transport across the plasma membrane of mammalian cells of *Leishmania* HASPB as revealed by a CHO export mutant. J Cell Sci **118:**517-27.

Stossel, T. P., Condeelis, J., Cooley, L., Hartwig, J. H., Noegel, A., Schleicher, M. and Shapiro, S. S. 2001. Filamins as integrators of cell mechanics and signalling. Nat Rev Mol Cell Biol **2:**138-45.

Stossel, T. P., Fenteany, G. and Hartwig, J. H. 2006. Cell surface actin remodeling. J Cell Sci **119:**3261-4.

Straight, A. F., Cheung, A., Limouze, J., Chen, I., Westwood, N. J., Sellers, J. R. and Mitchison, T. J. 2003. Dissecting temporal and spatial control of cytokinesis with a myosin II Inhibitor. Science **299:**1743-7.

Summy, J. M., Qian, Y., Jiang, B. H., Guappone-Koay, A., Gatesman, A., Shi, X. and Flynn, D. C. 2003. The SH4-Unique-SH3-SH2 domains dictate specificity in signaling that differentiate c-Yes from c-Src. J Cell Sci **116:**2585-98.

Swanson, J. A. and Watts, C. 1995. Macropinocytosis. Trends Cell Biol **5:**424-8.

Takeya, R. and Sumimoto, H. 2003. Fhos, a mammalian formin, directly binds to F-actin via a region N-terminal to the FH1 domain and forms a homotypic complex via the FH2 domain to promote actin fiber formation. J Cell Sci **116:**4567-75.

Thomas, S. M. and Brugge, J. S. 1997. Cellular functions regulated by Src family kinases. Annu Rev Cell Dev Biol **13:**513-609.

Thoulouze, M. I., Sol-Foulon, N., Blanchet, F., Dautry-Varsat, A., Schwartz, O. and Alcover, A. 2006. Human immunodeficiency virus type-1 infection impairs the formation of the immunological synapse. Immunity **24:**547-61.

Tojo, H., Kaieda, I., Hattori, H., Katayama, N., Yoshimura, K., Kakimoto, S., Fujisawa, Y., Presman, E., Brooks, C. C. and Pilch, P. F. 2003. The Formin family protein, formin homolog overexpressed in spleen, interacts with the insulin-responsive aminopeptidase and profilin IIa. Mol Endocrinol **17:**1216-29.

Tominaga, T., Sahai, E., Chardin, P., McCormick, F., Courtneidge, S. A. and Alberts, A. S. 2000. Diaphanous-related formins bridge Rho GTPase and Src tyrosine kinase signaling. Mol Cell **5:**13-25.

Tomiyoshi, G., Horita, Y., Nishita, M., Ohashi, K. and Mizuno, K. 2004. Caspase-mediated cleavage and activation of LIM-kinase 1 and its role in apoptotic membrane blebbing. Genes Cells **9:**591-600.

Torgerson, R. R. and McNiven, M. A. 1998. The actin-myosin cytoskeleton mediates reversible agonist-induced membrane blebbing. J Cell Sci **111:**2911-22.

Treisman, R. 1992. The serum response element. Trends Biochem Sci **17:**423-6.

Trinkaus, J. P. 1973. Surface activity and locomotion of Fundulus deep cells during blastula and gastrula stages. Dev Biol **30:**69-103.

Tsukita, S. and Yonemura, S. 1999. Cortical actin organization: lessons from ERM (ezrin/radixin/moesin) proteins. J Biol Chem **274:**34507-10.

Ueda, K., Ohta, Y. and Hosoya, H. 2003. The carboxy-terminal pleckstrin homology domain of ROCK interacts with filamin-A. Biochem Biophys Res Commun **301:**886-90.

Uetz, P., Fumagalli, S., James, D. and Zeller, R. 1996. Molecular interaction between limb deformity proteins (formins) and Src family kinases. J Biol Chem **271:**33525-30.

Vandekerckhove, J. and Weber, K. 1978. At least six different actins are expressed in a higher mammal: an analysis based on the amino acid sequence of the amino-terminal tryptic peptide. J Mol Biol **126:**783-802.

Vaughan, K. T. 2005. Microtubule plus ends, motors, and traffic of Golgi membranes. Biochim Biophys Acta **1744:**316-24.

Venzke, S., Michel, N., Allespach, I., Fackler, O. T. and Keppler, O. T. 2006. Expression of Nef downregulates CXCR4, the major coreceptor of human immunodeficiency virus, from the surfaces of target cells and thereby enhances resistance to superinfection. J Virol **80:**11141-52.

Verhoef, P. A., Estacion, M., Schilling, W. and Dubyak, G. R. 2003. P2X7 receptor-dependent blebbing and the activation of Rho-effector kinases, caspases, and IL-1 beta release. J Immunol **170:**5728-38.

Verhoef, P. A., Kertesy, S. B., Estacion, M., Schilling, W. P. and Dubyak, G. R. 2004. Maitotoxin induces biphasic interleukin-1beta secretion and membrane blebbing in murine macrophages. Mol Pharmacol **66:**909-20.

Vidali, L., Chen, F., Cicchetti, G., Ohta, Y. and Kwiatkowski, D. J. 2006. Rac1-null mouse embryonic fibroblasts are motile and respond to platelet-derived growth factor. Mol Biol Cell **17:**2377-90.

Wade, R. H., Meurer-Grob, P., Metoz, F. and Arnal, I. 1998. Organisation and structure of microtubules and microtubule-motor protein complexes. Eur Biophys J **27:**446-54.

Wallar, B. J. and Alberts, A. S. 2003. The formins: active scaffolds that remodel the cytoskeleton. Trends Cell Biol **13:**435-46.

Wang, W., Eddy, R. and Condeelis, J. 2007. The cofilin pathway in breast cancer invasion and metastasis. Nat Rev Cancer **7:**429-40.

Wang, Y., El-Zaru, M. R., Surks, H. K. and Mendelsohn, M. E. 2004. Formin homology domain protein (FHOD1) is a cyclic GMP-dependent protein kinase I-binding protein and substrate in vascular smooth muscle cells. J Biol Chem **279:**24420-6.

Wasserman, S. 1998. FH proteins as cytoskeletal organizers. Trends Cell Biol **8:**111-5.

Watanabe, N., Kato, T., Fujita, A., Ishizaki, T. and Narumiya, S. 1999. Cooperation between mDia1 and ROCK in Rho-induced actin reorganization. Nat Cell Biol **1:**136-43.

Watanabe, N., Madaule, P., Reid, T., Ishizaki, T., Watanabe, G., Kakizuka, A., Saito, Y., Nakao, K., Jockusch, B. M. and Narumiya, S. 1997. p140mDia, a mammalian homolog of *Drosophila* diaphanous, is a target protein for Rho small GTPase and is a ligand for profilin. Embo J **16:**3044-56.

Weed, S. A. and Parsons, J. T. 2001. Cortactin: coupling membrane dynamics to cortical actin assembly. Oncogene **20:**6418-34.

Weeds, A. and Maciver, S. 1993. F-actin capping proteins. Curr Opin Cell Biol **5:**63-9.

Wegmann, D., Hess, P., Baier, C., Wieland, F. T. and Reinhard, C. 2004. Novel isotypic gamma/zeta subunits reveal three coatomer complexes in mammals. Mol Cell Biol **24:**1070-80.

Welch, M. D. and Mullins, R. D. 2002. Cellular control of actin nucleation. Annu Rev Cell Dev Biol **18:**247-88.

Welker, R., Harris, M., Cardel, B. and Krausslich, H. G. 1998. Virion incorporation of human immunodeficiency virus type 1 Nef is mediated by a bipartite membrane-targeting signal: analysis of its role in enhancement of viral infectivity. J Virol **72:**8833-40.

Wen, Y., Eng, C. H., Schmoranzer, J., Cabrera-Poch, N., Morris, E. J., Chen, M., Wallar, B. J., Alberts, A. S. and Gundersen, G. G. 2004. EB1 and APC bind to mDia to stabilize microtubules downstream of Rho and promote cell migration. Nat Cell Biol **15:**15.

Westendorf, J. J. 2001. The formin/diaphanous-related protein, FHOS, interacts with Rac1 and activates transcription from the serum response element. J Biol Chem **276:**46453-9.

Westendorf, J. J. and Koka, S. 2004. Identification of FHOD1-binding proteins and mechanisms of FHOD1-regulated actin dynamics. J Cell Biochem **92:**29-41.

Westendorf, J. J., Mernaugh, R. and Hiebert, S. W. 1999. Identification and characterization of a protein containing formin homology (FH1/FH2) domains. Gene **232:**173-82.

Westendorf, J. J., Yamamoto, C. M., Lenny, N., Downing, J. R., Selsted, M. E. and Hiebert, S. W. 1998. The t(8;21) fusion product, AML-1-ETO, associates with C/EBP-alpha, inhibits C/EBP-alpha-dependent transcription, and blocks granulocytic differentiation. Mol Cell Biol **18:**322-33.

Wolf, K., Mazo, I., Leung, H., Engelke, K., von Andrian, U. H., Deryugina, E. I., Strongin, A. Y., Brocker, E. B. and Friedl, P. 2003. Compensation mechanism in tumor cell migration: mesenchymal-amoeboid transition after blocking of pericellular proteolysis. J Cell Biol **160:**267-77.

Wolf, K., Muller, R., Borgmann, S., Brocker, E. B. and Friedl, P. 2003. Amoeboid shape change and contact guidance: T-lymphocyte crawling through fibrillar collagen is independent of matrix remodeling by MMPs and other proteases. Blood **102:**3262-9.

Woychik, R. P., Maas, R. L., Zeller, R., Vogt, T. F. and Leder, P. 1990. 'Formins': proteins deduced from the alternative transcripts of the limb deformity gene. Nature **346:**850-3.

Wyckoff, J. B., Pinner, S. E., Gschmeissner, S., Condeelis, J. S. and Sahai, E. 2006. ROCK- and myosin-dependent matrix deformation enables protease-independent tumor-cell invasion *in vivo*. Curr Biol **16:**1515-23.

Xu, Y., Moseley, J. B., Sagot, I., Poy, F., Pellman, D., Goode, B. L. and Eck, M. J. 2004. Crystal structures of a Formin Homology-2 domain reveal a tethered dimer architecture. Cell **116:**711-23.

Yamaguchi, H. and Condeelis, J. 2007. Regulation of the actin cytoskeleton in cancer cell migration and invasion. Biochim Biophys Acta **1773:**642-52.

Yamana, N., Arakawa, Y., Nishino, T., Kurokawa, K., Tanji, M., Itoh, R. E., Monypenny, J., Ishizaki, T., Bito, H., Nozaki, K., Hashimoto, N., Matsuda, M. and Narumiya, S. 2006. The Rho-mDia1 Pathway Regulates Cell Polarity and Focal Adhesion Turnover in Migrating Cells through Mobilizing Apc and c-Src. Mol Cell Biol **26:**6844-58.

Yamazaki, D., Kurisu, S. and Takenawa, T. 2005. Regulation of cancer cell motility through actin reorganization. Cancer Sci **96:**379-86.

Yayoshi-Yamamoto, S., Taniuchi, I. and Watanabe, T. 2000. FRL, a novel formin-related protein, binds to Rac and regulates cell motility and survival of macrophages. Mol Cell Biol **20:**6872-81.

Yoshida, K. and Soldati, T. 2006. Dissection of amoeboid movement into two mechanically distinct modes. J Cell Sci **119:**3833-44.

Zhang, J., Driscoll, T. A., Hannun, Y. A. and Obeid, L. M. 1998. Regulation of membrane release in apoptosis. Biochem J **334 (Pt 2):**479-85.

Zigmond, S. H., Evangelista, M., Boone, C., Yang, C., Dar, A. C., Sicheri, F., Forkey, J. and Pring, M. 2003. Formin leaky cap allows elongation in the presence of tight capping proteins. Curr Biol **13:**1820-3.

Zimmerberg, J. and Kozlov, M. M. 2006. How proteins produce cellular membrane curvature. Nat Rev Mol Cell Biol **7:**9-19.

Zuniga, A., Michos, O., Spitz, F., Haramis, A. P., Panman, L., Galli, A., Vintersten, K., Klasen, C., Mansfield, W., Kuc, S., Duboule, D., Dono, R. and Zeller, R. 2004. Mouse limb deformity mutations disrupt a global control region within the large regulatory landscape required for Gremlin expression. Genes Dev **18:**1553-64.

12 DANKSAGUNG

Prof. Dr. Hans-Georg Kräusslich gilt mein erster Dank für die Möglichkeit, die vorliegende Arbeit in seinem Institut anfertigen zu können sowie für zahlreiche Anregungen und seine Unterstützung während meiner Promotionszeit.

Mein besonderer herzlicher Dank gilt meinem Mentor Prof. Dr. Oliver T. Fackler für die Vergabe des spannenden Themas und für seine Unterstützung und Förderung meiner wissenschaftlichen Laufbahn. Ich danke ihm für die stets kreativen und motivierenden Diskussionen und sein Vertrauen in meine Fähigkeiten

Als nächstes möchte ich mich bei Prof. Dr. Walter Nickel und Prof. Dr. Michael Lanzer für die freundliche Teilnahme an der Prüfungskommission bedanken.

Während meiner Dissertation hatte ich die Möglichkeit, mit zahlreichen Arbeitsgruppen eng und erfolgreich zusammenzuarbeiten. Daher möchte ich mich hier für die fruchtbare Kooperation bedanken, die einen großen Teil zum Gelingen dieser Arbeit beigetragen hat. Besonders erwähnen möchte ich an dieser Stelle die Gruppen um Dr. Robert Grosse, insbesondere Thomas und Xenia, um Prof. Dr. Walter Nickel, vor allem Stella und Julia, sowie der Gruppe um Dr. Matthias Geyer, hier besonders André.

Den Initiatoren des internationalen Graduiertenkollegs GK1188 "Quantitative Analysis of Dynamic Processes in Membrane Transport and Translocation" gilt mein Dank für die Finanzierung dieser Doktorarbeit sowie die Möglichkeit, im Rahmen des Programms zahlreiche Eindrücke und Erfahrungen zu sammeln. Den anderen „Fellows“ danke ich besonders für den guten Zusammenhalt in unserer kleinen Gruppe.

Dr. Judith Gasteier gilt besonderer Dank für das Einarbeiten in Thema und Arbeitstechniken. Außerdem danke ich meinen Laborkollegen Bettina, Claudia, Jana, Jaz, Nadine, Simone, Steffi und Susi für die stete Hilfs- und Diskussionsbereitschaft sowie die freundschaftliche Atmosphäre.

Auch dem ganzen Rest der Virologie möchte ich danken für die freundliche Atmosphäre, die dafür gesorgt hat, dass das Arbeiten immer Spaß gemacht hat. Besonders erwähnen möchte ich an dieser Stelle meine Mitstreitern der ersten Stunde: Christine, Marko, Patrick, Steffi J. und Steffi V.

Dem Frauenabend um den harten Kern Daniela, Sonja und Frau Rauch danke ich für die herzliche Aufnahme in ihren erlesenen Kreis.

Meinen Freunden aus dem guten alten Braunschweiger Kreis möchte ich ebenfalls danken für die Ablenkung von der Arbeit bei diversen Besuchen und die vielen schönen Abende in Eurer Mitte.

Mein besonders herzlicher Dank gilt meiner Familie und vor allem meinen Eltern und meinem Bruder, ohne die diese Arbeit nicht möglich gewesen wäre.

Schließlich soll mein größter Dank meiner Freundin Ilka gelten, die immer an meiner Seite war und immer an mich geglaubt hat.